INVESTIGATIONS INTO THE INTERACTIONS OF THE HIGH MOBILITY GROUP BOX 1 PROTEIN AND THEIR TOXICOLOGICAL RELEVANCE

Thesis submitted in accordance with the requirements of the University of Liverpool for the degree of Doctor of Philosophy

By

Hannah Louise Aucott
January 2014

DECLARATION

This thesis is the result of my own work. The material contained within this thesis has not been presented, nor is currently being presented, either wholly or in part for any other degree or qualification.

Hannah Louise Aucott

This research was carried out in the Department of Pharmacology and Therapeutics, The University of Liverpool, UK.

CONTENTS

ABSTRACT

Drug Induced Liver Injury (DILI) is associated with high morbidity and mortality rates. It is the leading cause of acute liver failure, accounting for 50% of all cases. Moreover, DILI is the most frequent cause of post marketing drug withdrawal and is often cited as a cause of compound attrition during the drug-development process. The High Mobility Group Box 1 (HMGB1) protein is an important inflammatory mediator which alters the immune system to tissue stress and injury. HMGB1 has been implicated in the pathogenesis of multiple inflammatory diseases including immune-mediated DILI. It has been identified as a potential biomarker of hepatic injury and a target for therapeutic intervention. Research is required to elucidate the pro-inflammatory role of HMGB1. HMGB1 has been reported to interact with a diverse range of endogenous (IL-1, DNA, nucleosomes, CXCL12) and exogenous (LPS) molecules to promote inflammation. However, the mechanisms responsible for these synergistic interactions remain poorly defined and therefore, the overall aim of this work was to characterise the interactions of HMGB1. Specifically, this work has focused on the interaction with IL-1β, which is of particular interest since both molecules often co-exist at the site of inflammation.

The interaction between HMGB1 and IL-1β was investigated using combined cellular and Nuclear Magnetic Resonance (NMR) methodologies. LPS-free, isotopically labelled recombinant HMGB1 (full length protein, amino acids 1-215) and IL-1β proteins were expressed and purified from BL21 (DE3) cells. To facilitate these studies, three additional HMGB1 mutants were sub-cloned from the HMGB1 plasmid: Δ30 (1-185), A box (1-85) and B box (89-163). The recombinant proteins were characterised using Mass Spectrometry (MS) and NMR spectroscopy.

Synovial fibroblasts were isolated from synovial tissue obtained from rheumatoid arthritis patients undergoing joint replacement surgery. Cells were treated with HMGB1 (full length, Δ30, A box or B box) alone or combination with IL-1β. Cell supernatants were collected after 24hr and IL-6 levels were quantified by ELISA. Untreated fibroblasts or cells treated with any HMGB1 construct, or IL-1β alone had no detectable IL-6 release (<9.375pg/mL). In contrast, full length HMGB1, the Δ30 and the B box domain (but not the A box domain) all acted in synergy with IL-1β to substantially enhance IL-6 production. In one patient, HMGB1, Δ30 and the B box in combination with IL-1β induced IL-6 levels of 28,473 ± 127pg/mL, 18,491 ± 2388pg/mL and 18,710 ± 2792pg/mL, respectively. The synergistic interaction was mediated via the Interleukin-1 receptor (IL-1R) and could be inhibited when the cells were pre-treated with 5μg/mL anakinra, a selective IL-1R antagonist but not detoxified LPS, a TLR4 receptor antagonist.

To investigate if there is a direct interaction between HMGB1 and IL-1β, a comprehensive biophysical analysis was performed using NMR methodologies. However, despite performing the experiments in various ways, no evidence of a direct interaction between IL-1β and either full length HMGB1, Δ30 or the B box was detected. This suggests that the synergistic interaction between HMGB1 and IL-1β is mediated via an alternative cellular mechanism in which HMGB1 is required.

In conclusion, the work presented in this thesis has identified that the B box domain of HMGB1 is critical for the synergistic effect observed with IL-1β. However, this is not due to the formation of a binary complex between HMGB1 and IL-1β. Instead, it

would appear that the synergistic effect is mediated via an alternative cellular mechanism in which HMGB1 is required and additional proteins are involved. Future work could focus on discovering what these other proteins might be. These findings help to elucidate the pro-inflammatory role of HMGB1 and provide a novel an insight into HMGB1 biology.

ACKNOWLEDGMENTS

Firstly, I would like to thank my supervisors Dr Dominic Williams, Dr Daniel Antoine, Prof Lu-Yun Lian and Prof Kevin Park for their continued advice, support and encouragement. I would especially like to thank Dom for giving me the opportunity to do this PhD and for his continued guidance throughout.

I am also very grateful to our collaborators at the Karolinska Institutet in Stockholm, Sweden for all their help during my two placements. I would like to especially thank Helena Erlandsson Harris, Ulf Andersson, Peter Lundbäck and Heidi Wähämaa for their advice and technical expertise. Thank-you also to Dr Roz Jenkins and Dr Mark Prescott for MS assistance. A special thanks to Luke Palmer, Phill Roberts and Pete Metcalf for technical help. Of course, I must also say a huge thank-you to Dr Robert Gibson and Dr Marie Phelan for their invaluable help, advice and friendship. I doubt that I would have been able to complete this thesis without all of your prep talks and it really is much appreciated. I would also like to acknowledge the financial support received from the MCR ITTP.

I would like to thank all of the PhD students and post-docs in the CDSS, Biosciences Lab C and the NMR Centre who I've become good friends with during my PhD. There's not room to name you all but hopefully you know who you are! A special thanks to Jon, my HMGB1 buddy, for all of his help and support.

I would also like to say a big thank-you all of my friends and family outside of the lab. Thanks to Jo, Bhav, Nicola, Lorna and Sam for some great sangria nights. A big thanks to Emily for providing me with numerous cups of tea at any time of the day or night, especially during this last year. A special thanks to the 'Avignon 3', Matt, Phil and Catherine. Matt, thanks for some lovely 'Come-Dine-with-Me' nights and a great trip to Avignon. Phil, thanks for educating me on the Cables, introducing me to some 'interesting' pubs and being a great housemate for the last year. Of course Catherine deserves a special mention for putting up with me for 3 years, listening to all my moaning and helping to keep things in perspective. A special thanks also to Emma, George, Katie, Matt, James and Sophie. You've kept me sane throughout and I hope that I can see more of you all from now on.

Of course, I must also say a massive thank all of my family, especially my Auntie Yasmin, Ryan and Natasha. However, the biggest thank-you must go to my mum for her continued love and encouragement. I really couldn't have finished this PhD without your support.

Finally, this PhD is dedicated to my grandparents, my Auntie Rubina and my Auntie Betty.

PUBLICATIONS

ABSTRACTS

BTS, 2011 Development and optimisation of a suitable method to generate soluble recombinant high mobility group box 1 protein (*Toxicology*, 2011; 290(s 2–3))

World Congress: HMGB1 Elucidating the interaction between HMGB1 and IL-1β using combined cellular and NMR methodologies (*J Mol. Med*, 2013, *Abstract accepted*)

PAPERS

Investigating the interaction between HMGB1 and IL-1β using combined cellular and NMR methodologies *(Manuscript in preparation)*

ABBREVIATIONS

ACN	acetonitrile
ADR	adverse drug reaction
ALT	alanine aminotransferase
amu	atomic mass units
APAP	acetaminophen**,** paracetamol
APC	antigen presenting cell
AST	aspartate aminotransferase
ATP	adenosine triphosphate
BMRB	biological magnetic resonance biobank
^{13}C	carbon 13
1D	one dimensional
2D	two dimensional
3D	three dimensional
D_2O	deuterium oxide, ^2H_2O
DAMP	damage associated molecular pattern
dH_2O	distilled water
DILI	drug-induced liver injury
DTT	dithiothreitol
E.coli	*Escherichia coli*
EDTA	ethylenediaminetetraacetic acid
ELISA	enzyme-linked immunosorbant assay
ESI-MS	electrospray ionisation MS
EU	endotoxin unit
FDA	food and drug administration
FID	free induction decay
FL	forward long
FS	forward short
His	histidine
HIV	human immuno-deficiency
HMGB1	high mobility group box 1
HSP	heat shock protein
HSQC	heteronuclear single quantum coherence
Hz	hertz
ICE	interleukin-1 converting enzyme
IEX	ion exchange
IFN	interferon
IL	interleukin
IL-1R	interleukin-1 receptor
IL-1RA	IL-1R antagonist
IL-1RAcP	IL-1R accessory protein
IP	immunoprecipitation

IPTG	isopropyl β-D-1-thiogalactopyranoside
KC	kupffer cell
kDa	kilodalton
LB	lysogeny broth
LC-ESI-MS/MS	liquid chromatography ESI-MS/MS
LPC	lysophosphatidylcholine
LPS	lipopolysaccharide
MIP	macrophage inflammatory protein
MHz	mega hertz
MMP	matrix metalloproteinase
MS	mass spectrometry
MWCO	molecular weight cut off
m/z	mass-to-charge ratio
^{15}N	nitrogen 15
NaCl	sodium chloride
NAPQI	N-acetyl-p-benzoquinonimine
NCBI	national centre for biotechnology information
NCE	new chemical entities
NEM	N-ethylmaleimide
NES	nuclear export signal
NF-κB	nuclear factor-kappa B
NHS	national health service
NK	natural killer
NKT	natural killer T cell
NLS	nuclear localisation signal
NMR	nuclear magnetic resonance
NS	number of scans
OA	osteoarthritis
PAMP	pathogen associated molecular pattern
PBMC	peripheral blood mononucleated cell
PBS	phosphate buffered saline
PCR	polymerase chain reaction
p-i	pharmacological interaction
pI	isoelectric point
PolyI:C	polyinosinic: polycytidylic acid
ppm	parts per million
PRR	pattern recognition receptor
PTM	post translational modification
RA	rheumatoid arthritis
RAGE	receptor for advanced glycation endproducts
RL	reverse long
ROS	reactive oxygen species
rpm	revolutions per minute
RS	reverse short

SD	standard deviation
SDS-PAGE	sodium dodecyl sulfate-polyacrylamide gel electrophoresis
SEM	standard error of the mean
SF	synovial fibroblast
SLIM	site-directed ligase independent mutagenesis
SOB	super optimal broth
SOC	super optimal broth with catabolite repression
SPR	surface plasmon resonance
TAE	tris-acetic acid-EDTA
TBS	tris-buffered saline
TEV	tobacco etch virus
TIR	toll/IL-1R
TLR	toll-like receptor
TNF	tumour necrosis factor α
V	volts

CHAPTER ONE

GENERAL INTRODUCTION

TABLE OF CONTENTS

1.1. INTRODUCTION

Adverse Drug Reactions (ADRs) are a major clinical problem impacting on patient morbidity and mortality rates. In the US, ADRs rank between the 4th and 6th leading cause of death (Lazarou et al., 1998; Zou et al., 2009). A prospective study conducted in UK found that 6.5% of all hospital admissions are directly related to an ADR (Pirmohamed et al., 2004). ADRs are also a significant financial burden for the pharmaceutical industry and are associated with high compound attrition and drug withdrawal rates (Kola and Landis 2004).

ADRs can affect any organ system. However, the liver is highly susceptible to drug-induced toxicity due to its central role in the metabolism and distribution of xenobiotics. To date, nearly 1000 drugs have been linked to an adverse hepatic reaction and Drug-Induced Liver Injury (DILI; hepatotoxicity) is the leading cause of acute liver failure (Ostapowicz et al., 2002). Moreover, it is the most frequent reason for post-marketing drug withdrawal and is often cited as a cause of compound attrition during the drug development process (Kaplowitz 2005) (Lasser et al., 2002).

The cellular mechanisms leading to DILI are still not defined although two pathways appear to be involved: direct hepatotoxicity and adverse immune reactions. Chemically reactive drugs, or their metabolites, are able to damage cellular macromolecules, including proteins, lipids and nuclei acids, leading to hepatic cellular dysfunction and cell death. Emerging evidence suggests that hepatic cellular damage leads to activation of both innate and adaptive immunological responses. Inflammation, the first line innate immune response, has been identified as a key process involved in the modulation of liver injury during drug toxicity. Damaged or dying hepatocytes release proteins that are normally sequestered intracellularly into the extracellular environment (Iyer et al., 2009). These danger signals are termed Damage Associated Molecular Pattern Molecules (DAMPs) or alarmins. DAMPs activate neighbouring immune cells, triggering the production of multiple pro- and anti-inflammatory mediators. These mediators contribute to the progression of DILI by recruiting further innate and adaptive immune cells to the site of injury. The overall severity of the hepatic injury is determined by the balance of pro- and anti-inflammatory mediators produced. To date, more than 20 DAMPs have been identified including the High Mobility Group Box 1 (HMGB1) protein, the Heat Shock Protein (HSP) family, DNA and ATP (Kubes and Mehal 2012).

HMGB1 is a ubiquitous, non-histone chromatin binding protein released following cell activation or cell death. Extracellular HMGB1 has a diverse range of biological activities that promote inflammation and tissue repair. HMGB1 mediates cytokine production (Andersson et al., 2000), chemotaxis (Orlova et al., 2007), cell proliferation, dendritic cell and T-cell activation (Dumitriu et al., 2005), cell differentiation (Melloni et al., 1995) and autophagy (Tang et al., 2010). HMGB1 has been reported to have a pathogenic role in multiple inflammatory diseases and has been implicated as a pro-inflammatory mediator of DILI. HMGB1 appears to interact with a diverse range of endogenous (Interleukin-1 (IL-1), DNA, nucleosomes and CXCL12) and exogenous (Lipopolysaccharide, LPS) molecules to initiate and enhance inflammation. However, despite intense research the mechanisms responsible for these synergistic interactions are still largely unknown. Investigations into these mechanisms will clarify the pro-inflammatory role of HMGB1 and may identify novel cellular pathways that can be targeted to reduce inflammation during DILI.

1.2. ADVERSE DRUG REACTIONS (ADRs)

ADRs are a major public health concern impacting on both patient mortality and morbidity rates (Lazarou et al., 1998; Moore et al., 2007). A prospective observational study conducted at two large Merseyside hospitals between 2001 and 2002 concluded that 1225 (6.5%) out of 18,820 hospital admissions are due to an ADR. This accounted for 4% of the total bed capacity and was projected to cost the NHS up to £466 million per year (Pirmohamed et al., 2004). ADRs also contribute significantly to high compound attrition and drug withdrawal rates within the pharmaceutical industry (Kola and Landis 2004). Between 1975 and 1999, 548 New Chemical Entities (NCEs) were approved by the US Food and Drug Administration (FDA). 45 (8.2%) of these compounds were subsequently given a black box warning and 16 (2.9%) were withdrawn from the market (Lasser et al., 2002).

ADRs can be categorised as ‘on’ or ‘off’ target reactions. ‘On target’ reactions are predictable and are directly related to the primary or secondary pharmacology of the drug. These reactions are dose-dependent and can be alleviated if the dose is reduced or the drug is withdrawn. ‘On target’ reactions are not generally associated with high mortality rates. An example of an ‘on target’ ADR is hemorrhage with anticoagulants, such as warfarin. In contrast, ‘off target’ ADRs cannot be predicted

as they are not related to the known pharmacological activity and are dose-independent. 'Off target' ADRs are more commonly described as idiosyncratic reactions as patients display marked inter-individual susceptibility. Idiosyncratic reactions are less common than 'on target' ADRs but are more serious, normally occurring at therapeutic concentrations, and associated with higher mortality rates. These reactions usually occur after an initial delay or latency period which may range from a few days to several months. An example of an idiosyncratic reaction is hypersensitivity reactions with anticonvulsant drugs.

Any organ system is susceptible to ADRs. The liver is the central organ responsible for the metabolism and distribution of all endogenous and exogenous compounds and thus, the liver is a frequent target of drug-induced toxicity. A three year prospective study conducted in France reported that the annual incidence of DILI was 13.9 per 100,000 inhabitants (Sgro et al., 2002). Moreover, DILI is the most frequently citied cause of post-marketing drug withdrawal (Kaplowitz 2005) and a leading cause of compound attrition during the drug-development process.

1.3. DRUG INDUCED LIVER INJURY (DILI)

A prospective study conducted by the US Acute Liver Failure Study Group concluded that DILI is responsible for more than 50% of all cases of acute liver failure (Ostapowicz et al., 2002). It is associated with high morbidity and mortality rates, with the survival rate in the absence of a liver transplant approximately 20% (Bernal et al., 2009; Verma and Kaplowitz 2009). To date, nearly 1000 drugs have been associated with DILI (Zimmerman 1999; Kaplowitz 2004). Acetaminophen (paracetamol, APAP) overdose accounts for a significant proportion of all cases of DILI (Ostapowicz et al., 2002) and is responsible for 200-500 deaths annually in the UK (Hawton et al., 1995; Makin et al., 1995).

Idiosyncratic DILI is responsible for the majority of the remaining cases of acute liver failure (Ostapowicz et al., 2002). The mechanisms mediating idiosyncratic toxicities are largely unknown with a number of susceptibility factors implicated in the progression of these reactions including age, gender, metabolism and pre-existing inflammation. Idiosyncratic DILI reactions are rare and occur at a frequency of 1 in every 1000 to 1 in every 10,000 patients (Lee 2003). Due to the infrequent

occurrence of these reactions it is difficult to predict compounds that may cause idiosyncratic DILI during drug development and preclinical testing.

Clinically, DILI can mimic various forms of naturally occurring liver disease including hepatitis and cholestasis. Symptoms can vary from mild asymptomatic biochemical changes to fulminant hepatic failure. It is difficult to predict and diagnose DILI in the clinic due to the occurrence of pre-existing liver injury or inflammation in some patients, an incomplete understanding of the underlying mechanisms, particularly during cases of idiosyncratic drug toxicity, and a lack of sensitive and informative clinical biomarkers that detect early liver injury. Currently, measurement of serum and plasma levels of aminotransferases, such as Alanine Amino-Transferase (ALT) and Aspartate Amino-Transferase (AST), is regarded as the 'gold standard' method to detect DILI. However, these enzymes are not organ specific and are only significantly elevated following overt liver damage.

1.4. MECHANISMS OF DILI

The exact mechanisms mediating DILI are not fully understood, although it appears that two pathways are involved: direct hepatotoxicity and immune-mediated damage (Figure 1.1). Most xenobiotic compounds are metabolised in the liver and in some instances, DILI can be initiated by the bioactivation of a drug to a chemically reactive metabolite. Unless detoxified, the parent drug or reactive metabolite may covalently bind to cellular macromolecules including proteins, lipids and nucleic acids resulting in protein dysfunction, lipid peroxidation, DNA damage and oxidative stress. Impaired hepatic cell function ultimately leads to cell death and liver injury (Park et al., 2011).

APAP, a commonly used analgesic and antipyretic drug, is considered to be very safe at therapeutic doses (4 g/day) but causes acute liver failure during overdose. Metabolic activation has been demonstrated to be an essential pre-requisite for APAP-induced hepatotoxicity (Mitchell et al., 1973). APAP is bioactivated to the electrophilic intermediate N-acetyl-p-benzoquinonimine (NAPQI) (Dahlin et al., 1984). The reactive NAPQI metabolite has been demonstrated to bind to a number of target proteins including glutamine synthestase, glutamate dehydrogenase and aldehyde dehydrogenase (Bulera et al., 1995; Halmes et al., 1996; Landin et al.,

1996). APAP-induced hepatotoxicity has been widely studied and the APAP-mouse model is routinely used as a tool to investigate DILI.

Hepatocyte cell stress and damage can trigger both innate and adaptive immune responses. Stressed or dying hepatocytes release danger signals that activate local cells, particularly those of the innate immune system including Natural Killer (NK) cells, Natural Killer T (NKT) cells and kupffer cells (KCs). Prototypical danger signals include Tumour Necrosis Factor α (TNFα), Interleukin-1β (IL-1β), Interferons (IFNs), ATP and HMGB1 (Matzinger 1994; Gallucci and Matzinger 2001). The activation of local resident immune cells stimulates the release of multiple pro- and anti-inflammatory cytokines and chemokine mediators. These proteins activate and recruit further inflammatory cells to the liver with the overall severity of the hepatic injury depending on the balance of pro- and anti-inflammatory mediators produced. One type of cell recruited to the liver during DILI is the neutrophil cell (You et al., 2006). Neutrophils are critical to host defence as they phagocytose and digest foreign material. Depletion of these cells reduces susceptibility to liver injury induced by some drugs (You et al., 2006).

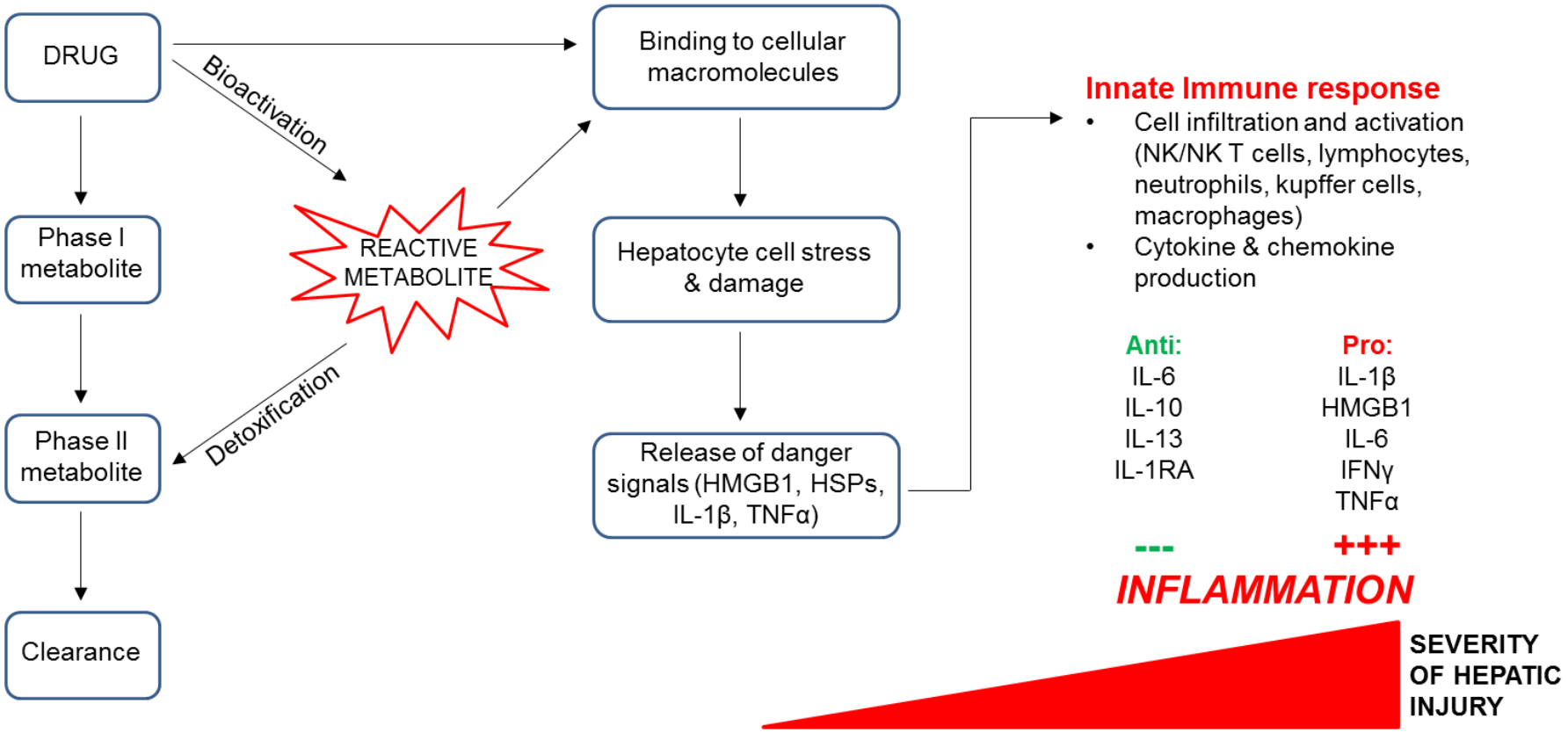

Figure 1.1 Mechanisms of DILI Schematic showing the pathways involved in DILI. Chemically reactive drugs or metabolites can interact with cellular macromolecules, including proteins, lipids and nucleic acids, leading to impaired hepatic cell dysfunction, cell death and possible liver injury. The severity of hepatic damage is determined by the balance of pro- and anti-inflammatory mediators produced. Figure adapted from (Kaplowitz 2005; Laverty et al., 2010).

1.5. IMMUNOLOGICAL RESPONSES IN DILI

The immune system is composed of innate immunity and adaptive immunity. Cells of the innate immune system include macrophages, NK cells, NKT cells and leukocytes. The innate immune response provides rapid, non-specific, first-line defence to recognise and eliminate invading pathogens. Innate immune cells can also function as Antigen Presenting Cells (APCs) to activate the adaptive immune response, which is specific to the invading pathogen.

Regulated physiological immune responses are important for tissue repair and regeneration. However, dysfunction of inflammatory pathways is associated with excessive cytokine production, tissue damage and a pathogenic role in multiple liver diseases. There is growing evidence to support the role of immune-mediated reactions in DILI caused by some drugs, particularly during idiosyncratic toxicity. Table 1.1 provides an overview of the drugs that cause idiosyncratic DILI with evidence of immune involvement.

Table 1.1 Overview of drugs that cause idiosyncratic DILI with evidence of immune involvement $^{+}$Evidence for both allergic and non-allergic DILI reactions. Table adapted from (Kaplowitz 2005; Laverty et al., 2010).

Drug class	Drug name
Anaesthetic	Halothane
Analgesic	Diclofenac^{+}
	Sulindac
Antibiotic	Amoxicillin
	Rifampicin^{+}
	Nitrofluantoin
	Minocycline
	Erthromycins
Anti-convulsant	Phenytoin
	Phenothiazines
Anti-epileptic	Carbamazepine^{+}
Antihypertensive	Dihydralazine
	Methyldopa
	Tienilic acid
Anti-thyroid	Propylthiouracil
Antidepressant	Tricyclic antidepressants
Gout	Allopurinol
Hypertension	ACE inhibitors

1.5.1. THE ROLE OF INNATE IMMUNE RESPONSES IN DILI

1.5.1.1. Sterile inflammation and Damage Associated Molecular Pattern (DAMP) molecules

Inflammation, the first line innate immune response to evading microbial pathogens, is a physiological process that promotes tissue repair and regeneration. However, if the inflammatory process is not tightly controlled, inflammation spreads and tissue damage can occur (Nathan 2002). Recent reports have shown that inflammation can occur in the absence of evading pathogens in response to necrotic cell death (Figure 1.2) (Chen et al., 2007; Hoque et al., 2013). This phenomenon is termed sterile inflammation and can occur in all tissues. Hepatic cell necrosis is known to occur in response to toxic insults (Grattagliano et al., 2002) and sterile inflammation has been identified as a key process involved in DILI. Clinical features of inflammation include redness, swelling, heat, neutrophil infiltration and tissue damage (Kubes and Mehal 2012).

Damaged or dying hepatocytes release proteins that are normally sequestered intracellularly into the extracellular environment (Figure 1.2). These host-derived proteins are termed DAMP molecules or alarmins as their extracellular release alerts the immune system to impending liver injury. HMGB1 (Scaffidi et al., 2002), ATP (Mariathasan et al., 2006), DNA (Jahr et al., 2001), hyaluronic acid and HSPs (Quintana and Cohen 2005) have all been identified as DAMPs that are able to trigger an immune response. DAMPs are recognised by the Pattern Recognition Receptors (PRRs), a group of highly conserved proteins that were initially identified as receptors for evading Pathogen Associated Molecular Pattern (PAMPs) molecules (e.g. LPS and polyinosinic: polycytidylic acid (poly: IC)). The most studied members of PRR family are the Toll-Like Receptors (TLRs), which are a family of transmembrane proteins expressed by cells of the innate immune system. Release and recognition of DAMPs by PRRs activates neighbouring cells of the innate immune system including macrophages, KCs, NK cells and NKT cells (Holt and Ju 2006). This triggers the activation of two interrelated cell signalling pathways that up-regulate the production of multiple inflammatory mediators. The first pathway activates Nuclear Factor-κB (NF-κB)-mediated gene expression resulting in the up-regulation of the transcription of a number of genes encoding pro-inflammatory cytokines, adhesion molecules, chemokines and growth factors (Siebenlist et al.,

1994; Barnes and Karin 1997). Many of these newly transcribed proteins are involved in the second pathway and contribute to the formation of the inflammasome. The inflammasome is a cytosolic multi-protein complex, activated following a second signal, which is critical for caspase-1 (also known as the Interleukin-1 Converting Enzyme (ICE); (Alnemri et al., 1996)) dependent processing and secretion of many inflammatory mediators including IL-1 and IL-18 (Martinon et al., 2002). Recent reports have demonstrated that the sterile inflammatory response to necrotic cells is mediated via the Nalp3 inflammasome (Iyer et al., 2009). Activated innate immune cells also secrete TNF, IFNγ, IL-6 and multiple chemokine mediators (Blazka et al., 1995; Ishida et al., 2002; Masubuchi et al., 2003). These proteins mediate the progression of DILI by promoting the recruitment of further innate and adaptive immune cells to the site of injury.

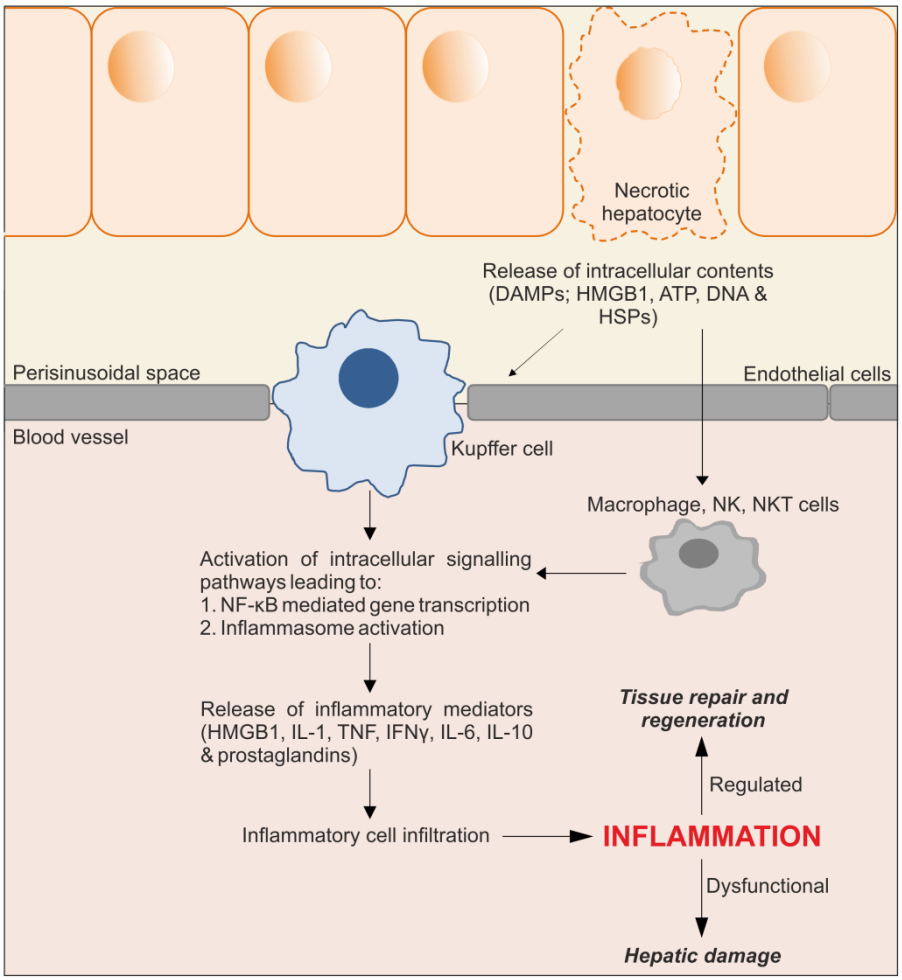

Figure 1.2 Overview of sterile inflammation and the effects of DAMPs on DILI
Necrotic hepatocytes passively release their intracellular contents (DAMPs; HMGB1, HSPs, DNA & ATP) into the extracellular environment and blood, triggering the activation of local innate immune cells including macrophages, KCs, NK cells and NKT cells. Multiple inflammatory mediators, including HMGB1, are up-regulated via two interrelated pathways, which involve NF-κB-mediated gene transcription and inflammasome formation and activation. Inflammatory mediators promote the recruitment of innate and adaptive immune cells, contributing to the progression of inflammation and liver injury (Siebenlist et al., 1994; Barnes and Karin 1997; Martinon et al., 2002; Scaffidi et al., 2002; Holt and Ju 2006).

1.5.1.2 The role of innate immunity as a promoter of DILI

Genetic and environmental factors are known to influence susceptibility to drug toxicity. In particular, it has been hypothesised that cellular stress or inflammatory responses due to concurrent or pre-existing infection may increase the risk of DILI (the inflammatory stress hypothesis). There is clinical evidence to support this theory with studies showing that patients infected with the Human Immuno-deficiency Virus (HIV) or hepatitis C virus have an elevated risk of developing hepatic ADRs

(Levy 1997; Nguyen et al., 2008). The mechanism is not completely understood but it is known that cells of the innate immune system are activated during infection leading to the production of multiple pro-inflammatory mediators. It is generally believed that this lowers the threshold for drug toxicity, contributing to the development of many idiosyncratic ADRs. Recent testing into this hypothesis has resulted in the development of multiple animal models that appear to reproduce some of the idiosyncratic drug toxicities observed in the clinic. Most of these models have involved co-treating animals with non-toxic doses of LPS, a bacterial endotoxin, to replicate pre-existing or concurrent inflammatory stress. LPS (Figure 1.3) is a major component of the outer membrane of gram negative bacteria and a potent activator of the immune response, inducing systemic inflammation and septic shock via TLR4-mediated NF-κB signalling (Shakhov et al., 1990; Hoshino et al., 1999; Beutler and Rietschel 2003). LPS has been extensively used by researchers to induce and study inflammatory responses. Studies using rodent models have shown that co-exposure to non-toxic doses of LPS increases the susceptibility to a number of hepatotoxic agents (Table 1.2).

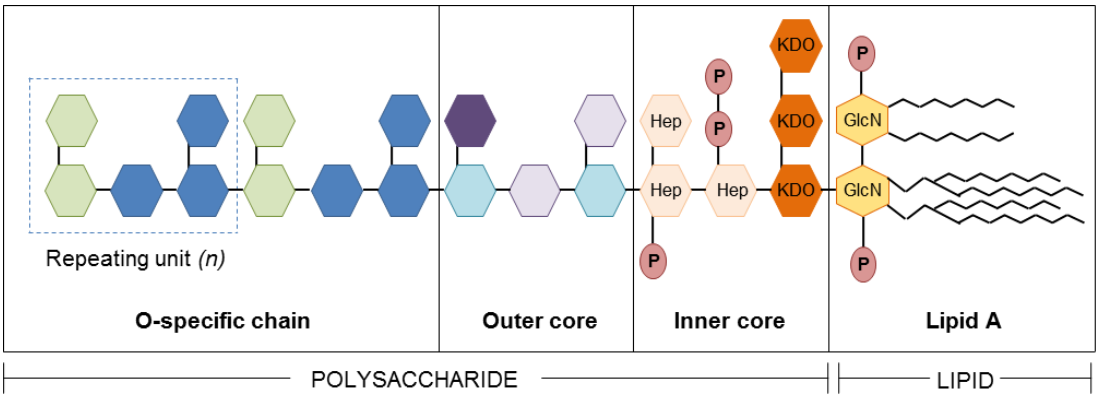

Figure 1.3 Structure of LPS The bacterial endotoxin, LPS, is present in the outer cell membrane of gram negative bacteria and is composed of polysaccharide and lipid moieties. (Hep, $_{L}$-glycero-$_{D}$-manno-heptose; KDO, 2-keto-3-deoxy-octulosonic acid; P, phosphate; GlcN, $_{D}$-glucosamine). Figure adapted from (Beutler and Rietschel 2003).

Table 1.2 Drugs with increased hepatotoxic activities in the presence of moderate inflammatory stress. Compounds listed below had a reduced toxicity threshold when co-administered with bacterial or viral products.

Hepatotoxin	Drug Class/ Use	Inflammagen(s)	References
APAP	Analgesic/ antipyretic	LPS & reovirus	(Maddox et al., 2010)
Chlorpromazine	Antipsychotic	LPS	(Buchweitz et al., 2002)
Diclofenac	Analgesic	LPS	(Deng et al., 2006)
Halothane	Anaesthetic	LPS	(Lind et al., 1984)
Ranitidine	Histamine-2 receptor antagonist (Indicated for gastric disease)	LPS	(Luyendyk et al., 2003)
Sulindac	Analgesic	LPS	(Zou et al., 2009)
Trovafloxacin	Antibiotic (Restricted use due to hepatotoxicity)	LPS	(Waring et al., 2006; Shaw et al., 2007)

1.5.2. THE ROLE OF ADAPTIVE IMMUNE RESPONSES IN DILI

Adaptive immunological responses have been implicated in DILI reactions caused by some drugs including halothane, diclofenac and carbamazepine (Maddrey et al., 2011). These reactions are often associated with fever, rash and eosinophilia, typically occurring after a short latency period of around 1-8 weeks.

Despite intense research it is still not clear how drugs or their metabolites can activate adaptive immune responses. Two hypotheses have been postulated: the hapten hypothesis and the Pharmacological Interaction (p-i) hypothesis. The hapten hypothesis proposes that chemically reactive drugs or metabolites covalently bind to cellular proteins to form immunogenic drug-protein adducts. These adducts are recognised as foreign and induce specific immune responses (Park et al., 1998). Auto-antibodies directed towards drug-modified hepatic proteins have been detected in the sera of some patients, supporting this hypothesis (Satoh et al., 1989; Bourdi et al., 1994; Gunaratnam et al., 1995; Lecoeur et al., 1996). In contrast, the p-i hypothesis proposed by Pichler suggests that some drugs are able to directly bind and activate T cell receptors in the absence of drug metabolism or antigen presentation (Zanni et al., 1998; Pichler et al., 2006).

1.6. INTERLEUKIN-1 (IL-1) AS A CIRCULATING MEDIATOR OF INFLAMMATION

The IL-1 sub-family consists of three proteins: Interleukin-1 alpha (Il-1α), Interleukin-1 beta (IL-1β) and the endogenous Interleukin-1 Receptor antagonist (IL-1RA). IL-1α and IL-1β are potent pleiotropic cytokines that regulate a diverse range of biological activities including the pro-inflammatory response and hematopoiesis (Dinarello 1996) (Table 1.3). Specifically, IL-1β is a critical mediator of the acute-phase response to tissue injury or inflammation (Zheng et al., 1995). A pathogenic role of IL-1β has been reported for many inflammatory diseases including autoimmune diseases, such as rheumatoid arthritis, type 2 diabetes and heart failure (Dinarello 2011).

Table 1.3 Overview of the biological activities of the IL-1 protein Table adapted from (Dinarello 1991).

Biological effects of IL-1
Pyrogen
Promotes synthesis of hepatic acute-phase proteins
T-cell activation
B cell activation
Induces fibroblast differentiation
Endothelial cell activation
Modulation of gene expression:
Increased expression of IL-1, IL-6, TNFα and IL-8
Suppression of type 1 IL-1R and cytochrome P450 expression

The IL-1β protein is released by macrophages, monocytes and dendritic cells (Iwamoto et al., 1989; Eder 2009). Two signals are required for the production, processing and release of IL-1β. Firstly, PAMPs or DAMPs induce the transcription of the IL-1β mRNA and the subsequent translational of the IL-1β protein. IL-1β is initially synthesised as a 31kDa precursor protein (Pro-IL-1β) and a second signal is required to activate the inflammasome and caspase-1 dependent processing and release of mature IL-1β (17 kDa) (Kostura et al., 1989); (Thornberry et al., 1992). The mechanism of IL-1β secretion is not well defined, however as IL-1β lacks a secretory signal peptide it cannot be released via the classical ER-Golgi pathway. Instead, it has been suggested that IL-1β may be released from secretory lysosomes

or exosomes during exocytosis, by shredding of plasma membrane microvesicles or by active transport using specialised membrane transporters (Eder 2009).

Extracellular IL-1 binds to the type I and II transmembrane IL-1 receptors (IL-1Rs) (Figure 1.4). The type I IL-1R is predominantly expressed on fibroblasts, endothelial cells, T cells and hepatocytes. IL-1 binds to the type 1 IL-1R and recruits the IL-1R accessory protein (IL-1RAcP) leading to the formation of a pro-inflammatory heterodimeric signalling complex (Greenfeder et al., 1995). The signalling complex activates the NF-κB pathway to induce the expression of a wide variety of genes including pro- and anti-inflammatory mediators (IL-1, IL-6, IL-8 and TNFα) and multiple inflammatory receptors, including the IL-1R (Dinarello 1996). In contrast, the type II IL-1R, located primarily on monocytes, neutrophils, B cells and bone marrow cells (Kuno and Matsushima 1994), contains a truncated cytoplasmic domain and cannot initiate intracellular signalling. Thus, the type II IL-1R acts as a decoy receptor, sequestering IL-1 and regulating the biological activity of the protein (McMahan et al., 1991). Furthermore, the endogenous IL-1RA can also bind to the IL-1R but cannot recruit the IL-1RAcP and therefore cannot initiate cell signalling and acts to regulate the pro-inflammatory activity of IL-1α and IL-1β (Arend et al., 1990; Greenfeder et al., 1995).

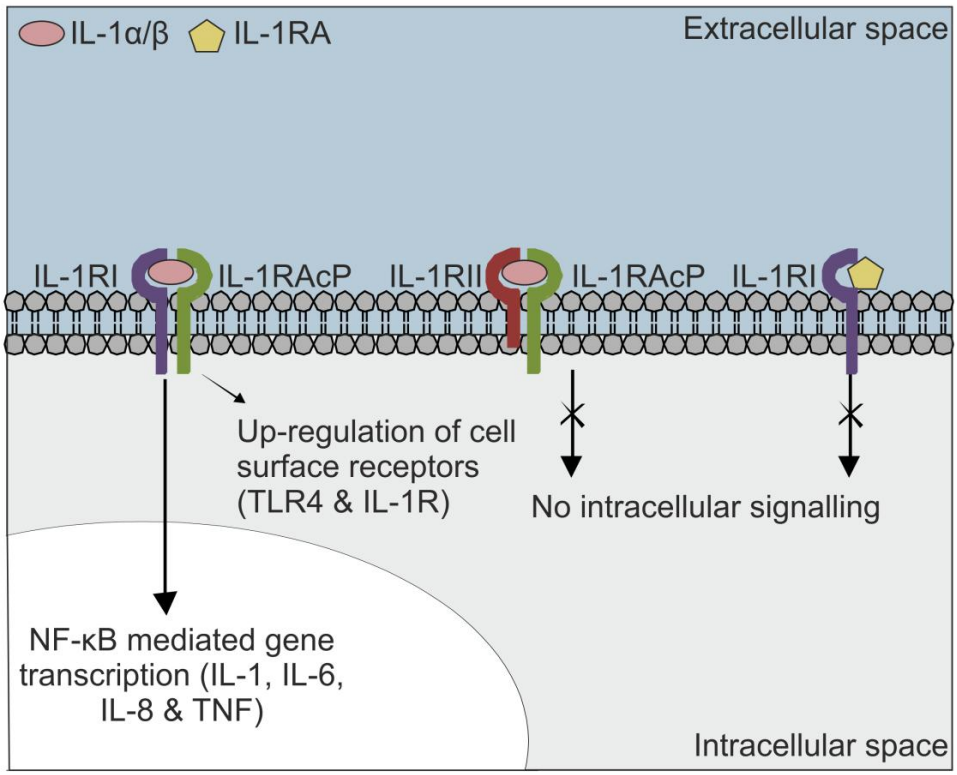

Figure 1.4 Overview of IL-1-mediated cell signalling IL-1α and IL-1β form a heterodimeric signalling complex by binding to the IL-1R type I (IL-1RI) and the IL-1RAcP. This results in NF-κB mediated gene transcription and up-regulation of multiple cell surface receptors including IL-1R and TLR4. In contrast, the IL-1R type II (IL-1RII) acts as a decoy receptor, as it contains a truncated cytoplasmic domain and cannot initiate intracellular signalling. The IL-1RA protein acts as a endogenous IL-1R antagonist as it can bind to the IL-1R but cannot recruit the IL-1RAcP (McMahan et al., 1991; Greenfeder et al., 1995; Dinarello 1996).

1.7. INTERLEUKIN-6 (IL-6) AS A CIRCULATING MEDIATOR OF INFLAMMATION

IL-6 (previously termed the hepatocyte stimulating factor; (Van Snick 1990)) is a pleotropic cytokine with a central role in host defence (Table 1.4). Macrophages and monocytes secrete IL-6 following activation of the NF-κB pathway in response to PAMPs or DAMPs (Iwamoto et al., 1989; Ju et al., 2002; Luckey et al., 2002). It has both pro- and anti-inflammatory activities that regulate the immune response, hematopoiesis and acute phase reactions (Simpson et al., 1997). Overproduction of IL-6 is associated with a number of autoimmune and inflammatory diseases (Ishihara and Hirano 2002; Kishimoto 2006).

IL-6 has important roles in liver repair and regeneration, protecting against APAP, ethanol and carbon tetrachloride induced hepatotoxicity (Kovalovich et al., 2000; Masubuchi et al., 2003; Bourdi et al., 2007). When subjected to acute carbon

tetrachloride treatment, IL-6 deficient mice have increased liver necrosis and impaired liver regeneration compared to wild-type animals (Kovalovich et al., 2000). Moreover, elevated IL-6 levels have been reported in animal models of APAP-induced hepatotoxicity (James et al., 2003) and IL-$6^{-/-}$ mice have an increased susceptibility to APAP-induced hepatic injury (Masubuchi et al., 2003).

Table 1.4 Biological activities of the IL-6 protein

Function	Reference(s)
Induction of B cell differentiation	(Hirano et al., 1985)
Hepatocyte stimulating factor: induces acute phase inflammatory response	(Gauldie et al., 1987)
T cell activation	(Lotz et al., 1988)
Hematopoietic activity	(Ikebuchi et al., 1987)
Induction of nerve cell differentiation	(Satoh et al., 1988)
Stimulates secretion of nerve growth factor by astrocytes	(Frei et al., 1989)

1.8. HIGH MOBILITY GROUP BOX-1 (HMGB1) AS A CIRCULATING MEDIATOR OF INFLAMMATION

1.8.1. Discovery and function of HMGB1

The HMGB1 protein (previously referred to as HMG-1, amphoterin or P30; (Bustin 2001)) is a ubiquitous and abundant non-histone chromatin binding protein first purified in the 1970s (Goodwin et al., 1973; Bustin 2001). The protein belongs to the HMG Box (HMGB) family, which also includes HMGB2 and HMGB3. The proteins have a highly conserved structure and were named after their ability to migrate quickly during electrophoresis. The average cell has up to 10^6 HMGB1 molecules (Muller et al., 2004) and HMGB1-deficient mice die within hours of birth due to hypoglycaemia, demonstrating a vital role for HMGB1 in growth and development. (Calogero et al., 1999).

HMGB1 has multiple, compartment-specific functions (Figure 1.5). HMGB1 is present in the nucleus of all eukaryotic cells where it acts as an ‘architectural’ DNA-binding protein (Bustin et al., 1978; Travers and Thomas 2004). Nuclear HMGB1 binds to the minor groove of double-stranded DNA in a sequence-independent manner. HMGB1 recognises distorted DNA structures like DNA-bulges, four-way junctions, kinks and cisplatin-modified DNA (Agresti and Bianchi 2003; Reeves

2010). HMGB1 induces bends into the DNA structure (Onate et al., 1994; Agresti and Bianchi 2003) which in turn facilitates the interaction between the DNA and various proteins, including the NF-κB and p53 transcription factors (Jayaraman et al., 1998; McKinney and Prives 2002; Rowell et al., 2012). HMGB1, therefore, facilitates gene transcription and DNA replication (Czura et al., 2001; Reeves 2010). Moreover, nuclear HMGB1 is also involved in cell replication, DNA repair and nucleosome assembly (Lange et al., 2008; Celona et al., 2011).

Extracellular HMGB1 has a diverse range of biological activities that promote inflammation and tissue repair. HMGB1 mediates cytokine production (Andersson et al., 2000), chemotaxis (Orlova et al., 2007), cell proliferation, dendritic cell and T-cell activation (Dumitriu et al., 2005), cell differentiation (Melloni et al., 1995) and autophagy (Tang et al., 2010). HMGB1 has been reported to have a pathogenic role in many diseases including arthritis (Kokkola et al., 2002), sepsis (Wang et al., 1999) and cancer (Lotze and Tracey 2005; Sims et al., 2010).

HMGB1 has also been identified as an inflammatory mediator of liver injury. Elevated HMGB1 levels have been reported in experimental models of hepatic reperfusion injury and DILI (Ilmakunnas et al., 2008). Recent studies have identified HMGB1 as a potential early and sensitive mechanistic biomarker of DILI, with significant HMGB1 elevations reported during APAP-induced hepatotoxicity (Antoine et al., 2009; Martin-Murphy et al., 2010). Moreover, HMGB1 has been identified as a potential target for therapeutic intervention during DILI. Administration of neutralising HMGB1 antibodies has been reported to be beneficial in mice models of APAP-overdose and is associated with increased survival rates (Antoine et al., 2010).

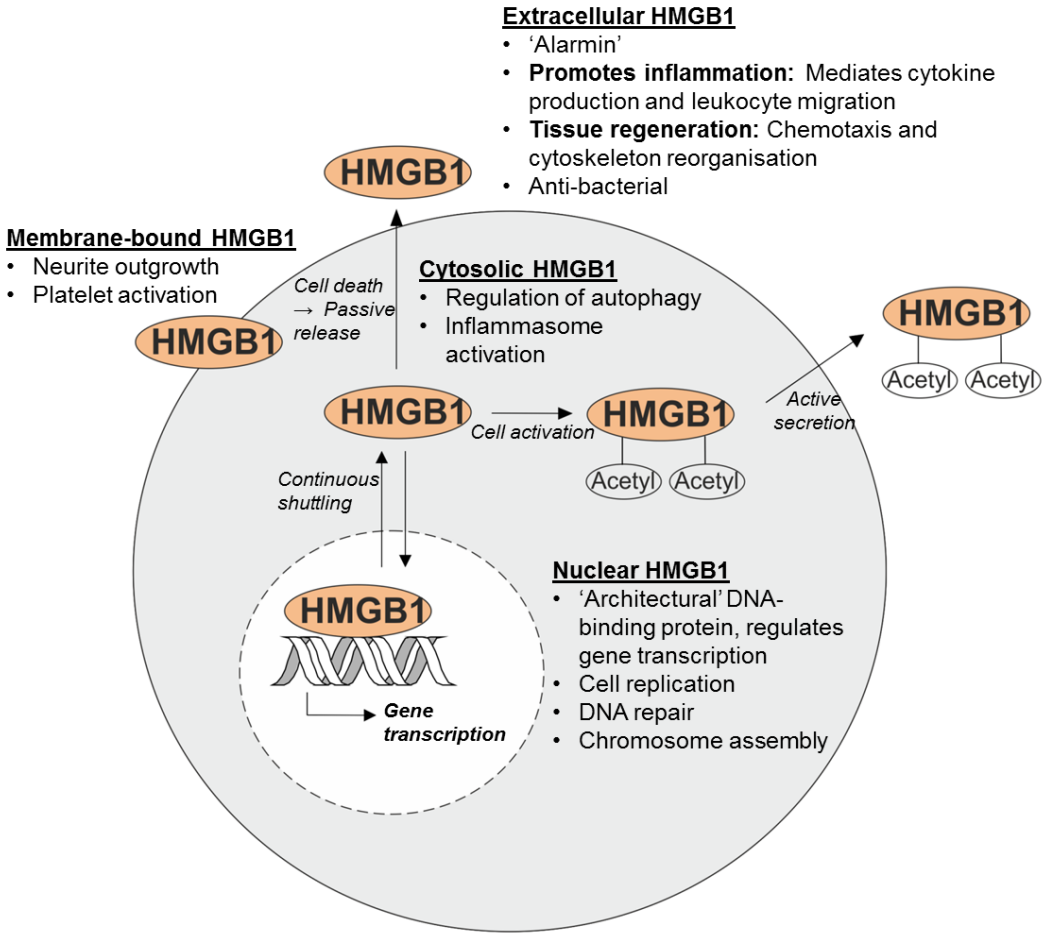

Figure 1.5 Compartment-specific functions of the HMGB1 protein HMGB1 is a multifunctional cytokine with a diverse range of intra- and extra-cellular activities. HMGB1 is highly expressed in the nucleus where it acts as an architectural DNA-binding protein that regulates gene transcription and chromatin structure. HMGB1 is also present in the cytoplasm where it is involved in autophagy and inflammasome activation. Membrane-bound HMGB1 promotes neurite outgrowth in cerebral neurons and platelet activation. Additionally, HMGB1 is released into the extracellular environment following cell activation (active secretion, requires HMGB1 acetylation) or cell death (passive secretion). Extracellular HMGB1 is an alarmin, promoting inflammation and tissue regeneration. Figure adapted from (Yang et al., 2013).

1.8.2. The structure of the HMGB1 Protein

The gene encoding human HMGB1 is located on chromosome 13q12 (Ferrari et al., 1996). HMGB1 is a 25 kDa protein containing 215 amino acids organised into a tripartite domain structure consisting of 2 HMG box domains (Boxes A and B) and a polyacidic negatively charged tail (Figure 1.6). The HMG domains are highly

conserved DNA-binding motifs present in a variety of architectural proteins. The HMGB1 protein is highly conserved between species with 99% homology in the primary sequence of the rodent and human forms. The sequences differ in only 2 amino acid residues located within the c-terminal tail: the glutamic acid at position 189 and the aspartic acid at position 202 in human HMGB1 are substituted by aspartic acid and glutamic acid residues respectively in the rodent protein.

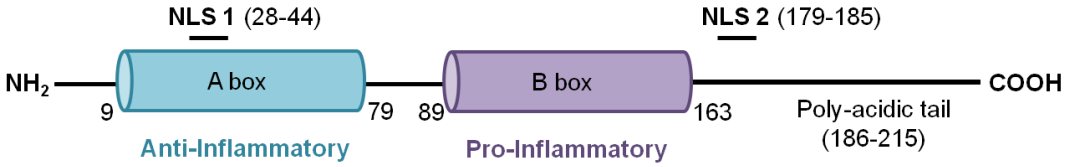

Figure 1.6 Domain structure of HMGB1 HMGB1, a 25 kDa nuclear protein consisting of 215 amino acid residues, has a tripartite domain structure comprising of two highly conserved DNA-binding motifs (boxes A and B, residues 9-79 and 89-163 respectively) and a polyacidic negatively charged tail (residues 186-215). The B box confers the pro-inflammatory activity whilst the A box is anti-inflammatory *in vivo*. The protein contains 2 NLS domains at residues 28-44 and 179-185 (as indicated). There are also two CRM1-dependent NES domains.

Boxes A and B correspond to residues 9-79 and 89-163 respectively (Figure 1.7). The boxes, which are connected by a short nine-residue linker region, have a low sequence similarity (29%) but share a conserved global fold, consisting of three α-helices arranged in an L-like structure (Weir et al., 1993; Hardman et al., 1995) (Figure 1.8). A 21-residue, unstructured and flexible linker region connects Box B to the 30-residue poly-acidic negatively charged tail. The tail is composed entirely of aspartic and glutamic acid residues (Residues 185-215; Figure 1.7) and interacts with the A and B boxes (Ramstein et al., 1999; Jung and Lippard 2003; Knapp et al., 2004; Watson et al., 2007; Stott et al., 2010). The interaction is believed to shield the boxes and has important functional implications. It modulates the interaction with DNA (Sheflin et al., 1993; Štros et al., 1994; Lee and Thomas 2000; Muller et al., 2001), is involved in the interaction with histones H1 and H3 (Cato et al., 2008; Watson et al., 2013) and modulates HMGB1 protein acetylation by histone acetyltransferases (Pasheva et al., 2004).

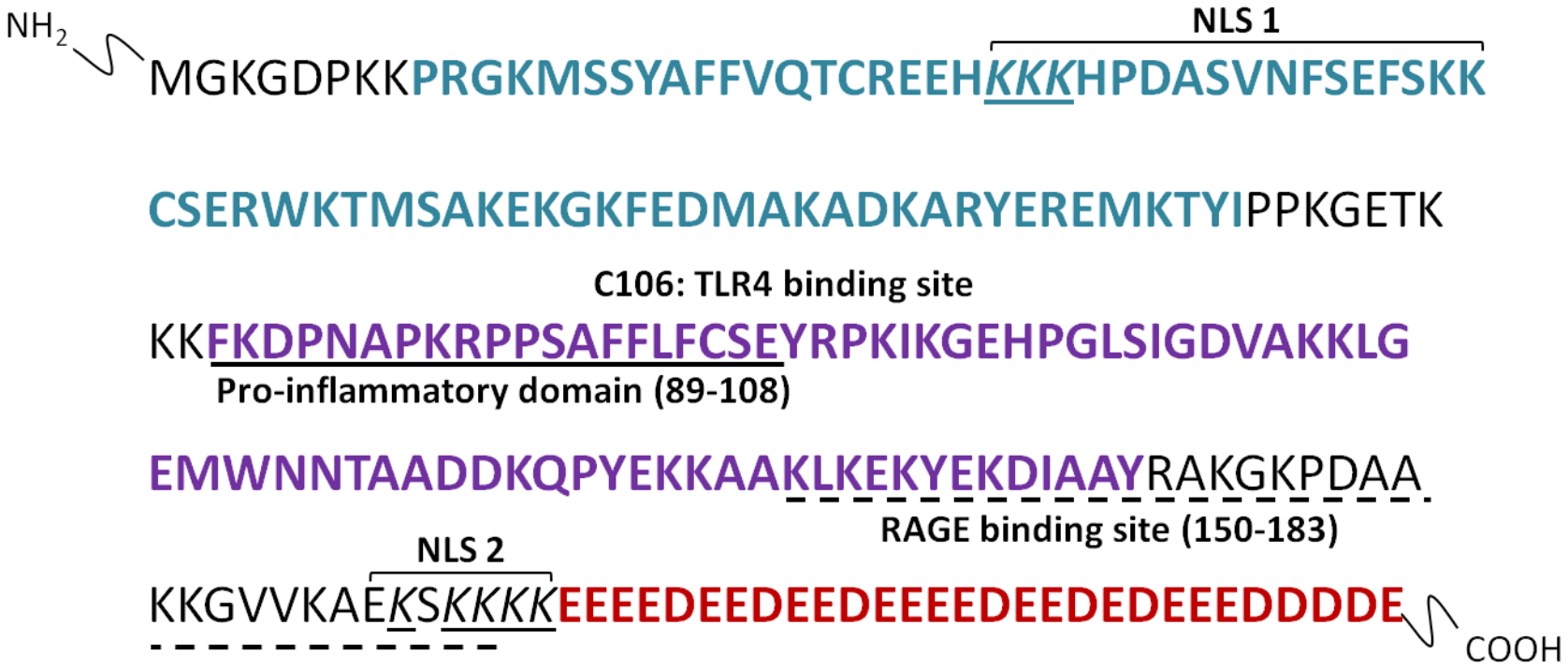

Figure 1.7 Linear representation of the amino acid structure of HMGB1 The HMGB1 protein contains 215 amino acid residues organised into three domains: the A (Blue) and B (Purple) boxes, at residues 9-79 and 89-163 respectively, and the negatively charged c-terminal tail composed of 30 acidic amino acid residues (Red;186-215). Box A is anti-inflammatory and B box is pro-inflammatory, a 20-residue region within the B box (89-108) represents the minimal region required for TNF activation. The TLR4 and RAGE binding sites are indicated. HMGB1 contains 43 lysine residues (20% of total amino acid content) and 8 of these, located within the NLS domains, are frequently acetylated *in vivo* (*K*) to aid active protein secretion.

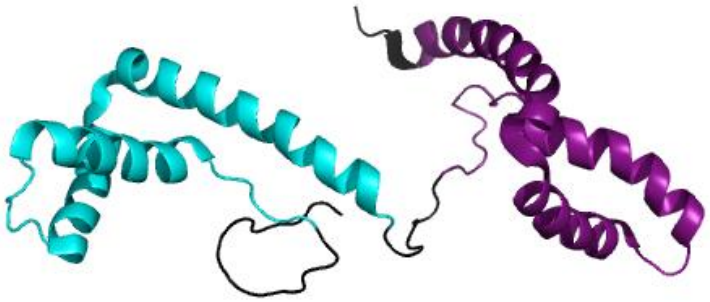

Figure 1.8 3D structure of HMGB1 A and B box domains HMGB1 is composed of 2 HMG boxes (Boxes A and B, also known as DNA-binding domains) and a polyacidic negatively charged tail. The 3D structure of HMGB1 amino acids 1-167 has been solved by solution NMR and is shown above. Image was prepared in PyMol using PDB entry 2YRQ (PyMoL).

HMGB1 also contains two Nuclear Localisation Signal (NLS) domains and two non-classical Nuclear Export Signal (NES) domains which allow the protein to continuously shuttle between the cell nucleus and cytoplasm.

1.8.3. Extracellular release of HMGB1

Under physiological conditions, HMGB1 is predominately localised to the nucleus but following cell injury or death it is released into the extracellular environment where it acts to initiate and amplify the inflammatory response. A number of mechanisms are involved in the regulation of HMGB1 release (Figure 1.9). HMGB1 is constitutively expressed in all nucleated cells and can be passively released during necrotic cell death following the loss of the cell membrane integrity (Figure 1.9A) (Scaffidi et al., 2002; Rovere-Querini et al., 2004). In this context HMGB1 is regarded as an early marker of cell death.

HMGB1 can also be actively secreted from innate immune cells in response to an inflammatory stimulus and in this context HMGB1 is regarded as a late mediator of cell activation (Figure 1.9B). Mouse macrophages stimulated with LPS, TNF or IL-1 secrete large amounts of HMGB1 (Wang et al., 1999). Similar to IL-1β, HMGB1 lacks a secretory signal peptide and cannot be secreted via the classical ER-Golgi pathway (Bonaldi et al., 2003). In resting cells, HMGB1 continually shuttles between the nucleus and cytoplasm. However, in activated macrophages and monocytes HMGB1 is post-translationally modified, preventing re-entry into the

nucleus and resulting in accumulation of HMGB1 into cytoplasmic vesicles (Bonaldi et al., 2003; Cato et al., 2008). HMGB1 is acetylated at lysine residues within the NLS domains, specifically lysine residues at positions 28, 29, 30, 180, 182, 183, 184 and 185 are frequently acetylated *in vivo* (Figure 1.7). Additionally, hyper-phosphorylation of HMGB1 has also been reported to occur in macrophages and monocytes (Youn and Shin 2006). The release of HMGB1 from the cytoplasmic vesicles into the extracellular environment is triggered by lysophosphatidylcholine (LPC) (Cato et al., 2008). LPC is a derived from phosphatidylcholine and is generated at the site of inflammation several hours after monocyte activation. Recent evidence suggests that active HMGB1 secretion from macrophages stimulated with LPS or polyI:C is dependent on the inflammasome and capase-1 activation (Lamkanfi et al., 2010; Lu et al., 2012).

Active secretion of HMGB1 has also been reported from a number of other cells including neutrophils, dendritic cells, NK cells, pituicytes and hepatocytes (Wang et al., 1999; Chen et al., 2004; Dumitriu et al., 2005; Semino et al., 2005; Tsung et al., 2007). Further investigation is required to fully elucidate the mechanisms that drive active release of HMGB1 from these cells. It has been reported that mono-methylation of K42 may promote the cytoplasmic accumulation of HMGB1 in neutrophils (Ito et al., 2007).

HMGB1 released from necrotic or activated cells, interacts with the TLRs and the Receptor for Advanced Glycation Endproducts (RAGE) to elicit an inflammatory response. It is not yet known if the different molecular forms activate distinct signalling pathways. In contrast, HMGB1 released from apoptotic cells undergoing secondary necrosis promotes immune tolerance (Figure 1.9C) (Kazama et al., 2008). During apoptosis, Reactive Oxygen Species (ROS) produced by the mitochondria oxidise HMGB1, at the C106 residue, preventing binding to the TLR4 and thereby neutralising the cytokine-inducing activity (Kazama et al., 2008; Yang et al., 2010). A study by Antoine *et al* illustrated the critical role of HMGB1 oxidation and subsequent immune tolerance during APAP-induced hepatotoxicity (Antoine et al., 2010). In the APAP-induced hepatotoxicity mouse model, diet restriction inhibited caspase-driven apoptosis and prevented HMGB1 oxidation leading to enhanced inflammation and increased mortality (Antoine et al., 2010).

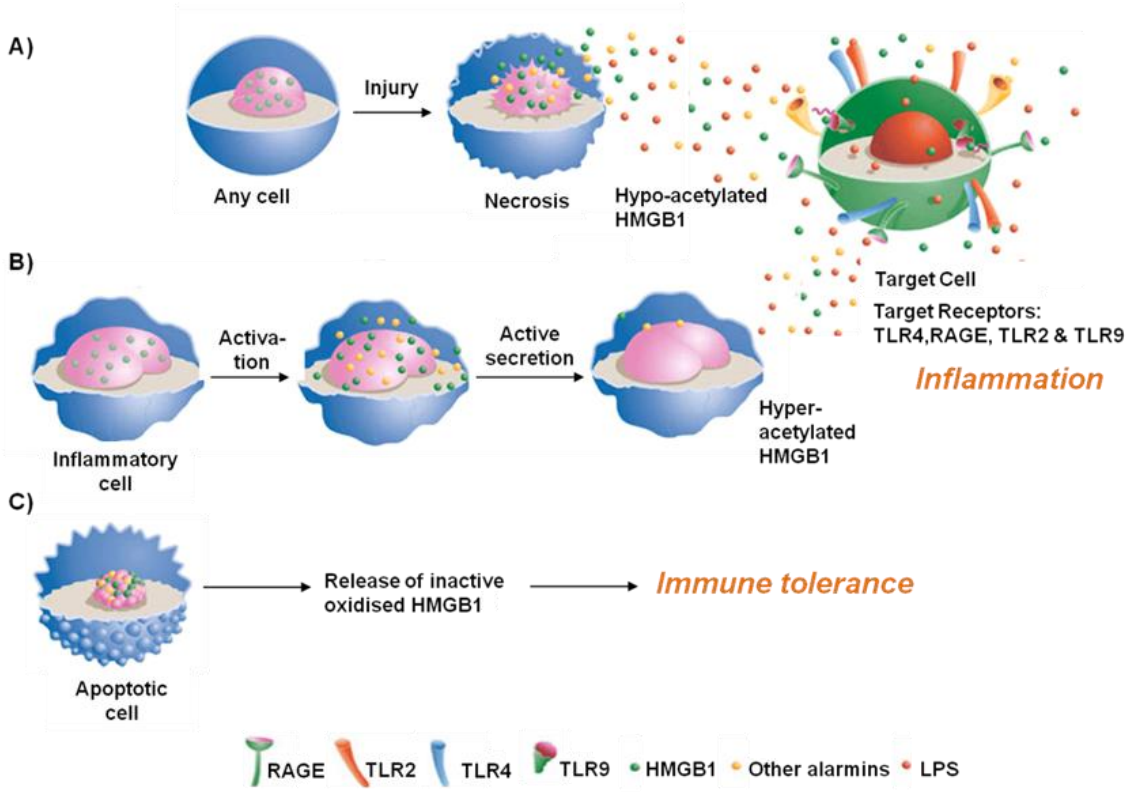

Figure 1.9 Mechanisms for the release of HMGB1 into the extracellular environment HMGB1 is released into the extracellular environment following cell death or injury where it may act to initiate and amplify the inflammatory response. A) Hypo-acetylated HMGB1 is passively released by necrotic cells. B) Hyper-acetylated HMGB1 is actively secreted from activated immune cells. Both molecular forms can bind to the TLRs (TLR2, TLR4 and TLR9 have been implicated in HMGB1 signalling) and the RAGE on the target cell to promote inflammation. In contrast, oxidised HMGB1 released from apoptotic cells during secondary necrosis promotes immune tolerance (C). Figure adapted from (Harris and Raucci 2006).

1.8.4. Receptors mediating HMGB1 activity

Extracellular HMGB1 interacts with multiple un-related receptors to mediate a diverse range of biological responses. A number of receptors have been identified for HMGB1 including RAGE, TLR2, TLR4, TLR9, Syndecan, Mac-1, and Siglec-10 (Salmivirta et al., 1992; Hori et al., 1995; Yu et al., 2006; Tian et al., 2007; Chen et al., 2009; Gao et al., 2011).

1.8.4.1. Receptor for Advanced Glycation Endproducts (RAGE)

RAGE, a multi-ligand member of the immunoglobulin superfamily, was the first receptor to be identified for HMGB1 (Hori et al., 1995). A recent study by Huttunen *et al*, has mapped the RAGE binding site to residues 150-183 (Huttunen et al., 2002)

(Figure 1.7). HMGB1-RAGE signalling mediates chemotaxis and cell growth, differentiation of immune cells and the up-regulation of inflammatory cell signalling receptors, including RAGE and TLR4 (Orlova et al., 2007; Andersson and Tracey 2011) (Figure 1.10).

1.8.4.2. Toll-Like Receptors (TLRs)

HMGB1 also interacts with TLR2, 4 and 9 (Figure 1.10) The interaction between HMGB1 and TLR4 is critical for HMGB1-induced cytokine release (Yang et al., 2010). Macrophages from TLR4-deficient mice do not release TNF, IL-6, IL-1β or IL-10 when exposed to HMGB1 (Yang et al., 2010). In contrast, $TLR2^{-/-}$ and $RAGE^{-/-}$macrophages secrete large amounts of cytokines in response to HMGB1 treatment, suggesting that these receptors are dispensable during HMGB1-induced cytokine production (Yang et al., 2010). Binding of HMGB1 to TLR4, activates the adaptor protein MyD88 which promotes the nuclear translocation of NF-κB and results in the up-regulation of multiple pro-inflammatory genes and inflammatory mediators (Park et al., 2004). HMGB1 signalling through TLR4 mediates macrophage activation, cytokine release and tissue injury (Andersson et al., 2000; Andersson and Tracey 2011). The interaction between HMGB1 and TLR4 has been studied in detail using Surface Plasmon Resonance (SPR) and is mediated via the B box domain of HMGB1 (Yang et al., 2010). Specifically, the C106 residue is critical for the interaction and the C106A HMGB1 mutant does not bind to TLR4 and cannot induce cytokine production in human macrophages (Yang et al., 2010).

1.8.5. HMGB1 as a pro-inflammatory cytokine mediator

One of the main functions of extracellular HMGB1 is to induce the release of pro-inflammatory cytokines. Human monocytes exposed to HMGB1 release TNF, IL-1, IL-6, IL-8, IL-1RA, Macrophage-Inflammatory Protein (MIP)-1α and MIP-1β (Andersson et al., 2000). HMGB1-induced cytokine production is mediated via two mechanisms of action. Firstly, HMGB1 is an endogenous cytokine mediator and secondly, HMGB1 is also reported to act in synergy with multiple unrelated molecules to promote and enhance inflammation (Figure 1.10).

HMGB1 has intrinsic cytokine-inducing activity, interacting with TLR4 to activate NF-κB mediated gene transcription and cytokine production. Recent reports have

shown that the redox status of the C23, C45 and C106 residues is critical for the functional activity of HMGB1, with the pro-inflammatory molecular form requiring a C23-C45 disulphide bond and a reduced C106 residue (Yang et al., 2011). In contrast, fully reduced or fully oxidised HMGB1 does not induce cytokine-production in human macrophages (Yang et al., 2011).

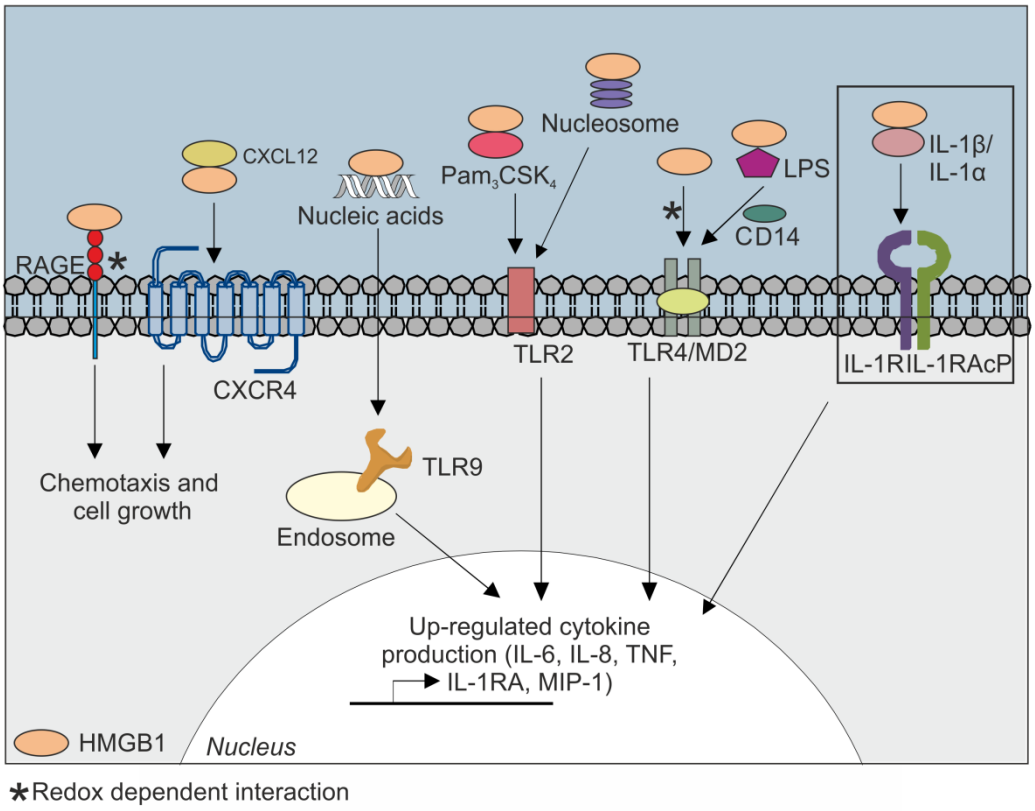

Figure 1.10 HMGB1 signalling pathways Extracellular HMGB1 activates multiple signalling pathways to promote inflammation and tissue repair. HMGB1 induced cytokine-production occurs via two mechanisms of action: 1) HMGB1 acts as an endogenous cytokine mediator interacting with the TLR4/MD2 complex and 2) HMGB1 acts in synergy with multiple endogenous (IL-1, CXCL12 and nucleosomes) and exogenous (LPS and Pam_3CSK_4) ligands. It is generally believed that HMGB1-partner molecules interactions signal via the partner molecule receptor. HMGB1 also interacts with RAGE and CXCL12/CXCR4 to promote chemotaxis and cell growth. The signalling pathway under investigation in this thesis is shown in the boxed region. Figure adapted from (Harris et al., 2012).

HMGB1 has also been demonstrated to act in synergy with a variety of endogenous and exogenous molecules to promote and enhance inflammation. Specifically, HMGB1 has been reported to interact with IL-1β, IL-1α, CXCL12, nucleosomes, LPS, CpG-DNA, Pam_3CSK_4 and lipoteichoic acid. A number of independent studies have shown that these synergistic interactions result in an enhanced inflammatory

response (Ivanov et al., 2007; Tian et al., 2007; Sha et al., 2008; Urbonaviciute et al., 2008; Hreggvidsdottir et al., 2009; Qin et al., 2009; Cox et al., 2012; Schiraldi et al., 2012). It has been proposed that these responses are mediated via the formation of highly active inflammatory complexes that interact with the partner molecule receptor. However, molecular studies are required to further characterise these interactions and to elucidate the mechanism of action.

The first study to describe this mechanism was reported by Sha *et al*, in 2008. In this study FLAG-tagged HMGB1 was expressed alone or in the presence of IL-1β. Mouse macrophages exposed to HMGB1 cultured in the presence of IL-1β had enhanced TNFα and MIP-2 production when compared to cells treated with HMGB1 alone (Sha et al., 2008). The authors proposed that this effect was mediated via the formation of a highly active pro-inflammatory complex between HMGB1 and IL-1β. To support this theory, they reported that FLAG-tagged HMGB1 and IL-1β could be co-isolated using a pull down assay. Additionally, several recent publications from independent groups support this hypothesis and demonstrate that HMGB1 and IL-1β also significantly enhance cytokine production in synovial fibroblasts (SFs) (Hreggvidsdottir et al., 2009; Ferhani et al., 2010; Garcia-Arnandis et al., 2010; Wähämaa et al., 2011). Moreover, HMGB1 has recently been shown to form similar complexes with CXCL12 and LPS (Schiraldi 2012, Youn 2008).

HMGB1 and IL-1β are circulating mediators of inflammation that often co-exist at the site of inflammation and signal via a common pathway. Both proteins have been implicated in the pathogenesis of DILI and thus, the synergistic interaction between HMGB1 and IL-1β is of particular interest. However, detailed cellular and biophysical studies characterising the interaction are lacking within the current literature and this project will make extensive use of Nuclear Magnetic Resonance (NMR) to probe the interactions between HMGB1 and IL-1β in the presence and absence of LPS. Further details of the NMR method are given in Chapter 2.

1.9. AIMS OF THESIS

HMGB1 has been described as a pathogenic mediator of immune-mediated DILI. It has been identified as a potential biomarker of hepatotoxicity and a target for therapeutic intervention. Further investigations are required to elucidate the pro-inflammatory role of HMGB1. HMGB1 interacts with a diverse range of unrelated

molecules to enhance inflammation. However, despite considerable research the role of HMGB1-partner molecule interactions in modulating the inflammatory response remain poorly defined and further investigations are needed. The overall aim of the work presented in this thesis was to characterise the interactions of HMGB1 using combined cellular and NMR methodologies. Specifically, this work has focused on the interaction with IL-1β, which is of particular interest, as both molecules often co-exist at the site of inflammation and have been implicated in the pathogenesis of DILI.

The specific aims of this work were to:

- Develop and optimise methods for the expression, purification and characterisation of LPS-free and isotopically labelled recombinant HMGB1 and IL-1β proteins (Chapter 1)
- Characterise the cellular response to HMGB1/IL-1β synergy (Chapter 2):
  - Identify which domain(s) of HMGB1 mediates the interaction with IL-1β
  - Explore the dynamics and kinetics of the HMGB1/IL-1β interaction to establish the clinical relevance of HMGB1/IL-1β synergy
- Test the hypothesis that HMGB1 and IL-1β directly interact to form a binary complex and, if appropriate, identify the residue(s) involved in the binding interaction (Chapter 3)

The findings from this work will help to elucidate the function of HMGB1 and will provide a novel insight into the biology of the HMGB1 protein.

CHAPTER TWO

MATERIALS AND METHODS

TABLE OF CONTENTS

2.1. MATERIALS

The HMGB1 I.M.A.G.E full length cDNA clone was purchased from Imagenes (Berlin, Germany) (Clone ID: IRAUp96H0588D). The I.M.A.G.E full length cDNA clone for IL-1β was obtained from Source Biosciences (UK) (Clone ID: IRATp970B129D). PCR primers used for cloning purposes were synthesised by Sigma Aldrich (UK). All PCR reagents were purchased from New England BioLabs (NEB, Hertfordshire, UK). XLI-blue *E.coli* cells were from Stratagene (San Diego, USA) and BL21 (DE3) cells were from Novagen (Merck Chemicals Ltd, Nottingham, UK). Kanamycin was purchased from Sigma Aldrich (UK) and used at a final concentration of 32 μg/mL. Ampicillin was from Melford (UK) and was used at a final concentration of 100 μg/mL. AKTA columns were from GE Healthcare (Buckinghamshire, UK). All AKTA buffers were passed through a 0.22 μM filter and de-gassed prior to use. SFs were cultured from synovial tissue isolated from Rheumatoid Arthritis (RA) patients at the Karolinska Institute, Stockholm, Sweden. Unless otherwise stated, all other reagents were purchased from Sigma Aldrich (UK).

2.2. GENERAL MOLECULAR BIOLOGY METHODS

2.2.1. Amplification of full length human HMGB1 DNA by Polymerase Chain Reaction (PCR)

The DNA sequence for the human HMGB1 protein (648 bp) was obtained from the NCBI website (BC008492.1). Forward and reverse primers were designed to clone the DNA encoding the full length protein from the I.M.A.G.E cDNA clone. Primer sequences are detailed in Table 2.1; Nco1 and EcoR1 restriction sites were incorporated into the forward and reverse primers respectively, as underlined. PCR reactions were set up in a final volume of 50 μL and contained 750 ng cDNA template, 1x polymerase buffer, 0.5 μM forward and reverse primers, 0.2 mM

Table 2.1 Sequences and technical information of the PCR primers used for the cloning of the HMGB1, Δ30, A box and IL-1β DNA from the respective cDNA clones Important features are underlined and include the Nco1 and EcoR1 restriction sites, added to the HMGB1 forward and reverse primers respectively, and the primer extension regions added to the IL-1β primers to aid the In-fusion cloning reaction.

Protein	Primer	Sequence (5' to 3')	Melting temperature (^{o}C)	GC content
HMGB1	Forward	ATATCCATGGGCAAAGGAGATCCTAAGAAGCCGAGAG	78.8	48.7
	Reverse	TATAGAATTCTTATTCATCATCATCATCTTCTTCTTCATC	69.4	27.5
A box	FL	GGAGACATGAAAGAAGTTCAAGGATCCCAATGCACCCAAGAG	82.7	47.7
	FS	CAAGGATCCCAATGCACCCAAGAG	73.1	54.2
	RL	AACTTCTTTCATGTCTCCCCTTTGGGAGGGATATAGGTTTTC	78.2	42.9
	RS	CCTTTGGGAGGGATATAGGTTTTC	65.3	45.9
Δ30	FL	AAAAAGAAGTGAGAAGAGGAGGAAGATGAGGAAGATGAAGAG	76.3	40.5
	FS	GAGGAAGATGAGGAAGATGAAGAG	63.3	45.9
	RL	GTCAAGGCTGAAAAAAGCAAGAAAAAGAAGTGAGAAGAGGAG	77.8	40.5
	RS	GTCAAGGCTGAAAAAAGCAAGAAA	66.2	37.5
IL-1β	Forward	AAGTTCTGTTTCAGGGCCCGGCACCTGTACGATCACTGAAC	84.7	53.7
	Reverse	ATGGTCTAGAAAGCTTTATTAGGAAGACACAAATTGCAT	72.6	33.4

dNTPs, 0.1 mM betaine and 0.5 units Phusion Hot Start polymerase. PCR reactions were carried out in an Eppendorf Mastercycler® as described in Table 2.2.

Table 2.2 PCR cycling conditions used to amplify HMGB1 DNA for the I.M.A.G.E cDNA clone

	Step	Temperature	Time
1	**Polymerase activation**	98°C	2 min
2	**Denaturation**	98°C	20 sec
3	**Annealing**	55°C	30 sec
4	**Extension**	72°C	30 sec
	Steps 2-4 were repeated for 24 cycles		

2.2.2. Analysis of DNA products using agarose gel electrophoresis

PCR products were analysed using agarose gel electrophoresis. 0.6% or 1% (w/v) agarose gels were prepared by dissolving 300 mg or 500 mg agarose respectively in 50 mL 1xTris-Acetic acid-EDTA (TAE) buffer (40mM Tris acetate, 20 mM Acetic acid, 1 mM EDTA). The mixture was heated until the agarose had fully dissolved and then allowed to cool to 40-50°C. Ethidium bromide to a final concentration of 1 µM was added; the gel was poured and left to set at room temperature. Agarose gels were run in 1 x TAE buffer. For each sample, 5 µL of the PCR products were mixed with 5 µL of loading buffer (30% glycerol, 0.25% bromophenol blue in dH_2O). 5 µL of the DNA ladder (1Kb ladder, NEB; N3232) and 10 µL of each sample was loaded to the wells and the gel was run at 80V for approximately 40 min. DNA bands were visualised under UV light.

2.2.3. Construction of the pETM-11-HMGB1 plasmid

PCR products were purified using the GenElute PCR Clean-Up Kit (Sigma Aldrich) according to the manufacturer's instructions. To obtain cut linear DNA the reaction products were digested using 10 U NcoI and 10 U EcoRI in a total volume of 60 µL dH_2O supplemented with 1 x NEBuffer EcoRI (NEB, Hertfordshire, UK). Reactions were allowed to proceed at 37°C for 1 h. Cut DNA was purified using the GenElute PCR Clean-Up Kit. A purified and pre-cut pETM-11 expression vector was supplied by Dr Robert Gibson, Institute of Integrative Biology, University of Liverpool.

Ligation of HMGB1 DNA into the pETM-11 vector was carried out at an insert: vector molar ratio of 5:1 at 20^{o}C for 25 min using the T4 DNA ligase (Invitrogen, UK) (Figure 2.1). Plasmid concentration was quantified using a ND-100 Spectrophotometer (NanoDrop®).

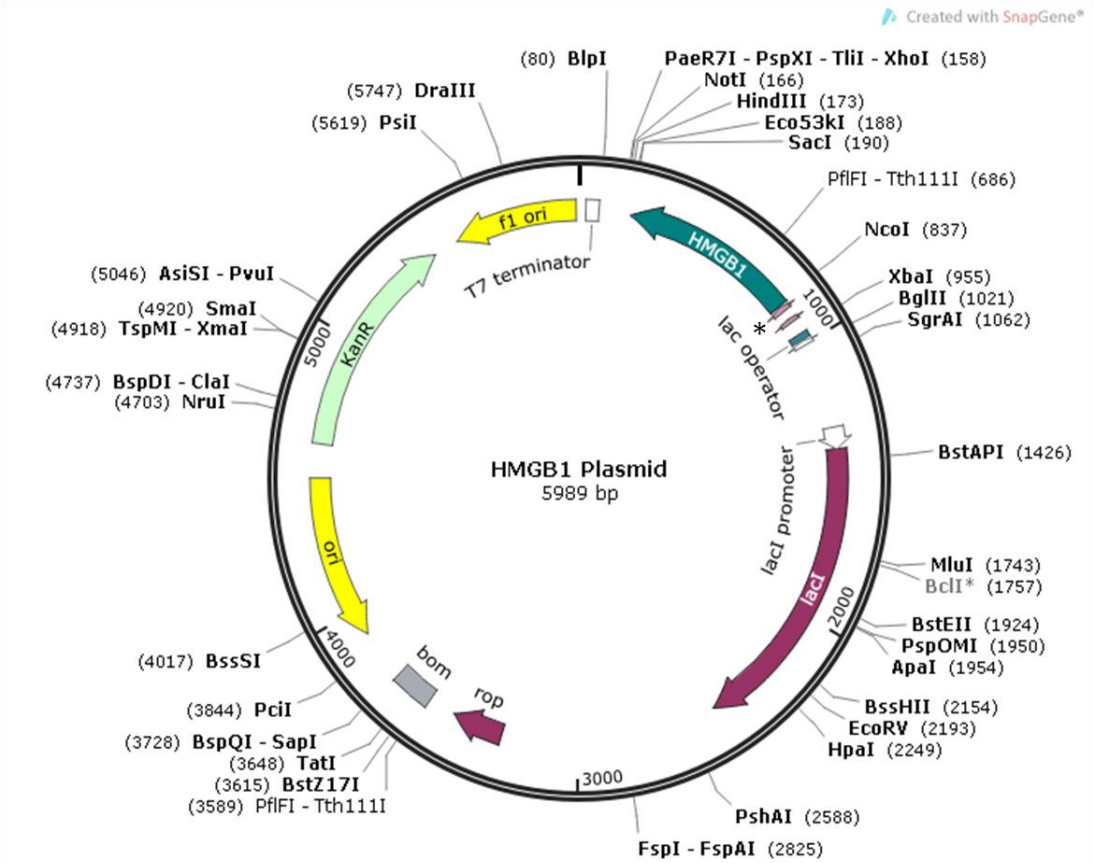

Figure 2.1 Schematic representation of the pETM-11-HMGB1 vector map HMGB1 was cloned into the pETM-11 plasmid at the NcoI and EcoRI restriction enzyme sites, as indicated, generating a recombinant vector with 5989 bp. The DNA for the Δ30, A box and B box mutants was cloned into the vector at the same sites generating plasmids of 5902 bp, 5602 bp and 5575 bp respectively. The key features of the plasmid are indicated and include the kanamycin resistance gene (KanR) and the T7 promoter region. * indicates the position of the 6-residue his tag incorporated into the N-terminus of all constructs for purification purposes. The vector map was created using SnapGene®.

2.2.4. Cloning of HMGB1 mutants using Site-Directed Ligase Independent Mutagenesis (SLIM)

The A box (residues 1-85) and Δ30 (residues 1-185) HMGB1 mutants were sub-cloned using the Site-directed Ligase Independent Mutagenesis (SLIM) method described by Chiu and colleagues (Chiu et al., 2004). An overview of the technique is shown in Figure 2.2. Briefly, SLIM comprises of a single inverse PCR reaction that uses four primers (Forward Long [FL], Forward Short [FS], Reverse Long [RL] and Reverse Short [RS]) to incorporate the desired substitution, insertion or deletion into the target DNA and produce complementary overhangs. This results in the generation of four PCR products and following subsequent denaturation and re-annealing 16 different hybrids are formed; two of these hybrids contain the correct complementary overhangs and can form stable, non-covalently joined DNA circles. When transformed into *Escherichia coli* (*E.coli*), in this case XL1-blue cells, only the circular DNA can produce colonies on the appropriate antibiotic selective agar plate.

To generate the A box and Δ30 mutants a stop codon (TGA) was inserted into the target DNA at positions 86 and 186 respectively. Sequences for the PCR primers used to incorporate this mutation are given in Table 2.1. pETM-11-HMGB1 plasmid DNA (prepared as previously described in Section 2.2.3) was used as the template DNA for the PCR reactions. Reactions contained 5 ng DNA template, 0.2 mM dNTPs, 100 mM betaine, 10 pmol of each primer, 1 x polymerase buffer and 0.5 U Phusion Hot start Fidelity DNA polymerase (NEB, UK) in a total volume of 25 µL dH_2O. PCR reactions were carried out in an Eppendorf Mastercycler® as detailed in Table 2.3.

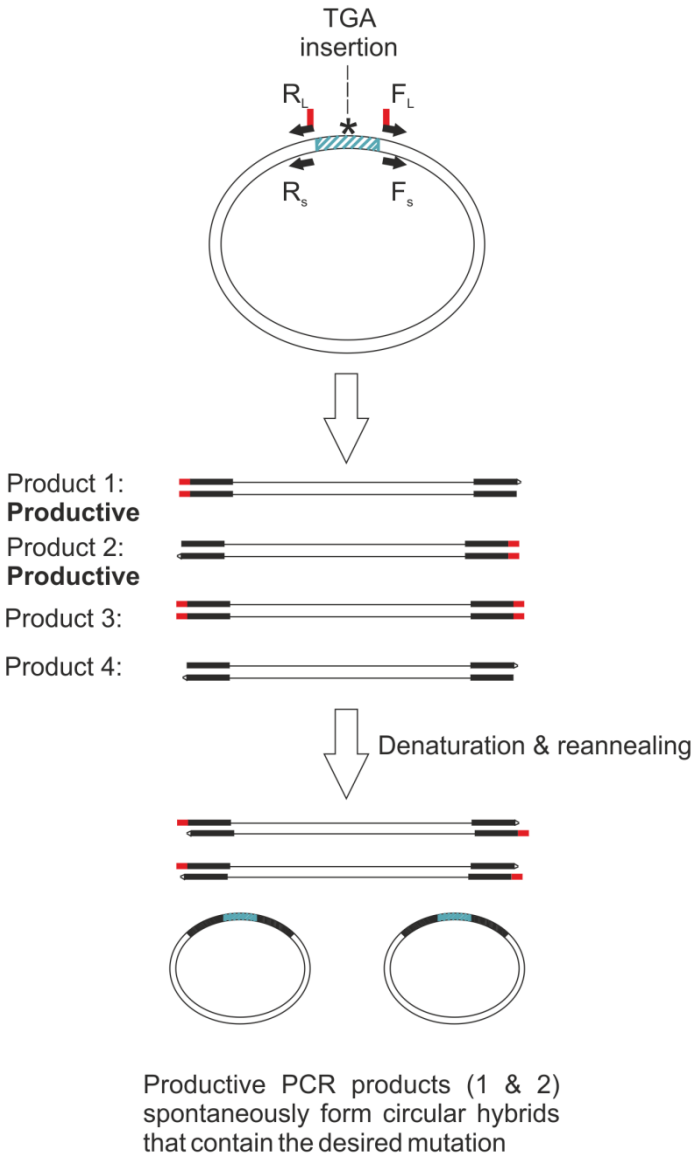

Figure 2.2 An overview of the Site-directed Ligase Independent Mutagenesis (SLIM) method used to clone the Δ30 and A box mutants SLIM is a novel PCR-based mutagenesis technique used for the insertion, substitution or deletion of nucleotides in plasmid DNA. SLIM comprises of an inverse PCR reaction that utilises four primers (Forward Long [FL], Forward Short [FS], Reverse Long [RL] and Reverse Short [RS]) to incorporate the desired modification into the target DNA and produce complementary overhangs. The FL and RL primers incorporate the described modification and the FS and RS primers amplify the region immediately prior to the mutation point. 4 PCR products are generated; products 1 and 2 are considered to be productive as they contain complementary overhangs. Subsequent denaturation and re-annealing of the PCR products results in the formation of 16 hybrids; 2 of these hybrids can form stable, non-covalently joined DNA circles. When transformed into *E.coli* only the circular DNA can produce colonies on the appropriate antibiotic selective agar plate. Figure was adapted from Chui et al, 2004 (Chiu et al., 2004).

Table 2.3 PCR conditions used to sub-clone the Δ30 and A box mutants from the petM-11 plasmid DNA using Site-directed Ligase Independent Mutagenesis (SLIM)

	Step	Temperature	Time
1	**Polymerase activation**	98°C	2 min
2	**Denaturation**	95°C	25 sec
3	**Annealing**	50°C	30 sec
4	**Extension**	68°C	7 min
	Steps 2-4 were repeated for 29 cycles		

To remove the template DNA, PCR products were digested using Dpn1. 20 µl of the PCR products were incubated with 10 U Dpn1 in 1 x NEB buffer 4 (B7004S, NEB, Hertfordshire, UK) at 37°C for 1 h. The reaction was terminated using 30 µl of a solution of 50 mM Tris HCl (pH 8), 300 mM NaCl and 20 mM EDTA. The products were denatured at 99°C for 3 min. To anneal the complementary overhangs of the DNA strands, thermo hybridisation was performed as described in Table 2.4. This resulted in the formation of circular hybrids that contained the desired mutation.

Table 2.4 Thermocycler conditions used for the thermo hybridisation of the linear Dpn1 digested pETM-11-Δ30 and pETM-11-A box PCR products

Step	Temperature	Time
1	99°C	3 min
2	65°C	5 min
3	30°C	15 min
Steps 2-3 were repeated for 3 cycles		

2.2.5. Construction of the pETM-11-B box plasmid

The B box domain was synthesised and sub-cloned into the pETM-11 vector (at the Nco1 and EcoR1 restriction sites) by GeneArt, Regensburg, Germany.

2.2.6. Amplification of the DNA encoding human IL-1β protein by PCR

The DNA sequence for the human IL-1β protein (459 bp) was obtained from the NCBI website (BC008678.1). Forward and reverse primers were designed to amplify the DNA from the I.M.A.G.E full length cDNA clone (Table 2.1). PCR reactions

contained 100 ng of the template DNA, 1x polymerase buffer, 0.6 µM forward and reverse primers, 0.2 mM dNTPs, 1 mM $MgCl_2$ and 1 U of KOD polymerase in a final volume of 50 µl. Reactions were carried out in an Eppendorf Mastercycler® as outlined in Table 2.5.

Table 2.5 An overview of the PCR cycling conditions used to amplify IL-1β DNA

	Step	Temperature	Time
1	**Polymerase activation**	94°C	2 min
2	**Denaturation**	94°C	30 sec
3	**Annealing**	60°C	30 sec
4	**Extension**	68°C	2 min
	Steps 2-4 were repeated for 29 cycles		
5	**Final elongation**	72°C	2 min

PCR products were analysed using agarose gel electrophoresis as previously described (Section 2.2.2).

2.2.7. Construction of the pOPINf-IL-1β recombinant plasmid

IL-1β DNA was expressed using the pOPINf vector system (Figure 2.3). The pOPINf plasmid was prepared as follows: a commercial glycerol stock of the plasmid was used to inoculate 5 mL of LB supplemented with 100 µg/mL ampicillin and incubated overnight at 37°C in a shaking incubator at 200 rpm. The following day the overnight culture was transferred to 100 mL ampicillin selective Lysogeny Broth (LB) medium and returned to the incubator for a further 24 h. The plasmid was purified using the GenElute™ HP Plasmid Midiprep kit (Sigma Aldrich) according to the manufacturer's instructions. Plasmid concentration was quantified using a ND-1000 Spectrophotometer (NanoDrop®) and was only used when the A_{260}:A_{280} ratio was between 1.8-2.1.

To obtain cut linear plasmid DNA, 5 µg of DNA was incubated with 1 x BSA, 50 U KpnI, 50 U HindIII and 1 x NEbuffer 2 (NEB, UK) in a total volume of 190 µL of dH_2O at 37°C for 2 h. The digested plasmid was purified using the GenElute PCR Clean-Up Kit (Sigma Aldrich) according to the manufacturer's instructions. The

purity of the plasmid DNA was analysed using agarose gel electrophoresis as described in Section 2.2.2.

Ligation of IL-1β DNA into the cut pOPINF vector was carried out using the In-Fusion® HD Cloning Kit (Clontech, Saint Germain-en-Lave, France) according to the manufacturer's instructions at an insert: vector molar ratio of 7:1.

2.2.8. Confirmation of gene insertion by DNA sequencing

To confirm that the recombinant plasmids contained the correct gene of interest, 1 mL bacterial cell cultures were sent to Source Bioscience, UK, for forward and reverse DNA strand sequencing using the T7 primer.

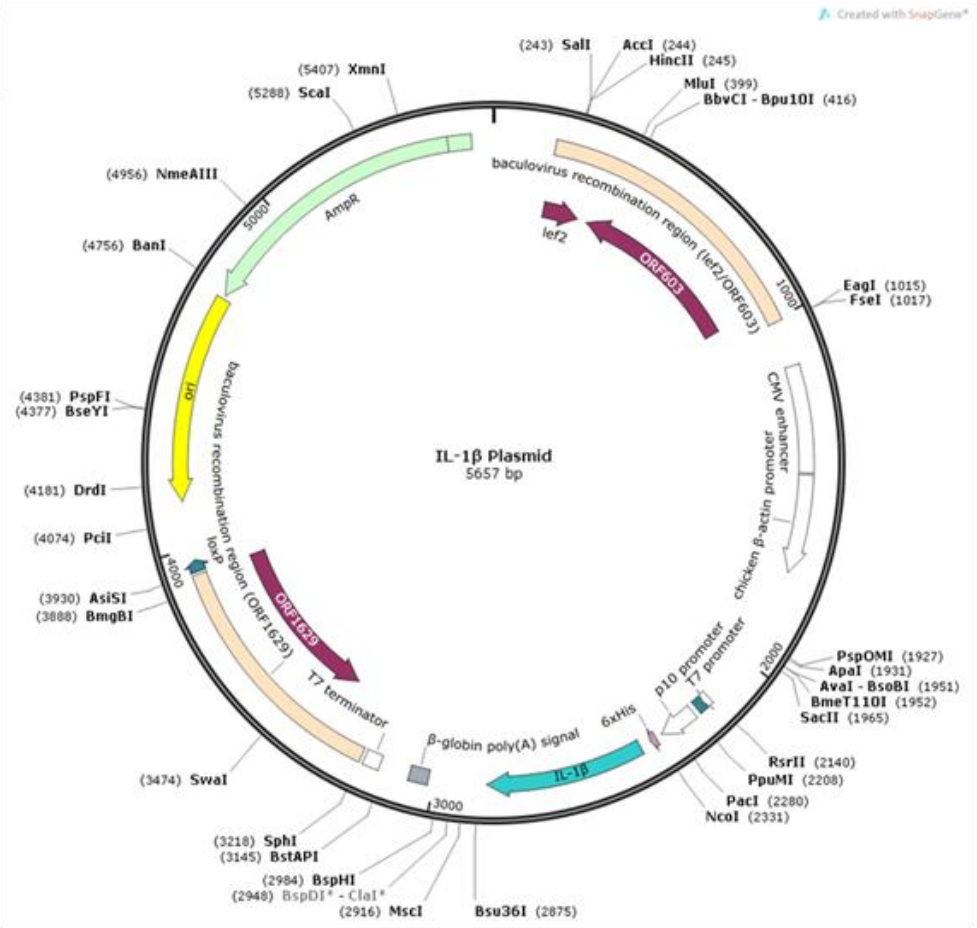

Figure 2.3 Schematic representation of the pOPINf-IL-1β vector map IL-1β DNA was cloned into the pOPINf plasmid using an In-Fusion® HD cloning Kit at the KpnI and HindIII restriction sites, as indicated, resulting in the formation of a recombinant plasmid of 5657 bp. Key features of the plasmid are indicated and include the ampicillin resistance gene (AmpR) and the T7 promoter region. The vector map was created using SnapGene®.

2.3. PREPARATION OF RECOMBINANT PROTEINS FROM ESCHERICHIA COLI (*E.COLI*): PROTEIN EXPRESSION AND PURFICATION METHODS

2.3.1. Preparation of chemically competent *E.coli* cells for the cloning and expression of recombinant plasmids

Two types of chemically competent *E.coli* cells were used: XL1-blue cells for cloning and BL21 (DE3) cells for expression purposes. Chemically competent cells were prepared using a variant of the Hanahan method (Hanahan 1983). The procedure was conducted in a sterile environment and all glass and plasticware used throughout was pre-chilled. Briefly, the commercial glycerol cell stock was streaked onto a LB-agar plate with the appropriate antibiotic resistance (XLI-blue = 20 µg/mL tetracycline & BL21 (DE3) = antibiotic free) and the plate was incubated overnight at 37^{o}C. A single colony from the plate was used to inoculate 5 mL LB and the medium was incubated overnight at 37^{o}C in a shaking incubator at 200 rpm. The following day, the 5 mL cell culture was added to 250 mL of Super Optimal Broth (SOB) medium and the cells were returned to the incubator until an OD_{600} of 0.3 was achieved. The cell culture was centrifuged at 3000g for 10 min at 4^{o}C; the supernatant was decanted and the cell pellet was gently resuspended in 80 mL ice cold CCMB80 buffer (10 mM KOAc pH7.0, 80 mM $CaCl_2.2H_2O$, 20 mM $MnCl_2.4H_2O$, 10 mM $MgCl_2$, 10% glycerol). The cells were incubated on ice for 20 min and centrifuged for a further 10 min. The cell pellet was resuspended in CCMB80 buffer to yield a final OD_{600} of 1.0-1.5 and cells were stored in 50 µl aliquots at -80^{o}C until required.

2.3.2. Transformation of recombinant plasmids into competent *E.coli* cells

Transformation of all recombinant plasmids (pETM-11-HMGB1, pETM-11 Δ30, pETM-11-A box, pETM-11-B box and pOPINF-IL-1β) into competent E.*coli* cells followed the same standard protocol. Briefly, 50 µL aliquots of competent cells were thawed on ice prior to the addition of 50 ng of plasmid DNA. The cells were incubated on ice for a further 30 min, heat shocked at 42^{o}C for precisely 1 min and returned to ice for a further 2 min. 300 µL of Super Optimal broth with Catabolite repression (SOC) medium was added and the cells were incubated at 37^{o}C for 1 h in a shaking incubator. Following this 100 µL of the cells were plated out onto

kanamycin or ampicillin selective agar plates and were incubated overnight at 37^{o}C in a non-shaking incubator. Colonies on the plate represented bacteria with antibiotic resistant that were successfully transformed with the desired plasmid.

2.3.3. Expression of recombinant HMGB1, HMGB1 mutants and IL-1β in LB media

Single discrete colonies were cultured overnight in 50 mL LB, supplemented with the appropriate antibiotic, at 37^{o}C in a shaking incubator at 200 rpm. The overnight culture was used to inoculate 500 mL LB to give a starting OD_{600} between 0.07-0.1. The cells were incubated at 37^{o}C at 200 rpm until an OD_{600} between 0.8-1.0 was achieved. Protein expression was induced with the addition of Isopropyl β-D-1-thiogalactopyranoside (IPTG) and cells were incubated at 200 rpm, as outlined in Table 2.6. Induced cells were harvested by centrifugation at 3000g for 15 min at 4^{o}C; the cell pellet was retained and stored at -80^{o}C prior to protein purification.

Table 2.6: An overview of the expression conditions used for the production of recombinant proteins in *E.coli* Recombinant plasmids were transformed into BL21 (DE3) cells and cultured in antibiotic selective LB or M9 media. Protein expression was induced using Isopropyl β-D-1-thiogalactopyranoside (IPTG) as indicated.

Construct	Antibiotic resistance	IPTG final concentration (mM)	Incubation conditions
HMGB1	Kanamycin	0.5	37^{o}C, 4 h
Δ30 HMGB1	Kanamycin	1	18^{o}C, overnight
A box	Kanamycin	1	24^{o}C, overnight
B box	Kanamycin	1	24^{o}C, overnight
IL-1β	Ampicillin	1	37^{o}C, 4 h

2.3.4. Expression of ^{15}N and/or ^{13}C-labelled recombinant proteins in minimal (M9) Medium

^{15}N and/or ^{13}C enriched proteins were prepared in minimal medium (also referred to as M9 media) using ^{15}N ammonium chloride and/or ^{13}C glucose as the sole sources of nitrogen and carbon respectively. Proteins were expressed as described in Section 2.3.3 with the following modifications: the M9 medium consisted of 88 mM Na_2HPO_4 and 55 mM KH_2PO_4 adjusted to pH7.2 and supplemented with 22 mM

^{13}C-labelled glucose, 18 mM $^{15}NH_4Cl$, 1 mM $MgSO_2.7H_2O$, 140 µM $CaCl_2.2H_20$ and 30 µM thiamine HCl. Discrete colonies were incubated in 2 mL LB, with the appropriate antibiotic, for 5 h at 37^{o}C in a shaking incubator set at 200 rpm. Cells were centrifuged at 3000g for 10 min and the cell pellet was re-suspended in 500 µL M9 media. 50 mL of M9 media, supplemented with the appropriate antibiotic, was inoculated with 250 µL of the resuspended cells and incubated overnight at 37^{o}C at 200 rpm. The following day, cells were centrifuged at 3000g for 10 min; the cell pellet was retained and re-suspended in 3-5 mL M9 media and used to inoculate 500 mL M9 media to give a starting OD_{600} between 0.07-0.1. Protein expression was induced as previously described (Table 2.6) with the following exemption; IL-1β was induced overnight at 18^{o}C.

2.3.5. Lysis of bacterial cell pellets

The bacterial cell pellets were allowed to gently thaw on ice and re-suspended in 10 mL of lysis buffer per 1 g of cell pellet. The lysis buffer consisted of 25 mM Tris HCl pH7.8, 350 mM NaCl, 250 mM sucrose, 0.5 mg/mL lysosyme and 0.1% (v/v) Triton X100. 12.5 µg/mL DNase 1 from bovine pancreas was added to the resuspended cells. The pellets were incubated on ice for 15-30 min prior to the addition an equal volume of 25 mM Tris HCl (pH7.8) supplemented with 350 mM NaCl. The cells were returned to the ice for a further 5 min. Cells were lysed using a Pressure Cell Homogeniser (Stansted Fluid Power Ltd, UK) at 1 bar. Lysed cells were centrifuged at 23-24,000g for 30 min at 4^{o}C to remove the bacterial debris and the lysate was retained and passed through a 0.22 µM syringe filter.

2.3.6. Purification of recombinant proteins by Ni^{2+} affinity chromatography

A cleavable 6 residue histidine (His) tag was incorporated into the N-terminus of all protein constructs for purifications purposes. His-tagged proteins were purified using a variation of the method originally described by Hochuli and colleagues (Hochuli et al., 1988) on a ÄKTApurifier system equipped with a P-960 sample pump and a frac-920 fraction collector. A 5 mL HisTrap HP column pre-charged with Ni^{2+} Sepharose beads was equilibrated with 15 mL buffer A (25 mM Tris HCl, 350 mM NaCl and 20 mM imidazole, pH7.8) at a constant flow rate of 3.5 mL/min. The lysate was loaded onto the column and the column was washed with a further 25 mL

of buffer A to remove any proteins that had formed non-specific interactions with the Ni^{2+} resin. Proteins of interest, interacted specifically with the Ni^{2+} mediumand were eluted using an increasing concentration of buffer B (25 mM Tris HCl, 250 mM NaCl and 0.5 M imidazole, pH7.8) delivered by a linear gradient over 90 mL (or 18 column volumes). Proteins were collected in 5 mL fractions and analysed using SDS gel electrophoresis as described in 2.3.7. Fractions containing the protein of interest were pooled and subjected to further purification.

All recombinant proteins were purified using Ni^{2+} affinity chromatography as described above with the following exception: for the IL-1β purification, buffers A and B consisted of 50 mM Tris HCl, 350 mM NaCl, 20 mM imidazole, pH 8.0 and 50 mM Tris HCl, 350 mM NaCl, 0.5 M imidazole pH 8.0 respectively.

2.3.7. SDS-PAGE gel electrophoresis analysis of protein samples

SDS-PAGE gel electrophoresis was used to analyse the purity of bacterially expressed recombinant proteins. Proteins were resolved on 12.5% (HMGB1 and Δ30) and 15% (A box, B box and IL-β) bis-acrylamide SDS-PAGE gels using the standard method described by Laemmli (Laemmli 1970) in a Bio-Rad gel electrophoresis system. Gel samples were prepared as indicated using a 4x SDS-PAGE loading buffer (200 mM Tris-HCl, pH6.8 supplemented with 400 mM DTT, 8% SDS, 0.4% bromophenol blue and 40% glycerol). Gels were run at 100 V for 10 min to allow the samples to stack evenly and then at 180 V for 45-60 min or until the loading dye had reached the bottom of the gel plate.

SDS-PAGE gels were stained using Coomassie R250 stain (0.25% [w/v] Coomassie R250 stain, 45% methanol and 10% acetic acid in dH_2O) at room temperature for 30 min. Stained gels were placed in a solution of 40% methanol, 10% acetic acid until the background was completely de-stained.

2.3.8. Cleavage of the 6-his tag from HMGB1 and HMGB1 mutants using TEV protease

The 6 residue poly-histidine tag, which was incorporated into the N-terminus of all HMGB1 constructs for purification purposes, was cleaved following the Ni^{2+} affinity chromatography using the Tobacco Etch Virus (TEV) protease. For optimal TEV cleavage, the protein was desalted into 25 mM Tris HCl, 50 mM NaCl, pH 7.8 using

a HiPrep 26 10 desalting column (GE Healthcare, Buckinghamshire, UK) according to the manufacturer's instructions. Incubations were conducted overnight at 4^{o}C at a TEV: protein ratio of 1:20 (w/w).

The cleaved protein was isolated by "reverse" Ni^{2+} affinity chromatography. Protein samples were adjusted to 300 mM NaCl and loaded onto a pre-equilibrated 5 mL HisTrap HP column at 3.5 mL/min. The flow through, containing the cleaved protein was retained. The cleaved his-tag and his-tagged TEV protease, which interacted specifically with the Ni^{2+} beads were eluted using 25 mM Tris HCl, 250 mM NaCl and 0.5 M imidazole, pH 7.8.

2.3.9. Cleavage of the 6-his tag from IL-1β using 3C protease

The 6 residue poly-histidine tag, incorporated into the N-terminus of the IL-1β protein, was cleaved after the Ni^{2+} affinity chromatography, using the 3C protease. The protease, produced in-house and kindly provided by Dr Thomas Zacharchenko, recognised the LEVLFQ-GP sequence and specifically cleaved between the glutamine (Q) and glycine (G) residues. For optimal cleavage, the protein was desalted into 50 mM TrisHCl, 50 mM NaCl, pH 8 using a HiPrep 26 10 desalting column (GE Healthcare, Buckinghamshire, UK) according to the manufacturer's instructions. Incubations were conducted overnight at 4^{o}C at a 3C: protein ratio of 1:25 (w/w).

The cleaved protein was isolated by "reverse" Ni^{2+} affinity chromatography. Protein samples were adjusted to 300 mM NaCl and loaded onto a pre-equilibrated 5 mL HisTrap HP column at a flow rate of 3.5 mL/min. The flow through, containing the cleaved protein was retained. The cleaved his-tag and his-tagged 3C protease bound specifically to the Ni^{2+} beads and were eluted using 50 mM Tris HCl, 350 mM NaCl and 0.5 M imidazole, pH 7.8.

2.3.10. Purification of recombinant proteins by Ion Exchange (IEX) chromatography

All recombinant proteins were subjected to Ion Exchange (IEX) chromatography following the reverse affinity purification. IEX chromatography separates molecules by exploiting the difference in their overall net surface charge. A protein has no net charge at a pH equivalent to its Isoelectric Point (pI). However, at a pH greater than

its pI a protein will have a negative net charge and will interact with positively charged medium or an anion exchanger (HiTrap Q FF column). At a pH lower than its pI a protein will have a positive net charge and interact with negatively charged medium or a cation exchanger (HiTrap S FF column).

The HMGB1 protein had a pI of 5.62 and was purified using anion exchange on a 5 mL HiTrap Q FF column (GE Healthcare, Buckinghamshire, UK). To allow optimal binding, the protein was desalted into buffer A (25 mM Tris HCl, 50 mM NaCl, pH 7.8) prior to IEX purification, using a HiPrep 26 10 desalting column (GE Healthcare, Buckinghamshire, UK) according to the manufacturer's instructions. The HiTrap Q FF column was pre-equilibrated with buffer A and the sample was loaded at constant flow rate of 3.5 mL/min. The protein was eluted using an increasing concentration of buffer B (25 mM Tris HCl, 1 M NaCl, pH 7.8) delivered over 90 mL (or 18 column volumes) and collected in 5 mL fraction. Fractions were analysed using SDS gel electrophoresis as described previously (Section 2.3.7). Fractions containing the protein of interest were pooled and purified further using size exclusion chromatography.

The cleaved IL-1β protein had a pI of 5.91 and was purified using anion exchange as described above but using the following buffers; Buffer A: 50 mM Tris HCl, 50 mM NaCl, pH 8.5 and buffer B contained 50 mM Tris HCl, 0.5 M NaCl, pH 8.5.

The cleaved Δ30, A box and B box had pI values of 9.87, 9.67 and 9.38 respectively and were purified by cation exchange using a 5 mL HiTrap S FF column, as described above but with the following modifications; Buffer A consisted of 50 mM potassium phosphate, 50 mM NaCl, pH 6.5 and buffer B contained 50 mM potassium phosphate, 1 M NaCl, pH 6.5.

2.3.11. Purification of recombinant proteins using size exclusion chromatography

The fractions retained from the IEX chromatography were subjected to size exclusion purification. Proteins were concentrated to approximately 5-8 mL using 6 or 20 mL Vivaspin centrifugal concentrators with a 5 kDa Molecular Weight Cut Off (MWCO) according to the manufacturer's instructions (Sigma Aldrich, UK).

The sample was loaded onto a Superdex 75 26 10 column (GE Healthcare, Buckinghamshire, UK), which was pre-equilibrated with PBS pH 7.2.

The column was washed with 320 mL (or 1 column volume) of PBS, delivered at constant flow rate of 1 mL/min and the protein was collected in 5 mL fractions. The retention time was determined by the size of the molecule. Proteins were analysed using SDS gel electrophoresis as described in Section 2.3.7.

Purified proteins were concentrated to an appropriate working concentration using the Vivaspin centrifugal concentrators according to the manufacturer's instructions.

2.3.12. Removal of contaminating endotoxin from recombinant protein preparations using the Triton-X114 protocol

Contaminating LPS was removed from bacterially expressed recombinant protein preparations using the Triton-X114 two phase extraction protocol originally described by Aida and Pabst (Aida and Pabst 1990). Briefly, Triton-X114 was added to the proteins at a final concentration of 1% (v/v) and the solution was gently inverted to ensure thorough mixing. Tubes were rotated at 4^{o}C for 30 min, heated to 37^{o}C for 10 min and centrifuged at 18,000g at 25^{o}C for 10 min. This resulted in the formation of a bi-layer and the top layer, containing the protein, was carefully aspirated into a sterile tube. The entire process was repeated 3 times. After the final spin, the samples were passed through a 0.22 µM syringe filter.

Protein aliquots (10 µg/mL) were sent to the Karolinska Institute in Stockholm, Sweden for endotoxin level quantification using the chromogenic LAL endotoxin assay. Proteins used for experiments had LPS levels of less than 5 Endotoxin Unit (EU)/mL.

2.3.13. Determining the total molecular mass of recombinant HMGB1 and IL-1β proteins using Electrospray Ionization Mass Spectrometry (ESI-MS) analysis

Recombinant proteins were prepared at 1 pg/µL in dH_2O for Electrospray Ionization Mass Spectrometry (ESI-MS) analysis. Samples were kindly analysed by Dr Mark Prescott at the Institute of Integrative Biology, University of Liverpool. Samples were analysed using a Waters Micromass Quadrupole Time of Flight (QToF) mass

spectrometer operated in the positive ion electrospray mode. The samples were dissolved in 50% aqueous acetonitrile (ACN), and infused into the mass spectrometer via a syringe pump. The mass range scanned was: m/z 2-80 kDa. Data were analysed using Waters MassLynx MS software.

2.3.14. Western blot analysis of the recombinant HMGB1 protein

5 µl of 4 x SDS-PAGE loading buffer was added to 1 µg of the recombinant HMGB1 protein in a final volume of 20 µl dH_2O. Proteins were resolved on a 10% bis-acrylamide SDS-PAGE gel using the standard method described by Laemmli (Laemmli 1970) in a Bio-Rad gel electrophoresis system. Gels were run at 100 V for 10 min to allow the samples to stack evenly and then at 180 V for 45-60 min or until the loading dye had reached the bottom of the gel plate. The proteins were transferred onto nitrocellulose membrane (Hybond ECL, GE Healthcare) in ice-cold transfer buffer (25 mM Tris base, 200 mM Glycine and 20% methanol in dH_2O) at 100 V for 1 h. The membrane was blocked in 10% milk (Bio-Rad, Hertfordshire, UK) for 30 min at room temperature. The membrane was washed four times using Tween-TBS buffer (0.1% Tween in 1 x TBS buffer. 1 x TBS buffer contained 20 mM Tris base and 137 mM NaCl). The membrane was incubated with a polyclonal rabbit anti-HMGB1 antibody (Abcam, UK) for 1 h at room temperature. The anti-HMGB1 antibody was diluted 1/5000 in 2% milk. The membrane was washed four times using Tween-TBS buffer. The membrane was incubated with an anti-rabbit IgG antibody (Sigma, A0545) for 1 h at room temperature. The anti-rabbit antibody was diluted 1/1000 in 2% milk. Protein bands were visualised using the Western Lightning™ Chemiluminescence Plus-ECL reagent (Perkin Elmer, UK) according to the manufacturer's instructions.

2.3.15. Determination of the redox status of HMGB1 using LC-ESI-MS/MS

100 µg of his-tagged HMGB1 was incubated with 50 µl of Ni^{2+} affinity beads for 15 min at room temperature. The beads were centrifuged at 13,000 rpm for 1 min; the pellet was retained and washed with PBS. The beads were re-suspended in 55 mM iodoacetamide (Figure 2.4A) and incubated at room temperature for a further 15 min. The beads were centrifuged at 13,000 rpm for 1 min; the pellet was retained and washed with PBS. The beads were re-suspended in 1 mM DTT and incubated for a further 15 min. The beads were centrifuged at 13,000 rpm for 1 min; the pellet was

retained and re-suspended in 20 mM N-ethylmaleimide (NEM; Figure 2.4B). The beads were incubated for a further 15 min at room temperature. The beads were centrifuged at 13,000 rpm for 1 min; the pellet was retained and washed with PBS. The his-tagged HMGB1 protein was digested on the Ni^{2+} beads using Glu-c (NEB, Hertfordshire, UK) at a final protein: Glu-c ratio of 1:100. The mixture was incubated for 16 h at 25^{o}C in a total volume of 100 µl in PBS. The following day, the beads were centrifuged at 13,000 rpm for 1 min and the supernatant was retained. The peptides were dried down using a speed vac and re-suspended in 20 µl 0.1% TFA. The peptides were purified using ZipTip C18 pipette tips (Millipore, UK) according to the manufacturer's instructions. Briefly, 1 µl 1% TFA was added to 10 µl of the peptides and the sample was vortexed. The C18 ZipTip was washed twice with 100% ACN and three times with 0.1% TFA. The sample was loaded onto the column and the tip was washed five times with 0.1% TFA. Peptides were eluted in 10 µl 0.1% TFA/60% ACN.

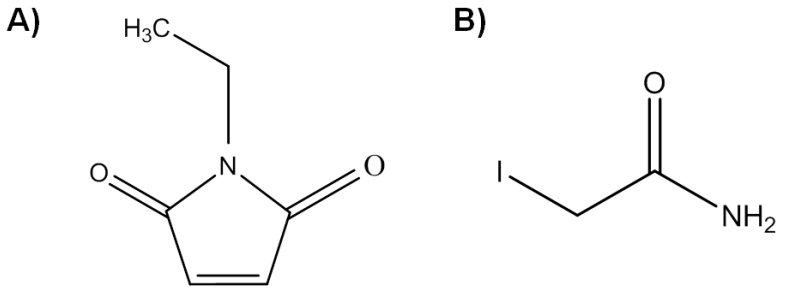

Figure 2.4 Chemical structures of (A) NEM and (B) iodoacetamide

Samples were kindly analysed using LC-ESI-MS/MS by Dr Rosalind Jenkins in the Centre for Drug Safety Science at the University of Liverpool. The alkylation with iodoacetamide generated a carboxyamidomethyl adduct resulting in a mass shift of 57 amu (atomic mass units). The alkylation with NEM yielded a mass shift of 125 amu.

2.3.16. Determination of the cytokine-inducing activity of rHMGB1 proteins on Peripheral Blood Mononuclear Cell (PBMC) cultures

PBMCs were purified using Ficoll centrifugation (Ficoll-Paque Plus, GE Healthcare) from the blood of a healthy volunteer drawn into sodium heparin tubes. Briefly, 18 mL of blood was collected and added to an equal volume of PBS along with 8 mL of Ficoll reagent. The mixture was immediately centrifuged at 440g for 20 min at 20^{o}C.

The PBMC layer was retained and cells were washed using 40-45 mL PBS. Cells were centrifuged at 300g for a further 7 min. The pellet was retained and the wash was repeated. Cells were counted and the viability with assessed using trypan blue; cells were only used when the viability > 95%.

Cells were plated at 100,000 cells/mL in a 96-well plate in OPTIMEM supplemented with 100 U/mL Penicillin and 100 µg/mL streptomycin and cultured at 37^{o}C with 5% CO_2. Cells cultures were stimulated with HMGB1, Δ30, A box and B box at a final concentration of 0, 0.625, 1.25, 2.5, 5 and 10 µg/mL for 16 h. Cell supernatants were collected and stored at -20^{o}C. IL-6 levels were quantified by ELISA as described in Section 2.4.8.

2.4. IN VITRO ASSAYS TO INVESTIGATE THE INTERACTIONS OF HMGB1

2.4.1. Culturing of SFs isolated from RA patients

SFs were cultured from synovial tissue isolated from arthritic patients undergoing joint replacement surgery at the Karolinska Institute, Stockholm, Sweden as previously described (Wahamaa 2011). Cells were cultured in DMEM supplemented with 10% heat-inactivated FCS (PAA Laboratories, Linz, Austria), 100U/mL penicillin, 100 µg/mL streptomycin and 1 x HEPES (Life Technologies, Paisley, Scotland, UK) at 37^{o}C with 5% CO_2.

Cells were sub-cultured when they were 80% confluent using 0.05% trypsin-EDTA (Gibco, UK). Briefly, cells were washed twice with PBS before 0.05% trypsin-EDTA was added (4 and 2 mL trypsin solution was added to T175 and T75 flasks respectively) and cells were incubated at room temperature for approximately 5 min or until all the cells had detached from the flask. The detached cells were diluted to 15 mL using DMEM medium and were centrifuged at 300g for 5 min at room temperature. The cell pellet was retained and re-suspended in DMEM. Cell viability was assessed using trypan blue (Merck, Darmstadt, Germany) and was between 95-100%. As a general rule, cells were sub-cultured at a ratio of 1:3.

2.4.2. Investigating the synergistic activity of HMGB1 and IL-1β in SFs

SFs were plated at 6,000 cells/well in a 96-well plate and allowed to rest for 15-17 h. The medium was discarded and the cells were washed with OPTIMEM (Invitrogen, UK), supplemented with 100 U/mL penicillin and 100 µg/mL streptomycin (Invitrogen, UK). Cells were treated with a final concentration of 100 ng/mL HMGB1 and 0.5 ng/mL or 0.05 ng/mL IL-1β. Proteins were pre-incubated as a 50 x stock solution in PBS (without $CaCl_2$ and $MgCl_2$, pH7.2; Invitrogen, UK) for 16 h at 4^{o}C prior to the experiment. For the simultaneous addition the diluted HMGB1 and IL-1β stocks were incubated separately overnight at 4^{o}C and were combined immediately prior to dosing. The proteins were diluted in OPTIMEM immediately prior to cell treatment to provide the final indicated concentrations. Cells were dosed for 24 h and the cell supernatants were collected and stored at -80^{o}C until analysis.

2.4.3. HMGB1 and IL-1β dose response in SFs

SFs were plated at 6,000 cells/well in a 96-well plate and allowed to rest for 15-17 h. The medium was discarded and the cells were washed with OPTIMEM (Invitrogen, UK), supplemented with 100 U/mL penicillin and 100 µg/mL streptomycin (Invitrogen, UK). HMGB1 and IL-1β were prepared as a 50 x stock solution and incubated for 16 h at 4^{o}C. Proteins were diluted in OPTIMEM immediately prior to cell dosing to provide a final concentration of 3.25-100 ng/mL HMGB1 and 0.5 ng/mL IL-1β. Cells were dosed for 34 h and the cell supernatants were collected and stored at -80^{o}C until analysis.

2.4.4. Investigating the kinetics of the synergistic interaction between HMGB1 and IL-1β in SFs

SFs were plated at 6,000 cells/well in a 96-well plate and allowed to rest for 15-17 h. The medium was discarded and the cells were washed with OPTIMEM (Invitrogen, UK), supplemented with 100 U/mL penicillin and 100 µg/mL streptomycin (Invitrogen, UK). Fibroblasts were treated with a final concentration of 100 ng/mL HMGB1 and 0.5 ng/mL IL-1β. The proteins were prepared as 50 x stock solutions using freshly made dilutions and pre-incubated at 4^{o}C, room temperature or 37^{o}C for 0-24 h. Stock solutions were diluted in OPTIMEM immediately prior to cell dosing.

Cells were dosed for 24 h and the cell supernatants were collected and stored at -80^{o}C until analysis.

2.4.5. Investigating the synergistic interaction between IL-1β and the different HMGB1 domains (Full length HMGB1, Δ30, A box or B box)

SFs were plated at 6,000 cells/well in a 96-well plate and allowed to rest for 15-17 h. The medium was discarded and the cells were washed with OPTIMEM (Invitrogen, UK), supplemented with 100 U/mL penicillin and 100 µg/mL streptomycin (Invitrogen, UK). Cells were treated with HMGB1, Δ30, A box or B box in combination with IL-1β. Proteins were prepared as a 50 x stock solution and incubated for 16 h at 4^{o}C. Stock solutions were diluted in OPTIMEM immediately prior to dosing to provide a final concentration of 100 ng/mL HMGB1, 86 ng/mL Δ30, 40 ng/mL A box or 35 ng/mL B box with 0.05 or 0.5 ng/mL IL-1β. Different concentrations of the HMGB1 constructs were used to maintain the same molar ratio (1:137 or 1:1370, IL-1β: HMGB1/Δ30/A box or B box). Cells were dosed for 24 h, the supernatants were collected and stored at -80^{o}C until analysis.

2.4.6. Determining if the synergy between HMGB1, Δ30 or B box and IL-1β is mediated via the IL-1R or TLR4 receptor

SFs were plated at 6,000 cells/well in a 96-well plate and allowed to rest for 15-17 h. The medium was discarded and the cells were washed with OPTIMEM (Invitrogen, UK), supplemented with 100 U/mL penicillin and 100 µg/mL streptomycin (Invitrogen, UK). Cells were pre-treated with 5 µg/mL anakinra (Kineret®; a synthetic IL-1R antagonist) or 10 µg/mL detoxified LPS for 1-2 h. The cells were treated with HMGB1, Δ30, A box or B box in combination with IL-1β. Proteins were prepared as described in Section 2.4.5. Cells were dosed for 24 h, the supernatants were collected and stored at -80^{o}C until analysis.

2.4.7. Investigating the effect of LPS on HMGB1 and IL-1β synergy

SFs were plated at 6,000 cells/well in a 96-well plate and allowed to rest for 15-17 h. The medium was discarded and the cells were washed with OPTIMEM (Invitrogen, UK), supplemented with 100 U/mL penicillin and 100 µg/mL streptomycin (Invitrogen, UK). The HMGB1, IL-1β and LPS used to dose the cells were prepared as 50 x stock solutions. 5 µg/mL HMGB1 was pre-incubated with 1.25 ng/mL LPS

for 1 h at 4°C. 25 ng/mL IL-1β was added to the mixture and the proteins were incubated for a further 16 h at 4°C. The proteins were diluted in OPTIMEM immediately prior to cell dosing. Additionally, 5 µg/mL HMGB1 and 25 ng/mL IL-1β were incubated for 16 h at 4°C. Following the overnight incubation, 1.25 ng/mL LPS was added to the proteins for 2, 1, 0.5 or 0 h. The stock solutions were diluted 1/50 in OPTIMEM immediately prior to cell stimulations to provide a final cellular concentration of 100 ng/mL HMGB1, 0.5 ng/mL and 25 pg/mL LPS. Cells were dosed for 24 h; supernatants were collected and stored at -80°C until analysis.

2.4.8. Quantification of IL-6 levels in synovial fibroblast cell supernatants by ELISA

IL-6 cytokine levels were quantified using the Human IL-6 DuoSet ELISA kit (R & D systems) according to the manufacturer's instructions. The limit of quantification was 9.37 pg/mL and samples below this limit were assigned a value of 0.1 for statistical analysis.

2.4.9. Statistical analysis

All data are provided as absolute IL-6 values ± SD, with the following exception: for Figure 4.2, data are expressed as mean IL-6 value ± SEM. The limit of quantification for the IL-6 ELISA was 9.37 pg/mL and samples below this limit were assigned a value of 0.10 for statistical analysis. Data were analysed for normality using a Shapiro Wilk test. For normal data statistical significance was determined using a T-test. Non-normal data were analysed using a Kruskal Wallis one-way ANOVA on ranks test.

2.5. NMR METHODS TO INVESTIGATE HMGB1 PROTEIN INTERACTIONS

2.5.1. An Introduction to NMR spectroscopy

(The following references were used throughout this section (Cavanagh et al., 2006; Muskett 2011; Takeda and Kainosho 2011)).

In 1957, Saunders *et al* recorded the first ^{1}H NMR spectrum for the pancreatic ribonuclease protein using a 40 MHz spectrometer (Saunders et al., 1957). Since then, NMR tools have developed considerably with the introduction of two-

dimensional (2D) spectroscopy in the 1970s allowing for the study of multiple nuclei within a single experiment.

All molecules are composed of atoms, which in turn consist of a nucleus that contains protons and neutrons and is surrounded by orbital negatively charged electrons. Nuclei have an intrinsic quantum mechanical property known as the nuclear spin angular momentum, which is defined by the nuclear spin quantum number (*I*). As a result, when certain atomic nuclei are exposed to a strong magnetic field they will align parallel to the applied field. It is important to note that nuclei with $I = ½$ are commonly studied by NMR spectroscopy. This includes the ^{1}H, ^{15}N and ^{13}C isotopes, which have a natural abundance of 99.99%, 0.37% and 1.11% respectively. As such, enrichment of the ^{15}N and ^{13}C isotopes is required for the production of labelled proteins for heteronuclear NMR experiments.

NMR experiments utilise a stable magnetic field and when the sample is placed into the spectrometer the nuclei align to this resting state. During the experiment, radiofrequency pulses perturb the alignment and the resulting signal is detected. The signal is measured until the nuclei have re-aligned to the magnetic field (resting state). The amplified and digitised signal is known as the Free Induction Decay (FID) signal and is a measurement of the intensity of the signal over time (intensity vs. time). The FID signal must be processed prior to data analysis and this is achieved using a mathematical process known as Fourier transformation. The FID signal is converted from a plot of the intensity vs. time to intensity vs. frequency (frequency may also be referred to as chemical shift), with the frequency measured in MHz. However, the MHz signal is dependent upon the magnetic field strength and is not a standardised measurement across different spectrometers. To compensate for this, the signal is converted to parts per million (ppm) and expressed relative to a reference peak and the final NMR spectrum is a plot of the chemical shift (ppm) vs. intensity.

2.5.2. Protein NMR spectroscopy: Types of experiments and their applications

Protein NMR spectroscopy has many practical applications; it can be employed to elucidate three dimensional (3D) protein structures and can be used to investigate and characterise macromolecular interactions. For the work described within this thesis, standard 1D, 2D and 3D experiments were employed. One dimensional (1D)

^{1}H NMR spectroscopy can provide vital information about a protein; for example it can be used to determine if the protein of interest is correctly folded and to identify any small molecule contaminants. 2D Heteronuclear Single Quantum Coherence (HSQC) experiments are used to obtain more detailed information about the protein of interest. HSQC experiments measure the chemical shift of both the proton and the heteronuclear atom (^{15}N or ^{13}C). They are used to obtain one-bond correlation spectra and each peak on a HSQC spectrum is a plot of the proton frequency (direct dimension) vs. the frequency of the corresponding heteronuclei (indirect dimension). 2D HSQC experiments are an extremely useful tool for investigating protein interactions. If two macromolecules interact to form a binary complex then the electronic environment of the atoms involved or affected by the interaction will be changed and the peaks on the HSQC spectrum will be perturbed. For the purpose of this work, protein NMR spectroscopy has been utilised to investigate HMGB1 interactions. Specifically, this work was performed to determine if a direct interaction occurs between HMGB1 and IL-1β.

A combination of 2D and 3D NMR experiments were performed for the assignment of the A box domain of HMGB1. Standard HSQC-based 3D triple resonance (^{1}H, ^{15}N and ^{13}C) experiments were used to assign the backbone residues (Clubb et al., 1992; Grzesiek and Bax 1992; Grzesiek and Bax 1992). Briefly, 3D HNCO and HNCACO experiments were used to sequentially assign the backbone NH via the carboxyl group and CBCACONH and HNCACB experiments were used to assign the backbone NH via the backbone Cα and side-chain Cβ groups (Figure 2.5).

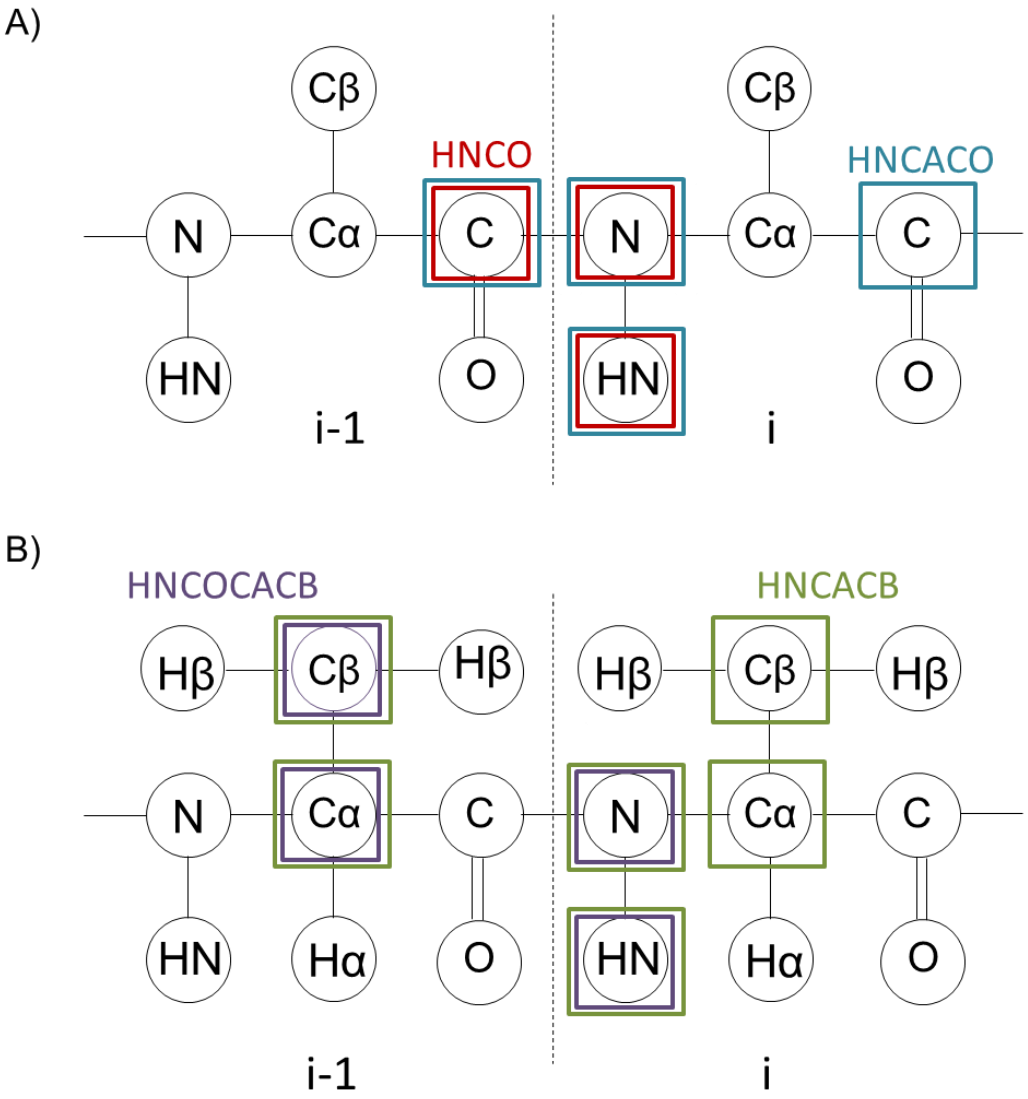

Figure 2.5 Overview of the experiments carried out for the assignment of the A box domain of HMGB1 Standard HSQC-based 3D triple resonance experiments were used to assign the backbone NH groups of the A box domain. A) HNCO and HNCACO spectra were used to sequentially assign the backbone NH via the carboxyl group. B) CBCACONH and HNCACB experiments were used to assign the backbone NH via the backbone Cα and side-chain Cβ groups. Circled nuclei represent resonances assigned using each experiment via i NH root resonances.

2.5.3. Preparation of NMR samples

For NMR analysis ^{15}N and/or ^{13}C-labelled recombinant proteins were expressed in minimal medium and purified as previously described in Section 2.3. Detailed information on the samples used for NMR experiments is provided in **Table 2.7**. As a general rule, NMR samples were prepared at 10-100 μM in PBS, pH 7.2, and contained a final concentration of 10% D_2O (Deuterium oxide, ^2H_2O). For NMR experiments, the samples were placed in either standard 5 mm NMR tubes (Sample

volumes of >500 μL; Goss Scientific, UK) or Shigemi reduced volume NMR tubes (Sample volume between 300-500 μL; Sigma Aldrich, UK). Between samples, NMR tubes were cleaned using 100% nitric acid overnight and washed thoroughly with ultrapure water prior to use.

2.5.4. NMR data collection

All NMR spectra were collected on Bruker Avance II 600 or 800 MHz spectrometers equipped with triple (TCI) resonance cryoprobes at 25^{o}C (298 K) unless otherwise stated.

2.5.5. NMR data processing and analysis

All NMR data were processed using Topspin 3.1 (Bruker) and analysed using CCPN analysis.

Table 2.7 An overview of the NMR sample preparation and experimental acquisition parameters NMR spectra were collected on 600MHz or 800MHz Bruker Advance spectrometers equipped with triple resonance cryoprobes at 25°C (298K) unless stated otherwise. All samples contained a final concentration of 10% D_20. (PBS; 8.06mM $Na_2HPO_4.7H_2O$, 1.47mM KH_2PO_4, 137.93mM NaCl and 2.67mM KCl, pH7.2)

Thesis figure(s)	Sample	LPS Free (<0.05EU/ mL)	Buffer/pH	Field strength (MHz)	Number of scans (NS)	T1 Increments	Resolution in the indirect dimension (Hz)
3.4	23 μM unlabelled HMGB1	Yes	PBS, pH 7.2	600	512	-	-
3.6	100 μM ^{15}N his-tagged Δ30	Yes	PBS, pH 7.2	600	64	160	18.24
3.7	50 μM ^{15}N A box	Yes	PBS, 10 mM DTT, pH 7.2	800	16	150	21.80
3.8	10 μM ^{15}N B box	Yes	PBS, pH 7.2	800	192	256	15.80
3.9	25 μM ^{15}N IL-1β	Yes	PBS, pH 7.2	600	32	160	21.00
3.11	100 μM ^{15}N A box pH titration from 5.5 to 7.2	No	20 mM potassium phosphate, 100 mM potassium chloride and 10 mM DTT, pH 5.5 to7.2	800	8	150	21.09
3.13	50 μM ^{15}NA box ± 10 mM DTT	Yes	PBS, pH 7.2	800	16	150	21.08

3.14	Pre-LPS removal: 40 µM ^{15}N his-tagged Δ30 Post-LPS removal 100 µM ^{15}N his-tagged Δ30	No Yes	PBS, pH 7.2	600	64	160	18.24
3.15	Pre-LPS removal: 77 µM ^{15}N A box Post-LPS removal 50 µM ^{15}N A box	No Yes	PBS, 10 mM DTT, pH 7.2	800	16	150	21.08
3.16	Pre-LPS removal: 10 µM ^{15}N B box Post-LPS removal 10 µM ^{15}N B box	No Yes	PBS, pH 7.2	800	192	256	15.80
5.1 & 5.2	25 µM IL-1β (Apo) 12.5 µM ^{15}N IL-1β ± 11.5 µM HMGB1 (IL-1β: HMGB1 1:1)	Yes	PBS, pH 7.2	600	32	160	21.00
5.3 & 5.4	100 µM ^{15}N IL-1β (Apo) 50 µM ^{15}N IL-1β ± 195 µM HMGB1 (IL-1β: HMGB1 1:4)	Yes	PBS, pH 7.2	600 10°C (283 K)	64 256	250 384	12.67 12.67
5.6	10 µM ^{15}N his-tagged Δ30 ± 90 µM IL-1β (Δ30: IL-1β ratio = 1:9)	Yes	PBS, pH 7.2	800	192	256	15.80
5.7	100 µM ^{15}N IL-1β ± 300 µM Δ30	Yes	20 mM Phosphate, 100 mM potassium chloride, 10 mM DTT, pH 6.8	800	4	210	16.99

5.8	10 µM ^{15}N B box ± 100 µM IL-1β (B Box: IL-1β ratio = 1:10)	Yes	PBS, pH 7.2	800	192	256	15.80
5.9	100 µM ^{15}N A box ± 500 µM IL-1β (A box: IL-1β ratio = 1:5)	Yes	20 mM Phosphate, 100 mM potassium chloride, 10 mM DTT, pH 6.8	800	8	150	21.09

CHAPTER THREE

EXPRESSION, PURIFICATION AND CHARACTERISATION OF RECOMBINANT HMGB1AND IL-1β PROTEINS

TABLE OF CONTENTS

3.1. INTRODUCTION

HMGB1 was first isolated from calf thymus in 1973 by Goodwin and colleagues (Goodwin et al., 1973). Originally HMGB1 was discovered as a nuclear protein that is involved in the regulation of protein transcription (Travers and Thomas 2004). However, subsequent studies have demonstrated that HMGB1 has multiple distinct functions in the nucleus and cytoplasm (Figure 1.5).

Increasingly, HMGB1 is reported to be an important cytokine mediator in both sterile and infectious inflammation. Studies have identified HMGB1 as a pathogenic mediator of sepsis, autoimmune diseases including arthritis, pancreatitis, respiratory disorders, gastrointestinal inflammation, ischemia-reperfusion injury and cancer (Andersson and Tracey 2011). Additionally, HMGB1 has been identified as an important inflammatory mediator in animal and clinical studies of DILI (Antoine et al., 2009; Antoine et al., 2010; Craig et al., 2011; Antoine et al., 2012). Recently, a study by Antoine and colleagues has identified acetylated HMGB1 as a prognostic indicator of acute liver injury during acetaminophen hepatotoxicity (Antoine et al., 2012).

To initiate and enhance inflammation, HMGB1 signals alone or via an unidentified mechanism to act in synergy with other endogenous or exogenous molecules. The overall aim of this thesis was to investigate and characterise the molecular interaction between HMGB1 and IL-1β using both cellular and NMR methodologies. To facilitate these studies, this chapter describes the development and optimisation of methods for the expression, purification and characterisation of the human HMGB1 and IL-1β proteins. This chapter also reports the successful sub-cloning of three human HMGB1 mutants (Table 3.1). The individual A and B box domains (corresponding to residues 1-85 and 89-163 respectively) and the Δ30 protein, which contains residues 1-185 and does not incorporate the 30-residue C-terminal polyacidic tail. The different HMGB1 domains will be used to further investigate the cellular and biophysical interaction between HMGB1 and IL-1β and to identify which domain(s) of HMGB1 is critical for the synergistic response.

Table 3.8 Domain structure of recombinant HMGB1, Δ30, A box and B box proteins produced in this thesis.

Construct	Domain structure
HMGB1	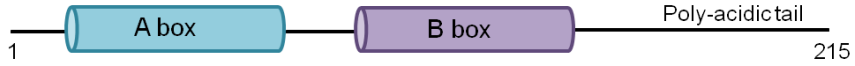
Δ30	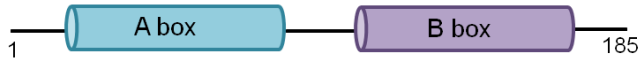
A box	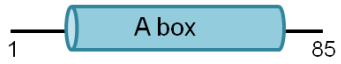
B box	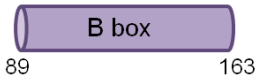

As discussed in Section 1.8.2, HMGB1 is a 25 kDa protein consisting of 215 amino acid residues organised into a tripartite domain structure (Figure 1.6 & Figure 1.7). The expression and purification of recombinant cytokine-inducing rat HMGB1 in *E.coli* has been previously reported and is associated with low protein yields (Bianchi 1991; Li et al., 2003). A further complication associated with the production of recombinant HMGB1 proteins is the presence of LPS contaminants in the purified protein sample. LPS is a major component of the outer membrane of gram negative bacteria and a potent activator of the innate immune system. LPS induces septic shock in humans and studies have demonstrated that LPS-treated macrophages release large quantities of TNF (Beutler et al., 1985). HMGB1 and LPS both signal via the TLR4 to increase nuclear translocation of NF-$_K$B (Andersson and Tracey 2011). It has been reported that HMGB1 and LPS act synergistically to enhance the inflammatory response and it is proposed that this is mediated via the formation of a highly active pro-inflammatory complex (Youn et al., 2008; Hreggvidsdottir et al., 2009). Efficient removal of LPS contaminants is essential (Wakelin et al., 2006) particularly since HMGB1 is reported to have a high affinity for LPS (Youn et al., 2008). A number of removal methods have been described including Triton-X 114 phase extraction, polymyxin B treatment and anion-exchange purification (Petsch and Anspach 2000).

The production of isotopically labelled recombinant proteins is required for heteronuclear NMR experiments and backbone assignment. For the purpose of this work, the proteins were uniformly labelled using the ^{15}N and/or ^{13}C isotopes. Isotope labelling increases the sensitivity and peak resolution and additionally helps to simplify the complexity of the NMR spectra (Lian and Middleton 2001). The production of isotopically labelled HMGB1 constructs has been previously reported. However, published NMR studies have not considered the effect of LPS contaminants and their removal. An additional aim of this work was to investigate the effect of LPS removal on the NMR spectra for the HMGB1 proteins.

This chapter describes the development and optimisation of methods for the expression, purification and characterisation of LPS-free and isotopically labelled recombinant human HMGB1 and IL-1β proteins.

3.2. MATERIALS AND METHODS

Recombinant HMGB1, Δ30, A box, B box and IL-1β proteins were expressed, purified and characterised as described in Chapter 2, Sections 2.2 and 2.3. A schematic overview of the methods employed is provided in Figure 3.1.

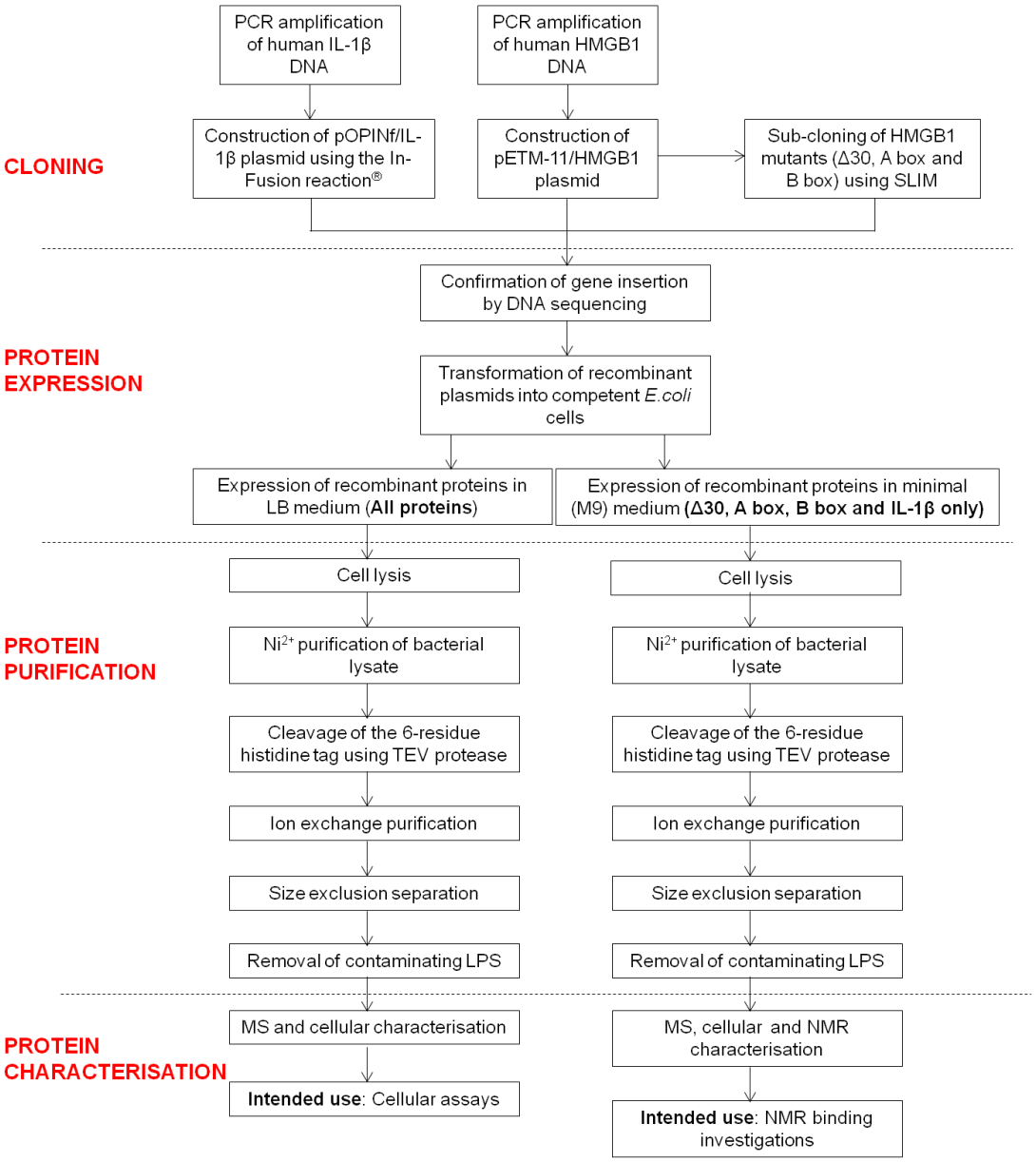

Figure 3.5 Schematic overview of the cloning, expression, purification and characterisation protocols

3.3. RESULTS

3.3.1. Production of recombinant human HMGB1 proteins from *E.coli*

The pETM-11/HMGB1 plasmid was transformed into *E.coli* BL21 (DE3) cells and the protein was expressed in LB medium at 37^{o}C for 4 h, as this was determined to be the optimal expression conditions. The bacterial cell lysate was initially purified using Ni^{2+} affinity chromatography and SDS-PAGE gel electrophoresis analysis of the purification fractions identified two over expressed protein bands (Figure 3.2A). The two bands were successfully separated using anion exchange chromatography (Figure 3.2B), which exploited the difference in the overall net surface charge. ESI MS analysis determined that the upper band had a molecular weight (MW) of 28.03 kDa (Figure 3.2C). The predicted MW of his-tagged HMGB1 was 28.02 kDa and the MS analysis confirmed that the upper band was full length HMGB1. Furthermore, western blot analysis confirmed this finding (Figure 3.2D). The lower band was found to have a MW of 25.80 kDa by ESI-MS and represented a C-terminal truncated HMGB1 protein (Figure 3.2C). Predicted MW data suggests that the final 18 residues of the polyacidic C-terminal tail are absent in the truncated HMGB1 protein (corresponding to residues 198-215; EEEEDEEDEDEEEDDDDE).

In future preparations, the 6 residue poly-his tag was cleaved using TEV protease prior to the ion-exchange purification as described in Section 2.3.8. Additionally, to increase the purity the HMGB1 protein was further purified using size exclusion chromatography (as described in Section 2.3.11). Purified HMGB1 was visualised as a single band on a SDS-PAGE gel. In LB medium, the final yield of purified protein was approximately 0.75 – 1 mg/L. Due to the low protein yield, full length HMGB1 was not expressed in minimal medium.

The Δ30, A box and B box proteins were sub-cloned from the pETM-11/HMGB1 plasmid using SLIM as described in Chapter 2, Section 2.2.4. Recombinant plasmids were transformed into BL21 (DE3) cells and the proteins were expressed in LB and minimal medium. The purification protocol used for the mutants was identical to the HMGB1 purification strategy. Purified proteins were visualised as a single band on a SDS-PAGE gel. In comparison to HMGB1 the yields of protein obtained for the mutants were significantly higher (Table 3.2).

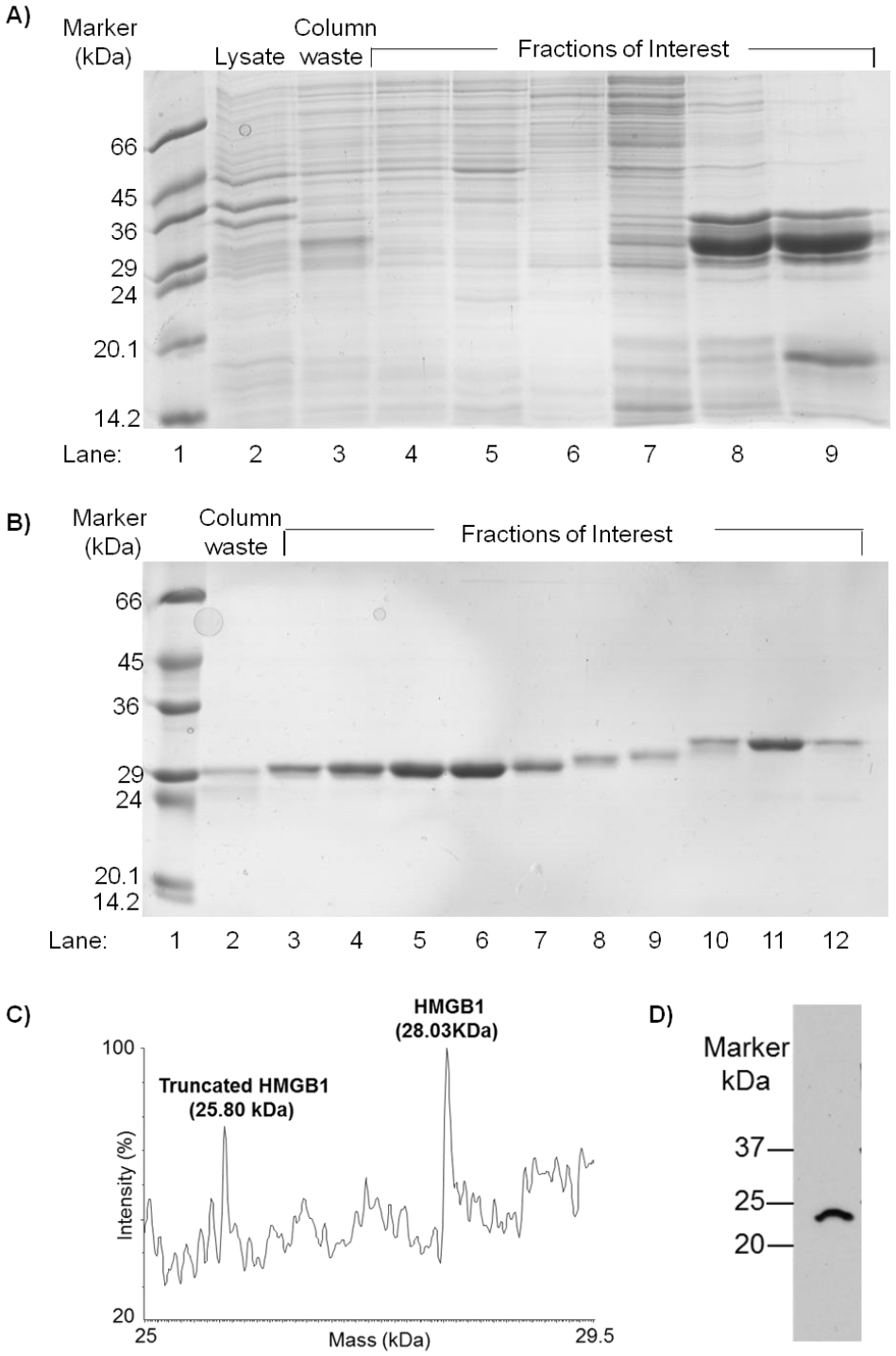

Figure 3.6 Production of recombinant human HMGB1 in BL21 (DE3) cells The pETM-11/HMGB1 plasmid was transformed into BL21 (DE3) cells and expressed in LB medium at 37^{o}C for 4 h. The cell lysate (lane 2) was purified using Ni^{2+} affinity chromatography and the fractions of interest (lanes 4-9) were analysed on a 12.5% SDS-PAGE gel (A). Two over-expressed protein bands were detected (lanes 8 & 9) and were separated using anion exchange chromatography (lower band lanes 3-7, upper band lanes 11-12) (B). ESI-MS analysis confirmed that the upper band corresponded to the full length HMGB1 and the lower band was a C-terminal truncated HMGB1 protein (C). Western blot analysis confirmed that the upper HMGB1 band was HMGB1 (D).

Table 3.9 Typical yields of LPS-free proteins obtained from BL21 (DE3) cells expressed in 1L of LB or minimal medium*

Construct	LB medium (mg/L)	Minimal medium (mg/L)
HMGB1	0.75 - 1	-
Δ30	3 - 5	1.5 – 2.5
A box	8 - 10	4 – 5
B box	8 - 10	4 – 5
IL-1β	36	20

3.3.2. Production of recombinant human IL-1β from *E.coli*

The DNA for the human IL-1β protein was sub-cloned into the pOPINF vector using the In-Fusion® reaction. A 6-residue his tag was incorporated into the N-terminus for purification purposes (Figure 2.3). The pOPINF/IL-1β plasmid was transformed into BL21 (DE3) cells and the protein was expressed in LB medium at 37^{o}C for 4 h. The bacterial cell lysate was purified using Ni^{2+} affinity chromatography and the fractions were analysed using SDS-PAGE gel electrophoresis (Figure 3.3B). A high yield of the IL-1β protein was obtained and contaminating proteins were removed using anion exchange chromatography (Figure 3.3C). ESI-MS analysis confirmed that the IL-1β protein had a total molecular weight of 19.39 kDa (predicted molecular weight = 19.5 kDa).

In future preparations, the 6 residue poly-his tag was cleaved using the 3C protease prior to the ion-exchange purification as described in Section 2.3.9. For NMR experiments, the protein was further purified using size exclusion separation. Purified IL-1β was visualised as a single band on a SDS-PAGE gel. In LB medium, the final yield of purified protein was approximately 36 mg/L of cell culture (Table 3.2). For the production of ^{15}N-labelled IL-1β, transformed *E.coli* cells were grown in minimal medium to an OD of 0.8-1.0 and after induction with IPTG, protein expression was carried out overnight at 18^{o}C. The purification of labelled proteins was identical to the protocols used for the purification of LB expressed proteins. Approximately 20 mg of purified IL-1β protein was obtained from 1L of minimal medium.

* For a description of the LPS removal see Section 3.3.3

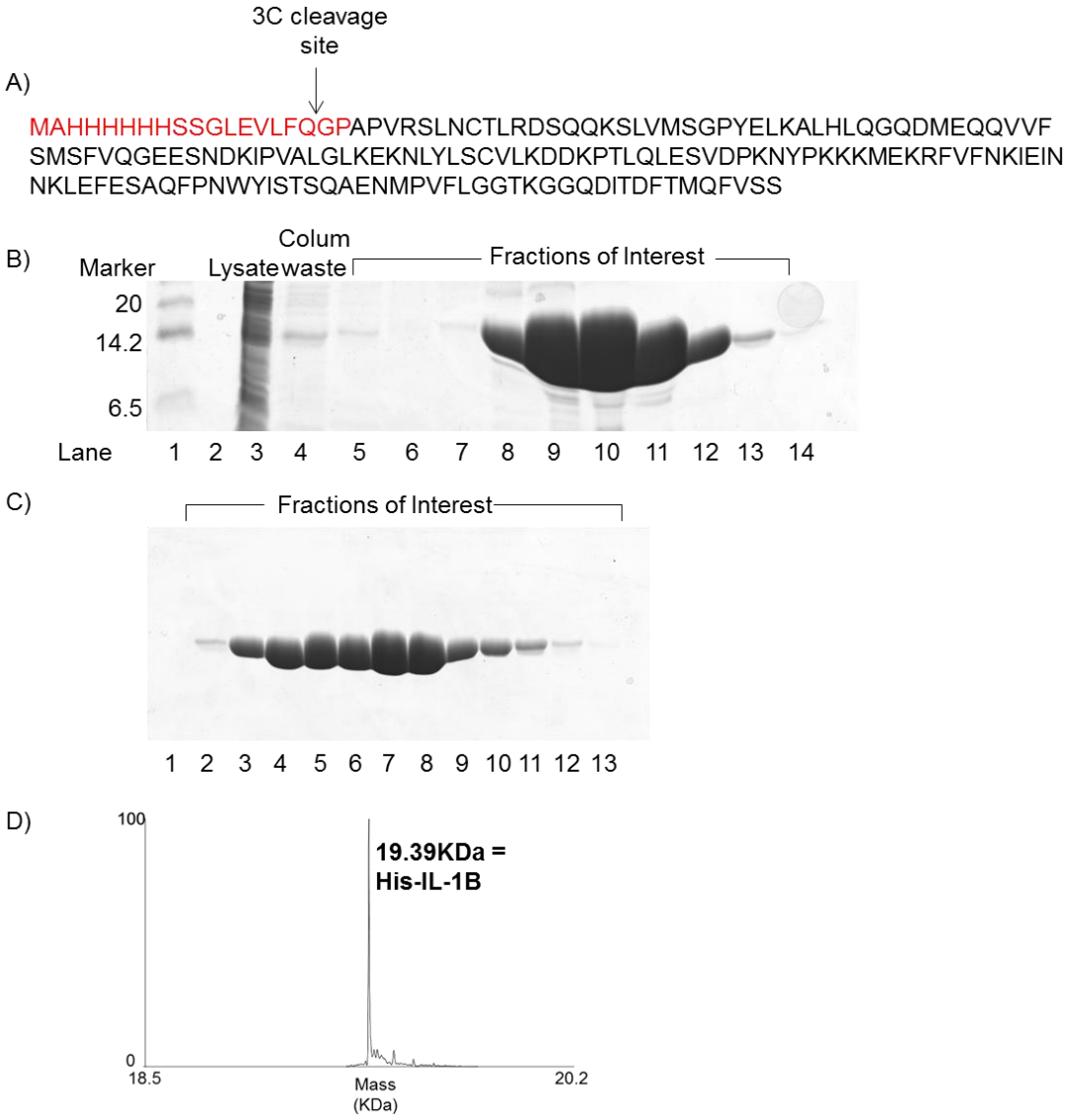

Figure 3.7 Production of recombinant IL-1β from BL21 (DE3) cells DNA for the human IL-1β protein was cloned into the pOPINF vector. A cleavable 6-residue his tag was incorporated into the construct for purification purposes (A). The plasmid was transformed into BL21 (DE3) cells and the protein was expressed in LB medium at 37^{o}C for 4 h. The cell lysate (lane 3) was purified using Ni^{2+} purification and the fractions of interest (lane 5-14) were analysed using SDS-PAGE gel electrophoresis (B). Protein contaminants were removed using anion exchange chromatography (lanes 2-12) over an increasing salt concentration (C). For NMR experiments, the protein was further purified using size exclusion separation. ESI-MS analysis confirmed that the total molecular weight of his-tagged IL-1β protein was 19.39 kDa (D).

3.3.3. Removal of LPS from recombinant protein preparations

LPS is a major component of the outer membrane of gram negative bacteria and a potent stimulator of the TLR4. Contaminating LPS was removed from protein preparations using a Triton X-114-based two-phase extraction protocol (Aida and Pabst 1990). It has previously been shown that this method is more effective at removing LPS from recombinant HMGB1 preparations than polymyxin B purification (Li et al., 2004). LPS levels in protein preparations were determined before and after Triton-X114 purification. LPS molecules vary considerably between different species and strains of bacteria (Erridge et al., 2002) and to account for this variation the LPS levels are expressed as EU/mg of protein (EU/mg). This is a standardised measurement that describes the biological activity or potency.

The level of LPS in bacterially expressed recombinant full length HMGB1 was typically greater than 500 EU/mg (Table 3.3). Considerably less LPS was detected in the Δ30 (approx. 126 EU/mg) and A box (Approx. 52 EU/mg) preparations. The LPS content in the B box preparation before LPS removal was not determined but previous studies have demonstrated that both HMG boxes have a similar affinity for LPS (Li et al., 2004). Importantly, the LPS content after the Triton X-114 purification in all protein preparations was consistently less than 5 EU/mg. Recombinant IL-1β protein preparations were also subjected to Triton X-114 extraction and consistently exhibited levels of less than 5 EU/mg after purification.

Table 3.10 Typical LPS content in recombinant protein preparations before and after Triton X-114 purification (LPS levels are expressed as Endotoxin Units per mg of protein (EU/mg). 1EU/mg is approximately equal to 100 pg endotoxin)

Construct	Typical LPS before (EU/mg)	Typical LPS after (EU/mg)
HMGB1	> 500	< 5
Δ30	Approx. 126	< 5
A box	Approx. 52	< 5
B box	-	< 5
IL-1β	-	< 5

3.3.4. NMR characterisation of recombinant proteins

3.3.4.1. 1D NMR characterisation of full length HMGB1

The full length HMGB1 protein was characterised using 1D NMR analysis. A ^{1}H NMR spectrum was collected on a 23 µM unlabelled HMGB1 sample in PBS at pH 7.2 using a 600 MHz Bruker Avance II spectrometer at 25^{o}C (Figure 3.4). Peaks were detected between 0.5 to 10 ppm and the spectral dispersion is characteristic of a folded protein (Figure 3.4). As previously described, LPS contaminants were removed using a Triton-X114 two phase extraction protocol and residual Triton-X114 impurities were identified in the ^{1}H HMGB1 spectrum.

The ^{1}H spectrum for full length HMGB1 was compared with the ^{1}H spectrum for the ^{15}N-labelled Δ30 and B box proteins. As indicated in Figure 3.5, conserved peaks were identified in the different spectra and, as expected, all three constructs appear to express proteins with folded regions, rather than being random coil.

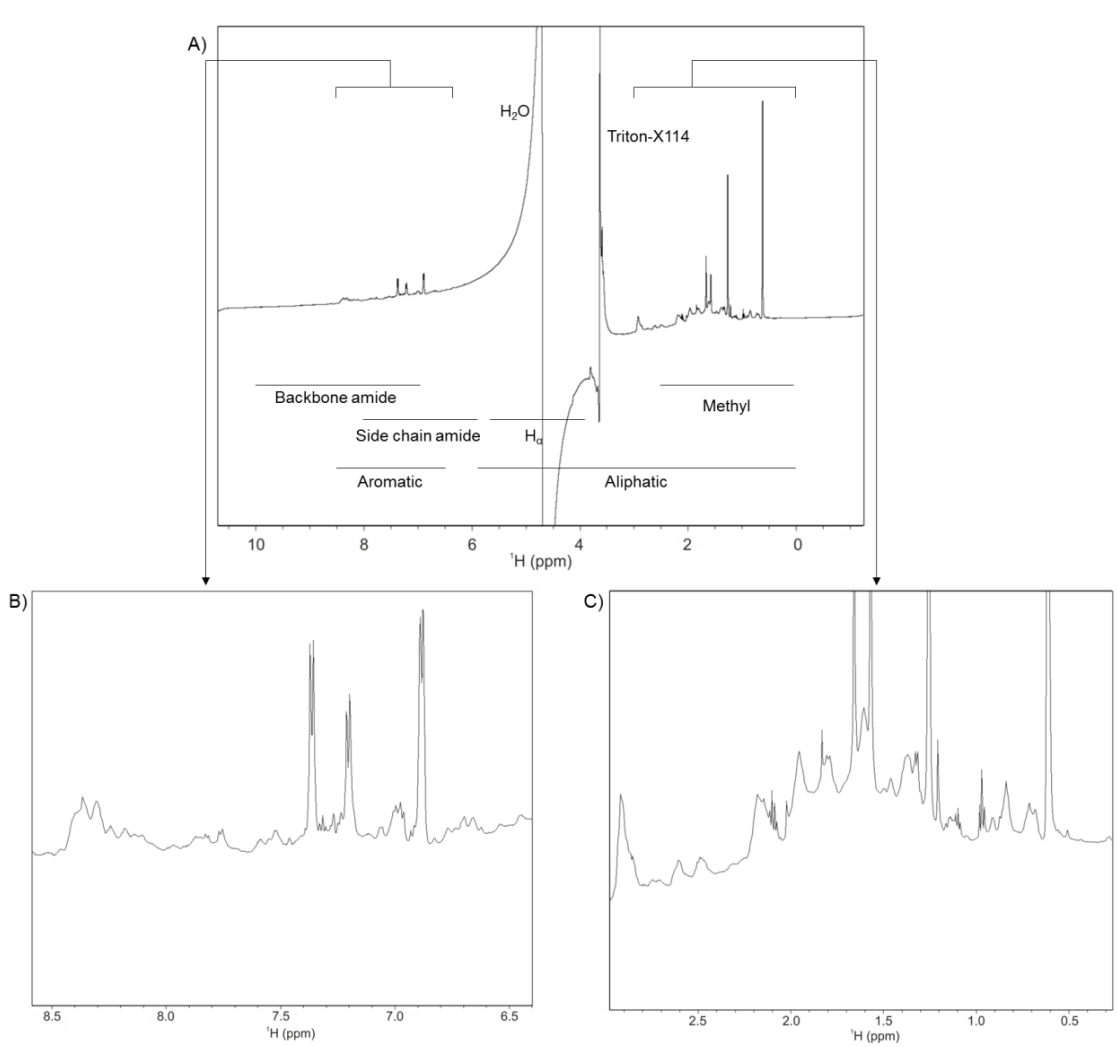

Figure 3.8 ^{1}H NMR spectrum for full length HMGB1 The NMR spectrum was collected on a 23 µM HMGB1 sample on a 600 MHz Bruker spectrometer equipped with triple resonance cryoprobes at 25^{o}C (298 K) in PBS, pH 7.2. The full ^{1}H spectrum for HMGB1 is presented with typical ^{1}H chemical shifts highlighted (A). An expanded section of the amide region is shown in (B) and an expanded section of the aliphatic region is displayed in (C). For (B) and (C) the spectrum was baseline corrected using the auto-correct spectra range function between -1–3 ppm and 6-10 ppm to reduce the effect of water suppression.

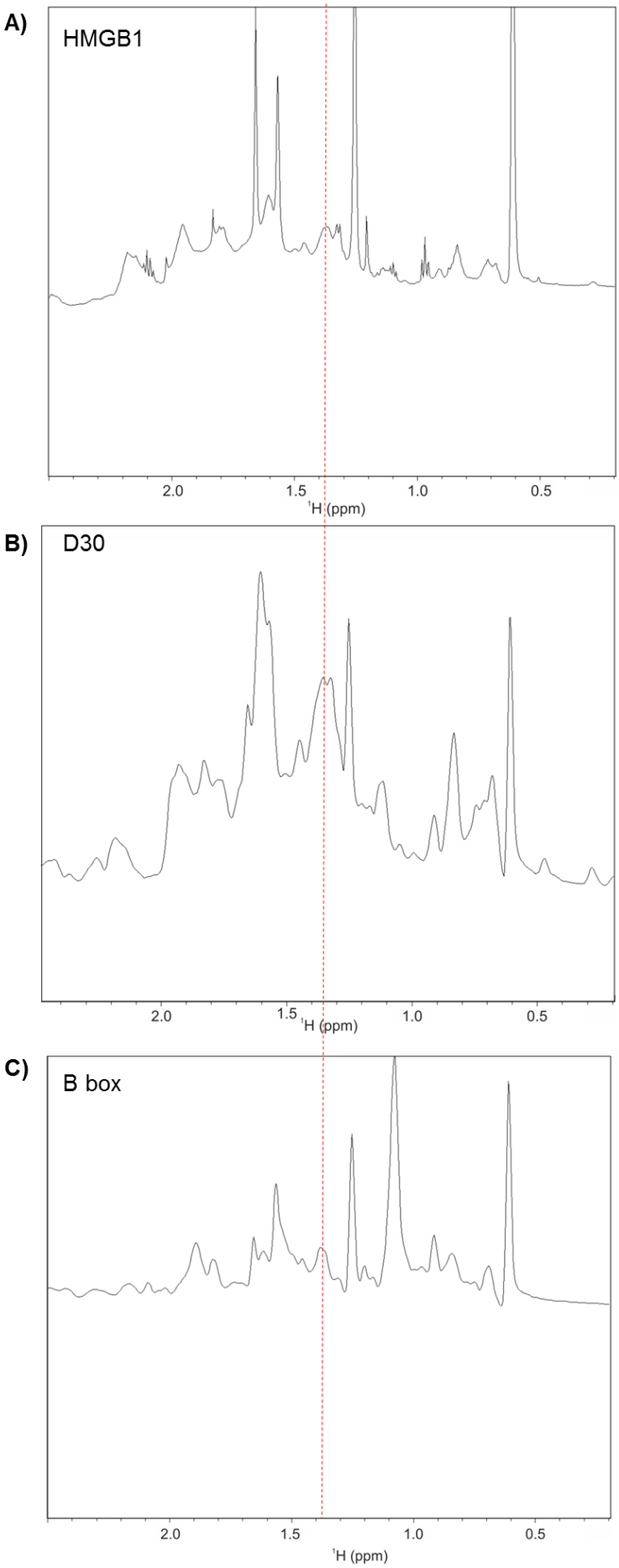

Figure 3.9 Comparison of ^{1}H NMR spectra for full length HMGB1, Δ30 and B box An expanded section of the aliphatic region is presented for full length HMGB1 (A), Δ30 (B) and B box (C). An example of a conserved peak is shown (---). Based on the line-widths of the peaks all three domains appear to contain folded regions.

3.3.4.2. 2D NMR characterisation of Δ30, A box, B box and IL-1β proteins

The HMGB1 constructs were characterised using 2D NMR analysis. ^{1}H-^{15}N HSQC spectra were collected for ^{15}N-labelled LPS-free Δ30, A box and B box proteins in PBS, pH 7.2 at 25^{o}C. The number of expected peaks for each spectrum was calculated as follows: number of backbone amides (total number of residues with proline deducted) plus the number of asparagine and glutamine side-chain amides (Table 3.4). Under these conditions, 159 peaks were detected on the ^{1}H-^{15}N HSQC spectrum for the ^{15}N-labelled his-tagged Δ30 (Figure 3.6). The peaks were well dispersed and resolved and the spectrum was indicative of a folded protein. However, 22% of the expected peaks were missing from the spectrum, probably due to the fast chemical exchange with the solvent, as expected from the pH used for the solution.

On the ^{1}H-^{15}N HSQC spectrum for the reduced ^{15}N-labelled A box 67 out of 84 predicted peaks were detected (Figure 3.7). The peaks were well resolved and the spectral dispersion indicated that the protein was folded.

On the ^{1}H-^{15}N HSQC spectrum for the ^{15}N-labelled B box, 69 out of 73 expected peaks were detected (5% missing) (Figure 3.8). The peaks were well resolved and dispersed. The spectrum indicated that the protein was folded.

The IL-1β protein was also characterised using 2D NMR analysis. A ^{1}H-^{15}N HSQC spectrum was collected on a 25 μM LPS-free ^{15}N-labelled Il-1β protein in PBS, pH 7.2 at 25^{o}C. The spectral dispersion was indicative of a folded protein and the peaks were well resolved. In total, 161 peaks were resolved out of an expected 168 (4% missing).

Table 3.11 Number of peaks detected on the ^{1}H-^{15}N HSQC spectra for the Δ30, A box, B box and IL-1β proteins at pH 7.2 NMR spectra were collected in PBS, pH 7.2. The number of predicted peaks was calculated as follows: N^{o} of backbone amides (total residues with proline deducted) plus Asn and Gln side-chain amides.

Construct	Predicted peaks	N^{o} of resolved peaks	% of peaks missing
His-Δ30	204	159	22
A box	84	67	20
B box	73	69	5
IL-1β	168	161	4

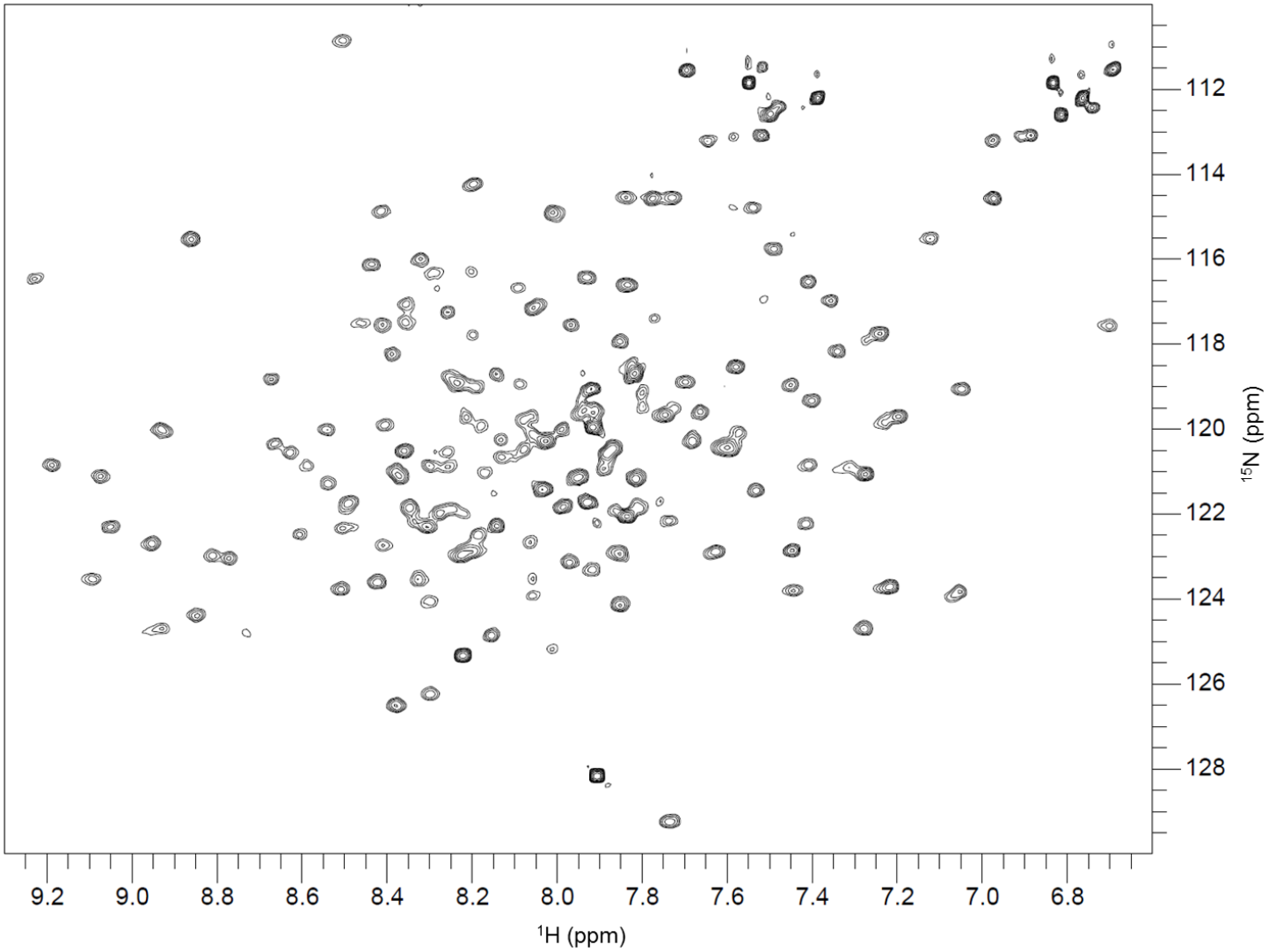

Figure 3.10 ^{1}H-^{15}N HSQC spectrum for 100 µM LPS-free his-tagged Δ30 at pH 7.2 A ^{1}H-^{15}N HSQC spectrum was collected for 100 µM LPS-free ^{15}N-labelled his-tagged Δ30 protein in PBS at pH 7.2 at 25^{o}C. The spectrum was recorded on a 600 MHz spectrometer using 64 scans with 160 increments and with a resolution in the indirect dimension of 18.24 Hz. Under these conditions 159 peaks were identified (22% of predicted peaks were absent). The well resolved and dispersed peaks indicate a folded protein.

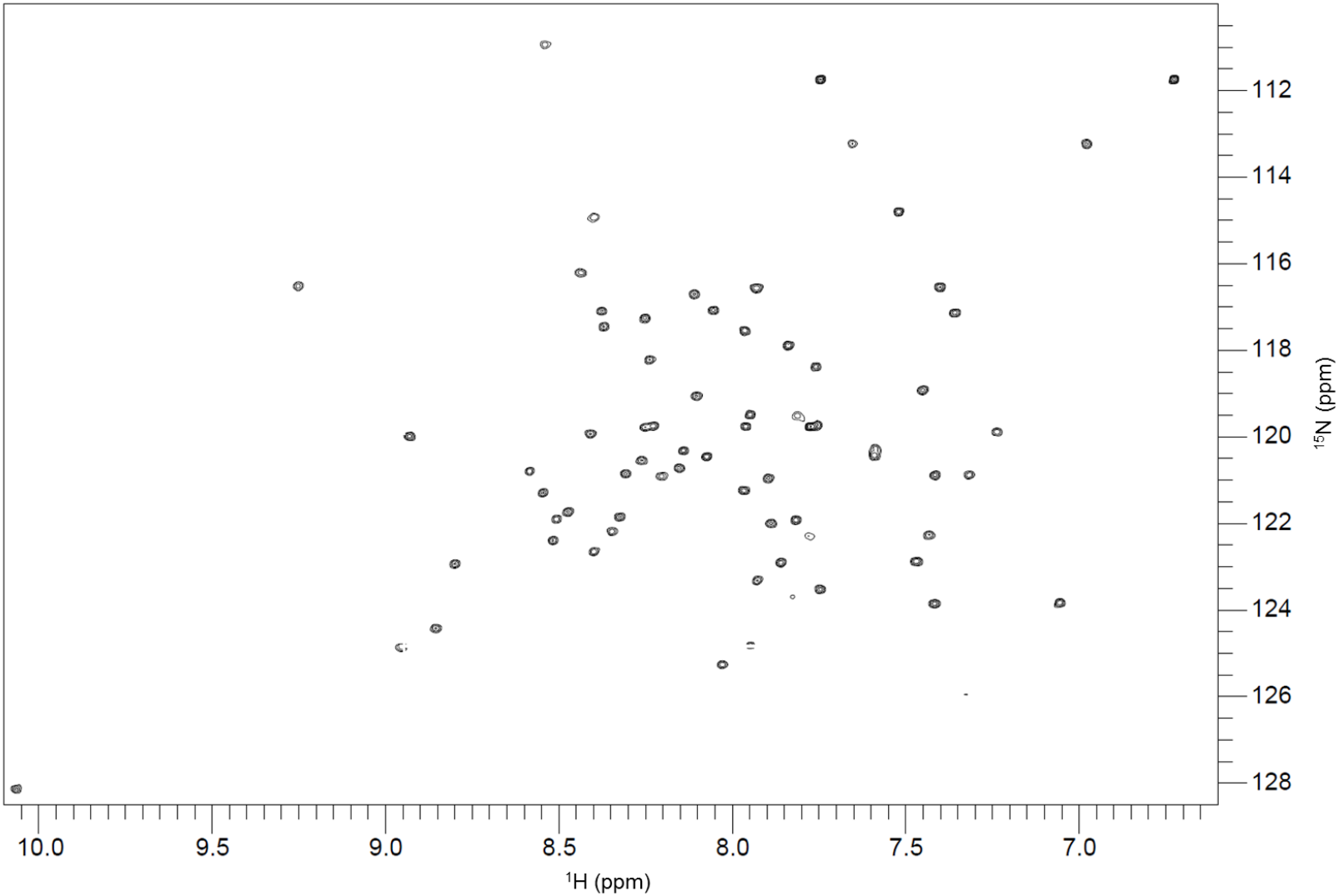

Figure 3.11 ^{1}H-^{15}N HSQC spectrum for 50 µM ^{15}N-labelled A box at pH 7.2 The ^{1}H-^{15}N HSQC spectrum for 50 µM ^{15}N-labelled A box was collected in PBS, 10 mM DTT at pH 7.2. The spectrum was collected on an 800 MHz spectrometer using 16 scans and 150 increments with a resolution in the indirect dimension of 21.80 Hz. Under these conditions 67 of the 84 predicted peaks were detected (20% missing). All of the peaks were well resolved and dispersed and the spectrum is indicative of a folded protein.

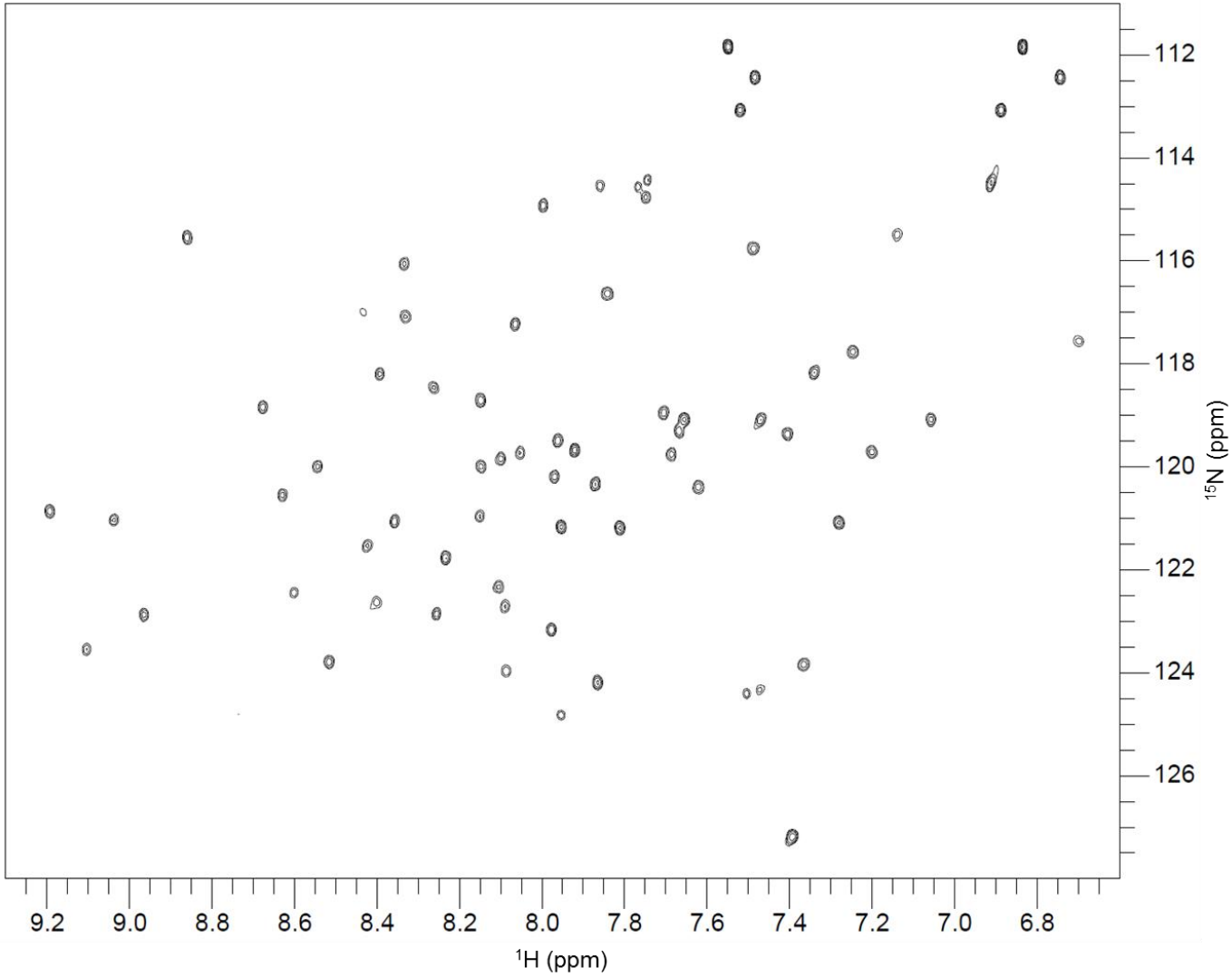

Figure 3.12 ^{1}H-^{15}N HSQC spectrum for B box The ^{1}H-^{15}N HSQC spectrum for 10 µM LPS-free B box was collected in PBS at pH 7.2 using a 800 MHz spectrometer. The spectrum was recorded at 25^{o}C using 192 scans with 256 increments and with a resolution in the indirect dimension of 15.80 Hz. Under these conditions 69 out of 73 predicted peaks were detected (5% missing). All peaks were well resolved and dispersed and the spectrum is indicative of a folded protein.

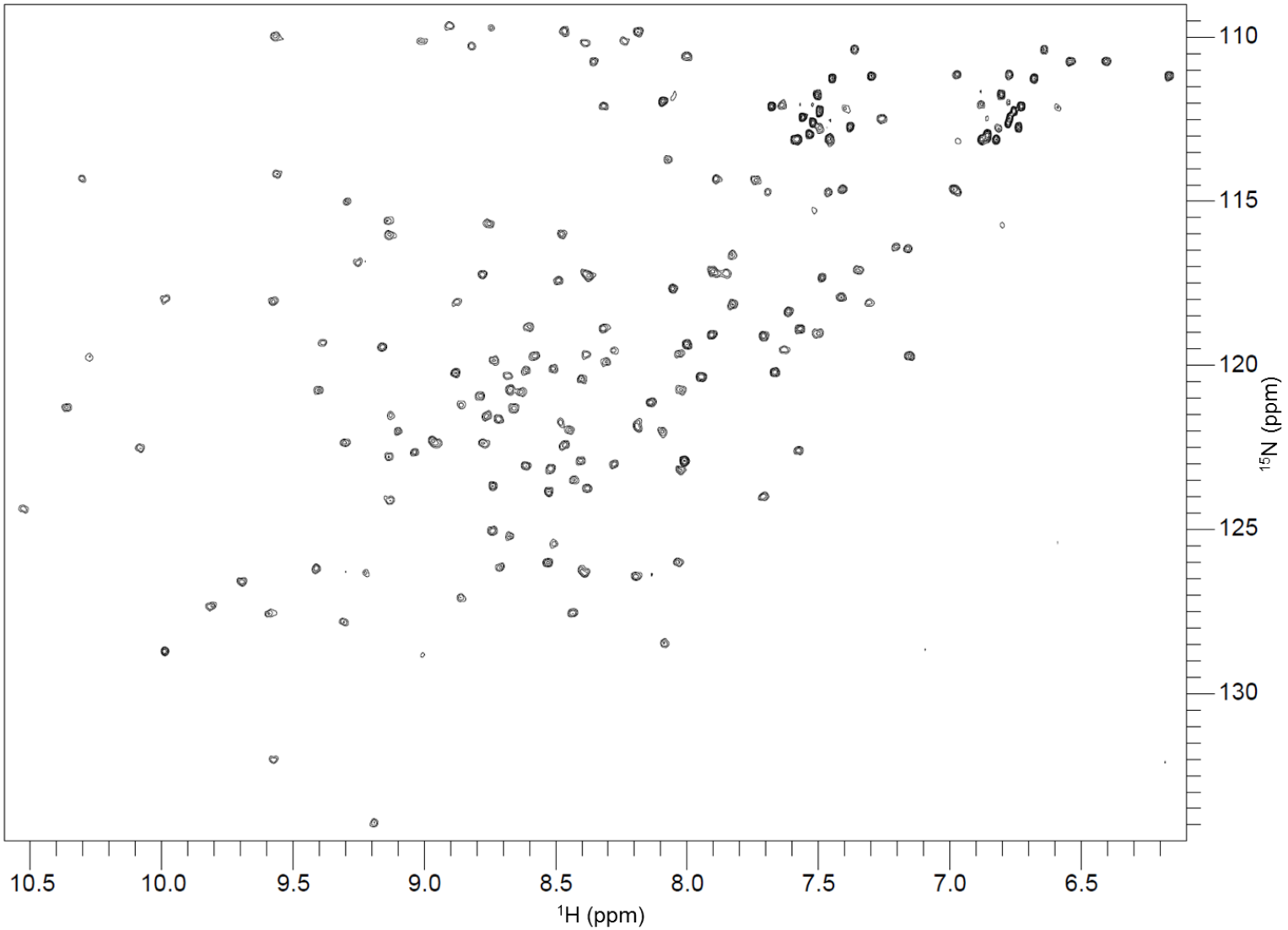

Figure 3.13 ^{1}H-^{15}N HSQC spectrum for 25 µM ^{15}N-labelled IL-1β at pH 7.2 The ^{1}H-^{15}N HSQC spectrum for 25 µM LPS-free ^{15}N-labelled IL-1β protein was collected in PBS at pH 7.2. The spectrum was collected on an 600 MHz spectrometer at 25^{o}C using 32 scans with 160 increments and with a resolution in the indirect dimensional of 21.00 Hz. Under these conditions 161 of 168 predicted peaks were detected (4% missing). All peaks were well resolved and dispersed and the spectrum is indicative of a folded protein.

3.3.4.3. Characterisation of the ^{1}H-^{15}N HSQC spectrum for the reduced A box domain of HMGB1

A partial assignment of the A box domain of HMGB1 was performed using a combination of 2D and 3D experiments. Spectra were collected on a 350 µM ^{15}N-^{13}C-labelled A box sample in 20 mM potassium phosphate, 100 mM potassium chloride and 10 mM DTT at pH 6.8. In total, it was predicted that there should be 84 peaks observed on the ^{1}H-^{15}N HSQC spectrum (82 backbone and 2 side-chain amides). Under these conditions, 70 peaks were detected and 63 residues were assigned (Figure 3.10).

^{1}H-^{15}N HSQC spectra were collected on a 100 µM A box sample in 20 mM potassium phosphate, 100 mM potassium chloride and 10 mM DTT at a pH range of 5.5 to 7.2. Spectra were acquired on an 800 MHz Bruker spectrometer at 25^{o}C using comparable NMR parameters (8 scans with 150 increments at a resolution in the indirect dimension of 21.08 Hz).

An overlay of the spectra is presented in Figure 3.11. At pH 5.5 83 of the 84 peaks were detected. However, up to 20% of the peaks disappeared with increasing pH conditions (Table 3.5) and as previously noted at pH 7.2 only 67 of the 84 peaks were detected. It was possible to identify 8 of the 17 residues that are missing from the spectrum at pH 7.2 using the partial A box assignment as M1, G2, G4, D5, S35, V36, A54 and K55. As shown in Figure 3.12, these residues are surface exposed and are dispersed across the molecule.

Table 3.12 Percentage of peaks missing from the A box ^{1}H-^{15}N HSQC spectra at pH 5.5-7.2 NMR spectra were collected on a 100 µM A box sample in 20 mM potassium phosphate, 100 mM potassium chloride and 10 mM DTT at pH 5.5 – 7.2. Expected peaks were calculated as follows: number of backbone amides (total number of residues with proline deducted) plus the number of asparagine and glutamine side-chain amides. 84 peaks were expected for the A box.

pH	N^{o} of peaks	% of peaks missing
5.5	83	1
6.0	78	7
6.5	75	11
6.8	70	17
7.2	67	20

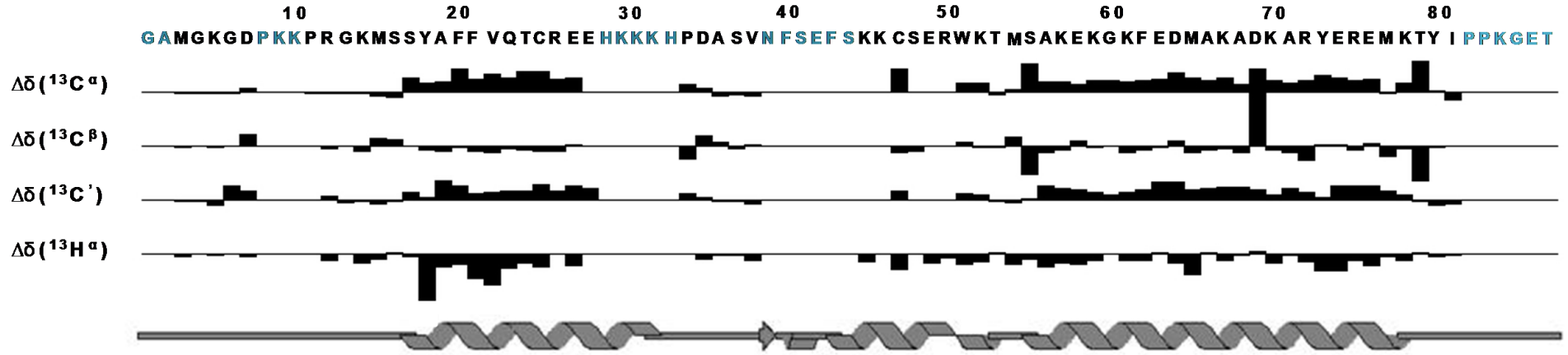

Figure 3.14 Chemical Shift Index (CSI) for A box assignment The A box domain (residues 1 -85) was assigned using sequential assignment. A change from the random coil chemical shift provides information on the structural identify of each amino acid residue. Based on the partial assignment, the majority of the secondary structure is alpha helical. (Black = assigned residues, Blue = residue not assigned).

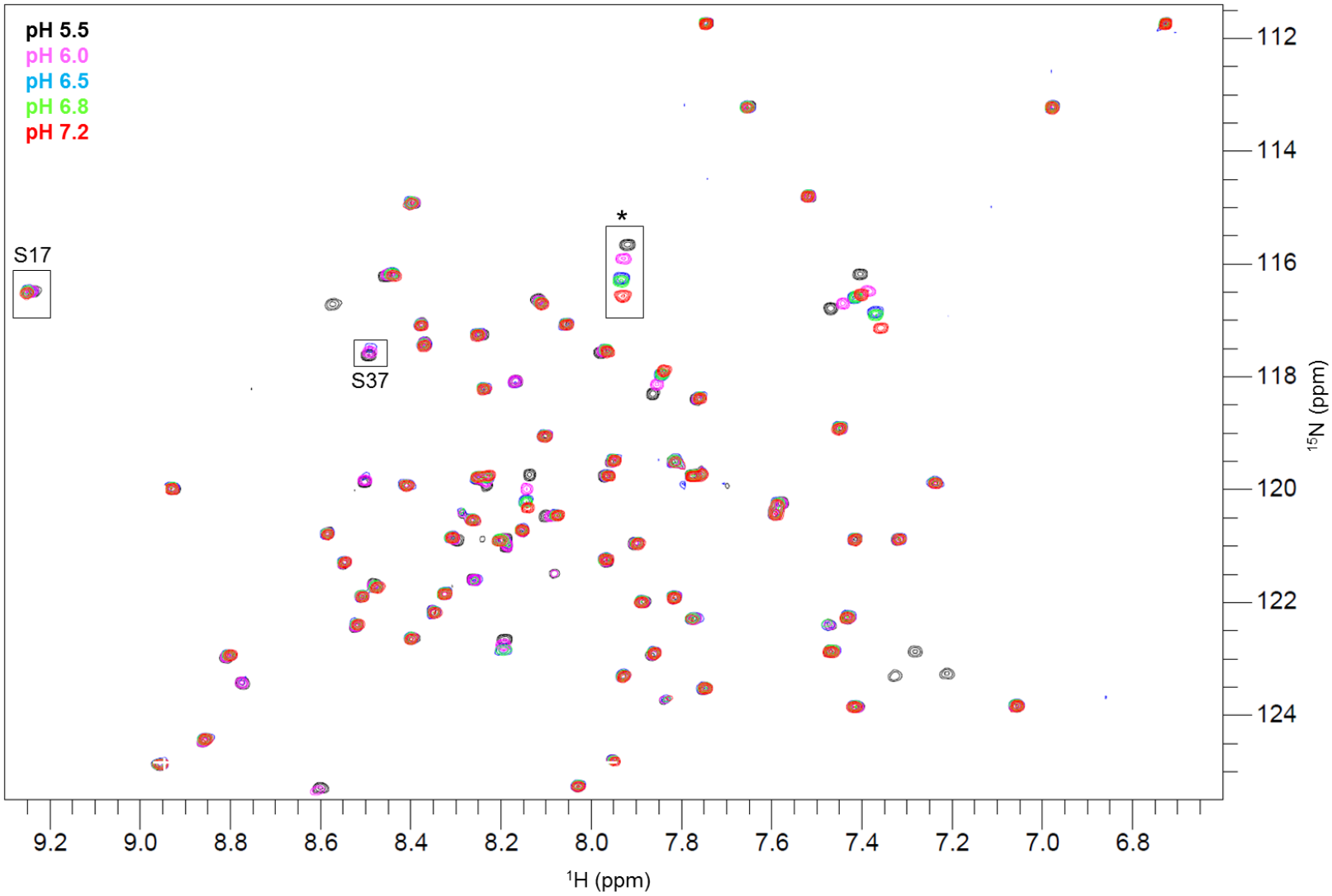

Figure 3.15 ^{1}H-^{15}N HSQC spectra for reduced A box at pH 5.5 to 7.2 Spectra were collected on a 100 µM A box sample in 20 mM potassium phosphate, 100 mM potassium chloride and 10 mM DTT on a 800 MHz spectrometer at 25^{o}C using comparable NMR acquisition parameters. Spectra were recorded at pH 5.5 (black), 6.0 (pink), 6.5 (blue), 6.8 (green) and 7.2 (red). For clarity an expanded section of the amine region is presented. No significant chemical shift perturbations were observed from some residues (S17). Some residues were not detected at every pH (S37). Some residues exhibited significant chemical perturbations at every pH point (*).

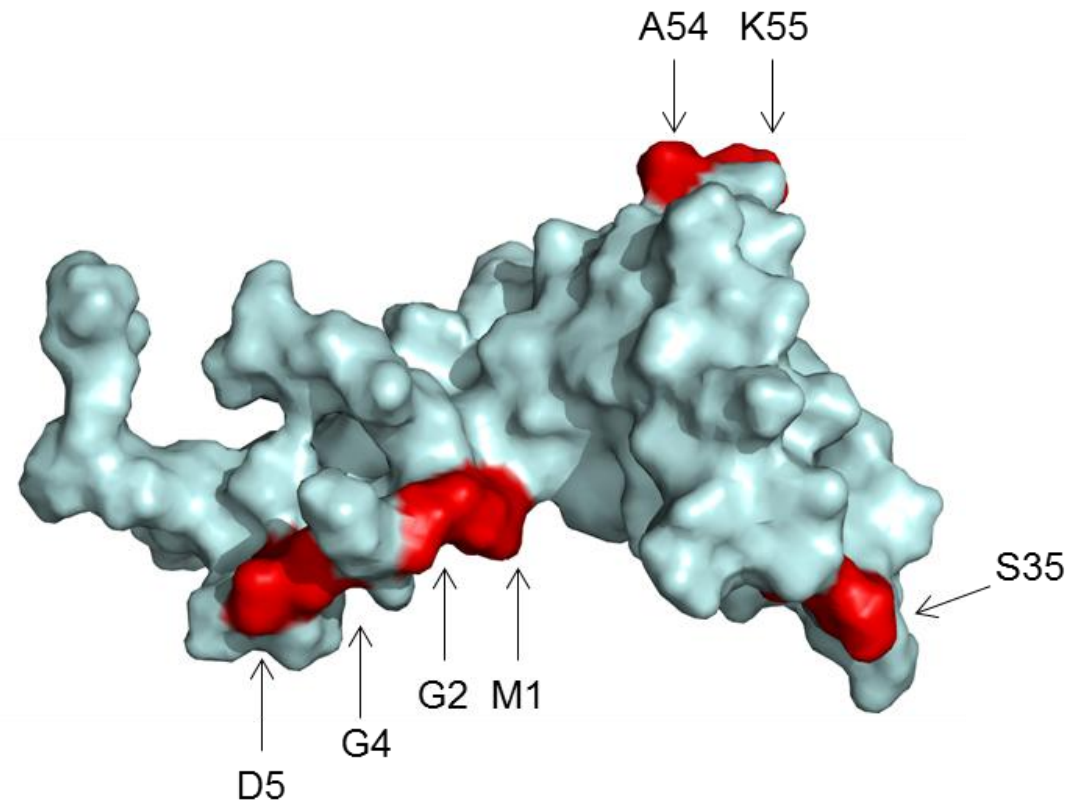

Figure 3.16 3D structure of A box highlighting the residues that disappear from the ^{1}H-^{15}N HSQC spectrum at pH 7.2 At pH 7.2 20% of the predicted peaks are missing from the ^{1}H-^{15}N HSQC spectrum for ^{15}N-labelled A box. A partial backbone assignment of the A box domain has identified 8 (M1, G2, G4, D5, S35, V36, A54 and K55) of these residues and these are highlighted on the 3D structure of A box. The V36 residue is not visible at this angle. Image was produced in PyMOL (PyMoL) using PDB entry 2YRQ.

3.3.4.4. NMR characterisation of the reduced and un-treated A box domain

^{1}H-^{15}N HSQC spectra were recorded for the reduced and un-treated A box domain. NMR spectra were recorded on an 800 MHz spectrometer at 25^{o}C in 20 mM potassium phosphate and 100 mM potassium chloride at pH 6.8. Spectra were collected in the absence and presence of 10 mM DTT using identical acquisition parameters; 16 scans with 150 increments and with a resolution in the indirect dimension of 21.08 Hz. As can be seen in Figure 3.13, the spectra for reduced and non-reduced A box differ considerably with significant chemical shift perturbations observed in the majority of peaks following the addition of 10 mM DTT. The formation of a di-sulphide bond between the C23 and C45 residues has been previously reported and is critical for TLR4 receptor binding (Yang et al., 2010; Yang et al., 2011). Using the partial A box assignment it was possible to identify these two residues in the reduced A box spectra (Figure 3.13).

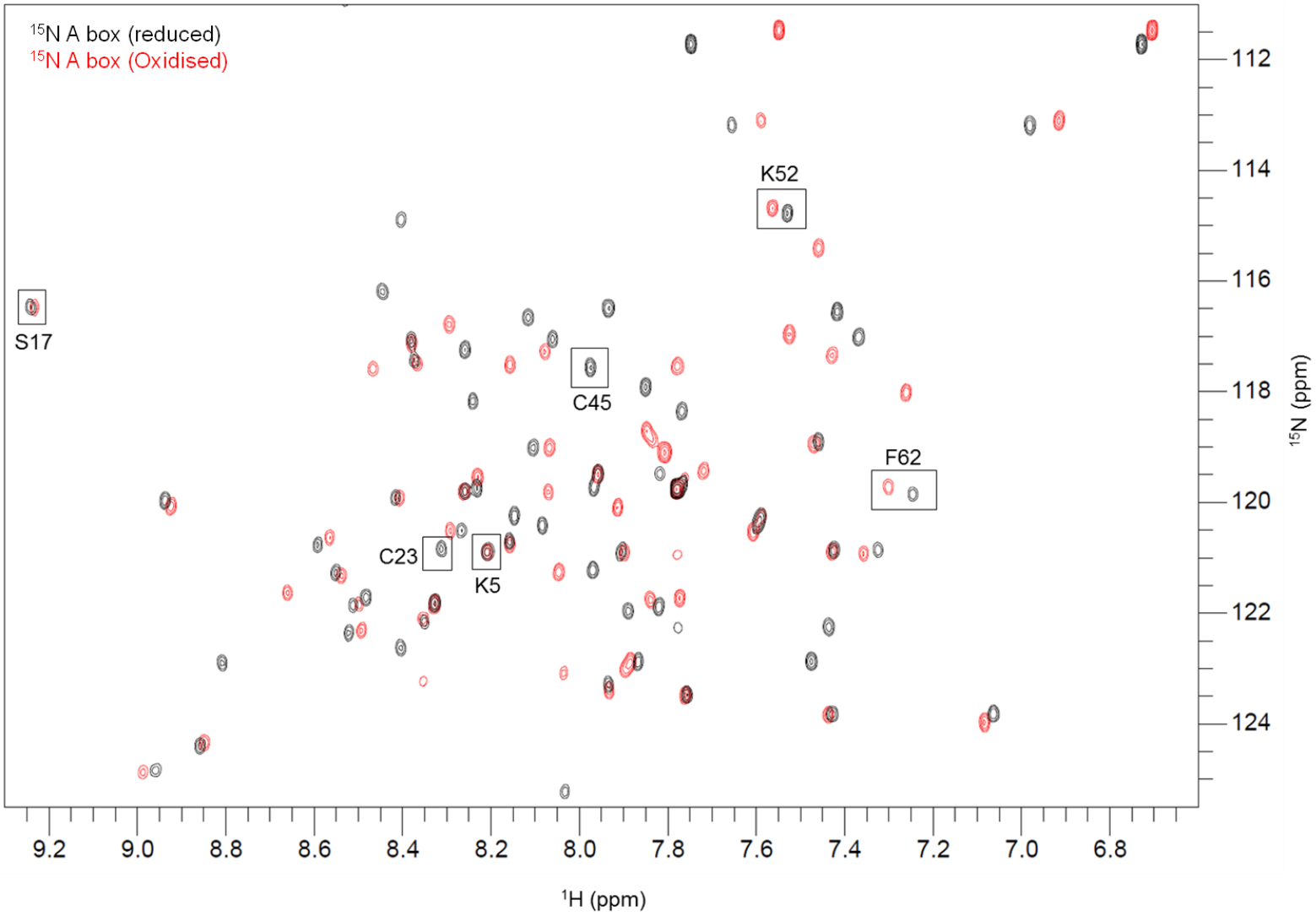

Figure 3.17 ^{1}H-^{15}N HSQC spectra for reduced and non-treated A box Spectra were recorded for a 50 µM A box sample in PBS, pH 7.2, with (black) and without (red) 10 mM DTT. Samples were analysed on a Bruker Avance II 800 MHz spectrometer at 25°C (298 K) using identical NMR parameters: 16 scans with 150 increments with a resolution in the indirect dimension of 21.08 Hz. Following the addition of DTT significant chemical shift perturbations were observed for some residues (For example, K52 & F62), while no or minor perturbations were observed for some residues (S17 & K5). The C23 and C45 in reduced A box are also indicated.

3.3.4.5. Investigating the effect of LPS removal on the NMR spectra for Δ30, A box and B box

As discussed previously, LPS contaminants were successfully removed using Triton-X114 purification (Section 3.3.3). To ensure that this process did not alter the NMR spectra, ^{1}H-^{15}N HSQC spectra were collected for ^{15}N-labelled HMGB1 proteins before and after LPS removal. Overlays of the spectra for ^{15}N-labelled Δ30, A box and B box are presented in Figure 3.14, Figure 3.15 and Figure 3.16, respectively. Prior to purification, the levels of LPS in the Δ30 and A box proteins were approximately 126 EU/mg and 52 EU/mg. The LPS content after the Triton-X114 purification in all protein preparations was consistently less than 5 EU/mg. No significant chemical shift perturbations were detected for any of the proteins following LPS removal although some minor perturbations were observed in the ^{1}H-^{15}N HSQC spectra for the B box (Figure 3.16).

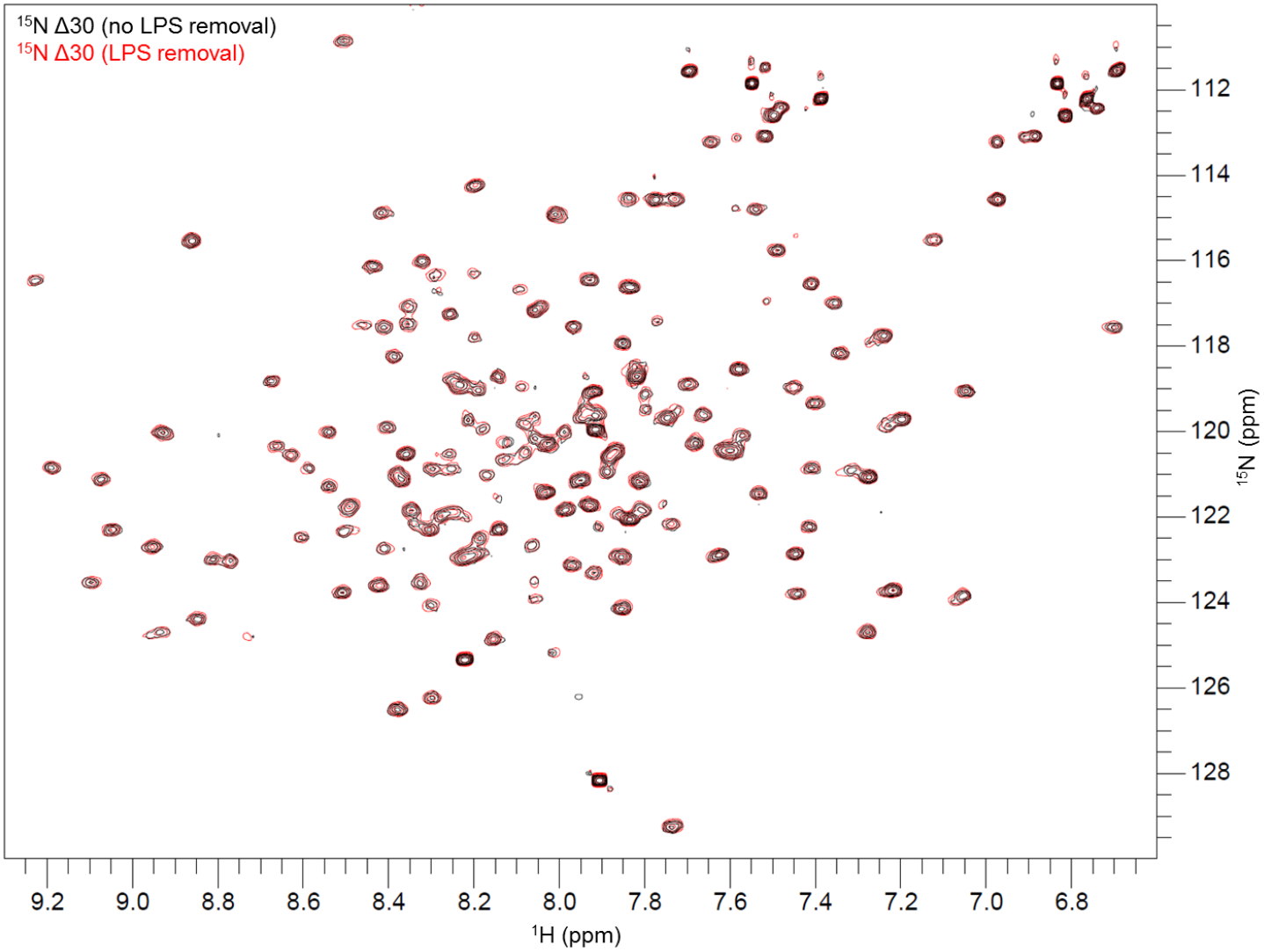

Figure 3.18 Effect of LPS removal on the Δ30 ^{1}H-^{15}N HSQC spectra A ^{1}H-^{15}N HSQC spectrum was collected on a 40 µM ^{15}N-labelled his-tagged Δ30 sample before the sample was subjected to Triton-X114 purification to remove contaminating LPS (Black). A ^{1}H-^{15}N HSQC spectrum was collected on a 100 µM ^{15}N-labelled his-tagged Δ30 sample after (red) purification. The spectra were collected in PBS at pH 7.2 on an 600 MHz spectrometer using 64 scans with 160 increments and with a resolution in the indirect dimension of 18.24 Hz. The LPS level was approximately 126 EU/mL before LPS removal and < 3 EU/mL after removal. No significant chemical shift perturbations were detected.

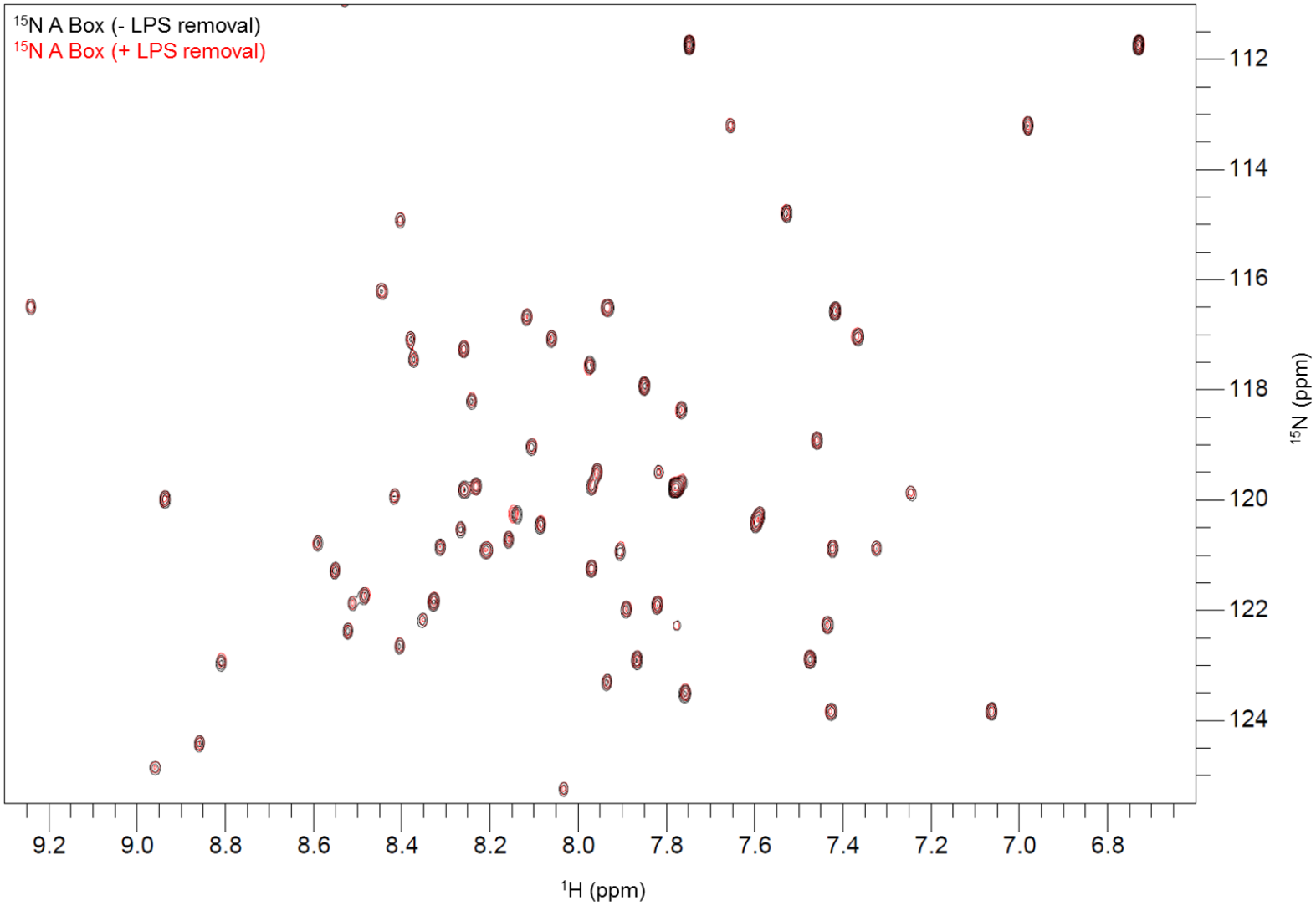

Figure 3.19 Effect of LPS removal on the A box ^{1}H-^{15}N HSQC spectra ^{1}H-^{15}N HSQC spectra were collected on a 50 µM A box sample in PBS with 10 mM DTT, pH 7.2 at 25^{o}C (298 K) on a Bruker Avance II 800 MHz spectrometer using identical acquisition parameters (NS = 16, increments = 150 and ^{15}N resolution = 21.08). HSQC spectra were collected before (black) and after (red) the sample was subjected to a specific LPS removal step using a Triton-X114 based two phase extraction protocol. The LPS content in the sample was > 50 EU/mL before LPS removal and < 3 EU/mL after removal. No significant chemical shift perturbations were detected.

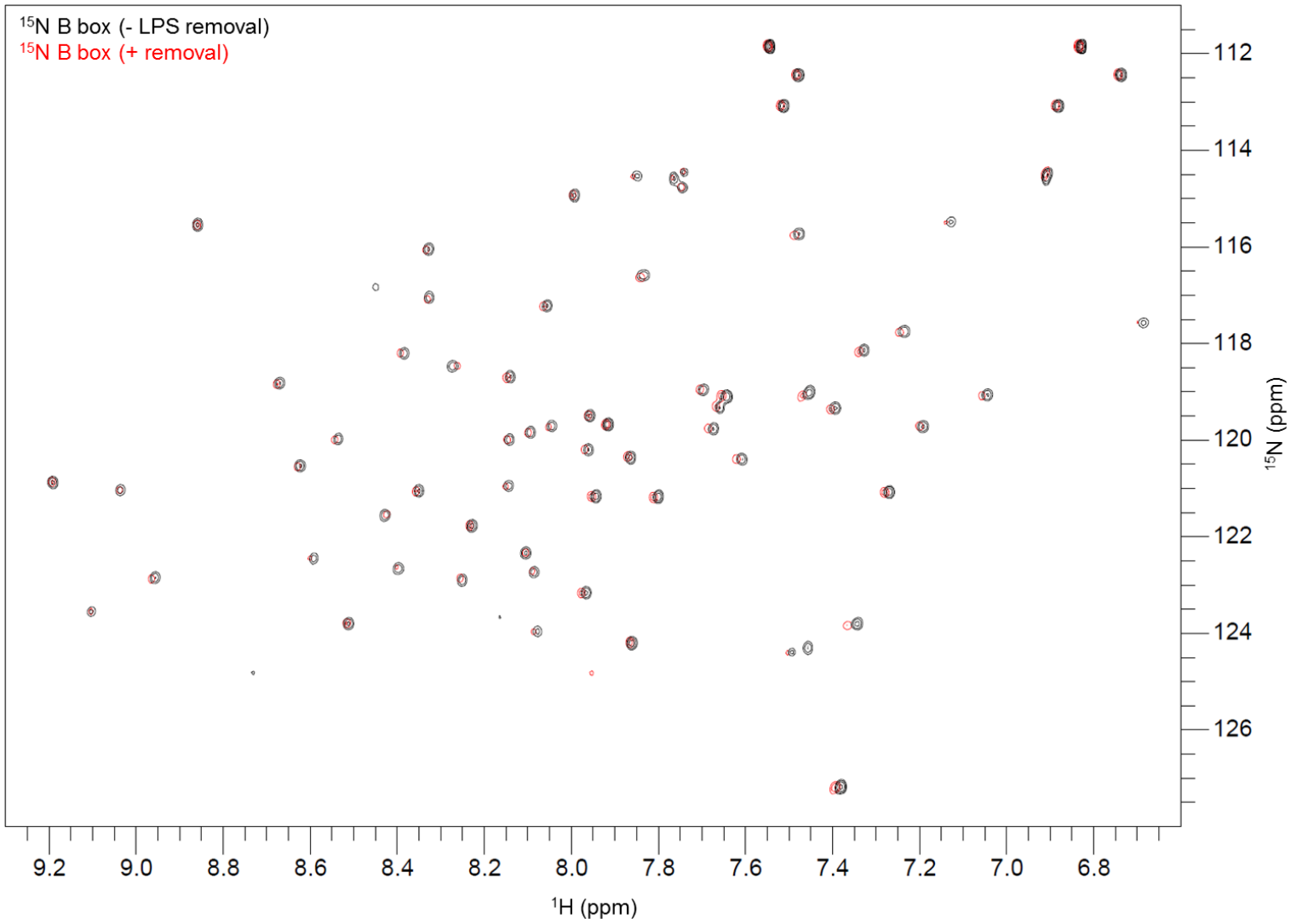

Figure 3.20 Effect of LPS removal on the B box ^{1}H-^{15}N HSQC spectra ^{1}H-^{15}N HSQC spectra were collected on a 10 µM B box sample in PBS, pH 7.2 at 25°C (298 K) on a Bruker Avance II 800 MHz spectrometer using identical NMR parameters (NS = 192, increments = 256 and ^{15}N resolution = 15.80). Spectra were collected before (black) and after (red) the sample was subjected to a specific LPS removal step using a Triton-X114 based two phase extraction protocol. Some minor chemical shift perturbations were observed.

3.3.5. Analysis of the cytokine-inducing activity of the recombinant HMGB1 proteins

The cytokine-inducing activity of the recombinant HMGB1 proteins was assessed in PBMCs isolated from a healthy volunteer. Un-induced cells or cells treated with PBS (vehicle control) had minimal IL-6 release. 10 µg/mL recombinant HMGB1, Δ30, A box or B box also failed to induce IL-6 production in the PBMCS with low or un-detectable IL-6 levels recorded (< 154 pg/mL). However, the positive control, a recombinant HMGB1 with known cytokine-inducing activity, (supplied by Peter Lundbäck, Karolinska Institute, Stockholm, Sweden) induced IL-6 levels of 27,612 ± 836 pg/mL.

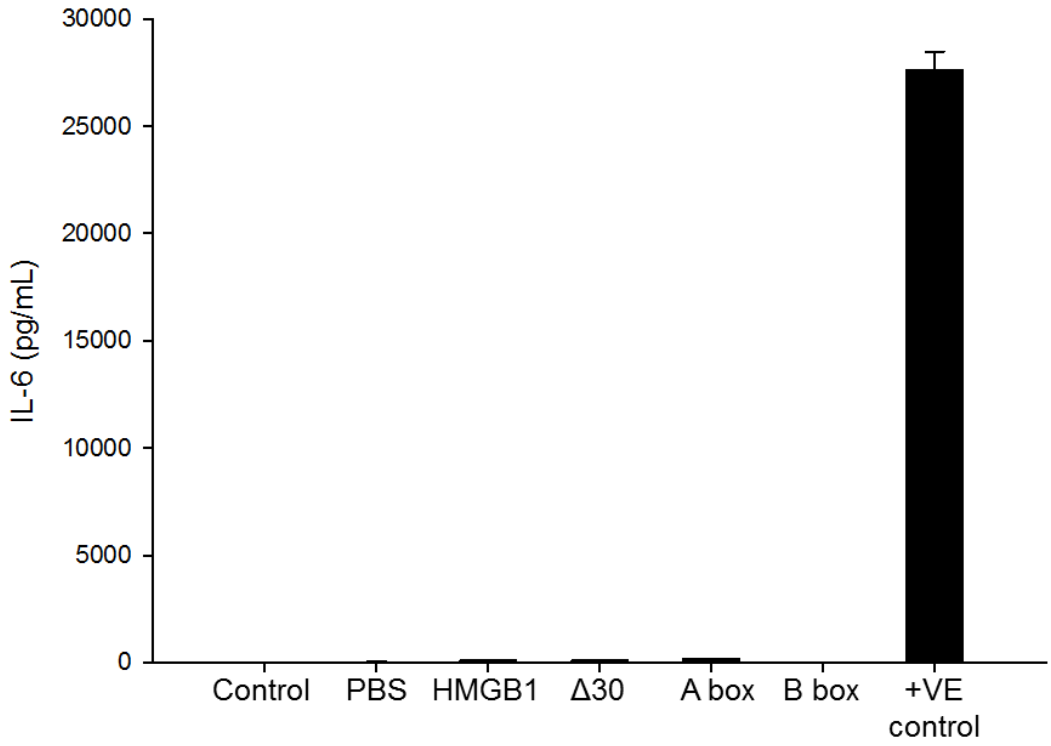

Figure 3.21 Induction of IL-6 release in PBMCs by bacterially expressed rHMGB1 constructs Cells were isolated from a healthy volunteer and treated with PBS (Vehicle control), HMGB1, Δ30, A box or B box at a final concentration of 10 µg/mL. Cell supernatants were collected after 16 h and IL-6 levels were quantified by ELISA. Recombinant HMGB1 with known cytokine-inducing activity was used as a positive control (n = 1 experiment performed in triplicate wells). +VE control = recombinant HMGB1 with known cytokine-inducing activity.

3.3.6. LC-ESI-MS/MS characterisation of the redox state of the C23, C45 and C106 residues in full length HMGB1

Recent evidence has shown that the redox status of the three cysteine residues (23, 45 and 106) in HMGB1 is critical for the interaction with the TLR4 (Yang et al., 2010; Yang et al., 2011). The redox status of the three residues was determined using LC-ESI- MS/MS analysis. Reduced cysteine residues within his-tagged HMGB1 were initially capped using iodoacetamide. The alkylation with iodoacetamide generates a carboxyamidomethyl adduct resulting in a mass shift of 57 amu (atomic mass units). Next, the protein was incubated with 1 mM DTT and newly reduced cysteine residues were capped using NEM. The alkylation with NEM yields a mass shift of 125 amu. The protein was digested using Glu-C and peptides were analysed using LC-ESI-MS/MS analysis. A thiol-capped NEM adduct was detected in the peptide containing residues 2-26 (Figure 3.18A). This corresponded to the C23 residue. The same adduct was detected in a second peptide which contained residues 17-26 (Figure 3.18B). A thiol-capped NEM adduct, corresponding to the C45 residue, was detected in the peptide containing amino acids 41-47 (Figure 3.18C). Furthermore, in a peptide comprising residues 103-108 a thiol-capped NEM adduct was detected that corresponded to the C106 residue. Collectively, these results show that all three cysteine residues were oxidised in the *E.coli* expressed his-tagged HMGB1 protein, prior to the addition of DTT.

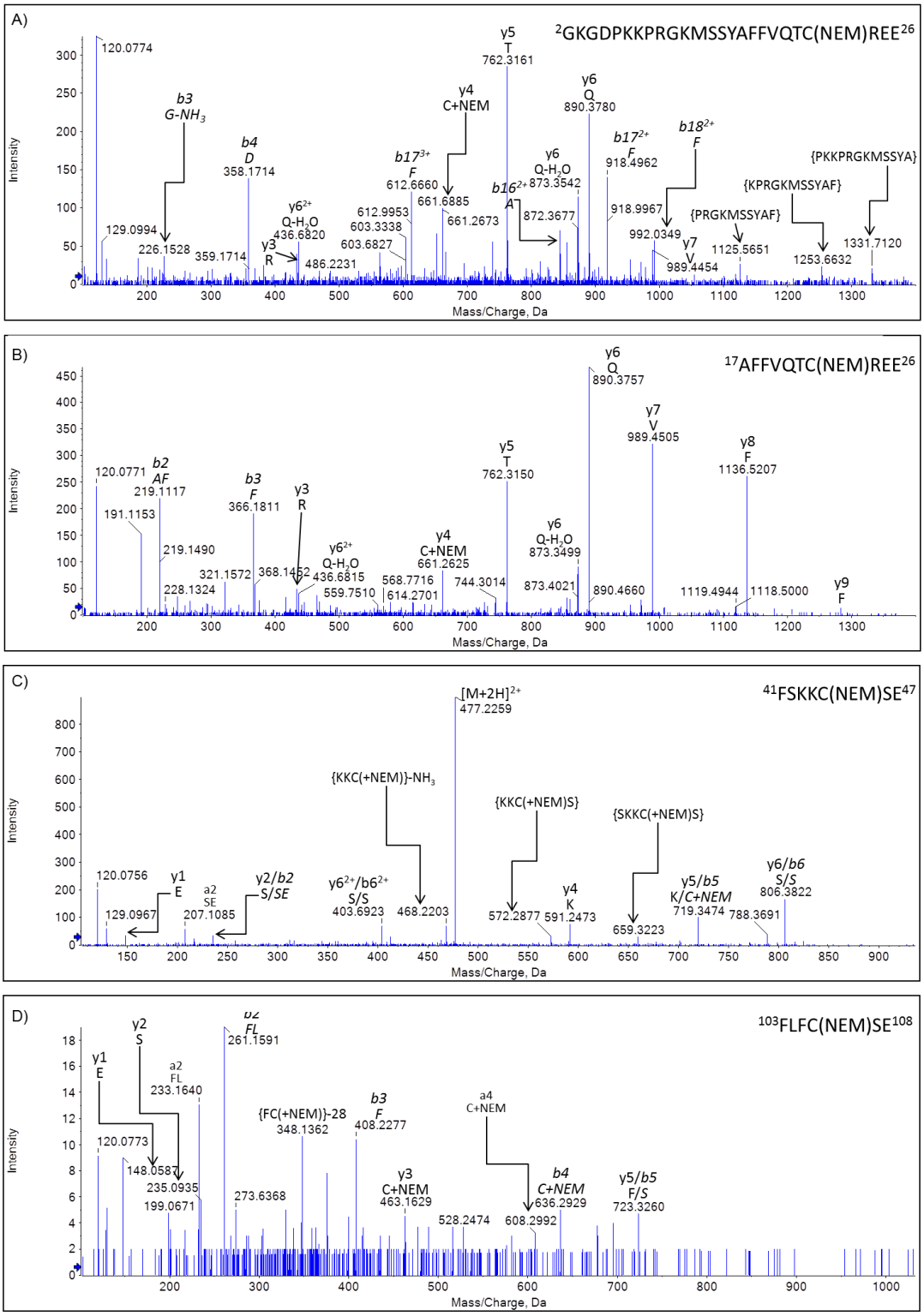

Figure 3.22 Mass spectrometric identification of C23, C45 and C106 redox state LC-MS/MS spectra of Glu-C-derived peptides confirming that the C23 (A and B), C45 (C) and C106 (D) residues in his-tagged HMGB1 are all oxidised.

3.4. DISCUSSION

For the purpose of this work, human HMGB1 and three HMGB1 domains were expressed in *E.coli* BL21 (DE3) cells. Approximately 0.75-1 mg of full length human HMGB1 protein was obtained from 1 L of LB medium. Expression of recombinant HMGB1 in bacterial cells has been previously associated with low protein yields (Bianchi 1991; Lee et al., 1998; Li et al., 2003). This has been partially attributed to the toxicity of the 30-residue C-terminal polyacidic tail, which is composed entirely of repeating aspartic and glutamic acid residues. Additionally, it has been reported previously that the HMGB1 protein may be toxic to the *E.coli* cells and may interact with the bacterial DNA (Bianchi 1991). Degradation of HMGB1 by bacterial cells has been previously reported (Bianchi 1991) and a C-terminal truncated HMGB1 protein was also over expressed in the BL21 (DE3) cell cultures (Figure 3.2). Li *et al* demonstrated that both full length and truncated HMGB1 can induce comparable TNF-release in mouse macrophages (Li et al., 2003). Three recombinant HMGB1 mutants, Δ30, A box and B box, were also generated for use in the cellular assays and NMR characterisation. In comparison to the full length protein, the yields of protein obtained for the HMBG1 domains and truncated mutant were considerably higher (Table 3.2). Typically 3-5 mg of Δ30 and 8-10 mg of the A and B box proteins was obtained for 1 L of LB medium. All of the proteins were visualised as a single band on a SDS-PAGE gel.

Efficient removal of LPS contaminants from recombinant protein preparations was of critical importance as contaminating LPS can activate TLR4 and induce a similar biological response to HMGB1 (Hoshino et al., 1999). Until recently, it was believed that the Heat Shock Protein (HSP) 60 and HSP70 induced TNF secretion and APC activation via the TLR4. However, it has now been demonstrated that these effects were in fact a direct result of low amounts of endotoxin contamination (Bausinger et al., 2002; Gao and Tsan 2003; Gao and Tsan 2003). In comparison to other proteins, HMGB1 is reported to have a high affinity for LPS, binding to both the polysaccharide and lipid-A moieties (Youn et al., 2011). Additionally, HMGB1 and LPS have been demonstrated to act synergistically to enhance cytokine production in SFs and it is proposed that this effect is mediated via the formation of a highly active pro-inflammatory complex (Hreggvidsdottir et al., 2009; Wähämaa et al., 2011). Consequently, in agreement with previous findings bacterially expressed HMGB1

had high levels of contaminating LPS (<500 EU/mL) (Bianchi 1991). In comparison, the HMGB1 mutants had considerably less LPS contamination. This suggests that the C-terminal tail of HMGB1 is involved in the interaction and that the HMGB1 mutants have a reduced affinity for LPS (Table 3.2). LPS contaminants were successfully removed using a two-phase Triton-X114 extraction protocol which consistently reduced LPS levels to less than 3 EU/mg of protein.

The work presented in this chapter also describes the NMR characterisation of the recombinant HMGB1 and IL-1β proteins. Uniformly ^{15}N and/or ^{13}C -labelled proteins were expressed and purified in minimal media with final yields of approximately half of that obtained from LB media (Table 3.2). ^{1}H-^{15}N HSQC spectra were collected for the ^{15}N-labelled Δ30, A box, B box and IL-1β proteins. All of the peaks were well resolved and the spectral dispersions were indicative of folded proteins. However, up to 22% of the predicted peaks were missing from the spectrum at pH 7.2 (Table 3.4) due to chemical exchange of the amide protons with water. The removal of contaminating LPS did not alter the Δ30, A box and B box NMR spectra and no significant chemical shift perturbations were observed following Triton-X114 purification (Figure 3.14, Figure 3.15 and Figure 3.16).

Further NMR characterisation was performed for the A box domain and a partial assignment of the ^{1}H-^{15}N HSQC spectrum was undertaken. A pH titration was conducted and NMR spectra were collected at pH 5.5 to 7.2. A total of 84 peaks were expected on the ^{1}H-^{15}N HSQC spectrum and at pH 5.5 only 1% of the peaks were undetectable. In comparison, at pH 7.2 20% of the peaks were missing from the spectrum (Figure 3.11 and Table 3.5). These residues were dispersed across the protein and did not cluster to a specific region. Future NMR spectra were collected at pH 7.2 as this is more physiologically relevant. Additionally, Li *et al* have previously reported that at pH 6.0 the cytokine-inducing activity of HMGB1 is inhibited (Li et al., 2004).

Previous studies have reported conflicting results on the intrinsic pro-inflammatory activity of HMGB1 (Andersson et al., 2000; Rouhiainen et al., 2007; Sha et al., 2008). Recently, Yang *et al* have demonstrated that the redox status of the C23, C45 and C106 residues is critical for the functional activity of the protein. The pro-inflammatory molecular form requires a C23-C45 disulphide bond and a reduced

C106 residue, with other forms of HMGB1 unable to induce cytokine-production (Yang et al., 2011). LC-ESI-MS/MS characterisation of the bacterially expressed recombinant his-tagged HMGB1 protein identified that the C23, C45 and C106 residues were all oxidised (Figure 3.18). However, it was not possible to deduce the specific cysteine modification using this method. HMGB1 expressed in BL21 (DE3) cells is unlikely to contain any post-translational modifications and it can be assumed that the oxidation occurred during the purification procedure. Consequently, the recombinant HMGB1 proteins did not induce IL-6 cytokine production in PBMCs (Figure 3.17). However, evidence within the literature also supports the hypothesis that HMGB1 acts synergistically with endogenous and exogenous molecules to initiate and amplify the inflammatory response and emerging evidence suggests that this mechanism may be independent of the oxidation state (Wähämaa et al., 2011; Leclerc et al., 2013). The synergistic potential of the recombinant HMGB1 has not been examined within this chapter but will be the focus of future experiments.

In conclusion, this chapter describes the successful optimisation of methods to express, purify and characterise recombinant HMGB1, Δ30, A box, B box and IL-1β proteins in *E.coli*. The recombinant proteins contain minimal endotoxin contamination (< 5 EU/mg of protein) and the NMR characterisation has indicated that they are well folded. However, the recombinant HMGB1 proteins did not induce IL-6 cytokine production in PBMCs and this requires further investigation. Previous studies have suggested that HMGB1 and IL-1β act synergistically to promote inflammation. It is proposed that this response is mediated by the formation of a highly active pro-inflammatory complex in which HMGB1 and IL-1β directly interact. However, the molecular interaction between the two proteins requires further investigation; the folded, purified and LPS-free proteins generated in this chapter will be used to elucidate the cellular and biophysical interaction between HMGB1 and IL-1β.

CHAPTER FOUR

IN VITRO CHARACTERISATION OF THE INTERACTION BETWEEN HMGB1 AND IL-1β

TABLE OF CONTENTS

4.1. INTRODUCTION

In 1999, Wang and colleagues identified HMGB1 as a late cytokine mediator of lethal endotoxemia (Wang et al., 1999). Subsequent studies have demonstrated that HMGB1 has a board range of immunological activities. Extracellular HMGB1 promotes inflammation and tissue regeneration by mediating the production of multiple cytokine mediators from macrophages and monocytes, chemotaxis, angiogenesis, cell proliferation and autophagy (Andersson et al., 2000; Orlova et al., 2007; Tang et al., 2010; Andersson and Tracey 2011).

As discussed in Section 1.8.5, human monocytes exposed to recombinant HMGB1 secrete multiple cytokine mediators including TNFα, IL-1α, IL-1β, IL-1RA, IL-6, IL-8 and the MIP (Andersson et al., 2000). It has been proposed that HMGB1 induced cytokine production is mediated via the formation of highly active pro-inflammatory complexes with both endogenous and exogenous molecules (Figure 1.10) (Ivanov et al., 2007; Tian et al., 2007; Sha et al., 2008; Urbonaviciute et al., 2008; Youn et al., 2008; Hreggvidsdottir et al., 2009; Schiraldi et al., 2012). Specifically, HMGB1 has been shown to act in synergy with IL-1β and LPS to enhance NF-κB-mediated cytokine production (Hreggvidsdottir et al., 2009; Garcia-Arnandis et al., 2010; Wähämaa et al., 2011).

The synergistic effect of HMGB1 with IL-1β is of particular interest since both molecules are regarded as classical cytokine mediators that activate related intracellular signalling pathways to mediate a similar range of biological responses. Moreover, the HMGB1 and IL-1β proteins often co-exist at the site of injury or infection, with both danger signals secreted by activated immune cells in response to hepatocyte cell stress or damage.

HMGB1 and IL-1β synergy is not well defined and the molecular mechanism mediating the synergistic response is unknown. In 2008, Sha and colleagues reported that FLAG-tagged HMGB1 expressed in the presence of IL-1β has enhanced pro-inflammatory activity compared to HMGB1 alone. In this study, macrophage and neutrophil cells treated with HMGB1, expressed in the presence of IL-1β, had enhanced pro-inflammatory cytokine production (Sha et al., 2008). Subsequent studies confirmed this finding with HMGB1 and IL-1β also shown to act synergistically on SFs isolated from RA and osteoarthritis (OA) patients

(Hreggvidsdottir et al., 2009; Garcia-Arnandis et al., 2010; Wähämaa et al., 2011). To date, it has been reported that HMGB1 and IL-1β act synergistically to enhance the production of multiple inflammatory mediators including IL-6, IL-8, TNF and MIP (Sha et al., 2008; Hreggvidsdottir et al., 2009; Garcia-Arnandis et al., 2010; Wähämaa et al., 2011). These mediators contribute to the immune response with IL-6, in particular, known to have multiple biological activities that promote hepatic acute phase inflammatory responses and tissue regeneration.

Although HMGB1 and IL-1β have been shown to act synergistically, there are no detailed studies investigating the effects of this interaction within the current literature. Therefore, the overall aim of this chapter was to characterise the cellular response to HMGB1 and IL-1β synergy. This was investigated by addressing the following points:

1. Accessing the synergistic activity of bacterially expressed recombinant HMGB1 and IL-1β proteins.
2. Investigating the dynamics of the synergistic interaction. Specifically, determining the minimal incubation time and optimal conditions required to enhance the inflammatory response
3. Investigating the kinetics of the synergy; do different ratios of HMGB1/ IL-1β show similar synergistic responses?
4. Identifying which domain(s) of HMGB1 mediates the synergistic activity with IL-1β. This was achieved by investigating whether the three HMGB1 mutants (Δ30, A box and B box proteins) act synergistically with IL-1β.
5. Confirming that HMGB1/IL-1β synergy is mediated by the IL-1R
6. Determining if LPS inhibits the synergistic interaction with IL-1β

4.2. MATERIALS AND METHODS

LPS-free recombinant HMGB1 (Full length, Δ30, A box and B box) and IL-1β proteins were expressed and purified from *E.coli* as described in Chapter 2, Sections 2.2 and 2.3. Proteins were characterised as detailed in Chapter 3. The LPS content in all proteins was <5 EU per mg of protein.

SFs were used as a model cell system to investigate HMGB1-IL-1β synergy. Cells were cultured from synovial tissue isolated from arthritic patients undergoing joint replacement surgery at the Karolinska Institute, Stockholm, Sweden, as described in Chapter 2, Section 2.4. Cell experiments were performed as described in Chapter 2, Sections 2.4.2 to 2.4.7. IL-6 cytokine levels were quantified by ELISA (Chapter 2, Section 2.4.8). All results are expressed as absolute IL-6 content ± SD, with the exception of Figure 4.2 where data are expressed as mean IL-6 content ± SEM. Data were analysed as described in Chapter 2, Section 2.4.9.

4.3. RESULTS

4.3.1. HMGB1 and IL-1β act in synergy to increase pro-inflammatory cytokine levels in SFs

The synergistic activity of the recombinant HMGB1 and IL-1β proteins was assessed in SFs isolated from four arthritic patients. The patients were aged between 30-71 years of old and had been clinically diagnosed with either RA or poly-arthritis (Table 4.1). Cells were treated with 100 ng/mL HMGB1 alone or with HMGB1 that had been pre-incubated overnight at 4^{o}C with 0.05 or 0.5 ng/mL IL-1β. Cell supernatants were collected 24 h after stimulation and the IL-6 release was quantified by ELISA.

Table 4.13 Summary of patient information SFs were isolated and cultured from the synovial tissue of four arthritic patients undergoing joint replacement therapy at the Karolinska Institute, Stockholm, Sweden. Background details for each patient are provided.

Cell ID	Gender	Age	Clinical diagnosis
0-247	Female	71	RA
0-248	Male	43	Poly-arthritis
0-253	Female	60	RA
0-255	Female	30	RA

The results for each patient are provided in Figure 4.1. Un-treated fibroblasts or cells treated with HMGB1 or IL-1β alone had no detectable IL-6 release, or IL-6 levels that were below the limit of detection for the ELISA assay (9.37 pg/mL; samples below this limit were assigned a value of 0.1 pg/mL for statistical analysis). However, in all four patients, HMGB1 acted in synergy with both 0.05 and 0.5 ng/mL IL-1β to substantially enhance the IL-6 release. A similar trend was seen in all patients, although the individual cytokine levels differed considerably; for example, when treated with 100 ng/mL HMGB1 in combination with 0.5 ng/mL IL-1β patients 0-247, 0-248, 0-253 and 0-255 had IL-6 levels of 7603 ± 260, 8066 ± 1030, 15,385 ± 2688 and 28,473 ± 127 pg/mL respectively. To account for the inter-patient variability, data are also expressed as a percentage of the 100 ng/mL HMGB1-0.5 ng/mL IL-1β group in Figure 4.2. Statistical analysis confirmed that cells treated with HMGB1 in combination with 0.5 ng/mL IL-1β had significantly increased IL-6 secretion when compared to un-treated cells or cells treated with HMGB1 or IL-1β alone ($p < 0.05$). However, the increase observed in fibroblasts

treated with HMGB1 and 0.05 ng/mL IL-1β was not found to be statistically significant from the control cells. Additionally, the synergistic activity of HMGB1 with ^{15}N-labelled-IL-1β was tested and the results were found to be consistent with the data obtained for the un-labelled proteins (Figure 4.25).

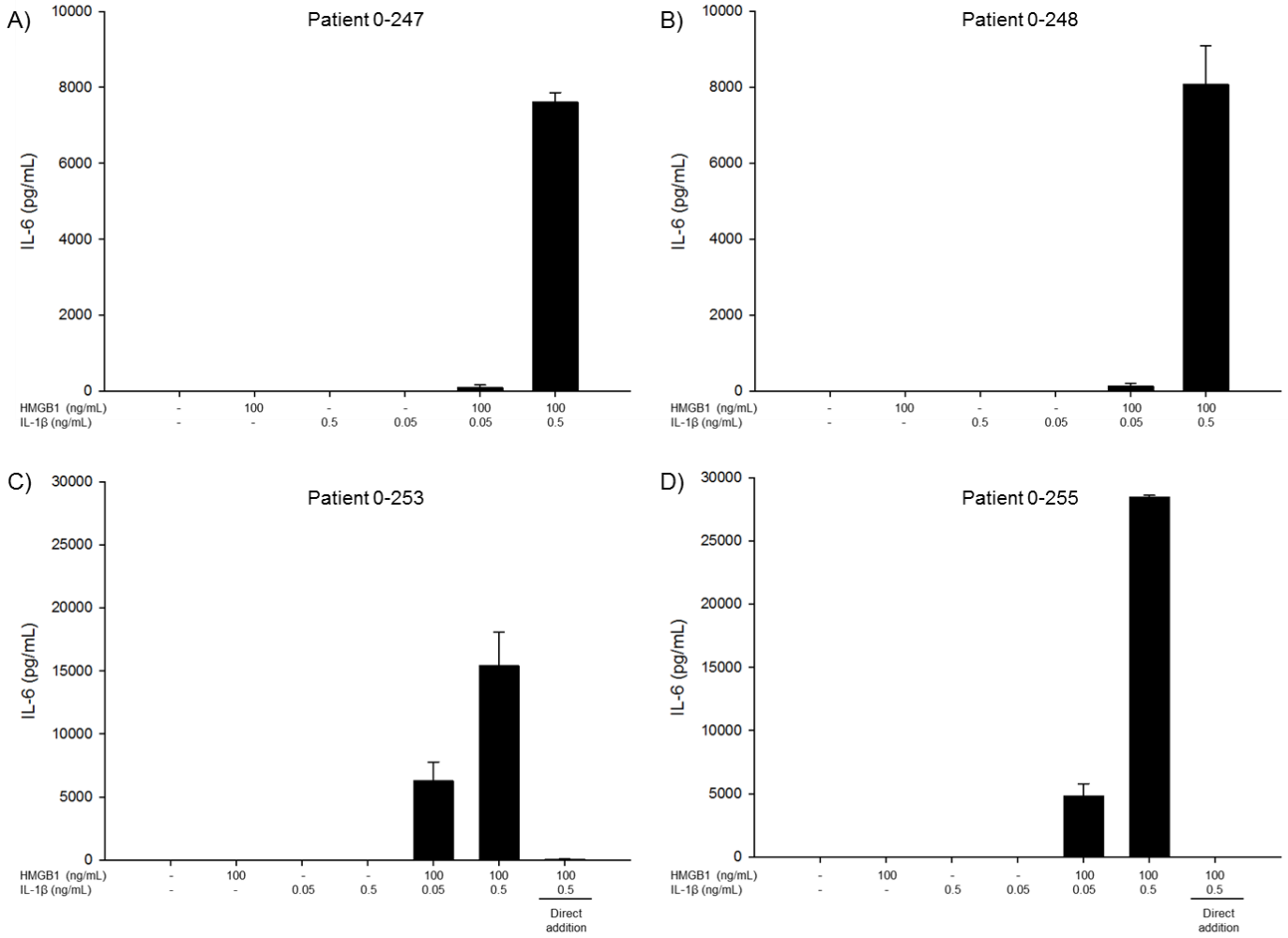

Figure 4.23 HMGB1 and IL-1β act synergistically to enhance the inflammatory response in SFs: Individual patient data SFs were isolated from four arthritic patients and treated with HMGB1 alone or HMGB1 in combination with IL-1β for 24 h. IL-6 cytokine levels were quantified by ELISA. A), B), C) & D) show data for patients 0-247, 0-248, 0-253 and 0-255 respectively. Untreated fibroblasts or cells treated with HMGB1 or IL-1β alone had minimal or no detectable IL-6 release (<9.37 pg/mL; SD values < 7.00 pg/mL). However, treatment with 100 ng/mL HMGB1 that was pre-incubated with 0.5 ng/mL IL-1β enhanced the IL-6 cytokine levels. n = 1 experiment/patient performed in triplicate wells; data are expressed as absolute IL-6 level ± SD.

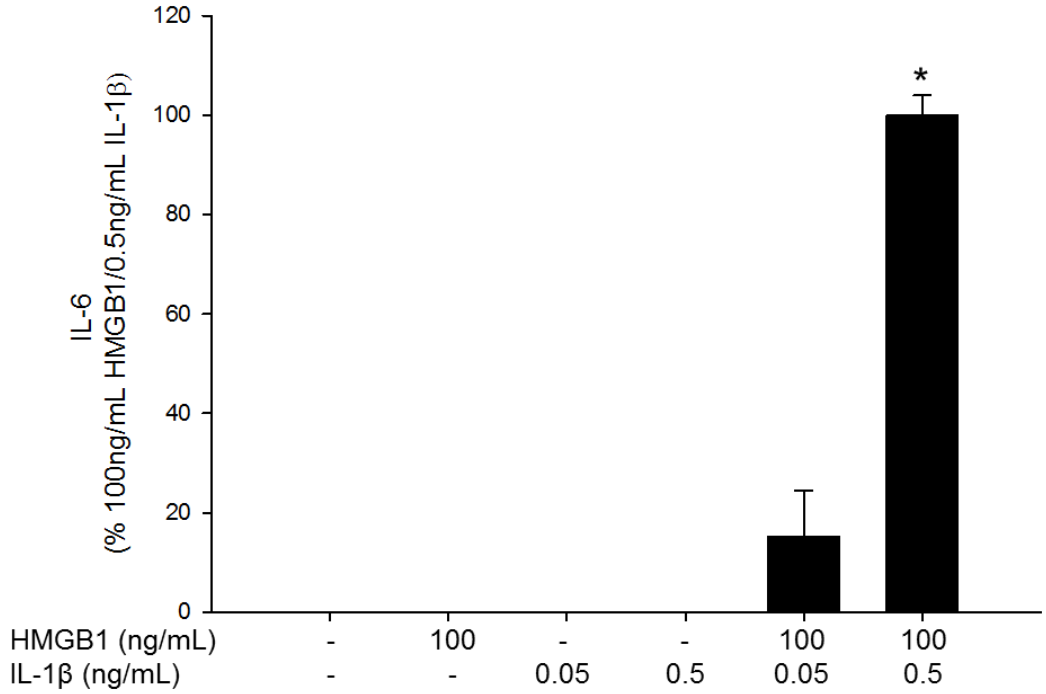

Figure 4.24 HMGB1 and IL-1β act synergistically to enhance the inflammatory response in SFs; combined patient data SFs were isolated from four arthritic patients and treated with 100 ng/mL HMGB1 alone or in combination with IL-1β for 24 h. IL-6 cytokine levels were quantified by ELISA. Un-treated, IL-1β- and HMGB1-treated cells had no detectable IL-6 release (IL-6 levels were below the limit of detection (9.37 pg/mL) and were assigned a value of 0.1 pg/mL for statistical analysis; SEM values for these groups were <0.1%). To account for inter-patient variability, data are expressed as a % of the HMGB1/0.5 ng/mL IL-1β group ± SEM. Data were analysed for statistical significance using a Kruskal Wallis one-way ANOVA on ranks test. Cells treated with HMGB1 in combination with IL-1β had significantly increased IL-6 levels (p <0.05). n = four experiments performed in triplicate wells.

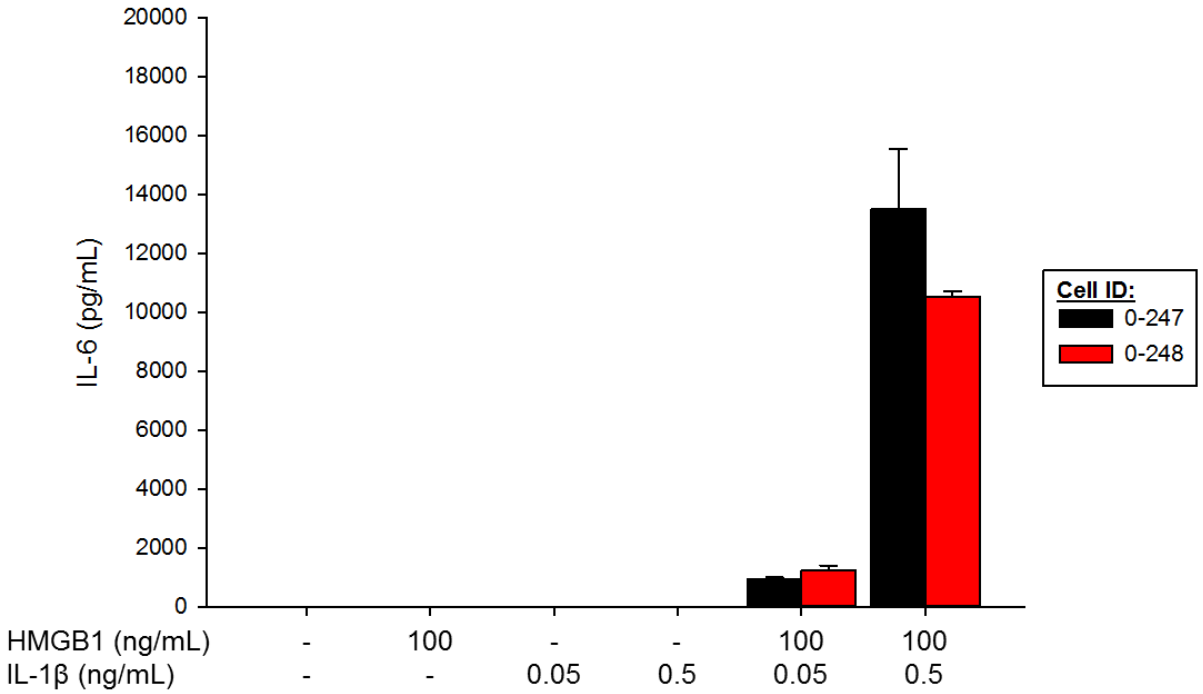

Figure 4.25 HMGB1 acts in synergy with ^{15}N-labelled IL-1β to enhance the IL-6 release from SFs SFs were isolated from two RA patients (0-247 and 0-248) and treated with 100 ng/mL HMGB1 or 0.05/0.5 ng/mL IL-1β alone or following 16 h co-incubation. Un-treated, IL-1β- and HMGB1-treated cells had no detectable IL-6 release (IL-6 levels were below the limit of detection (9.37 pg/mL) and were assigned a value of 0.1 pg/mL for statistical analysis; SD values for these groups = 0). n = two experiments performed in triplicate wells. Data are expressed as IL-6 level ± SD.

4.3.2. HMGB1 enhances the cytokine-stimulating activity of IL-1β in a dose-dependent manner

Previous studies reporting the synergistic interaction between HMGB1 and IL-1β have utilised an excess of the HMGB1 protein in comparison to IL-1β and in the previous expeirment the final molar ratio of HMGB1:IL-1β in the cells was 137:1 or 1370:1, respectively. The aim of this experiment was to determine if HMGB1 enhances the activity of the IL-1β protein in a dose-dependent manner and to investigate whether the synergistic interaction is still relevant at lower molar ratios.

SFs, isolated from two RA patients (0-253 and 0-255), were treated with increasing concentrations of HMGB1 (0-100 ng/mL) that had been pre-incubated with 0.5 ng/mL IL-1β for 16 h at 4^{o}C. This provided a molar ratio range of from 4:1 to 137:1 (HMGB1: IL-1β). Cells were stimulated for 24 h and the IL-6 content was quantified by ELISA. As previously observed, un-treated cells or cells treated with the recombinant proteins alone had minimal or un-detectable IL-6 levels (Figure 4.4). Additionally, fibroblasts treated with 3.25-25 ng/mL HMGB1 together with 0. 5 ng/mL IL-1β (4:1 to 34:1; HMGB1: IL-1β) had low IL-6 cytokine levels (<12 pg/mL). In contrast, cells from both patients had increased IL-6 levels when treated with 50 or 100 ng/mL HMGB1 in combination with I-1β. However, the relationship between the molar ratio used and the IL-6 release did not appear to be linear; for example, 100 ng/mL HMGB1 with 0.5 ng/mL IL-1β resulted in IL-6 levels of 10,332 ± 6.25 and 12,983 ± 9.90 pg/mL in patients 0-253 and 0-255, respectively. In contrast, treatment with 50 ng/mL HMGB1/ 0.5 ng/mL IL-1β induced IL-6 levels of 178 ± 0.20 and 145 ± 0.05 pg/mL in patients 0-253 and 0-255, respectively.

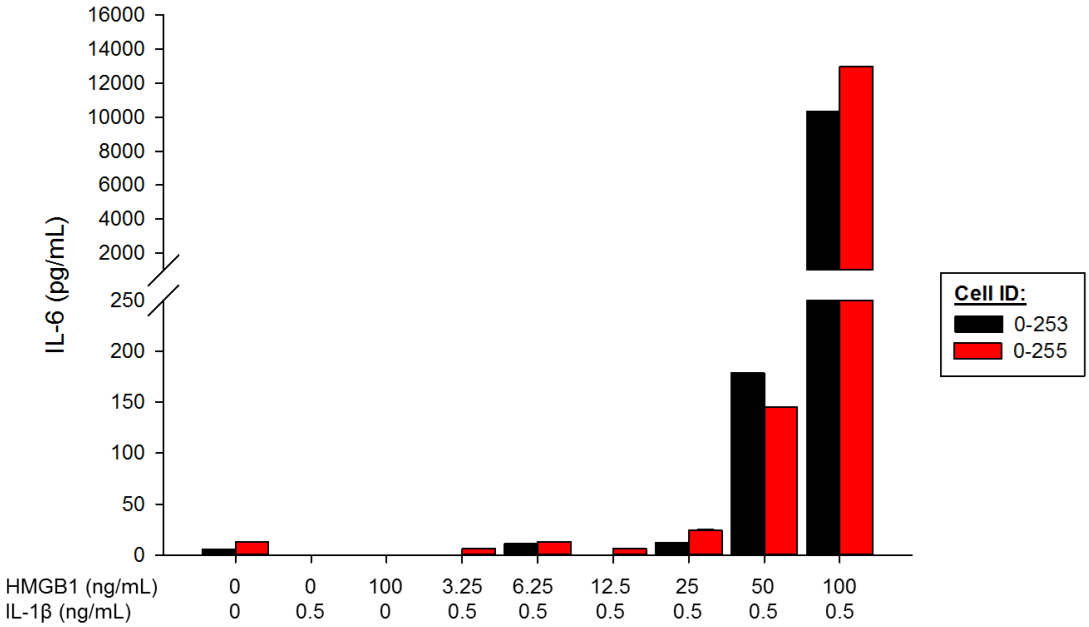

Figure 4.26 The effect of HMGB1 concentration on the synergistic interaction with IL-1β SFs isolated from two RA patients (0-253 and 0-255) were treated with increasing concentrations of HMGB1 (0-100 ng/mL) in complex with 0.5 ng/mL IL-1β. No detectable IL-6 secretion was detected in cells treated with IL-1β alone. However, treatment with IL-1β in combination with HMGB1 increased IL-6 levels considerably in a dose-dependent manner. n = 1 experiment per patient, performed in triplicate wells. Data are expressed as IL-6 value ± SD with all SD values < 10 pg/mL.

4.3.3. Investigating the kinetics of the synergistic interaction between HMGB1 and IL-1β

It has been previously reported that pre-incubation of HMGB1 and IL-1β for 16 h at 4^{o}C is an important prerequisite for the synergistic interaction (Hreggvidsdottir et al., 2009; Wähämaa et al., 2011). However, Garcia-Arnandis *et al* (2010) reported that simultaneous protein addition also results in enhanced cytokine production. Therefore, the aim of this experiment was to determine if pre-incubation of HMGB1 and IL-1β is necessary for the cellular response and if so, to identify the minimal incubation time required.

SFs from two patients (0-253 and 0-255) were stimulated with HMGB1 that had been pre-incubated with IL-1β for 0-24 h prior to cell stimulation. To determine the physiological relevance of the interaction, the proteins were incubated at 4^{o}C, room temperature and 37^{o}C. Cell supernatants were collected after 24 h and the IL-6 release was quantified by ELISA. As can be seen in Figure 4.27, pre-incubation of HMGB1 and IL-1β is not required for the synergistic response and the IL-6 induction was not dependent upon the incubation time. Additionally, in this experiment simultaneous addition of HMGB1 and IL-1β induced an enhanced cellular response resulting in IL-6 levels of 2,796 ± 2.17 pg/mL and 2,785 ± 1.56 pg/mL, in patients 0-253 and 0-255, respectively.

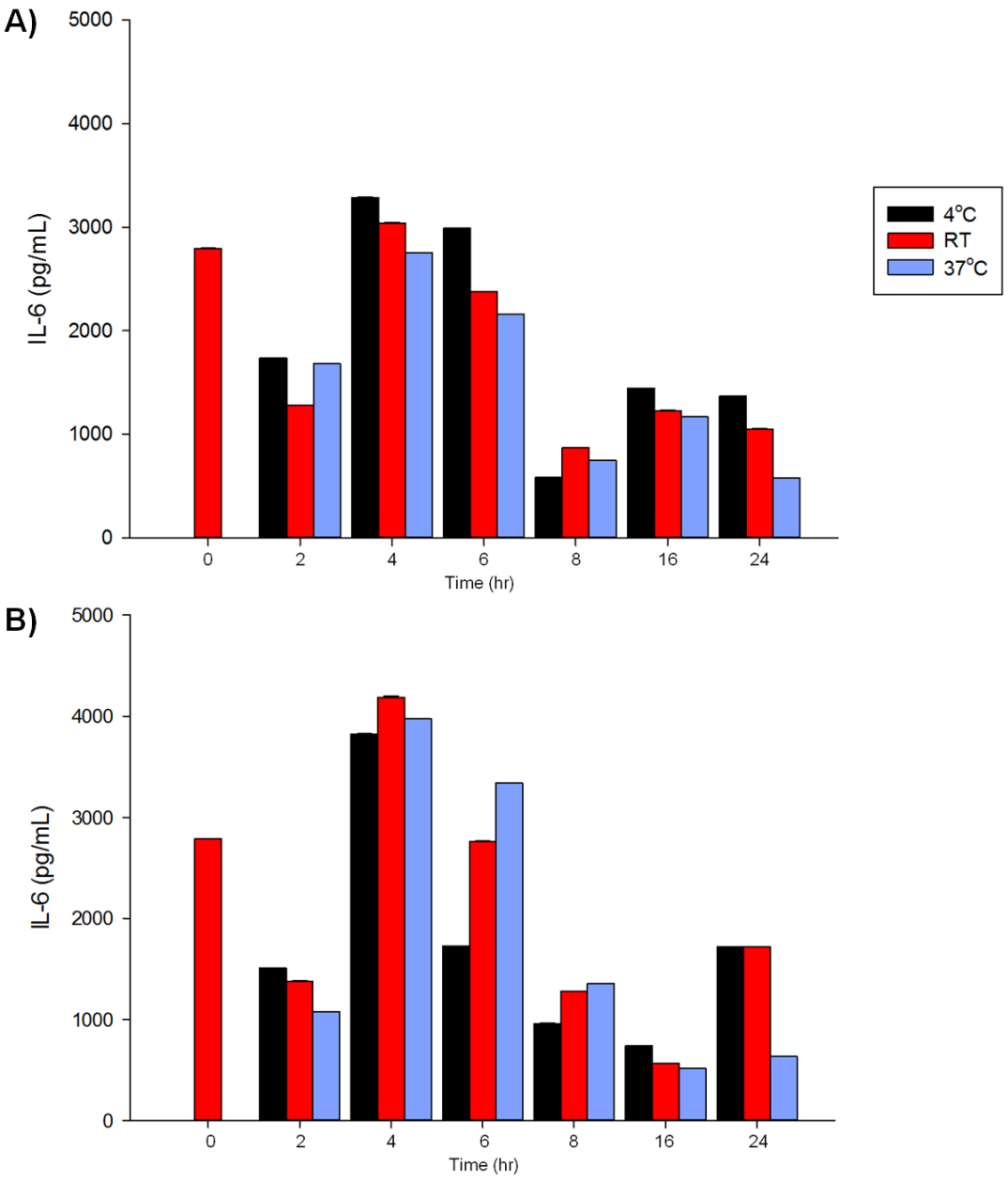

Figure 4.27 The effect of pre-incubation on the synergistic interaction between HMGB1 and IL-1β SFs from two patients (0-253 (A) and 0-255 (B)) were stimulated with 100 ng/mL HMGB1 that had been pre-incubated with 0.5 ng/mL IL-1β for 0-24 h at 4°C, room temperature or 37°C. Cells were stimulated for 24 h, supernatants were collected and the extracellular IL-6 release was quantified by ELISA. Data are expressed as absolute IL-6 value ± SD. n = 1 experiment performed in triplicate wells. All SD values were < 13 pg/mL. Note: Proteins were incubated as a 50 x stock solution (5 µg/mL HMGB1 and 25 ng/mL IL-1β) and diluted in OPTIMEM immediately prior to dosing.

4.3.4. The Δ30 and B box proteins act in synergy with IL-1β to increase IL-6 secretion from SFs but the A box does not interact with IL-1β

To determine which domain of HMGB1 is critical for the synergistic activity observed between HMGB1 and IL-1β, SFs from two RA patients (0-253 and 0-255) were treated for 24 h with four different HMGB1 constructs – full length HMGB1, Δ30, A box or B box - in combination with either 0.05 or 0.5 ng/mL IL-1β. Different concentrations of the four constructs were used (100 ng/mL HMGB1, 86 ng/mL Δ30, 40 ng/mL A box and 35 ng/mL B box) to maintain the same molar ratio across all of the treatment groups (1 IL-1β: 137 HMGB1 or 1 IL-1β: 1370 HMGB1).

As previously observed, no detectable IL-6 secretion was seen in the supernatants obtained from untreated cells. Additionally, all of the recombinant proteins – HMGB1, Δ30, A box, B box and IL-1β – failed to elicit a cellular response alone. However, full length HMGB1, Δ30 and the B box all acted in synergy with IL-1β to noticeably enhance cytokine production in both patients. In SFs isolated from patient 0-255 treatment with HMGB1, Δ30 or the B box in combination with 0.5 ng/mL IL-1β resulted in IL-6 cytokine levels of 28,473 ± 127 pg/mL, 18,491 ± 2388 pg/mL and 18,710 ± 2792 pg/mL, respectively. A similar response was observed with cells isolated from patient 0-253 although to a lesser extent.

Interestingly, the A box did not act synergistically with either concentration of IL-1β and in both patients, treatment with 35 ng/mL A box in combination with 0.5 or 0.05 ng/mL IL-1β failed to induce detectable IL-6 production. This data would suggest that whilst the B box is critical for the interaction between HMGB1 and IL-1β, the A box does not contribute to the synergistic activity.

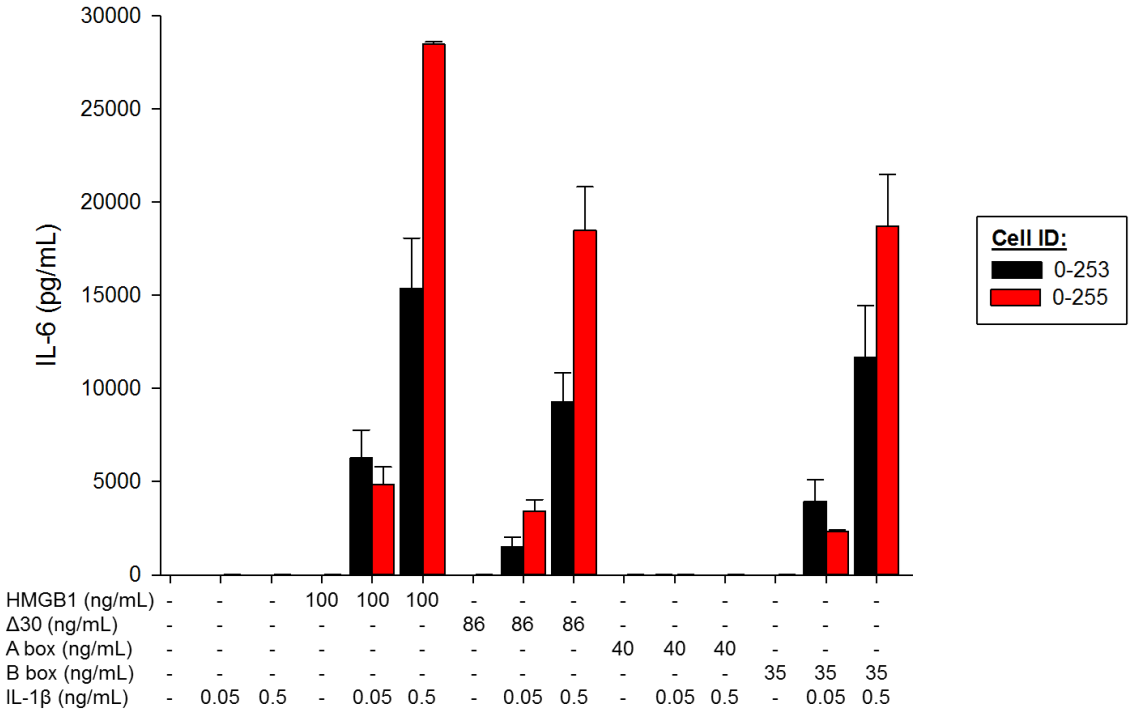

Figure 4.28 HMGB1, Δ30 and B box act in synergy with IL-1β to enhance cytokine production in SFs but the A box does not. SFs were treated with HMGB1, Δ30, A box or B box in combination with 0.5 or 0.05 ng/mL IL-1β for 24 h and IL-6 levels were analysed by ELISA (Note: Different concentrations of the HMGB1 constructs were used to maintain the same molar ratio). The HMGB1, Δ30 and B box constructs acted in synergy with IL-1β to increase IL-6 secretion in both patients (Black = Patient 0-253 and red = Patient 0-255) but the A box did not, indicating that the interaction between HMGB1 and IL-1β is specific to the B box domain. Data are expressed as IL-6 value ± SD. n = two experiments, performed in triplicate wells.

4.3.5. The synergistic activity of HMGB1, Δ30 or the B box with IL-1β is mediated via the IL-1 receptor

To determine if the synergy between HMGB1 and IL-1β is mediated by the IL-1R, the previous experiment (described in Section 4.3.4) was repeated in the presence of anakinra (Kineret®, a synthetic IL-1RA). SFs from patients 0-253 and 0-255 were pre-treated with 5 μg/mL anakinra for 1-2 h prior to cell stimulation. As previously observed, in the absence of anakinra, full length HMGB1, Δ30 and the B box all acted in synergy with IL-1β to promote an increase in IL-6 levels. However, pre-treatment with anakinra inhibited the synergistic effect and resulted in minimal or un-detectable cytokine levels (Figure 4.7).

Additionally, cells from patient 0-253 were pre-treated for 1-2 h with detoxified LPS, a TLR4 antagonist, and stimulated with 100 ng/mL HMGB1 pre-incubated with 0.5 ng/mL IL-1β. Detoxified LPS did not inhibit the enhanced cytokine release induced by HMGB1/IL-1β and in the absence and presence of detoxified LPS, SFs had IL-6 levels of 10,332 ± 6.25 and 10,498 ± 1.40 pg/mL, respectively.

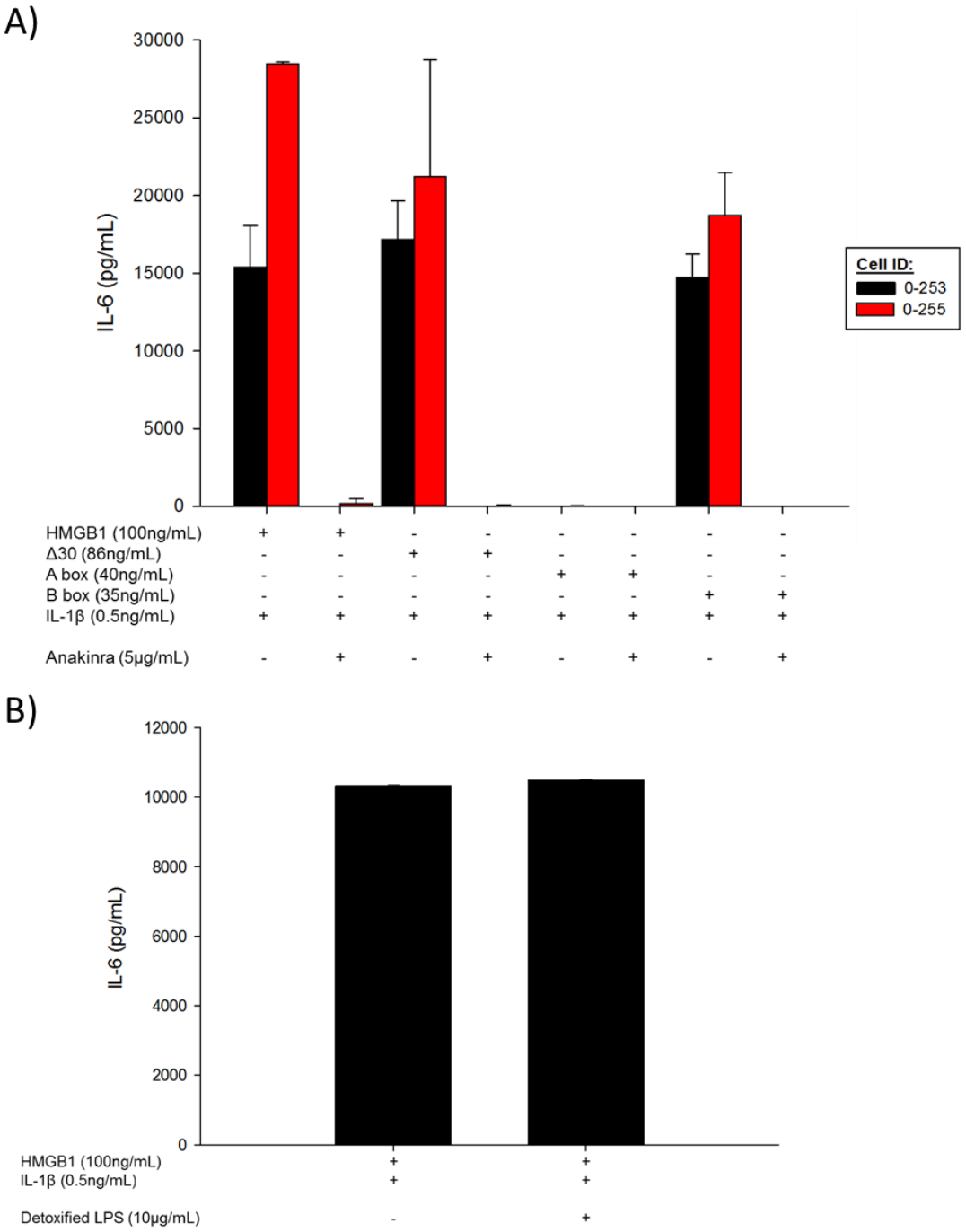

Figure 4.29 The synergistic activity between HMGB1 and IL-1β is mediated via the IL-1R A) SFs were pre-treated with 5 µg/mL anakinra, an IL-1RA, for 1-2 h prior to cell stimulation. Cells were stimulated with HMGB1, Δ30, A box or B box in combination with IL-1β for 24 h and the IL-6 levels were quantified by ELISA. (Data for patient 0-253 are shown in black and in red for patient 0-255). n = two experiments performed in triplicate wells **B)** Cells from patient 0-253 were pre-treated with detoxified LPS, a TLR4 antagonist, prior to stimulation with HMGB1 in combination with IL-1β. n = one experiment performed in triplicate wells. All data are expressed as IL-6 value ± SD (SD values were < 6.25 pg/mL).

4.3.6. HMGB1/IL-1β synergy can be inhibited using sub-optimal concentrations of LPS

HMGB1 is reported to form pro-inflammatory complexes with both IL-1β and LPS and it was hypothesised that LPS may inhibit the synergistic interaction. As previously observed, un-treated fibroblasts and cells treated with HMGB1 or IL-1β alone had minimal or no detectable IL-6 release (Figure 4.30). Additionally, the sub-optimal LPS concentration used in this experiment (25 pg/mL) did not enhance IL-6 levels alone or in combination with HMGB1 or IL-1β. To determine if LPS could prevent the interaction with IL-1β, 100 ng/mL HMGB1 was pre-incubated with LPS for 1 h prior to the addition of 0.5 ng/mL IL-1β. Pre-incubation with LPS partially inhibited the HMGB1/IL-1β induced IL-6 release. In the absence of LPS, HMGB1 and IL-1β induced IL-6 levels of 15,385 ± 2688 pg/mL and 28,473 ± 127 pg/mL in patients 0-253 and 0-255, respectively. However, this was reduced to 7371 ± 444.7 pg/mL and 6370 ± 753.1 pg/mL in the presence of LPS. Additionally, LPS was added to HMGB1/IL-1β combinations for 0-2 h post overnight incubation to determine if LPS could disrupt the synergistic interaction. In patient 0-253, LPS was not able to inhibit HMGB1/IL-1β induced IL-6 release. In cells treated with HMGB1 and IL-1β that had been incubated with LPS for 1 h post overnight incubation IL-6 levels of 17,753 ± 809 pg/mL were detected. Inconsistent results were recorded for patient 0-255 and IL-6 levels of 14,728 ± 279 pg/mL were detected following the addition of LPS for 1 h post overnight incubation with similar results recorded for 2, 0.5 and 0 h post incubation. These levels were considerably lower than the 28,473 ± 127 pg/mL IL-6 detected with HMGB1/IL-1β.

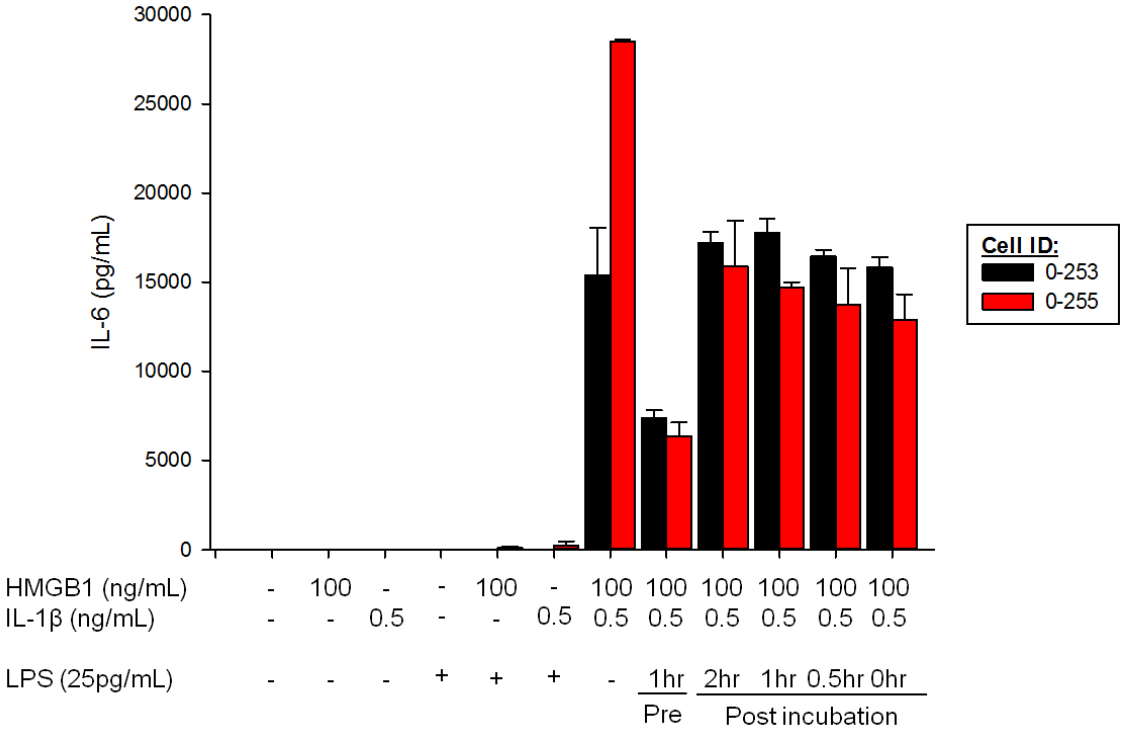

Figure 4.30 Pre-incubation of HMGB1 with sub-optimal concentrations of LPS partially inhibits the synergistic response with IL-1β 100 ng/mL HMGB1 was pre-incubated with 25 pg/mL LPS before (1 h) and addition (0-2 h) the addition of 0.5 ng/mL IL-1β and overnight incubation at 4°C. The HMGB1/IL-1β/LPS combinations were used to stimulate SFs from two patients (0-253 and 0-255) for 24 h. Cell supernatants were collected and IL-6 levels were quantified by ELISA. n = two experiments performed in triplicate wells. Data are expressed as absolute IL-6 value ± SD.

4.4. DISCUSSION

The overall aim of the work presented in this chapter was to characterise the cellular response to the synergistic interaction between HMGB1 and IL-1β. The recombinant HMGB1 and IL-1β proteins were shown to act synergistically on SFs to enhance cytokine production. Fibroblasts treated with 100 ng/mL HMGB1 that had been pre-incubated with 0.5 ng/mL IL-1β had significantly increased IL-6 release compared to un-treated fibroblasts or cells treated with HMGB1 or IL-1β alone ($p < 0.05$) (Figure 4.23 and Figure 4.24). These results are agreement with the findings published by Hreggvidsdottir *et al* (2009). Moreover, recent studies have reported that HMGB1 and IL-1β also act synergistically to promote PGE_2 biosynthesis and to enhance IL-8, TNF, and Matrix Metalloproteinase (MMP) production from SFs (Wähämaa et al., 2011; Leclerc et al., 2013).

Previous studies investigating the synergistic interaction between HMGB1 and IL-1β have utilised an excess of the HMGB1 protein in comparison to IL-1β (1:137 HMGB1: IL-1β) (Hreggvidsdottir et al., 2009; Wähämaa et al., 2011). To determine if the synergistic activity was dose-dependent, SFs were treated with increasing concentrations of HMGB1 (0-100 ng/mL) and IL-1β (0.5 ng/mL). The results suggest that an excess of the HMGB1 protein may be required for the synergistic interaction, with no or minimal IL-6 production detected in cells treated with low levels of HMGB1 (3.25-25 pg/mL) and IL-1β (Figure 4.4). In contrast, both 50 and 100 ng/mL HMGB1 acted in synergy with IL-1β to enhance IL-6 production, although this increase was not linear. When the concentration of HMGB1 was halved, from 100 to 50 ng/mL, the IL-6 secretion was reduced by up 89-fold (Figure 4.4). Overall this data suggests that HMGB1 and IL-1β only act synergistically during injury or infection, when HMGB1 levels are significantly elevated.

It has previously been reported that pre-incubation of HMGB1 and IL-1β, for up to 16 h, may be an important prerequisite for the synergistic response. However, simultaneous protein addition to cell cultures has generated conflicting results and one of the aims of this chapter was to determine if pre-incubation is required. Initially, in agreement with the findings of Hreggvidsdottir *et al* (2009) and Wähämaa *et al* (2011), simultaneous protein addition induced minimal or no-detectable IL-6 secretion (Figure 4.2). However, in the time course, simultaneous

addition of HMGB1 and IL-1β resulted in extracellular IL-6 levels of up to 2800 pg/mL (Figure 4.5). This data is concordant with the results reported by García-Arnandis *et al* (2010) and suggests that pre-incubation of HMGB1 and IL-1β is not required for the synergistic activity. The inconsistent results between experiments might, in part, be due to subtle differences in the experimental set up. Initially, the stock proteins were diluted and incubated overnight at 4^{o}C prior to cell addition. However, in subsequent experiments the stock solutions were diluted immediately prior to cell treatment and this may have been an important factor given the relatively low concentrations that were used in these studies (Li et al., 2004).

The next aim was to determine which domain of HMGB1 is critical for the synergistic activity and SFs were treated with the individual HMGB1 constructs in combination with IL-1β. Full length HMGB1, Δ30 and the B box all acted in synergy with IL-1β to substantially enhance IL-6 release in both patients (Figure 4.28): in patient 0-255 this resulted in IL-6 levels of 28,473 ±127 pg/mL, 18,490 ± 2337 pg/mL and 18,710 ± 2797 pg/mL respectively, and a similar trend was observed for patient 0-253. Previous studies have shown that the B box mediates the pro-inflammatory activity of full length HMGB1 and these results demonstrate, for the first time, that the B box domain is also critical for the synergistic interaction with IL-1β. Li *et al* identified that the amino acids at positions 89-108 are indispensable for HMGB1 induced macrophage activation and TNF release (Li et al., 2003) and further investigation is required to determine if this region also mediates the synergistic interaction with IL-1β. Additionally, these results imply that the c-terminal acidic tail may also contribute to the interaction as treatment with Δ30 in combination IL-1β induced lower levels of IL-6 than HMGB1 in combination IL-1β. The acidic tail has been previously shown to modulate the acetylation of HMGB1 (Pasheva et al., 2004) and the interactions with DNA (Sheflin et al., 1993; Stros et al., 1994; Muller et al., 2001) and nucleosomes (Bonaldi et al., 2002). These results also demonstrate that the A box domain is not required for the synergistic interaction and fibroblasts treated with the A box in combination with IL-1β had low IL-6 secretion, with 7.1 ± 0.9 pg/mL and 23.8 ± 4.2 pg/mL IL-6 detected in patients 0-253 and 0-255, respectively (Figure 4.28). This is not an unexpected finding, previous work has shown that the A box domain is anti-inflammatory and that it can competitively inhibit the pro-inflammatory activity of the full length protein.

Treatment with recombinant A box has been demonstrated to be beneficial in animal models of sepsis, arthritis, pancreatitis, ischemia-reperfusion injury, stroke and transplantation (Yang et al., 2004; Huang et al., 2007; Andrassy et al., 2008; Muhammad et al., 2008; Yuan et al., 2009; Ostberg et al., 2010). The mode of action for the A box inhibition is still not defined and it is not known yet if the A box can inhibit the synergistic interaction between HMGB1 and IL-1β.

Anakinra is a synthetic mimic of the endogenous IL-1RA, which can bind to the IL-1R but cannot recruit the IL-1RAcP, an essential co-factor, and does not initiate intracellular signalling (Figure 1.4) (Arend et al., 1990; Greenfeder et al., 1995). In Figure 4.7 it was demonstrated that the synergistic interaction between HMGB1, Δ30 or the B box with IL-1β can be inhibited using anakinra pre-treatment, indicating that the cellular response is mediated via the IL-1R. In patient 0-255, in the absence of anakinra, 35 ng/mL B box with 0.5 ng/mL IL-1β resulted in IL-6 levels of 18,710 ± 2,791 pg/mL, but in the presence of anakinra this was reduced by 99% to 12.4 ± 3.5 pg/mL. This finding is in agreement with recently published data which indicates that the synergistic activities of HMGB1 are mediated by the partner molecule receptor (Hreggvidsdottir et al., 2011). Additionally, it has been previously shown that HMGB1 and IL-1β do not act synergistically on PBMCs, which express low levels of the IL-1R (Hreggvidsdottir et al., 2009; Leclerc et al., 2013). Furthermore, pre-treatment with detoxified LPS, a competitive TLR4 antagonist, failed to inhibit the synergistic interaction and cells treated with HMGB1/IL-1β in the absence and presence of detoxified LPS had IL-6 levels of 10,332 ± 6.25 pg/mL and 10,498 ± 1.40 pg/mL, respectively.

HMGB1 is also reported to act in synergy with LPS. It has been reported that HMGB1 acts as an alternative LPS binding protein, transferring LPS monomers to the CD14 molecule to initiate TLR4-mediated pro-inflammatory responses (Youn et al., 2008). Recent investigations have identified two potential LPS-binding sites in the HMGB1 protein with boxes A and B reported to bind to the polysaccharide and lipid moieties of LPS, respectively (Hreggvidsdottir et al., 2009; Youn et al., 2011). Consequently, it was hypothesised that suboptimal concentrations of LPS (25 pg/mL) may inhibit the synergistic interaction with IL-1β. Pre-incubation of HMGB1 with LPS inhibited HMGB1/IL-1β induced IL-6 release by up to 52% (Figure 4.30). However, LPS was not able to inhibit HMGB1/IL-1β-induced IL-6

production when added after the overnight incubation (Figure 4.8). These findings support the hypothesis previously proposed, which suggests that HMGB1 and IL-1β promote inflammation by forming a highly active pro-inflammatory complex. Moreover, this data suggests that IL-1β and LPS may compete for the same binding site on the HMGB1 protein and that the interaction with LPS may block the IL-1β binding site and vice versa.

In conclusion, the work presented within this chapter demonstrates that HMGB1 and IL-1β act in synergy, via the IL-1R, to enhance cytokine production from SFs. For the first time, these results identify that the B box domain of HMGB1 is critical for this interaction. Previous studies have proposed that HMGB1 and IL-1β form a binary pro-inflammatory complex that initiates and promotes inflammation and, collectively, the findings from this chapter support that hypothesis. However, biophysical analysis of the interaction between HMGB1 and IL-1β is lacking within the current literature and further investigations are required to elucidate the mechanism of action.

CHAPTER FIVE

BIOPHYSICAL ANALYSIS OF THE INTERACTION BETWEEN HMGB1 AND IL-1β

TABLE OF CONTENTS

5.1. INTRODUCTION

HMGB1 and IL-1β have been shown to act synergistically to enhance inflammation (Sha et al., 2008; Hreggvidsdottir et al., 2009; Garcia-Arnandis et al., 2010; Wähämaa et al., 2011) and it has been proposed that this synergistic activity is mediated by the formation of a highly active pro-inflammatory complex in which HMGB1 and IL-1β directly interact. This hypothesis is supported by previous studies which have demonstrated that HMGB1 is able to interact with a diverse range of endogenous and exogenous molecules to mediate a range of biological activities (Dintilhac and Bernués 2002; Ivanov et al., 2007; Tian et al., 2007; Urbonaviciute et al., 2008; Youn et al., 2008; Schiraldi et al., 2012). Additionally, two independent groups have reported that an interaction between HMGB1 and IL-1β can be detected using immunoprecipitation (IP) methods (Sha et al., 2008; Ferhani et al., 2010). However, a detailed biophysical analysis of the molecular relationship between HMGB1 and IL-1β is not available within the current literature.

Protein NMR spectroscopy is a powerful biophysical technique that can be used to obtain physical, chemical and electronic information about proteins in solution. It is routinely used to characterise intermolecular interactions and can be used to identify the specific residues involved in a binding interaction. Protein NMR has been previously used to investigate the interactions of the HMGB1 protein. The interaction between the A and B boxes with the c-terminal acidic tail has been elucidated (Watson et al., 2007; Stott et al., 2010). Additionally, the binding to DNA and linker histones, which is essential for the physiological role of HMGB1, has been extensively characterised using this technique (Stott et al., 2006; Cato et al., 2008). Furthermore, Schiraldi *et al* have recently reported that HMGB1 forms a heterocomplex with the chemokine, CXCL12. They proposed a model in which one molecule of HMGB1 binds to two molecules of CXCL12 via the A and B boxes. The complex was shown to have enhanced binding to the CXCR4 receptor and increased cell infiltration (Schiraldi et al., 2012).

Evidence within the literature suggests that HMGB1 may form a similar complex with IL-1β. Therefore, the aim of this chapter was to conduct a comprehensive biophysical analysis of the interaction between HMGB1 and IL-1β using NMR methodologies. Specifically, this work was performed to test the hypothesis that

HMGB1 and IL-1β directly interact to form a binary complex and to identify the residue(s) involved in the binding interaction. The choice of using NMR for these studies is based on the fact that the method is able to detect interactions over a wide range of binding affinities. Furthermore, if binding is detected, the binding interface between HMGB1 and IL-1β can be determined since the resonance assignments of both proteins are available.

5.2. MATERIAL AND METHODS

LPS-free recombinant HMGB1, Δ30, A box, B box and IL-1β proteins were expressed and purified from *E.coli* as detailed in Chapter 2 and Chapter 3. The interaction between IL-1β and each of the individual HMGB1 constructs was determined using 2D ^{1}H-^{15}N HSQC experiments as described in Chapter 2, Section 2.5.

5.3. RESULTS

5.3.1. Investigating the intermolecular interaction between HMGB1 and IL-1β

Firstly, the interaction between full length HMGB1 and IL-1β was examined using NMR spectroscopy. ^{1}H-^{15}N HSQC spectra were collected on a 600 MHz Bruker Avance II spectrometer equipped with triple resonance cryoprobes. To allow a direct comparison to be made, the spectra were collected using identical acquisition parameters: 32 scans with 160 increments at a resolution in the indirect dimension of 21.00 Hz. To reproduce the conditions used in the cellular experiments (described in Chapter 4) the NMR spectra were collected in PBS at pH 7.2 and the HMGB1 and IL-1β proteins were incubated for 16 h at 4^{o}C prior to the experimental analysis.

Initially, a ^{1}H-^{15}N HSQC spectrum was collected on a 25 μM ^{15}N-labelled IL-1β sample in the absence of HMGB1 at 25^{o}C. The peaks on the spectrum were well resolved and dispersed and indicate that the IL-1β protein was well folded (Figure 5.31; black spectrum). Next, a 12.5 μM aliquot of the IL-1β protein was incubated overnight with 11.5 μM HMGB1; this resulted in a molar ratio of approximately 1:1 IL-1β: HMGB1. The HSQC spectrum was recorded again and an overlay of the spectra for IL-1β alone and in the presence of HMGB1 is presented in Figure 5.31. No interaction between HMGB1 and IL-1β was detected, under the conditions employed in this experiment, since there were no significant chemical shift perturbations for the IL-1β residues following the addition of HMGB1. This is illustrated more clearly in Figure 5.32, where a section of the amide region is shown in greater detail.

Next, the IL-1β and HMGB1 proteins were concentrated and the experiment was repeated at 10^{o}C (or 283 K) using a higher concentration of protein. A HSQC spectrum was collected for 100 μM ^{15}N-IL-1β in the absence of HMGB1 (Figure 5.33; black spectrum) using 64 scans with 250 increments at a resolution in the indirect dimension of 12.65 Hz. A 50 μM ^{15}N-IL-1β sample was then incubated overnight with 195 μM HMGB1 (1:4 molar ratio) and the spectrum were recorded again using 256 scans with 384 increments at a resolution in the indirect dimension of 12.67 Hz (Figure 5.33; red spectrum). For clarity an expanded section of the amide region of the spectra is also provided in Figure 5.4. Small chemical shift

perturbations were observed for five of the IL-1β residues in the presence of an excess of HMGB1. The deposited NMR spectra for IL-1β was obtained from the Biological Magnetic Resonance Bank (BMRB) database (BMRB accession number 434 (Driscoll et al., 1990; Ulrich et al., 2008)) and it was possible to identify two of the residues that displayed small chemical perturbations as histidine 30 (H30) and asparagine 129 (N129). Further analysis revealed that these two residues are both surface exposed and are in close physical proximity to each other (Figure 5.35). However, the identity of the other three residues could not be determined as it was not possible to transfer the complete IL-1β assignment from the deposited data to the current spectra. This was due to differences in the ionic strength and pH between IL-1β in PBS and in 100 mM sodium acetate-d_3 pH 5.4, the conditions under which the assignment was deposited in the BMRB.

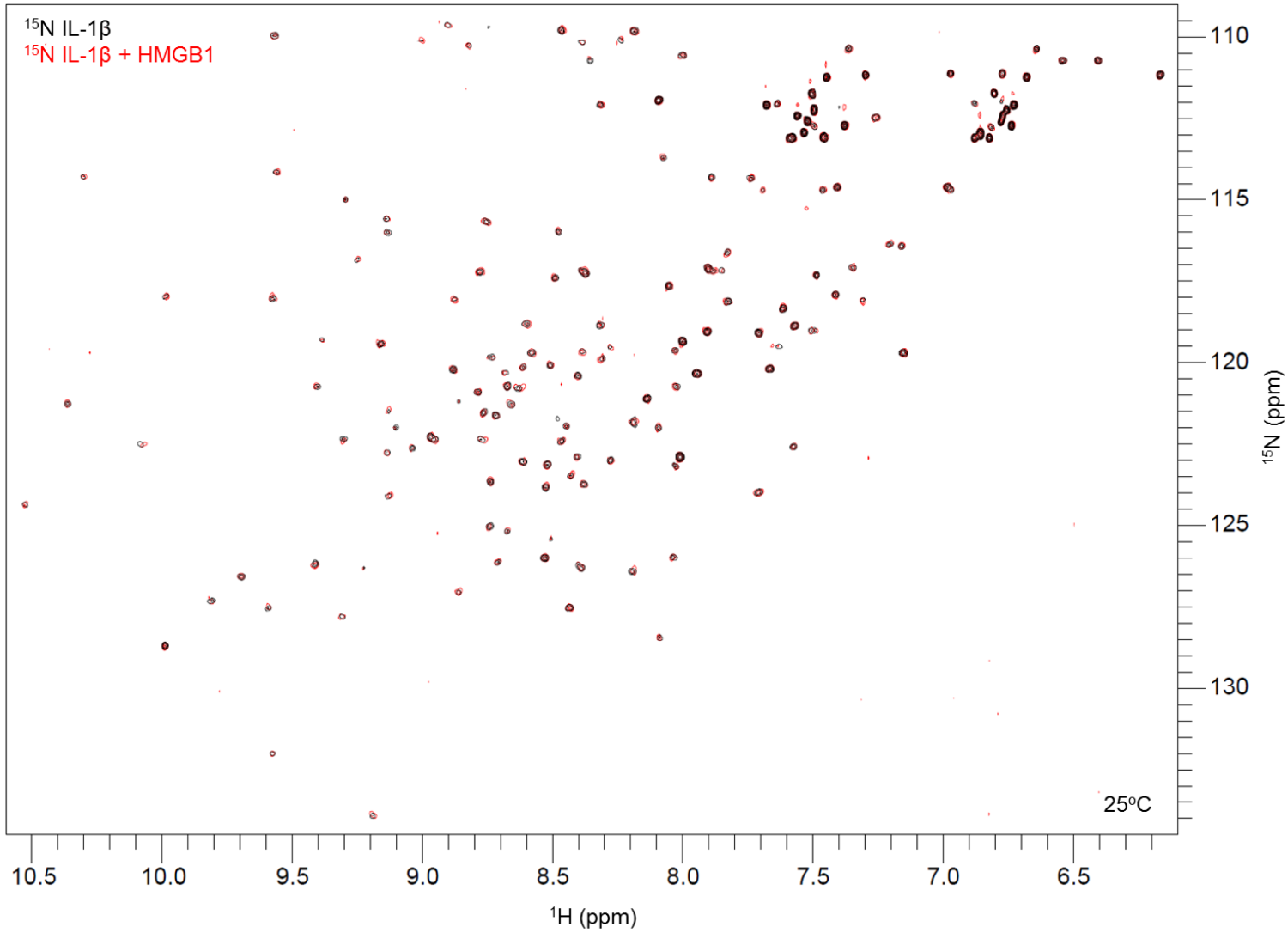

Figure 5.31 ^{1}H-^{15}N HSQC spectra for ^{15}N-IL-1β in the presence and absence of full length HMGB1 ^{1}H-^{15}N HSQC spectra were recorded for ^{15}N-labelled IL-1β in the absence and presence of HMGB1 on a 600 MHz Bruker Avance II spectrometer at 25°C (298 K) using identical acquisition parameters (^{15}N res = 21.00 Hz). Spectra were recorded on a 25 µM ^{15}N-labelled IL-1β alone (black) and for a 12.5 µM ^{15}N-IL-1β sample in the presence of 11.5 µM HMGB1 (red). No significant chemical shift changes were noted in the presence of HMGB1.

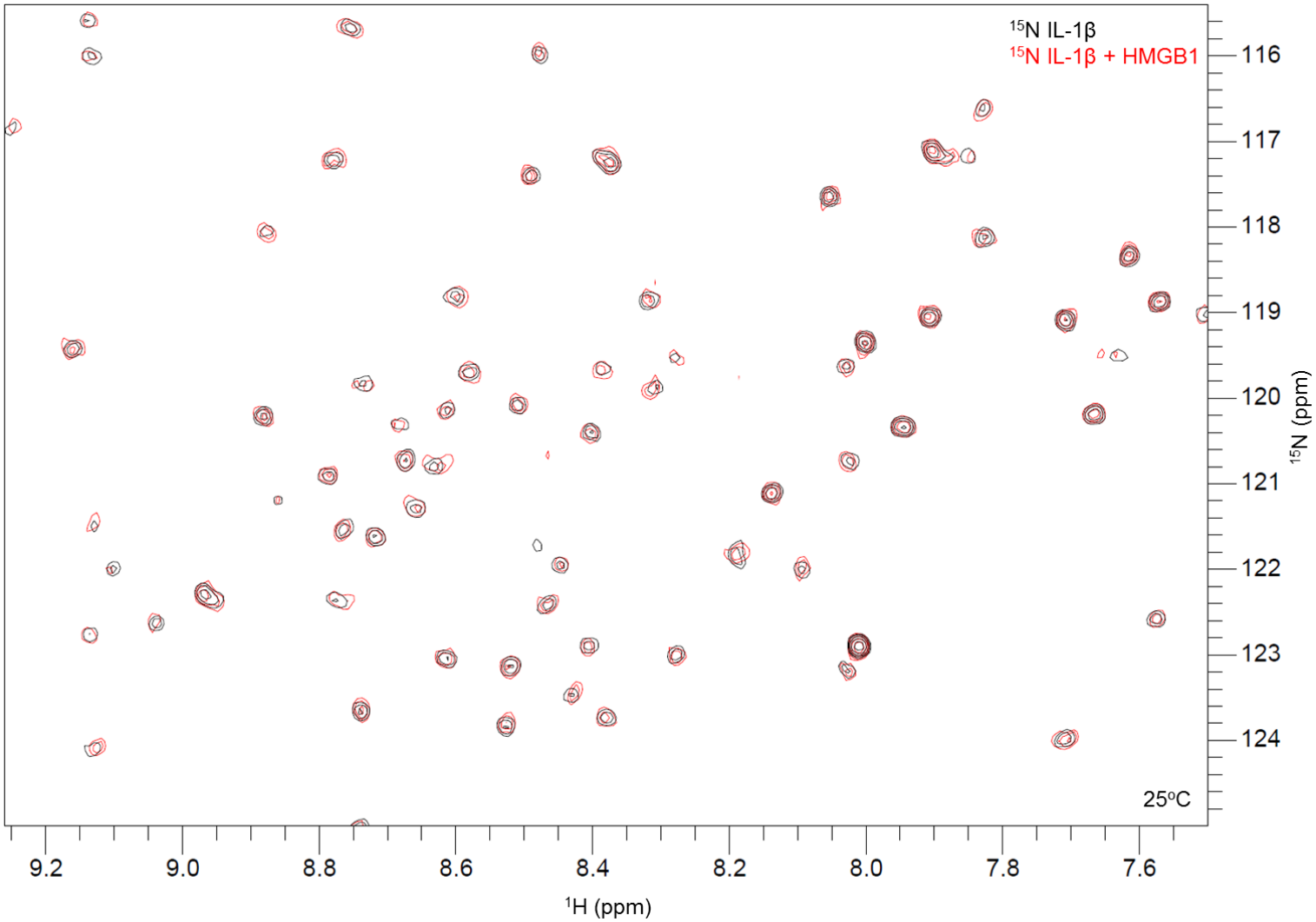

Figure 5.32 An expanded view of the amide region of the ^{1}H-^{15}N IL-1β HSQC spectra in the presence and absence of full length HMGB1 ^{1}H-^{15}N HSQC spectra were recorded for ^{15}N-IL-1β in the absence and presence of HMGB1 on a 600 MHz Bruker Avance II at 25°C (298 K) using identical acquisition parameters (^{15}N res = 21.00 Hz). Spectra were recorded on a 25 µM ^{15}N-labelled IL-1β alone (black) and for a 12.5 µM ^{15}N-IL-1β sample in the presence of 11.5 µM HMGB1 (red). For clarity an expanded section of the backbone amide region is shown. No significant chemical shift changes were detected following the addition of HMGB1.

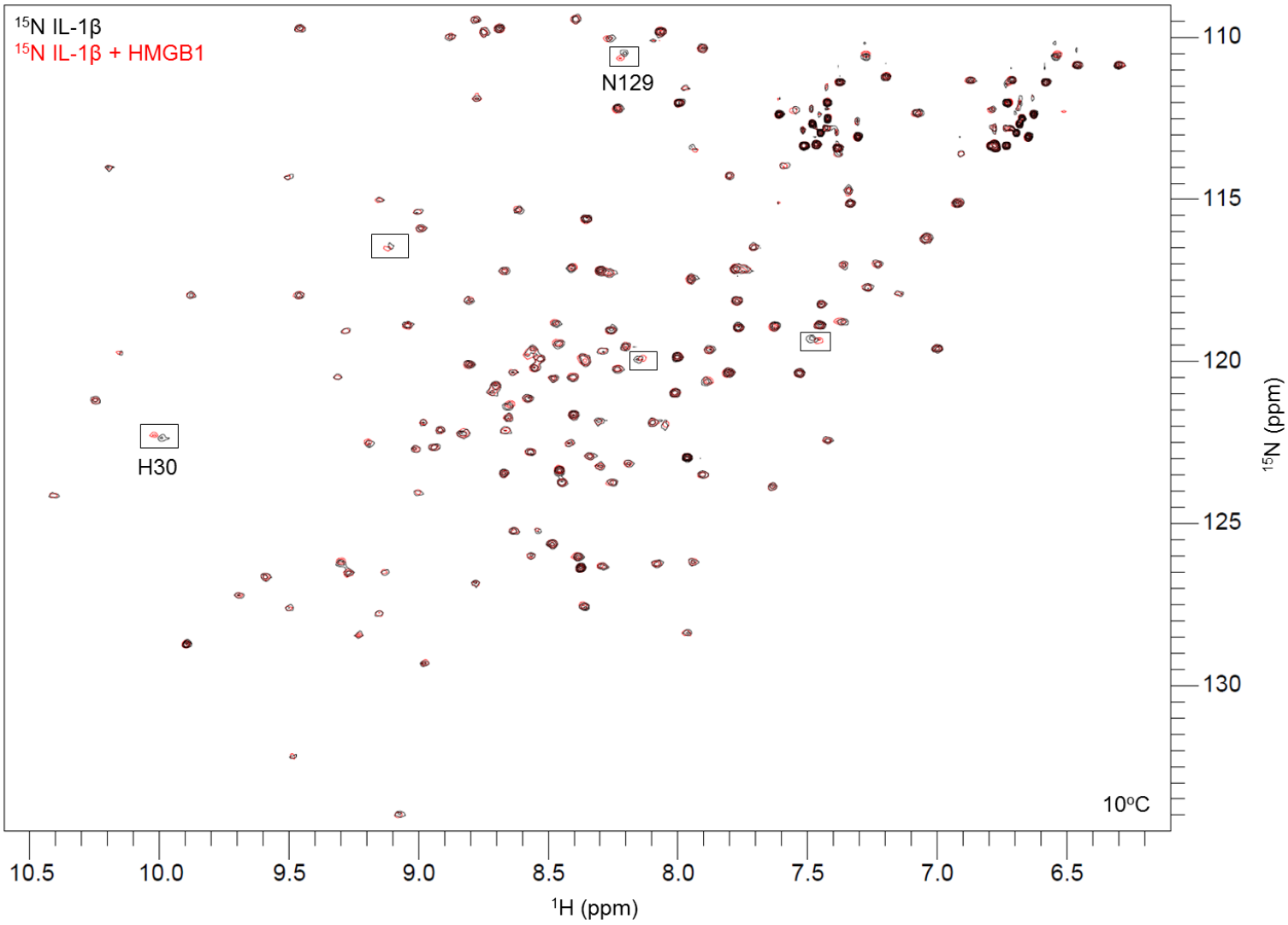

Figure 5.33 Full ^{1}H-^{15}N HSQC spectra recorded for ^{15}N-labelled IL-1β at 10°C in absence and presence of HMGB1 HSQC spectra were recorded on a 600 MHz Bruker Avance II spectrometer at 10°C (283 K) in PBS, pH 7.2, using an identical resolution in the indirect dimension of 12.67 Hz. Spectra were recorded for 100 µM IL-1β alone (black) and for 50 µM IL-1β in the presence of 195 µM HMGB1 (red; 1:4 molar ratio). Minor changes in the chemical shift of five peaks were observed (as indicated) and two of these residues could be assigned as H30 and N129.

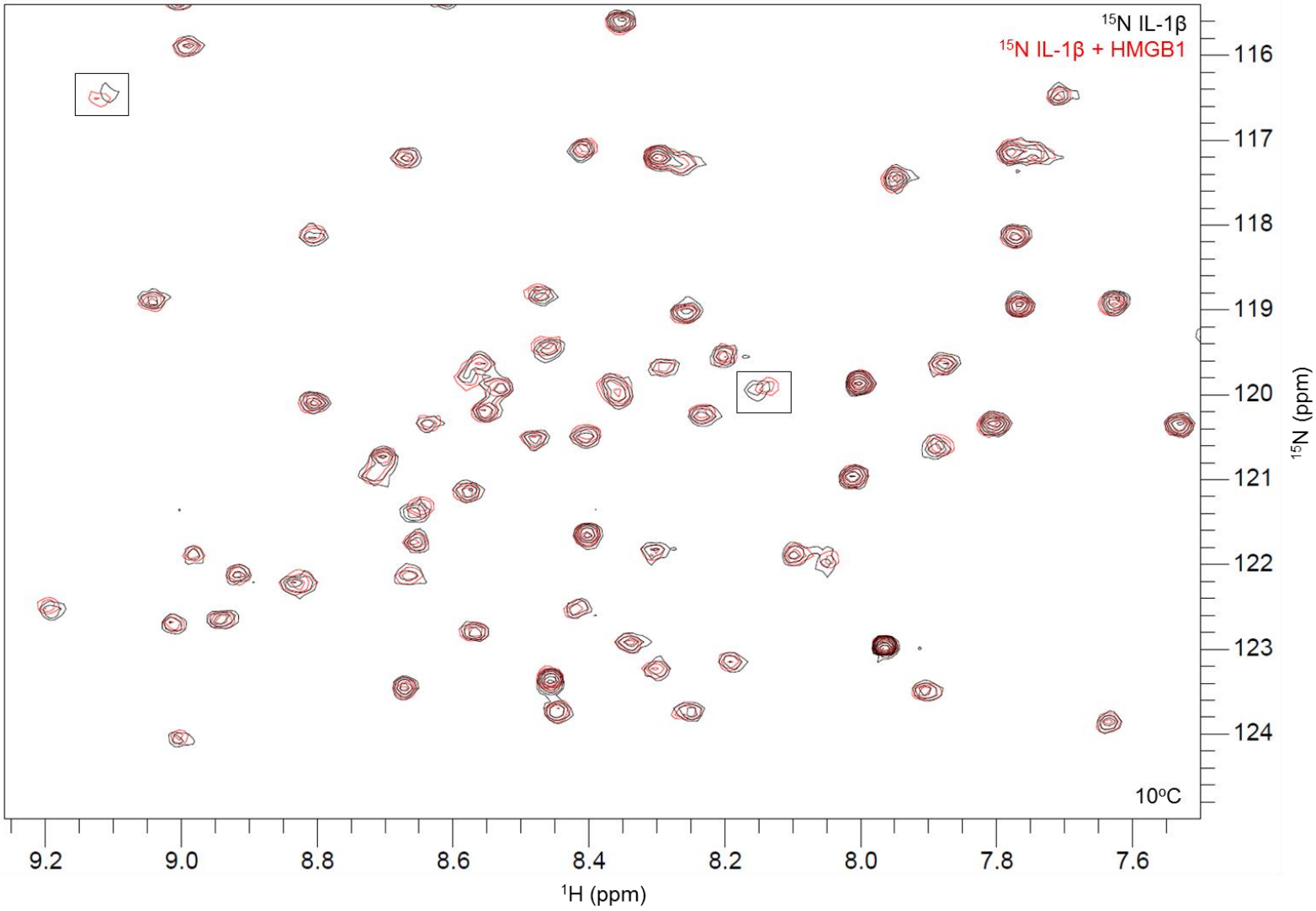

Figure 5.34 An expanded view of the amide region of the ^{1}H-^{15}N IL-1β HSQC spectra in the presence and absence of full length HMGB1 recorded at 10°C HSQC spectra were recorded on a 600 MHz Bruker Avance II spectrometer at 10°C (283 K) in PBS, pH 7.2, using an resolution in the indirect dimension of 12.67 Hz. The black spectra show 100 µM IL-1β alone and the red spectra correspond to 50 µM IL-1β with 195 µM HMGB1. An expanded region is shown for clarity with perturbations in the chemical shifts of two unassigned residues observed within this region (as indicated in the boxed regions).

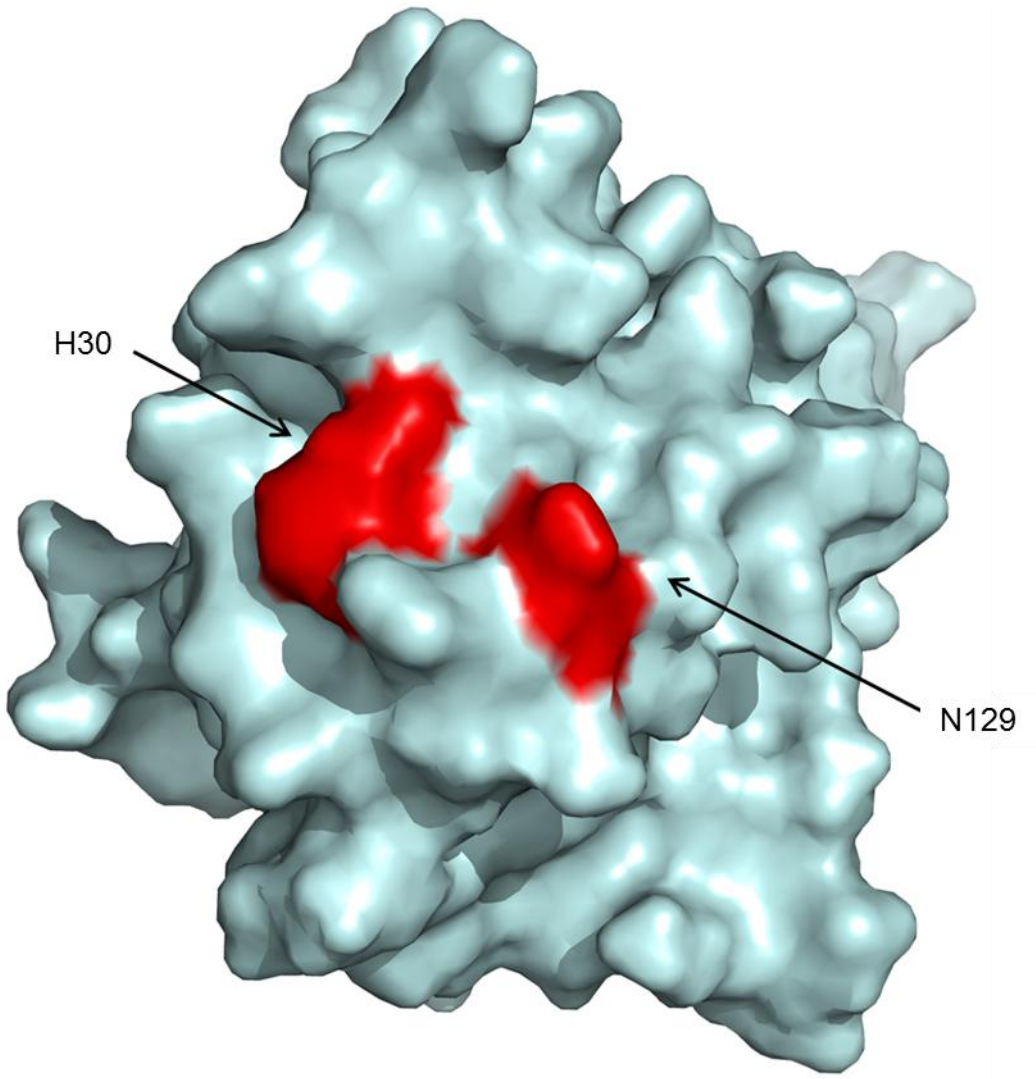

Figure 5.35 3D structure of the IL-1β protein highlighting the H30 and N129 residues NMR analysis detected small chemical shift perturbations for the H30 and N129 residues in the IL-1β protein in the presence of a 4:1 excess of HMGB1. As can be seen these residues are both surface exposed and in close physical proximity to each other. Figure was produced using PyMOL (PyMoL).

5.3.2. Investigating the intermolecular interaction between Δ30 and IL-1β

Due to the acidic nature of the C-terminal tail (residues 185-215) it was decided that further investigations into the interaction between HMGB1 and IL-1β would be carried out using the more stable Δ30 construct. In Chapter 4, it was demonstrated that the Δ30 protein acted in synergy with IL-1β to enhance IL-6 release in SFs (Chapter 4, Section 4.2.4). NMR spectra were collected on a 10 μM ^{15}N-labelled Δ30 sample in the absence and presence of 90 μM unlabelled IL-1β (1:9 molar ratio) on an 800 MHz Avance II Bruker spectrometer at 25^{o}C (298 K) in PBS at pH 7.2. To allow a direct comparison to be made between the spectra, identical acquisition parameters were used: 192 scans with 256 increments at a resolution in the indirect dimension of 15.80 Hz. An overlay of the ^{1}H-^{15}N HSQC spectra is presented in Figure 5.36. The Δ30 protein appeared to be well folded as the peaks on the HSQC spectra were well resolved and dispersed. When an excess of the IL-1β protein was added to the sample no significant changes in the chemical shift of the peaks was observed. It may appear that some small peaks disappear from spectrum following the addition of IL-β, however this is not the case as all of the peaks are present when the contour levels are increased. The reduction in the intensity is an unavoidable result of dilution effects. For increased clarity and to reduce the background noise levels the spectra are presented at reduced contour levels.

Next, the reverse experiment was conducted with ^{1}H-^{15}N HSQC spectra recorded for 100 μM IL-1β in the absence and presence of a three-fold excess of unlabelled Δ30 protein. The experiment was performed on an 800 MHz Bruker Avance II spectrometer in 20 mM phosphate, 100mM potassium chloride, and 10 mM DTT at pH 6.8 using comparable acquisition parameters: 4 scans with 210 increments at a resolution in the indirect dimension of 16.99 Hz. As shown in Figure 5.7 and Figure 5.8 minor chemical shift perturbations were observed for a number of the IL-1β residues; however, this did not appear to be a specific effect as most of the residues on the spectrum displayed some small perturbation. As observed previously (Figure 5.3), the H30 and N129 residues displayed the greatest chemical perturbations. However, it was difficult to replicate these results in subsequent experiments.

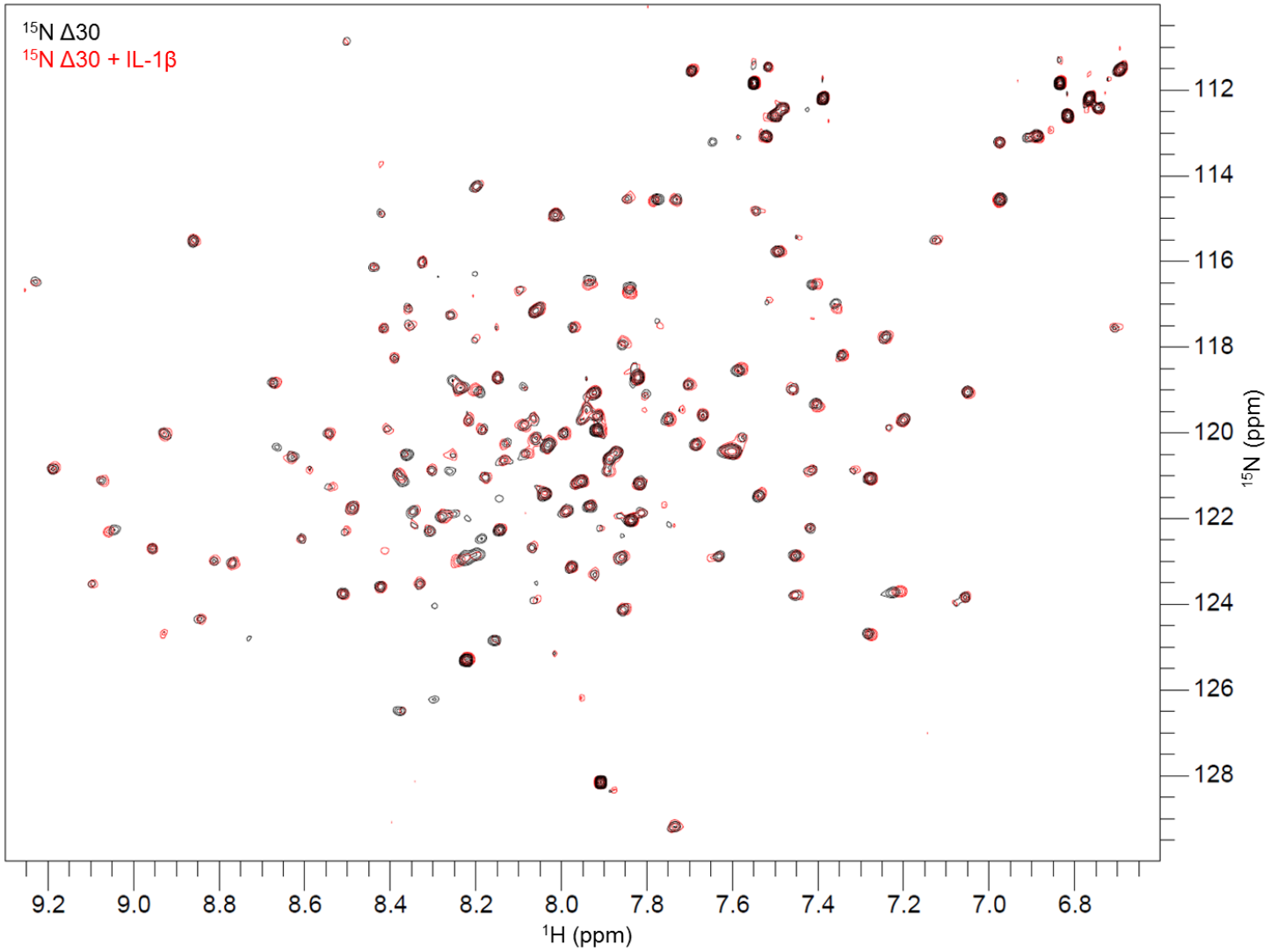

Figure 5.36 Effect of IL-1β on the ^{15}N-HSQC spectra of Δ30 ^{1}H-^{15}N HSQC spectra were collected using a 800 MHz Bruker Avance II spectrometer at 25^{o}C (298 K) on a 10 µM ^{15}N-labelled his-tagged Δ30 sample in PBS, pH 7.2. Spectra were recorded for Δ30 alone (black) and in the presence of 90 µM IL-1β (red) using identical acquisition parameters: NS = 192, increments = 256 and ^{15}N res = 15.80 Hz. No significant changes in the chemical shifts of the peaks were observed in the presence of IL-1β. From the spectra presented it would appear that some of peaks disappear following the addition of IL-1β. However, this was due the low concentration of the ^{15}N B box protein and all peaks were present when the contour levels were increased.

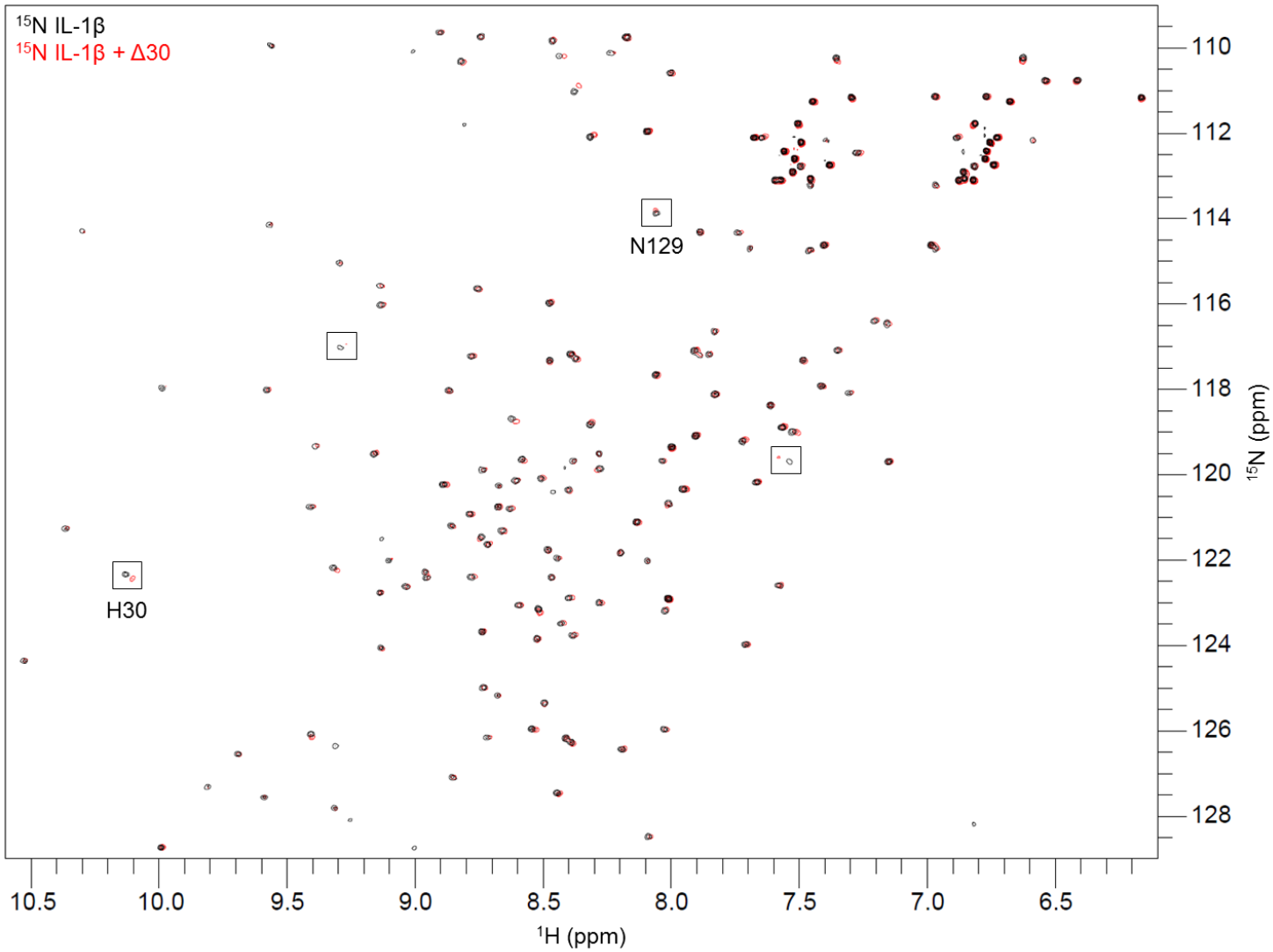

Figure 5.37 ^{1}H-^{15}N HSQC spectra for ^{15}N-labelled IL-1β before and after the addition of a three-fold excess of Δ30 NMR spectra were collected for 100 µM IL-1β in the absence and presence of 300 µM Δ30 on a Bruker 800 MHz spectrometer at 25^{o}C (298 K). Samples were analysed in 20mM potassium phosphate, 100mM potassium chloride and 10 mM DTT, pH 6.8, using 4 scans with 210 increments at a FID resolution of 16.99. Minor chemical shift perturbations were observed for the majority of residues and the residues that showed the greatest perturbations are indicated.

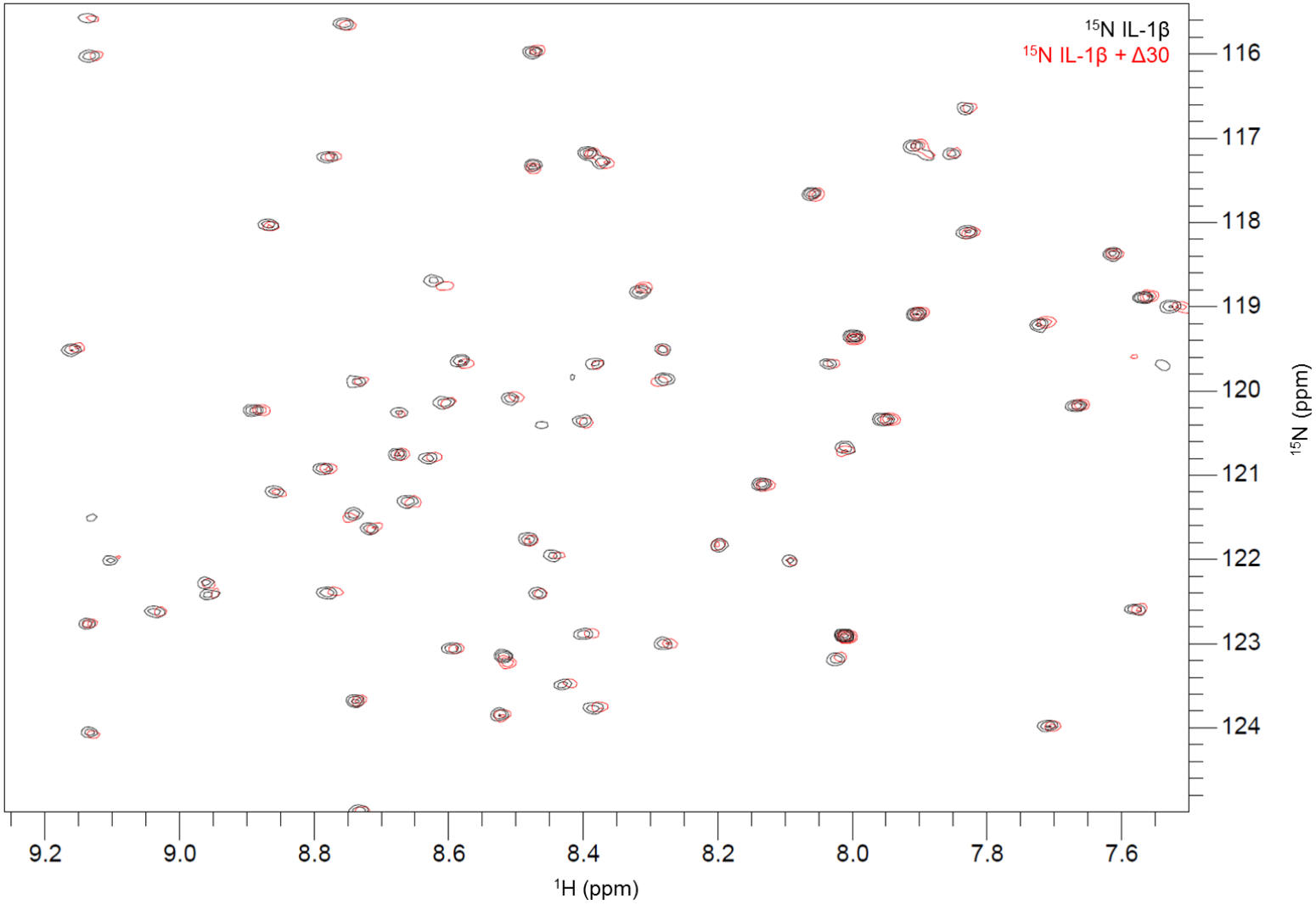

Figure 5.38 An expanded view of the amide region of the ^{1}H-^{15}N HSQC spectra for ^{15}N-labelled IL-1β in the absence and presence of Δ30 NMR spectra were collected for 100 µM IL-1β in the absence and presence of 300 µM Δ30 on a Bruker 800 MHz spectrometer at 25°C (298 K). Samples were analysed in 20 mM potassium phosphate, 100 mM potassium chloride and 10 mM DTT, pH 6.8, using 4 scans with 210 increments at a resolution in the indirect dimension of 16.99 Hz. Minor chemical shift perturbations were observed.

5.3.3. Investigating the intermolecular interaction between the B box and IL-1β

In Chapter 4 it was demonstrated that the B box domain of HMGB1 is critical for the synergistic interaction with IL-1β. The association between the B box and IL-1β was investigated using 2D NMR analysis, to determine if a direct interaction could be detected. NMR spectra were collected on an 800 MHz Bruker Avance II spectrometer equipped with triple resonance cryoprobes at 25^{o}C (298 K) using identical acquisition parameters: 192 scans with 256 increments at a resolution in the indirect dimension of 15.80 Hz. ^{1}H-^{15}N HSQC spectra were collected on a 10 μM ^{15}N-labelled B box sample before and after the addition of 100 μM IL-1β (B box: IL-1β ratio of 1:10). Samples were analysed in PBS at pH 7.2 to replicate the cellular buffer conditions.

An overlay of the two spectra is presented in Figure 5.9. In both cases the peaks are well defined and dispersed and the spectra are indicative of a folded B box protein. Following the addition of an excess of un-labelled IL-1β the HSQC spectra showed little variation; no significant change in the chemical shift of the peaks was observed. From Figure 5.9 it would appear that some of peaks disappear from the spectrum after the addition of IL-1β. However, this was due to the dilution effects of the ^{15}N-B box protein used in the experiment and all of the peaks were present when the contour levels were increased. However, the spectra are presented at reduced contour levels in the Figure for increased clarity as the background noise levels also increased significantly.

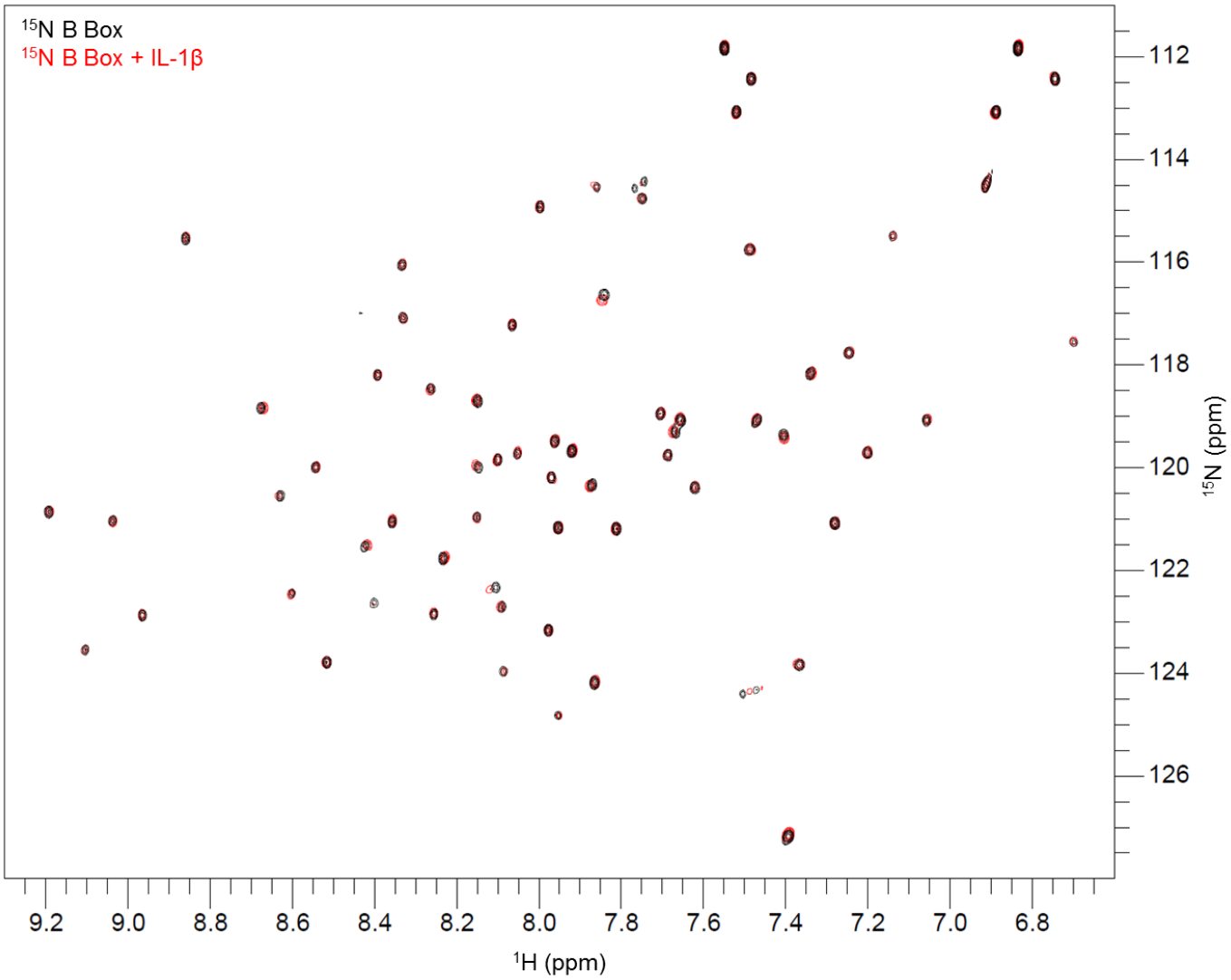

Figure 5.39 ^{1}H-^{15}N HSQC spectra for the ^{15}N-labelled B box domain in the presence and absence of IL-1β ^{1}H-^{15}N HSQC spectra were collected on a 10 µM ^{15}N B box sample in PBS, pH 7.2 at 25^{o}C (298 K) in the absence (Black) and presence (red) of 100 µM IL-1β (^{15}N B box: IL-1β ratio of 1:10). NMR spectra were collected on a Bruker Avance II 800 MHz spectrometer using identical experimental parameters (NS = 192, increments = 256 and ^{15}Nres = 15.80 Hz). In the presence of IL-1β, no significant change in the chemical shift of the peaks was observed. From the spectra it would appear that some of peaks disappear following the addition of IL-1β. However, this was due the low concentration of the ^{15}N B box protein and all peaks were present when the contour levels were increased.

5.3.4. Investigating the intermolecular interaction between the A box domain of HMGB1 and IL-1β

^{1}H-^{15}N HSQC spectra for a 100 μM ^{15}N-labelled A box sample were collected in the absence and presence of 500 μM IL-1β at 25^{o}C in 20 mM potassium phosphate, 100 mM potassium chloride and 10 mM DTT at pH 6.8 using a 800 MHz Bruker Avance II spectrometer. Figure 5.10 shows an overlay of the A box spectra without (black) and with (red) IL-1β. In order for a direct comparison to be made the spectra were collected using identical acquisition parameters: 8 scans with 150 increments at a resolution in the indirect dimension of 21.09 Hz. In both spectra the peaks are well defined and dispersed indicating that the A box protein used in the experiment was folded. As can be seen, no chemical shift perturbations were observed following the addition of an excess of IL-1β.

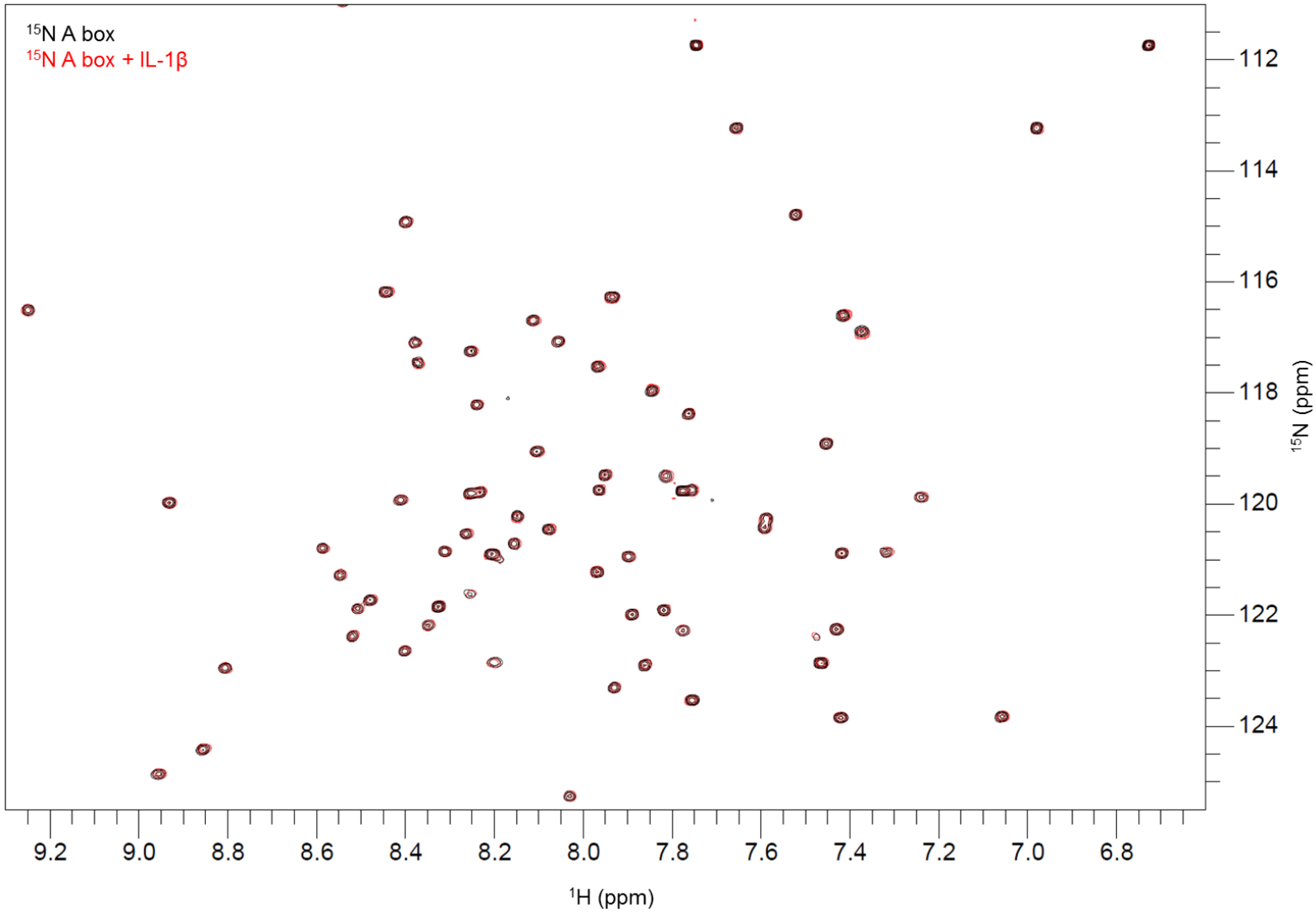

Figure 5.40 Investigating the intermolecular interaction between ^{15}N A box and IL-1β
^{1}H-^{15}N HSQC spectra were collected for a 100 µM ^{15}N-labelled A box sample in the absence (black) and presence (red) of 500 µM IL-1β at 25°C (298 K) in 20 mM potassium phosphate, 100 mM potassium chloride and 10 mM DTT, pH 6.8, on a 800 MHz Bruker Avance II spectrometer. No significant chemical shift changes were observed in the presence of IL-1β.

5.4. DISCUSSION

It has been previously demonstrated that HMGB1 and IL-1β act in synergy to amplify the inflammatory response and it has been postulated that this effect is mediated by the formation of a highly active pro-inflammatory complex in which HMGB1 and IL-1β directly interact (Sha et al., 2008; Ferhani et al., 2010; Wähämaa et al., 2011). However, there is currently limited evidence to prove that a direct association occurs, although it is known that HMGB1 can complex with a diverse range of endogenous and exogenous molecules. Two independent groups have demonstrated that HMGB1 and IL-1β can be co-purified using IP: in 2008, Sha and colleagues reported that IL-1β could be detected along with FLAG-tagged HMGB1 following FLAG-affinity IP purification (Sha et al., 2008). Additionally, in 2010, Ferhani *et al* (2010) reported that HMGB1/IL-1β complexes could be isolated from macrophages treated with recombinant HMGB1 and IL-1β proteins. However, the published data for this later study did not include an IL-1β positive control and it is possible that the IL-1β protein interacted non-specifically with the anti-HMGB1 antibody used in the experiment. Therefore, the work presented in this chapter was performed to elucidate the molecular interaction between *E.coli* expressed and purified recombinant HMGB1 and IL-1β, and to test the hypothesis that these proteins directly interact to form a binary complex that enhances the inflammatory response.

The first experiment was designed to investigate the intermolecular interaction between ^{15}N-labelled IL-1β and unlabelled full length HMGB1. The specific batch of proteins used in this experiment had been previously demonstrated to act synergistically on SFs to enhance the release of IL-6 in cells isolated from two RA patients (Figure 4.3). Neither protein induced detectable IL-6 secretion alone but they acted synergistically to induce IL-6 levels of up to 13,486 ± 2055 pg/mL. The NMR experiments performed in this chapter were designed to replicate the cellular experimental conditions as closely as possible: the HSQC spectra were collected in PBS and the proteins were incubated overnight at 4^{o}C prior to sample analysis, as it has been previously reported this was a prerequisite for the synergistic activity (Sha et al., 2008; Hreggvidsdottir et al., 2009; Wähämaa et al., 2011) although the results

from Chapter 4 indicate that pre-incubation may not be necessary. Initially, the experiment was conducted at 25^{o}C (298 K) and under the conditions examined in this thesis no direct protein-protein interaction was detected between IL-1β and HMGB1 with no chemical shift perturbations observed for any of the IL-1β residues, suggesting that the cellular response is not mediated by the formation of a highly active binary complex (Figure 5.31 and Figure 5.32). Somewhat different results were obtained when the experiment was repeated at 10^{o}C (283 K) as minor chemical shift perturbations were observed for five IL-1β residues (Figure 5.3 and Figure 5.4). Two of these residues, H30 and N129, were surface exposed and in close proximity to each other (Figure 5.35). However, given such small and limited chemical shifts, and the difficulties in replicating the results, it is likely that these small perturbations are not caused by a direct binding interaction but are the result of subtle pH differences, which are likely to affect charged residues.

In Chapter 4 the Δ30 protein was shown to act synergistically with IL-1β to enhance the inflammatory response (Section 4.2.4) and experiments were designed to determine if this effect was due to the formation of a binary complex. Initially, ^{1}H-^{15}N HSQC spectra were collected for a ^{15}N-labelled Δ30 sample in the absence and presence of a 9-fold excess of unlabelled IL-1β protein. No chemical shift perturbations for the Δ30 residues were observed following the addition of IL-1β (Figure 5.36) indicating that a detectable binary complex was not formed under the conditions utilised in this experiment. It should be noted that it was not practical to reproduce the 1:137 (IL-1β: HMGB1 protein) molar ratio used in the cellular experiments within the NMR studies. However, the total concentration of the HMGB1 constructs used in the NMR experiments exceeds the concentration used in the cellular assays. Additionally, an excess of the unlabelled protein was required for the experiments and this resulted in an excess of the IL-1β protein being used when spectra were collected for ^{15}N-labelled HMGB1 proteins. However, the reverse experiment was also performed with ^{1}H-^{15}N HSQC spectra recorded for ^{15}N-labelled IL-1β in the presence of a three-fold excess of Δ30 protein (Figure 5.7 and Figure 5.8). Under these conditions minor chemical shift perturbations were observed for several of the IL-1β residues, including once again the H30 and N129 peaks. It is unlikely that these small chemical shift perturbations are due to a specific binding interaction since minor changes were detected for many of the residues. Moreover,

the chemical shift of the H30 residue, a charged amino acid, is particularly susceptible to pH changes and once again it is likely that the perturbations were due to a subtle pH change following the addition of the Δ30 protein.

Subsequently, NMR experiments were conducted to investigate the interaction between IL-1β and the individual A and B box domains. Despite structural similarities, the two HMG boxes have opposing functions *in vivo*: the B box is essential for the pro-inflammatory activity of HMGB1 (Li et al., 2003; Yang et al., 2010) whilst the A box is anti-inflammatory and has been shown to neutralise the inflammatory activity of the full length HMGB1 protein in experimental animal models (Yang et al., 2004; Andrassy et al., 2008; Yuan et al., 2009; Ostberg et al., 2010). It was previously observed that the B box is critical for the synergistic interaction with IL-1β and that the A box is not required (Chapter 4, Section 4.2.4). Therefore, as predicted, the formation of a complex between ^{15}N-labelled A box and IL-1β was not detected, with no chemical shift perturbations observed in the A box spectrum (Figure 5.10). Additionally, no chemical shift perturbations were observed in the ^{1}H-^{15}N HSQC spectrum for the ^{15}N-labelled B box protein following the addition of a 10-fold excess of IL-1β (Figure 5.9), despite the fact that this combination of proteins induced increased IL-6 secretion *in vitro* (Figure 4.6). Once again, this implies that HMGB1 and IL-1β do not directly interact to form a binary complex under the conditions used in these experiments.

From the NMR data presented within this chapter it would appear that the synergistic interaction observed between HMGB1 and IL-1β is not mediated by the formation of a pro-inflammatory binary complex. Rather, an alternative cellular mechanism is needed in which HMGB1 is involved and additional co-factor(s) may be required. The HMGB1 and IL-1β proteins signal via a common pathway to initiate inflammation, binding to the TLR4 and IL-1R, respectively (Figure 5.11). Both receptors belong to the Toll/IL-1R (TIR) family, which is split into three sub-families: the TLR family, the IL-1 family and the MyD88 family. All of the members of the TIR family share a common, highly conserved cytoplasmic motif (Gay and Keith 1991), the TIR domain which is essential for the initiation of intracellular signalling (Leung et al., 1994). The synergistic interaction between HMGB1 and IL-1β is mediated via the IL-1R (Chapter 4; Hreggvidsdottir et al., 2011). The IL-1R subfamily contains 10 proteins including the type I and II IL-R's

and the IL-1RAcP, a co-factor that is essential for the initiation of intracellular signalling. The type I IL-1R and IL-1RAcP are composed of an extracellular region made of three immunoglobulin-like domains, a transmembrane domain and a cytoplasmic TIR domain, which contains approximately 215 residues (Sims et al., 1989). The type II IL-1R has a truncated 29-residue TIR domain, cannot initiate cell signalling and acts as a decoy receptor for IL-1 (McMahan et al., 1991).

IL-1 signalling is mediated by the MyD88/IRAK/TRAF6 pathway and the TIR domains play a central role in initiating the cellular response (Figure 5.11). IL-1 binds to the type I IL-1R and recruits the IL-1RAcP resulting in the formation of a heterodimeric signalling complex (Greenfeder et al., 1995). The TIR domains within the IL-1R and the IL-1RAcP interact, inducing a conformational change (Martin and Wesche 2002) leading to the recruitment of the MyD88 and Tollip/IRAK proteins (Muzio et al., 1997). Under normal conditions, the activity of IRAK-1 is sequestered by the Tollip protein; this association is lost when IRAK-1 is recruited to receptor complex (Burns et al., 2000). IRAK-1 is phosphorylated (Burns et al., 2000; Kollewe et al., 2004) and released into the cytoplasm, where it associates with the TAB2 and TRAF6 proteins (Jiang et al., 2002). TRAF6 is poly-ubiquitinated and active TRAF6 can interact with the TAK-1, which in turn activates the NF-κB, p38 and c-JNK pathways (Wang et al., 2001). NF-κB activates a diverse range of pro-inflammatory genes including the IL-6 gene (Libermann and Baltimore 1990). Our findings suggest that additional molecules may be involved in mediating HMGB1/IL-1β synergy. There is currently no evidence within the literature to suggest that HMGB1 can directly bind to and activate the IL-1R. However, HMGB1 and IL-1β may form a tertiary complex with the IL-1R or IL-1RAcP to enhance intracellular signalling and future studies will investigate this hypothesis.

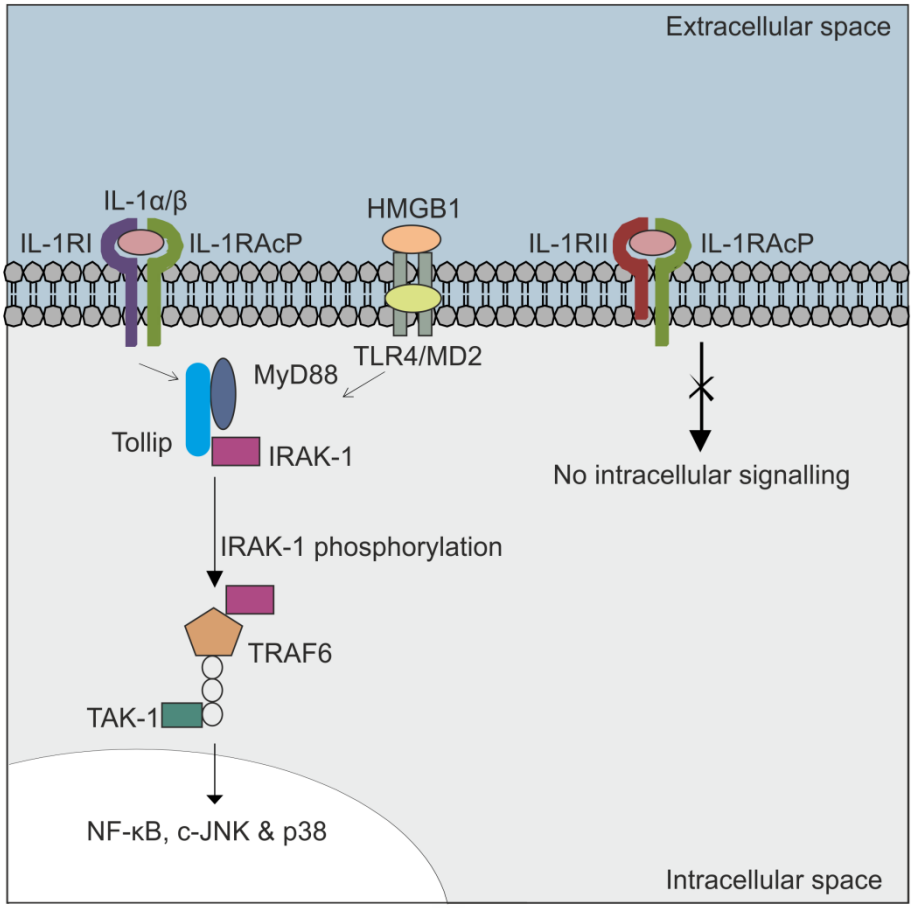

Figure 5.41 TIR family signal transduction pathway HMGB1 and IL-1β bind to the TLR4 and type I IL-1R (IL-1R1) proteins, respectively. Engagement of the receptor activates the MyD88/IRAK/TRAF6 intracellular signalling pathway. This results in activation of NF-κB-mediated gene transcription and the c-JNK and p38 signalling pathways.

In conclusion, the data presented within this chapter definitively shows that the synergistic effect between HMGB1 and IL-1β, observed in the cellular experiments, is not due to the formation of a binary complex between the two pro-inflammatory proteins. Despite performing the NMR experiments in various ways, there was no significant evidence to support the formation of a pro-inflammatory complex between IL-1β and either full length HMGB1, Δ30 or the B box. This suggests that HMGB1 and IL-1β elicit an inflammatory response via a novel cellular mechanism in which HMGB1 is required and additional proteins are involved. Future work will focus on discovering what these other proteins might be.

CHAPTER SIX

CONCLUDING DISCUSSION

TABLE OF CONTENTS

6.1. BACKGROUND

HMGB1 is an important mediator of inflammation which acts to alert the immune system to tissue stress and injury. It mediates cytokine production (Andersson et al., 2000), chemotaxis (Orlova et al., 2007), cell proliferation, dendritic cell and T-cell activation (Dumitriu et al., 2005), cell differentiation (Melloni et al., 1995) and autophagy (Tang et al., 2010). HMGB1 has been implicated in the pathogenesis of multiple inflammatory diseases including immune-mediated DILI, where it is a potential mechanistic biomarker and a target for therapeutic intervention. However, despite intense research the pro-inflammatory role of HMGB1 remains unresolved. Several studies have demonstrated that HMGB1 interacts with multiple unrelated ligands to enhance the inflammatory response, although currently these interactions are poorly defined. The overall aim of the work presented in this thesis was to specifically characterise the interaction between HMGB1 and IL-1β. This was achieved by:

- Developing and optimising methods for the production of LPS-free and isotopically-labelled recombinant HMGB1, Δ30, A box, B box and IL-1β proteins. The characterisation of these proteins in Chapter 3 enabled their use in further studies in Chapters 4 and 5, where a dual cellular and biophysical strategy was employed to study the synergistic response between HMGB1 and IL-1β.
- Performing an extensive cellular characterisation of the interaction between HMGB1 and IL-1β using established cell assays. In Chapter 4, SFs were used as a model cell system to investigate the cellular response to HMGB1 and IL-1β. These studies identified which domain of HMGB1 mediates the interaction and investigated the clinical relevance of the synergy by exploring the dynamics and kinetics of the response.
- Conducting an extensive biophysical analysis of the interaction between HMGB1 and IL-1β using NMR methodologies. The experiments described in Chapter 5 were undertaken to test the hypothesis that HMGB1 and IL-1β directly interact to form a binary pro-inflammatory complex. These are the first biophysical studies to investigate the interaction between HMGB1 and IL-1β.

The findings from these studies help to clarify the pro-inflammatory function of HMGB1 and are relevant to multiple inflammatory diseases where HMGB1 has been implicated as a pathogenic mediator.

6.2. HMGB1 AS AN INFLAMMATORY MEDIATOR OF DILI

There is an ever increasing awareness of the involvement of innate immunological responses during DILI. It is now widely accepted that DAMPs are released as a direct consequence of hepatic cellular dysfunction and death in response to a toxic insult. Amongst all DAMPs, HMGB1 is the most studied protein. HMGB1 drives inflammation during tissue injury or infection and is increasingly being identified as a pathogenic mediator of immune-mediated DILI, with elevated levels of up to 100 ng/mL reported during clinical APAP-induced hepatotoxicity (Antoine et al., 2012; Antoine et al., 2013). Additionally, HMGB1-targeted therapies have been reported to be beneficial in experimental animal models of DILI. Neutralising HMGB1 antibodies reduce hepatic inflammation and increase survival during APAP-induced DILI (Antoine et al., 2010), although the clinical potential of HMGB1-inhibition in hepatotoxicity is, as yet, unknown.

The renewed interest in HMGB1 biology has driven the need for a large quantity of recombinant HMGB1 protein. To facilitate this work, Chapter 3 describes the development and optimisation of methods for the production of recombinant HMGB1, Δ30, A box, B box and IL-1β proteins. To enable further cellular and biophysical studies in Chapters 4 and 5, the recombinant proteins were both LPS free and isotopically-labelled. To our knowledge, at the start of this work no other study had considered both of these factors when producing recombinant HMGB1 proteins.

Extracellular HMGB1 has been reported to act in synergy with multiple un-related endogenous and exogenous molecules to modulate the inflammatory response (Table 6.14). These interactions are ligand-specific as HMGB1 does not act synergistically with TNFα, RANKL, IL-18 or PolyI:C (Hreggvidsdottir et al., 2009). HMGB1 interactions with IL-1β, IL-1α, LPS and CpG-ODN are pro-inflammatory promoting the production and release of multiple cytokine mediators including IL-6, IL-8, TNF and MMP (Hreggvidsdottir et al., 2009; Wähämaa et al., 2011).

There is currently limited data available on the synergistic interaction between HMGB1 and IL-1β and prior to this study the kinetics of the interaction had not been well defined. In Chapter 4 an extensive *in vitro* analysis was undertaken to characterise the cellular response. SFs were isolated from RA patients and used as a model cell system. The results show that HMGB1 acts synergistically with IL-1β to initiate and enhance the inflammatory response following infection or injury when HMGB1 levels are significantly elevated. Full length HMGB1, Δ30 and the B box, but not the A box, all acted in synergy with IL-1β, via the IL-1R, to enhance cytokine production in these cells (Figure 4.6 and Figure 4.7). The B box was essential for the synergistic interaction with IL-1β (Figure 4.6), although further studies are needed to identify the critical residues involved. Previous studies have shown that a minimal 20-residue peptide (residues 89-108) (Figure 1.7) from within the B box domain is required for HMGB1-induced cytokine production and this region may be involved in the synergistic activity with IL-1β (Li et al., 2003).

Table 6.14 Overview of the key synergistic interactions of the HMGB1 protein HMGB1 interacts with multiple molecules to modulate the inflammatory response. The main findings from the work presented in this thesis are shown in the boxed region.

Partner molecule	Key findings	Receptor	Relevance of PTMs	Key reference(s)
PRO-INFLAMMATORY				
LPS	Enhances cytokine production LPS interacts with A and B boxes Alternative LBP-binding protein	TLR4		(Youn et al., 2008; Hreggvidsdottir et al., 2009; Wähämaa et al., 2011; Youn et al., 2011)
IL-1β	Enhances cytokine production B box domain of HMGB1 is critical Not due to the formation of a pro-inflammatory binary complex Mediated via an alternative cellular mechanism	IL-1R	Redox independent	Chapter 4 & 5 (Hreggvidsdottir et al., 2009; Hreggvidsdottir et al., 2011; Wähämaa et al., 2011)
IL-1α	Enhances cytokine production	IL-1R		(Wähämaa et al., 2011)
CXCL12	Promotes the recruitment of inflammatory cells to damaged tissue HMGB1 forms a heterocomplex with CXCL12 as shown by NMR	CXCR4	CXCL12 binds fully reduced HMGB1	(Schiraldi et al., 2012)
Nucleosomes	Enhance cytokine production Increases expression of co-stimulatory molecules on macrophages and dendritic cells	TLR2		(Urbonaviciute et al., 2008)
Nucleic acids	Enhances cytokine production	TLR9		(Ivanov et al., 2007)
ANTI-INFLAMMATORY				
CD24/Siglec-10	Ternary complex (HMGB1/CD24/Siglec-10) Negatively regulates HMGB1-induced NF-κB activation and cytokine production	CD24/Siglec-10		(Chen et al., 2009)

6.3. DIFFERENT MOLECULAR FORMS OF HMGB1 PRESENT DURING DILI AND THEIR SYNERGISTIC INTERACTIONS

It is now known that HMGB1 can undergo multiple post-translational modifications (PTMs) (Table 6.2). These PTMs regulate the release and function of HMGB1, with multiple molecular forms reported to be present during the inflammatory response. Emerging evidence suggests that different molecular forms of HMGB1 may function as informative mechanistic indicators of DILI.

Acetylation of HMGB1 is a prerequisite for protein secretion from activated immune cells and analysis of the acetylation status can provide insights into the mechanisms of DILI. Antoine and colleagues have shown that hypo-acetylated HMGB1, derived from necrotic cells, is an early marker of hepatocyte cellular dysfunction and cell death. In experimental rodent models, hypo-acetylated HMGB1 levels are significantly elevated from 3 h post APAP treatment, peaking at 5 h and returning to control values within 10 h. In contrast, hyper-acetylated HMGB1, a marker of cell activation and inflammation, is first significantly increased at 5 h post-treatment with levels remaining elevated for up to 24 h after APAP-administration (Antoine et al., 2009; Antoine et al., 2012). A recent clinical analysis of 84 patients presenting with acute liver failure to two major hospitals in the UK and USA has reported similar findings (Antoine et al., 2012). Moreover, from these patients it appears that quantification of the hyper-acetylated form of HMGB1 may be a predictive biomarker of the clinical outcome (Antoine et al., 2012).

Recent studies have demonstrated that the redox status of the three cysteine residues regulates HMGB1 receptor binding and bioactivity (Table 6.16). 'Cytokine-inducing' HMGB1 requires a C23-C45 disulphide bond and a reduced C106 residue (di-sulphide HMGB1) (Yang et al., 2011). The C106 residue is located within the B box domain and is critical for TLR4-binding. The results from Chapter 4 show that this region is also required for the synergistic interaction with IL-1β, although the effects of oxidation and other PTMs on HMGB1 synergy are still largely unknown. Recently, Park *et al* have shown that the C23-C45 di-sulphide bond reduces the binding affinity for cisplatin modified DNA (Park and Lippard 2011). Furthermore, it appears that all-thiol HMGB1 form a heterocomplex with CXCL12 that signals via the CXCR4 receptor to promote chemotaxis (Schiraldi et al., 2012).

Table 6.15: The functional importance of post-translational modifications in the HMGB1 protein

PTM	Target residue(s)	Significance	References
Acetylation	All lysine (K) residues are susceptible but K28, K29, K30, K180, K182, K183, K184 & K185 are frequently acetylated *in vivo*	Prerequisite for the active secretion from immune cells (Including macrophages and monocytes). Acetylation of K2 and K11 is required for binding to distorted DNA.	(Bonaldi et al., 2003; Assenberg et al., 2008)
Oxidation	C23, C45 & C106	Regulates pro-inflammatory activity C106 is critical for TLR4 binding	(Yang et al., 2011) (Venereau et al., 2012)
Methylation	K42	Promotes cytoplasmic accumulation	(Ito et al., 2007)
Phosphorylation	S35, S39, S42, S46, S53 and S181	Promotes cytoplasmic accumulation	(Youn and Shin 2006)

LC-MS/MS analysis of a batch of the recombinant HMGB1 produced in Chapter 3 revealed that the three cysteine residues were all oxidised (Figure 3.18). The biological function of C106- or fully-oxidised HMGB1 is still unknown (Table 6.3) and in agreement with previous findings, this recombinant HMGB1 did not induce IL-6 release in PBMCs or SFs alone (Figure 3.17 & Figure 4.1) (Yang et al., 2011). However, in Chapter 4, the recombinant HMGB1 was able to act synergistically with IL-1β to significantly enhance IL-6 production (Figure 4.1). This suggests that the synergistic activities of HMGB1 with IL-1 are independent of the oxidation status, TLR4 binding capability and the intrinsic cytokine-inducing activity. These results are in agreement with similar findings recently reported by Wähämaa and colleagues (Wähämaa et al., 2011) and suggest that an 'inactive cytokine-inducing' HMGB1 molecule may still be able to promote inflammation in the presence of IL-1β or other co-factors. However, to confirm this finding the synergistic activity between C106A and C106S HMGB1 mutants and IL-1β will need to be determined.

Table 6.16 Redox-state dependent functions of HMGB1 released during DILI Table adapted from (Yang et al., 2013).

Molecular form	Role in DILI	Source	Schematic representation	Cytokine-inducing (TLR4 binding)	Chemoattractant activity
All-thiol HMGB1	Promotes resolution and regeneration	Necrosis	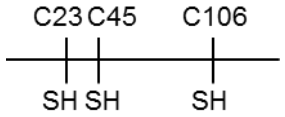	No	Yes
Di-sulphide HMGB1	Promotes Inflammation	Necrosis and pyroptosis		Yes	No
C106-oxidised HMGB1	Unknown function	Apoptosis	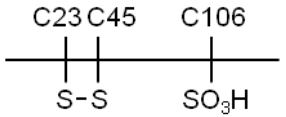	No	No
Fully-oxidised HMGB1	Unknown function	Apoptosis	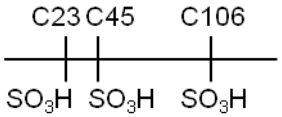	No	No

6.4. EXPLORING THE INTERACTION BETWEEN HMGB1 AND IL-1B

Biophysical analysis of the interaction between HMGB1 and IL-1β is not available within the current literature, although several publications have alluded to the formation of a pro-inflammatory binary complex. Protein NMR spectroscopy is a powerful technique used to investigate intermolecular interactions. In Chapter 5, an extensive biophysical analysis of the interaction between HMGB1 and IL-1β was conducted using NMR methodologies. The NMR findings conclusively show that HMGB1 and IL-1β do not directly interact to form a binary complex, under the conditions employed in these experiments. Despite the fact that the full length HMGB1, Δ30 and B box proteins had all been shown to act synergistically with IL-1β in the cellular assays described in Chapter 4 (Figure 4.6). This suggests that HMGB1 and IL-1β act via an alternative mode of action to synergistically enhance cytokine production during inflammation, although further studies are required to identify this pathway. Moreover, the results indicate that additional proteins involved in IL-1 signalling may be required for the synergistic interaction

6.5. FUTURE INVESTIGATIONS; ELUCIDATING THE MECHANISM OF ACTION FOR HMGB1/IL-1B SYNERGY

Future studies will investigate alternative mechanisms that may mediate the synergistic activity between HMGB1 and IL-1β. The findings presented in this thesis suggest that the interaction may require additional proteins. One possibility is that HMGB1 may form a ternary complex with IL-1β and the IL-1R or IL-1RAcP (Figure 6.42). It has recently been reported that HMGB1 forms a similar trimolecular complex with CD24, a glycosylated GDP-anchored membrane protein, and Siglec10 (or the mouse homologue Siglec-G), an inhibitory membrane receptor (Chen et al., 2009). It has been proposed that HMGB1 and CD24 first form a binary complex which, in turn, interacts with Siglec10. Chen *et al* have shown that the B box domain of HMGB1 is critical for this interaction. However, further biophysical experiments are needed to elucidate the specific binding site. In contrast, to the synergy between HMGB1 and IL-1β the ternary complex with CD24 and Siglec10 is anti-inflammatory, with the CD24 and Siglec10 proteins suppressing HMGB1-mediated NF-κB activation. Recent studies have shown that the HMGB1/CD24/Siglec10 pathway protects against DILI and sepsis with CD24 and SiglecG knockout mice

displaying an increased susceptibility to APAP-induced hepatotoxicity (Chen et al., 2009; Chen et al., 2011). This appears to be due to enhanced intracellular signalling in the absence of CD24 and SiglecG and administration of HMGB1-antibodies is beneficial in these models. This demonstrates a critical role for CD24 and Siglec10 in dampening the immune response to HMGB1. In contrast, a similar ternary complex between HMGB1, IL-1β and the IL-1R or IL-1RAcP would be pro-inflammatory, promoting inflammation in response to a toxic insult.

Additionally, it is also possible that HMGB1 may form a ternary complex with an alternative cellular protein prior to the interaction with the IL-1R receptor (Figure 6.42). This may result in enhanced intra-cellular signalling when compared IL-1β signalling alone. However, further experiments are required to test these hypotheses.

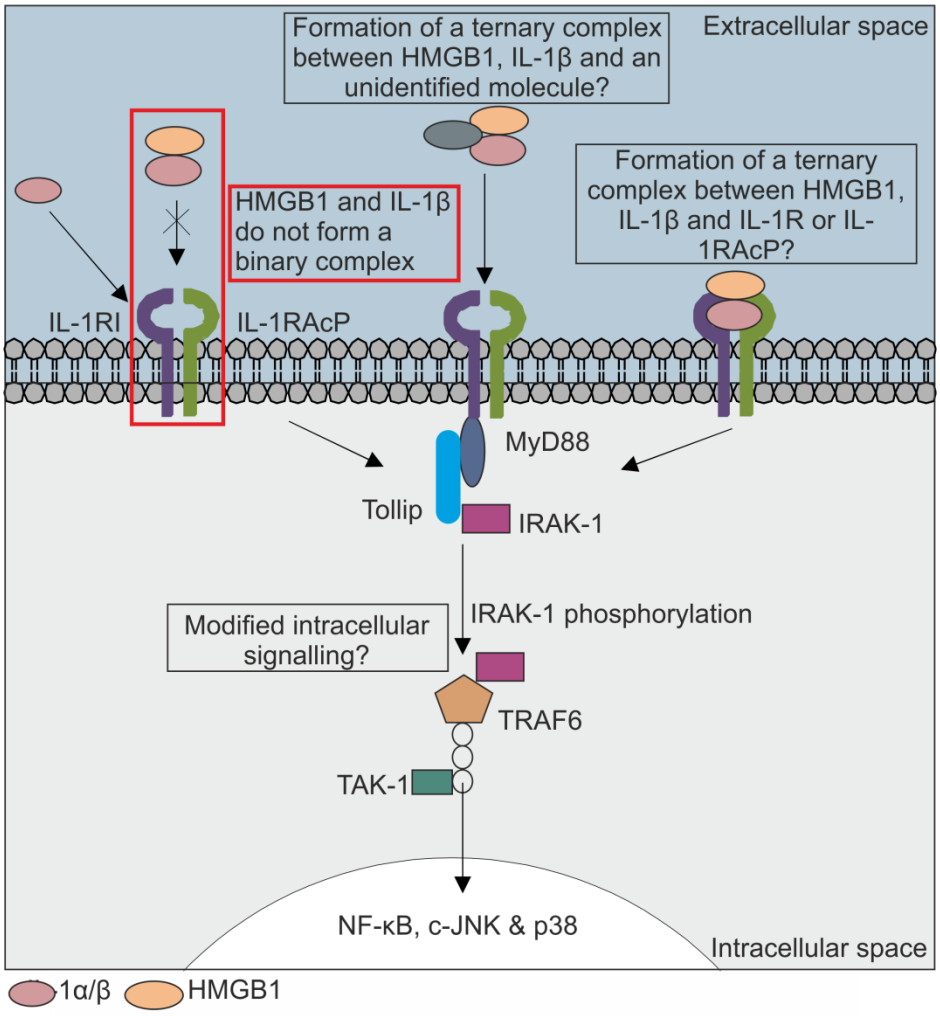

Figure 6.42 Overview of the potential mechanisms that may mediate the synergistic activity between HMGB1 and IL-1β The potential mechanism that has been investigated in this work is shown in the red box region. Based on the findings presented in this thesis, this mechanism can be excluded. Future experiments will investigate alternative mechanisms of action as outlined in the black box regions.

6.6. CONCLUDING REMARKS

In summary, the work presented in this thesis has used combined cellular and NMR methodologies to characterise the synergistic interaction between HMGB1 and IL-1β. The results show that the two proteins act synergistically to enhance cytokine production during the inflammatory response. Furthermore, these findings demonstrate that the B box domain of HMGB1 is critical for this effect. However, this is not due to the formation of a binary complex between HMGB1 and IL-1β, as shown by the NMR experiments. Instead, it appears that this occurs via an alternative cellular mechanism in which HMGB1 is required and other molecules may be involved. Future work will focus on identifying these other proteins. Overall

these studies help to clarify the pro-inflammatory role of extracellular HMGB1 released from stressed or dying hepatocytes during DILI. Moreover, these findings are relevant to multiple inflammatory diseases, where HMGB1 has been implicated as an important pathogenic mediator.

BIBLIOGRAPHY

Agresti, A. and Bianchi, M. E. (2003). "HMGB proteins and gene expression." *Curr Opin Genet Dev* 13(2): 170-178.

Aida, Y. and Pabst, M. J. (1990). "Removal of endotoxin from protein solutions by phase separation using Triton X-114." *J Immunol Methods* 132(2): 191-195.

Alnemri, E. S., Livingston, D. J., Nicholson, D. W., Salvesen, G., Thornberry, N. A., Wong, W. W. and Yuan, J. (1996). "Human ICE/CED-3 protease nomenclature." *Cell* 87(2): 171.

Andersson, U. and Tracey, K. J. (2011). "HMGB1 is a therapeutic target for sterile inflammation and infection." *Annu Rev Immunol* 29: 139-162.

Andersson, U., Wang, H., Palmblad, K., Aveberger, A. C., Bloom, O., Erlandsson-Harris, H., Janson, A., Kokkola, R., Zhang, M., Yang, H. and Tracey, K. J. (2000). "High mobility group 1 protein (HMG-1) stimulates proinflammatory cytokine synthesis in human monocytes." *J Exp Med* 192(4): 565-570.

Andrassy, M., Volz, H. C., Igwe, J. C., Funke, B., Eichberger, S. N., Kaya, Z., Buss, S., Autschbach, F., Pleger, S. T., Lukic, I. K., Bea, F., Hardt, S. E., Humpert, P. M., Bianchi, M. E., Mairbäurl, H., Nawroth, P. P., Remppis, A., Katus, H. A. and Bierhaus, A. (2008). "High-Mobility Group Box-1 in Ischemia-Reperfusion Injury of the Heart." *Circulation* 117(25): 3216-3226.

Antoine, D. J., Dear, J. W., Lewis, P. S., Platt, V., Coyle, J., Masson, M., Thanacoody, R. H., Gray, A. J., Webb, D. J., Moggs, J. G., Bateman, D. N., Goldring, C. E. and Park, B. K. (2013). "Mechanistic biomarkers provide early and sensitive detection of acetaminophen-induced acute liver injury at first presentation to hospital." *Hepatology* 58(2): 777-787.

Antoine, D. J., Jenkins, R. E., Dear, J. W., Williams, D. P., McGill, M. R., Sharpe, M. R., Craig, D. G., Simpson, K. J., Jaeschke, H. and Park, B. K. (2012). "Molecular forms of HMGB1 and keratin-18 as mechanistic biomarkers for mode of cell death and prognosis during clinical acetaminophen hepatotoxicity." *J Hepatol* 56(5): 1070-1079.

Antoine, D. J., Williams, D. P., Kipar, A., Jenkins, R. E., Regan, S. L., Sathish, J. G., Kitteringham, N. R. and Park, B. K. (2009). "High Mobility Group Box-1 protein and Keratin-18, circulating serum proteins informative of acetaminophen-induced necrosis and apoptosis in vivo." *Toxicol. Sci.*: kfp235.

Antoine, D. J., Williams, D. P., Kipar, A., Laverty, H. and Park, B. K. (2010). "Diet restriction inhibits apoptosis and HMGB1 oxidation and promotes inflammatory cell recruitment during acetaminophen hepatotoxicity." *Mol Med* 16(11-12): 479-490.

Arend, W. P., Welgus, H. G., Thompson, R. C. and Eisenberg, S. P. (1990). "Biological properties of recombinant human monocyte-derived interleukin 1 receptor antagonist." *J Clin Invest* 85(5): 1694-1697.

Assenberg, R., Webb, M., Connolly, E., Stott, K., Watson, M., Hobbs, J. and Thomas, J. O. (2008). "A critical role in structure-specific DNA binding for the acetylatable lysine residues in HMGB1." *Biochem J* 411(3): 553-561.

Barnes, P. J. and Karin, M. (1997). "Nuclear factor-kappaB: a pivotal transcription factor in chronic inflammatory diseases." *N Engl J Med* 336(15): 1066-1071.

Bausinger, H., Lipsker, D., Ziylan, U., Manie, S., Briand, J. P., Cazenave, J. P., Muller, S., Haeuw, J. F., Ravanat, C., de la Salle, H. and Hanau, D. (2002). "Endotoxin-free heat-shock protein 70 fails to induce APC activation." *Eur J Immunol* 32(12): 3708-3713.

Bernal, W., Cross, T. J., Auzinger, G., Sizer, E., Heneghan, M. A., Bowles, M., Muiesan, P., Rela, M., Heaton, N., Wendon, J. and O'Grady, J. G. (2009). "Outcome after wait-listing for emergency liver transplantation in acute liver failure: a single centre experience." *J Hepatol* 50(2): 306-313.

Beutler, B., Milsark, I. W. and Cerami, A. C. (1985). "Passive immunization against cachectin/tumor necrosis factor protects mice from lethal effect of endotoxin." *Science* 229(4716): 869-871.

Beutler, B. and Rietschel, E. T. (2003). "Innate immune sensing and its roots: the story of endotoxin." *Nat Rev Immunol* 3(2): 169-176.

Bianchi, M. E. (1991). "Production of functional rat HMG1 protein in Escherichia coli." *Gene* 104(2): 271-275.

Blazka, M. E., Wilmer, J. L., Holladay, S. D., Wilson, R. E. and Luster, M. I. (1995). "Role of proinflammatory cytokines in acetaminophen hepatotoxicity." *Toxicol Appl Pharmacol* 133(1): 43-52.

Bonaldi, T., Langst, G., Strohner, R., Becker, P. B. and Bianchi, M. E. (2002). "The DNA chaperone HMGB1 facilitates ACF/CHRAC-dependent nucleosome sliding." *EMBO J* 21(24): 6865-6873.

Bonaldi, T., Talamo, F., Scaffidi, P., Ferrera, D., Porto, A., Bachi, A., Rubartelli, A., Agresti, A. and Bianchi, M. E. (2003). "Monocytic cells hyperacetylate chromatin protein HMGB1 to redirect it towards secretion." *EMBO J* 22(20): 5551-5560.

Bourdi, M., Eiras, D. P., Holt, M. P., Webster, M. R., Reilly, T. P., Welch, K. D. and Pohl, L. R. (2007). "Role of IL-6 in an IL-10 and IL-4 double knockout mouse model uniquely susceptible to acetaminophen-induced liver injury." *Chem Res Toxicol* 20(2): 208-216.

Bourdi, M., Tinel, M., Beaune, P. H. and Pessayre, D. (1994). "Interactions of dihydralazine with cytochromes P4501A: a possible explanation for the appearance of anti-cytochrome P4501A2 autoantibodies." *Mol Pharmacol* 45(6): 1287-1295.

Buchweitz, J. P., Ganey, P. E., Bursian, S. J. and Roth, R. A. (2002). "Underlying endotoxemia augments toxic responses to chlorpromazine: is there a relationship to drug idiosyncrasy?" *J Pharmacol Exp Ther* 300(2): 460-467.

Bulera, S. J., Birge, R. B., Cohen, S. D. and Khairallah, E. A. (1995). "Identification of the mouse liver 44-kDa acetaminophen-binding protein as a subunit of glutamine synthetase." *Toxicol Appl Pharmacol* 134(2): 313-320.

Burns, K., Clatworthy, J., Martin, L., Martinon, F., Plumpton, C., Maschera, B., Lewis, A., Ray, K., Tschopp, J. and Volpe, F. (2000). "Tollip, a new component of the IL-1RI pathway, links IRAK to the IL-1 receptor." *Nat Cell Biol* 2(6): 346-351.

Bustin, M. (2001). "Revised nomenclature for high mobility group (HMG) chromosomal proteins." *Trends in Biochemical Sciences* 26(3): 152-153.

Bustin, M., Hopkins, R. B. and Isenberg, I. (1978). "Immunological relatedness of high mobility group chromosomal proteins from calf thymus." *J Biol Chem* 253(5): 1694-1699.

Calogero, S., Grassi, F., Aguzzi, A., Voigtlander, T., Ferrier, P., Ferrari, S. and Bianchi, M. E. (1999). "The lack of chromosomal protein Hmg1 does not disrupt cell growth but causes lethal hypoglycaemia in newborn mice." *Nat Genet* 22(3): 276-280.

Cato, L., Stott, K., Watson, M. and Thomas, J. O. (2008). "The Interaction of HMGB1 and Linker Histones Occurs Through their Acidic and Basic Tails." *Journal of Molecular Biology* 384(5): 1262-1272.

Cato, L., Stott, K., Watson, M. and Thomas, J. O. (2008). "The interaction of HMGB1 and linker histones occurs through their acidic and basic tails." *J Mol Biol* 384(5): 1262-1272.

Cavanagh, J., Fairbrother, W. J. and Palmer, A. G., III (2006). Protein NMR Spectroscopy : Principles and Practice. Burlington, MA, USA, Academic Press.

Celona, B., Weiner, A., Di Felice, F., Mancuso, F. M., Cesarini, E., Rossi, R. L., Gregory, L., Baban, D., Rossetti, G., Grianti, P., Pagani, M., Bonaldi, T., Ragoussis, J., Friedman, N., Camilloni, G., Bianchi, M. E. and Agresti, A. (2011). "Substantial histone reduction modulates genomewide nucleosomal occupancy and global transcriptional output." *PLoS Biol* 9(6): e1001086.

Chen, C. J., Kono, H., Golenbock, D., Reed, G., Akira, S. and Rock, K. L. (2007). "Identification of a key pathway required for the sterile inflammatory response triggered by dying cells." *Nat Med* 13(7): 851-856.

Chen, G.-Y., Chen, X., King, S., Cavassani, K. A., Cheng, J., Zheng, X., Cao, H., Yu, H., Qu, J., Fang, D., Wu, W., Bai, X.-F., Liu, J.-Q., Woodiga, S. A., Chen, C., Sun, L., Hogaboam, C. M., Kunkel, S. L., Zheng, P. and Liu, Y. (2011). "Amelioration of sepsis by inhibiting sialidase-mediated disruption of the CD24-SiglecG interaction." *Nat Biotech* 29(5): 428-435.

Chen, G., Li, J., Ochani, M., Rendon-Mitchell, B., Qiang, X., Susarla, S., Ulloa, L., Yang, H., Fan, S., Goyert, S. M., Wang, P., Tracey, K. J., Sama, A. E. and Wang, H. (2004). "Bacterial endotoxin stimulates macrophages to release

HMGB1 partly through CD14- and TNF-dependent mechanisms." *J Leukoc Biol* 76(5): 994-1001.

Chen, G. Y., Tang, J., Zheng, P. and Liu, Y. (2009). "CD24 and Siglec-10 selectively repress tissue damage-induced immune responses." *Science* 323(5922): 1722-1725.

Chiu, J., March, P. E., Lee, R. and Tillett, D. (2004). "Site-directed, Ligase-Independent Mutagenesis (SLIM): a single-tube methodology approaching 100% efficiency in 4 h." *Nucleic Acids Research* 32(21): e174.

Clubb, R. T., Thanabal, V. and Wagner, G. (1992). "A constant-time three-dimensional triple-resonance pulse scheme to correlate intraresidue 1HN, 15N, and 13C′ chemical shifts in 15N□13C-labelled proteins." *Journal of Magnetic Resonance (1969)* 97(1): 213-217.

Cox, K. H., Cox, M. E., Woo-Rasberry, V. and Hasty, D. L. (2012). "Pathways involved in the synergistic activation of macrophages by lipoteichoic acid and hemoglobin." *PLoS One* 7(10): e47333.

Craig, D. G., Lee, P., Pryde, E. A., Masterton, G. S., Hayes, P. C. and Simpson, K. J. (2011). "Circulating apoptotic and necrotic cell death markers in patients with acute liver injury." *Liver Int* 31(8): 1127-1136.

Czura, C. J., Wang, H. and Tracey, K. J. (2001). "Dual roles for HMGB1: DNA binding and cytokine." *J Endotoxin Res* 7(4): 315-321.

Dahlin, D. C., Miwa, G. T., Lu, A. Y. and Nelson, S. D. (1984). "N-acetyl-p-benzoquinone imine: a cytochrome P-450-mediated oxidation product of acetaminophen." *Proc Natl Acad Sci U S A* 81(5): 1327-1331.

Deng, X., Stachlewitz, R. F., Liguori, M. J., Blomme, E. A., Waring, J. F., Luyendyk, J. P., Maddox, J. F., Ganey, P. E. and Roth, R. A. (2006). "Modest inflammation enhances diclofenac hepatotoxicity in rats: role of neutrophils and bacterial translocation." *J Pharmacol Exp Ther* 319(3): 1191-1199.

Dinarello, C. A. (1991). "Interleukin-1 and interleukin-1 antagonism." *Blood* 77(8): 1627-1652.

Dinarello, C. A. (1996). "Biologic basis for interleukin-1 in disease." *Blood* 87(6): 2095-2147.

Dinarello, C. A. (2011). "Interleukin-1 in the pathogenesis and treatment of inflammatory diseases." *Blood* 117(14): 3720-3732.

Dintilhac, A. and Bernués, J. (2002). "HMGB1 Interacts with Many Apparently Unrelated Proteins by Recognizing Short Amino Acid Sequences." *Journal of Biological Chemistry* 277(9): 7021-7028.

Driscoll, P. C., Clore, G. M., Marion, D., Wingfield, P. T. and Gronenborn, A. M. (1990). "Complete resonance assignment for the polypeptide backbone of interleukin 1.beta. using three-dimensional heteronuclear NMR spectroscopy." *Biochemistry* 29(14): 3542-3556.

Dumitriu, I. E., Baruah, P., Valentinis, B., Voll, R. E., Herrmann, M., Nawroth, P. P., Arnold, B., Bianchi, M. E., Manfredi, A. A. and Rovere-Querini, P. (2005). "Release of High Mobility Group Box 1 by Dendritic Cells Controls T Cell Activation via the Receptor for Advanced Glycation End Products." *The Journal of Immunology* 174(12): 7506-7515.

Eder, C. (2009). "Mechanisms of interleukin-1beta release." *Immunobiology* 214(7): 543-553.

Erridge, C., Bennett-Guerrero, E. and Poxton, I. R. (2002). "Structure and function of lipopolysaccharides." *Microbes Infect* 4(8): 837-851.

Ferhani, N., Letuve, S., Kozhich, A., Thibaudeau, O., Grandsaigne, M., Maret, M., Dombret, M. C., Sims, G. P., Kolbeck, R., Coyle, A. J., Aubier, M. and Pretolani, M. (2010). "Expression of high-mobility group box 1 and of receptor for advanced glycation end products in chronic obstructive pulmonary disease." *Am J Respir Crit Care Med* 181(9): 917-927.

Ferrari, S., Finelli, P., Rocchi, M. and Bianchi, M. E. (1996). "The Active Gene That Encodes Human High Mobility Group 1 Protein (HMG1) Contains Introns and Maps to Chromosome 13." *Genomics* 35(2): 367-371.

Frei, K., Malipiero, U. V., Leist, T. P., Zinkernagel, R. M., Schwab, M. E. and Fontana, A. (1989). "On the cellular source and function of interleukin 6 produced in the central nervous system in viral diseases." *Eur J Immunol* 19(4): 689-694.

Gallucci, S. and Matzinger, P. (2001). "Danger signals: SOS to the immune system." *Curr Opin Immunol* 13(1): 114-119.

Gao, B. and Tsan, M. F. (2003). "Endotoxin contamination in recombinant human heat shock protein 70 (Hsp70) preparation is responsible for the induction of tumor necrosis factor alpha release by murine macrophages." *J Biol Chem* 278(1): 174-179.

Gao, B. and Tsan, M. F. (2003). "Recombinant human heat shock protein 60 does not induce the release of tumor necrosis factor alpha from murine macrophages." *J Biol Chem* 278(25): 22523-22529.

Gao, H. M., Zhou, H., Zhang, F., Wilson, B. C., Kam, W. and Hong, J. S. (2011). "HMGB1 acts on microglia Mac1 to mediate chronic neuroinflammation that drives progressive neurodegeneration." *J Neurosci* 31(3): 1081-1092.

Garcia-Arnandis, I., Guillen, M. I., Gomar, F., Pelletier, J. P., Martel-Pelletier, J. and Alcaraz, M. J. (2010). "High mobility group box 1 potentiates the pro-inflammatory effects of interleukin-1beta in osteoarthritic synoviocytes." *Arthritis Res Ther* 12(4): R165.

Gauldie, J., Richards, C., Harnish, D., Lansdorp, P. and Baumann, H. (1987). "Interferon beta 2/B-cell stimulatory factor type 2 shares identity with monocyte-derived hepatocyte-stimulating factor and regulates the major acute phase protein response in liver cells." *Proc Natl Acad Sci U S A* 84(20): 7251-7255.

Gay, N. J. and Keith, F. J. (1991). "Drosophila Toll and IL-1 receptor." *Nature* 351(6325): 355-356.

Goodwin, G. H., Sanders, C. and Johns, E. W. (1973). "A new group of chromatin-associated proteins with a high content of acidic and basic amino acids." *Eur J Biochem* 38(1): 14-19.

Grattagliano, I., Portincasa, P., Palmieri, V. O. and Palasciano, G. (2002). "Overview on the mechanisms of drug-induced liver cell death." *Ann Hepatol* 1(4): 162-168.

Greenfeder, S. A., Nunes, P., Kwee, L., Labow, M., Chizzonite, R. A. and Ju, G. (1995). "Molecular cloning and characterization of a second subunit of the interleukin 1 receptor complex." *J Biol Chem* 270(23): 13757-13765.

Grzesiek, S. and Bax, A. (1992). "Correlating backbone amide and side chain resonances in larger proteins by multiple relayed triple resonance NMR." *Journal of the American Chemical Society* 114(16): 6291-6293.

Grzesiek, S. and Bax, A. (1992). "An efficient experiment for sequential backbone assignment of medium-sized isotopically enriched proteins." *Journal of Magnetic Resonance (1969)* 99(1): 201-207.

Gunaratnam, N. T., Benson, J., Gandolfi, A. J. and Chen, M. (1995). "Suspected isoflurane hepatitis in an obese patient with a history of halothane hepatitis." *Anesthesiology* 83(6): 1361-1364.

Halmes, N. C., Hinson, J. A., Martin, B. M. and Pumford, N. R. (1996). "Glutamate dehydrogenase covalently binds to a reactive metabolite of acetaminophen." *Chem Res Toxicol* 9(2): 541-546.

Hanahan, D. (1983). "Studies on transformation of Escherichia coli with plasmids." *J Mol Biol* 166(4): 557-580.

Hardman, C. H., Broadhurst, R. W., Raine, A. R., Grasser, K. D., Thomas, J. O. and Laue, E. D. (1995). "Structure of the A-domain of HMG1 and its interaction with DNA as studied by heteronuclear three- and four-dimensional NMR spectroscopy." *Biochemistry* 34(51): 16596-16607.

Harris, H. E., Andersson, U. and Pisetsky, D. S. (2012). "HMGB1: a multifunctional alarmin driving autoimmune and inflammatory disease." *Nat Rev Rheumatol* 8(4): 195-202.

Harris, H. E. and Raucci, A. (2006). "Alarmin(g) news about danger." *Embo Reports* 7(8): 774-778.

Hawton, K., Ware, C., Mistry, H., Hewitt, J., Kingsbury, S., Roberts, D. and Weitzel, H. (1995). "Why patients choose paracetamol for self poisoning and their knowledge of its dangers." *BMJ* 310(6973): 164.

Hirano, T., Taga, T., Nakano, N., Yasukawa, K., Kashiwamura, S., Shimizu, K., Nakajima, K., Pyun, K. H. and Kishimoto, T. (1985). "Purification to homogeneity and characterization of human B-cell differentiation factor (BCDF or BSFp-2)." *Proc Natl Acad Sci U S A* 82(16): 5490-5494.

Hochuli, E., Bannwarth, W., Dobeli, H., Gentz, R. and Stuber, D. (1988). "Genetic Approach to Facilitate Purification of Recombinant Proteins with a Novel Metal Chelate Adsorbent." *Nat Biotech* 6(11): 1321-1325.

Holt, M. P. and Ju, C. (2006). "Mechanisms of drug-induced liver injury." *AAPS J* 8(1): E48-54.

Hoque, R., Farooq, A. and Mehal, W. Z. (2013). "Sterile inflammation in the liver and pancreas." *J Gastroenterol Hepatol* 28 Suppl 1: 61-67.

Hori, O., Brett, J., Slattery, T., Cao, R., Zhang, J., Chen, J. X., Nagashima, M., Lundh, E. R., Vijay, S., Nitecki, D. and et al. (1995). "The receptor for advanced glycation end products (RAGE) is a cellular binding site for amphoterin. Mediation of neurite outgrowth and co-expression of rage and amphoterin in the developing nervous system." *J Biol Chem* 270(43): 25752-25761.

Hoshino, K., Takeuchi, O., Kawai, T., Sanjo, H., Ogawa, T., Takeda, Y., Takeda, K. and Akira, S. (1999). "Cutting edge: Toll-like receptor 4 (TLR4)-deficient mice are hyporesponsive to lipopolysaccharide: evidence for TLR4 as the Lps gene product." *J Immunol* 162(7): 3749-3752.

Hreggvidsdottir, H. S., Lundberg, A. M., Aveberger, A. C., Klevenvall, L., Andersson, U. and Harris, H. E. (2011). "HMGB1-partner molecule complexes enhance cytokine production by signaling through the partner molecule receptor." *Mol Med*.

Hreggvidsdottir, H. S., Ostberg, T., Wahamaa, H., Schierbeck, H., Aveberger, A. C., Klevenvall, L., Palmblad, K., Ottosson, L., Andersson, U. and Harris, H. E. (2009). "The alarmin HMGB1 acts in synergy with endogenous and exogenous danger signals to promote inflammation." *J Leukoc Biol* 86(3): 655-662.

Huang, Y., Yin, H., Han, J., Huang, B., Xu, J., Zheng, F., Tan, Z., Fang, M., Rui, L., Chen, D., Wang, S., Zheng, X., Wang, C. Y. and Gong, F. (2007). "Extracellular Hmgb1 Functions as an Innate Immune-Mediator Implicated in Murine Cardiac Allograft Acute Rejection." *American Journal of Transplantation* 7(4): 799-808.

Huttunen, H. J., Fages, C., Kuja-Panula, J., Ridley, A. J. and Rauvala, H. (2002). "Receptor for advanced glycation end products-binding COOH-terminal motif of amphoterin inhibits invasive migration and metastasis." *Cancer Res* 62(16): 4805-4811.

Ikebuchi, K., Wong, G. G., Clark, S. C., Ihle, J. N., Hirai, Y. and Ogawa, M. (1987). "Interleukin 6 enhancement of interleukin 3-dependent proliferation of multipotential hemopoietic progenitors." *Proc Natl Acad Sci U S A* 84(24): 9035-9039.

Ilmakunnas, M., Tukiainen, E. M., Rouhiainen, A., Rauvala, H., Arola, J., Nordin, A., Makisalo, H., Hockerstedt, K. and Isoniemi, H. (2008). "High mobility group box 1 protein as a marker of hepatocellular injury in human liver transplantation." *Liver Transpl* 14(10): 1517-1525.

Ishida, Y., Kondo, T., Ohshima, T., Fujiwara, H., Iwakura, Y. and Mukaida, N. (2002). "A pivotal involvement of IFN-gamma in the pathogenesis of acetaminophen-induced acute liver injury." *FASEB J* 16(10): 1227-1236.

Ishihara, K. and Hirano, T. (2002). "IL-6 in autoimmune disease and chronic inflammatory proliferative disease." *Cytokine Growth Factor Rev* 13(4-5): 357-368.

Ito, I., Fukazawa, J. and Yoshida, M. (2007). "Post-translational methylation of high mobility group box 1 (HMGB1) causes its cytoplasmic localization in neutrophils." *J Biol Chem* 282(22): 16336-16344.

Ivanov, S., Dragoi, A. M., Wang, X., Dallacosta, C., Louten, J., Musco, G., Sitia, G., Yap, G. S., Wan, Y., Biron, C. A., Bianchi, M. E., Wang, H. and Chu, W. M. (2007). "A novel role for HMGB1 in TLR9-mediated inflammatory responses to CpG-DNA." *Blood* 110(6): 1970-1981.

Iwamoto, G. K., Monick, M. M., Burmeister, L. F. and Hunninghake, G. W. (1989). "Interleukin 1 release by human alveolar macrophages and blood monocytes." *Am J Physiol* 256(5 Pt 1): C1012-1015.

Iyer, S. S., Pulskens, W. P., Sadler, J. J., Butter, L. M., Teske, G. J., Ulland, T. K., Eisenbarth, S. C., Florquin, S., Flavell, R. A., Leemans, J. C. and Sutterwala, F. S. (2009). "Necrotic cells trigger a sterile inflammatory response through the Nlrp3 inflammasome." *Proc Natl Acad Sci U S A* 106(48): 20388-20393.

Jahr, S., Hentze, H., Englisch, S., Hardt, D., Fackelmayer, F. O., Hesch, R. D. and Knippers, R. (2001). "DNA fragments in the blood plasma of cancer patients: quantitations and evidence for their origin from apoptotic and necrotic cells." *Cancer Res* 61(4): 1659-1665.

James, L. P., McCullough, S. S., Lamps, L. W. and Hinson, J. A. (2003). "Effect of N-acetylcysteine on acetaminophen toxicity in mice: relationship to reactive nitrogen and cytokine formation." *Toxicol Sci* 75(2): 458-467.

Jayaraman, L., Moorthy, N. C., Murthy, K. G., Manley, J. L., Bustin, M. and Prives, C. (1998). "High mobility group protein-1 (HMG-1) is a unique activator of p53." *Genes Dev* 12(4): 462-472.

Jiang, Z., Ninomiya-Tsuji, J., Qian, Y., Matsumoto, K. and Li, X. (2002). "Interleukin-1 (IL-1) receptor-associated kinase-dependent IL-1-induced signaling complexes phosphorylate TAK1 and TAB2 at the plasma membrane and activate TAK1 in the cytosol." *Mol Cell Biol* 22(20): 7158-7167.

Ju, C., Reilly, T. P., Bourdi, M., Radonovich, M. F., Brady, J. N., George, J. W. and Pohl, L. R. (2002). "Protective role of Kupffer cells in acetaminophen-induced hepatic injury in mice." *Chem Res Toxicol* 15(12): 1504-1513.

Jung, Y. and Lippard, S. J. (2003). "Nature of full-length HMGB1 binding to cisplatin-modified DNA." *Biochemistry* 42(9): 2664-2671.

Kaplowitz, N. (2004). "Drug-induced liver injury." *Clin Infect Dis* 38 Suppl 2: S44-48.

Kaplowitz, N. (2005). "Idiosyncratic drug hepatotoxicity." *Nat Rev Drug Discov* 4(6): 489-499.

Kazama, H., Ricci, J. E., Herndon, J. M., Hoppe, G., Green, D. R. and Ferguson, T. A. (2008). "Induction of immunological tolerance by apoptotic cells requires caspase-dependent oxidation of high-mobility group box-1 protein." *Immunity* 29(1): 21-32.

Kishimoto, T. (2006). "Interleukin-6: discovery of a pleiotropic cytokine." *Arthritis Res Ther* 8 Suppl 2: S2.

Knapp, S., Muller, S., Digilio, G., Bonaldi, T., Bianchi, M. E. and Musco, G. (2004). "The long acidic tail of high mobility group box 1 (HMGB1) protein forms an extended and flexible structure that interacts with specific residues within and between the HMG boxes." *Biochemistry* 43(38): 11992-11997.

Kokkola, R., Sundberg, E., Ulfgren, A. K., Palmblad, K., Li, J., Wang, H., Ulloa, L., Yang, H., Yan, X. J., Furie, R., Chiorazzi, N., Tracey, K. J., Andersson, U. and Harris, H. E. (2002). "High mobility group box chromosomal protein 1: a novel proinflammatory mediator in synovitis." *Arthritis Rheum* 46(10): 2598-2603.

Kola, I. and Landis, J. (2004). "Can the pharmaceutical industry reduce attrition rates?" *Nat Rev Drug Discov* 3(8): 711-715.

Kollewe, C., Mackensen, A. C., Neumann, D., Knop, J., Cao, P., Li, S., Wesche, H. and Martin, M. U. (2004). "Sequential autophosphorylation steps in the interleukin-1 receptor-associated kinase-1 regulate its availability as an adapter in interleukin-1 signaling." *J Biol Chem* 279(7): 5227-5236.

Kostura, M. J., Tocci, M. J., Limjuco, G., Chin, J., Cameron, P., Hillman, A. G., Chartrain, N. A. and Schmidt, J. A. (1989). "Identification of a monocyte specific pre-interleukin 1 beta convertase activity." *Proc Natl Acad Sci U S A* 86(14): 5227-5231.

Kovalovich, K., DeAngelis, R. A., Li, W., Furth, E. E., Ciliberto, G. and Taub, R. (2000). "Increased toxin-induced liver injury and fibrosis in interleukin-6-deficient mice." *Hepatology* 31(1): 149-159.

Kubes, P. and Mehal, W. Z. (2012). "Sterile inflammation in the liver." *Gastroenterology* 143(5): 1158-1172.

Kuno, K. and Matsushima, K. (1994). "The IL-1 receptor signaling pathway." *J Leukoc Biol* 56(5): 542-547.

Laemmli, U. K. (1970). "Cleavage of structural proteins during the assembly of the head of bacteriophage T4." *Nature* 227(5259): 680-685.

Lamkanfi, M., Sarkar, A., Vande Walle, L., Vitari, A. C., Amer, A. O., Wewers, M. D., Tracey, K. J., Kanneganti, T. D. and Dixit, V. M. (2010).

"Inflammasome-dependent release of the alarmin HMGB1 in endotoxemia." *J Immunol* 185(7): 4385-4392.

Landin, J. S., Cohen, S. D. and Khairallah, E. A. (1996). "Identification of a 54-kDa mitochondrial acetaminophen-binding protein as aldehyde dehydrogenase." *Toxicol Appl Pharmacol* 141(1): 299-307.

Lange, S. S., Mitchell, D. L. and Vasquez, K. M. (2008). "High mobility group protein B1 enhances DNA repair and chromatin modification after DNA damage." *Proc Natl Acad Sci U S A* 105(30): 10320-10325.

Lasser, K. E., Allen, P. D., Woolhandler, S. J., Himmelstein, D. U., Wolfe, S. M. and Bor, D. H. (2002). "Timing of new black box warnings and withdrawals for prescription medications." *JAMA* 287(17): 2215-2220.

Laverty, H. G., Antoine, D. J., Benson, C., Chaponda, M., Williams, D. and Kevin Park, B. (2010). "The potential of cytokines as safety biomarkers for drug-induced liver injury." *Eur J Clin Pharmacol* 66(10): 961-976.

Lazarou, J., Pomeranz, B. H. and Corey, P. N. (1998). "Incidence of adverse drug reactions in hospitalized patients: a meta-analysis of prospective studies." *JAMA* 279(15): 1200-1205.

Leclerc, P., Wahamaa, H., Idborg, H., Jakobsson, P. J., Harris, H. E. and Korotkova, M. (2013). "IL-1beta/HMGB1 complexes promote The PGE2 biosynthesis pathway in synovial fibroblasts." *Scand J Immunol* 77(5): 350-360.

Lecoeur, S., Andre, C. and Beaune, P. H. (1996). "Tienilic acid-induced autoimmune hepatitis: anti-liver and-kidney microsomal type 2 autoantibodies recognize a three-site conformational epitope on cytochrome P4502C9." *Mol Pharmacol* 50(2): 326-333.

Lee, K. B., Brooks, D. J. and Thomas, J. O. (1998). "Selection of a cDNA clone for chicken high-mobility-group 1 (HMG1) protein through its unusually conserved 3'-untranslated region, and improved expression of recombinant HMG1 in Escherichia coli." *Gene* 225(1-2): 97-105.

Lee, K. B. and Thomas, J. O. (2000). "The effect of the acidic tail on the DNA-binding properties of the HMG1,2 class of proteins: insights from tail switching and tail removal." *J Mol Biol* 304(2): 135-149.

Lee, W. M. (2003). "Drug-induced hepatotoxicity." *N Engl J Med* 349(5): 474-485.

Leung, K., Betts, J. C., Xu, L. and Nabel, G. J. (1994). "The cytoplasmic domain of the interleukin-1 receptor is required for nuclear factor-kappa B signal transduction." *J Biol Chem* 269(3): 1579-1582.

Levy, M. (1997). "Role of viral infections in the induction of adverse drug reactions." *Drug Saf* 16(1): 1-8.

Li, J., Kokkola, R., Tabibzadeh, S., Yang, R., Ochani, M., Qiang, X., Harris, H. E., Czura, C. J., Wang, H., Ulloa, L., Warren, H. S., Moldawer, L. L., Fink, M. P., Andersson, U., Tracey, K. J. and Yang, H. (2003). "Structural basis for

the proinflammatory cytokine activity of high mobility group box 1." *Mol Med* 9(1-2): 37-45.

Li, J., Wang, H., Mason, J. M., Levine, J., Yu, M., Ulloa, L., Czura, C. J., Tracey, K. J. and Yang, H. (2004). "Recombinant HMGB1 with cytokine-stimulating activity." *J Immunol Methods* 289(1-2): 211-223.

Li, J., Wang, H., Mason, J. M., Levine, J., Yu, M., Ulloa, L., Czura, C. J., Tracey, K. J. and Yang, H. (2004). "Recombinant HMGB1 with cytokine-stimulating activity." *Journal of Immunological Methods* 289(1-2): 211-223.

Lian, L.-Y. and Middleton, D. A. (2001). "Labelling approaches for protein structural studies by solution-state and solid-state NMR." *Progress in Nuclear Magnetic Resonance Spectroscopy* 39(3): 171-190.

Libermann, T. A. and Baltimore, D. (1990). "Activation of interleukin-6 gene expression through the NF-kappa B transcription factor." *Mol Cell Biol* 10(5): 2327-2334.

Lind, R. C., Gandolfi, A. J., Sipes, I. G. and Brown, B. R., Jr. (1984). "The involvement of endotoxin in halothane-associated liver injury." *Anesthesiology* 61(5): 544-550.

Lotz, M., Jirik, F., Kabouridis, P., Tsoukas, C., Hirano, T., Kishimoto, T. and Carson, D. A. (1988). "B cell stimulating factor 2/interleukin 6 is a costimulant for human thymocytes and T lymphocytes." *J Exp Med* 167(3): 1253-1258.

Lotze, M. T. and Tracey, K. J. (2005). "High-mobility group box 1 protein (HMGB1): nuclear weapon in the immune arsenal." *Nat Rev Immunol* 5(4): 331-342.

Lu, B., Nakamura, T., Inouye, K., Li, J., Tang, Y., Lundback, P., Valdes-Ferrer, S. I., Olofsson, P. S., Kalb, T., Roth, J., Zou, Y., Erlandsson-Harris, H., Yang, H., Ting, J. P., Wang, H., Andersson, U., Antoine, D. J., Chavan, S. S., Hotamisligil, G. S. and Tracey, K. J. (2012). "Novel role of PKR in inflammasome activation and HMGB1 release." *Nature* 488(7413): 670-674.

Luckey, S. W., Taylor, M., Sampey, B. P., Scheinman, R. I. and Petersen, D. R. (2002). "4-hydroxynonenal decreases interleukin-6 expression and protein production in primary rat Kupffer cells by inhibiting nuclear factor-kappaB activation." *J Pharmacol Exp Ther* 302(1): 296-303.

Luyendyk, J. P., Maddox, J. F., Cosma, G. N., Ganey, P. E., Cockerell, G. L. and Roth, R. A. (2003). "Ranitidine treatment during a modest inflammatory response precipitates idiosyncrasy-like liver injury in rats." *J Pharmacol Exp Ther* 307(1): 9-16.

Maddox, J. F., Amuzie, C. J., Li, M., Newport, S. W., Sparkenbaugh, E., Cuff, C. F., Pestka, J. J., Cantor, G. H., Roth, R. A. and Ganey, P. E. (2010). "Bacterial- and viral-induced inflammation increases sensitivity to acetaminophen hepatotoxicity." *J Toxicol Environ Health A* 73(1): 58-73.

Maddrey, W., Schiff, E. R. and Sorrell, M. F. (2011). Schiff's Diseases of the Liver. Hoboken, NJ, USA, Wiley.

Makin, A. J., Wendon, J. and Williams, R. (1995). "A 7-year experience of severe acetaminophen-induced hepatotoxicity (1987-1993)." *Gastroenterology* 109(6): 1907-1916.

Mariathasan, S., Weiss, D. S., Newton, K., McBride, J., O'Rourke, K., Roose-Girma, M., Lee, W. P., Weinrauch, Y., Monack, D. M. and Dixit, V. M. (2006). "Cryopyrin activates the inflammasome in response to toxins and ATP." *Nature* 440(7081): 228-232.

Martin-Murphy, B. V., Holt, M. P. and Ju, C. (2010). "The role of damage associated molecular pattern molecules in acetaminophen-induced liver injury in mice." *Toxicol Lett* 192(3): 387-394.

Martin, M. U. and Wesche, H. (2002). "Summary and comparison of the signaling mechanisms of the Toll/interleukin-1 receptor family." *Biochim Biophys Acta* 1592(3): 265-280.

Martinon, F., Burns, K. and Tschopp, J. (2002). "The inflammasome: a molecular platform triggering activation of inflammatory caspases and processing of proIL-beta." *Mol Cell* 10(2): 417-426.

Masubuchi, Y., Bourdi, M., Reilly, T. P., Graf, M. L., George, J. W. and Pohl, L. R. (2003). "Role of interleukin-6 in hepatic heat shock protein expression and protection against acetaminophen-induced liver disease." *Biochem Biophys Res Commun* 304(1): 207-212.

Matzinger, P. (1994). "Tolerance, danger, and the extended family." *Annu Rev Immunol* 12: 991-1045.

McKinney, K. and Prives, C. (2002). "Efficient specific DNA binding by p53 requires both its central and C-terminal domains as revealed by studies with high-mobility group 1 protein." *Mol Cell Biol* 22(19): 6797-6808.

McMahan, C. J., Slack, J. L., Mosley, B., Cosman, D., Lupton, S. D., Brunton, L. L., Grubin, C. E., Wignall, J. M., Jenkins, N. A., Brannan, C. I. and et al. (1991). "A novel IL-1 receptor, cloned from B cells by mammalian expression, is expressed in many cell types." *EMBO J* 10(10): 2821-2832.

Melloni, E., Sparatore, B., Patrone, M., Pessino, A., Passalacqua, M. and Pontremoli, S. (1995). "Extracellular release of the 'differentiation enhancing factor', a HMG1 protein type, is an early step in murine erythroleukemia cell differentiation." *FEBS Lett* 368(3): 466-470.

Mitchell, J. R., Jollow, D. J., Potter, W. Z., Davis, D. C., Gillette, J. R. and Brodie, B. B. (1973). "Acetaminophen-induced hepatic necrosis. I. Role of drug metabolism." *J Pharmacol Exp Ther* 187(1): 185-194.

Moore, T. J., Cohen, M. R. and Furberg, C. D. (2007). "Serious adverse drug events reported to the Food and Drug Administration, 1998-2005." *Arch Intern Med* 167(16): 1752-1759.

Muhammad, S., Barakat, W., Stoyanov, S., Murikinati, S., Yang, H., Tracey, K. J., Bendszus, M., Rossetti, G., Nawroth, P. P., Bierhaus, A. and Schwaninger, M. (2008). "The HMGB1 receptor RAGE mediates ischemic brain damage." *J Neurosci* 28(46): 12023-12031.

Muller, S., Bianchi, M. E. and Knapp, S. (2001). "Thermodynamics of HMGB1 interaction with duplex DNA." *Biochemistry* 40(34): 10254-10261.

Muller, S., Ronfani, L. and Bianchi, M. E. (2004). "Regulated expression and subcellular localization of HMGB1, a chromatin protein with a cytokine function." *J Intern Med* 255(3): 332-343.

Muskett, F. W. (2011). Protein NMR Spectroscopy : Practical Techniques and Applications. L. Y. Lian and G. Roberts. Hoboken NJ, USA, Wiley.

Muzio, M., Ni, J., Feng, P. and Dixit, V. M. (1997). "IRAK (Pelle) Family Member IRAK-2 and MyD88 as Proximal Mediators of IL-1 Signaling." *Science* 278(5343): 1612-1615.

Nathan, C. (2002). "Points of control in inflammation." *Nature* 420(6917): 846-852.

Nguyen, G. C., Sam, J. and Thuluvath, P. J. (2008). "Hepatitis C is a predictor of acute liver injury among hospitalizations for acetaminophen overdose in the United States: a nationwide analysis." *Hepatology* 48(4): 1336-1341.

Onate, S. A., Prendergast, P., Wagner, J. P., Nissen, M., Reeves, R., Pettijohn, D. E. and Edwards, D. P. (1994). "The DNA-bending protein HMG-1 enhances progesterone receptor binding to its target DNA sequences." *Mol Cell Biol* 14(5): 3376-3391.

Orlova, V. V., Choi, E. Y., Xie, C., Chavakis, E., Bierhaus, A., Ihanus, E., Ballantyne, C. M., Gahmberg, C. G., Bianchi, M. E., Nawroth, P. P. and Chavakis, T. (2007). "A novel pathway of HMGB1-mediated inflammatory cell recruitment that requires Mac-1-integrin." *EMBO J* 26(4): 1129-1139.

Ostapowicz, G., Fontana, R. J., Schiodt, F. V., Larson, A., Davern, T. J., Han, S. H., McCashland, T. M., Shakil, A. O., Hay, J. E., Hynan, L., Crippin, J. S., Blei, A. T., Samuel, G., Reisch, J. and Lee, W. M. (2002). "Results of a prospective study of acute liver failure at 17 tertiary care centers in the United States." *Ann Intern Med* 137(12): 947-954.

Ostberg, T., Kawane, K., Nagata, S., Yang, H., Chavan, S., Klevenvall, L., Bianchi, M. E., Harris, H. E., Andersson, U. and Palmblad, K. (2010). "Protective targeting of high mobility group box chromosomal protein 1 in a spontaneous arthritis model." *Arthritis Rheum* 62(10): 2963-2972.

Park, B. K., Laverty, H., Srivastava, A., Antoine, D. J., Naisbitt, D. and Williams, D. P. (2011). "Drug bioactivation and protein adduct formation in the pathogenesis of drug-induced toxicity." *Chem Biol Interact* 192(1-2): 30-36.

Park, B. K., Pirmohamed, M. and Kitteringham, N. R. (1998). "Role of drug disposition in drug hypersensitivity: a chemical, molecular, and clinical perspective." *Chem Res Toxicol* 11(9): 969-988.

Park, J. S., Svetkauskaite, D., He, Q., Kim, J. Y., Strassheim, D., Ishizaka, A. and Abraham, E. (2004). "Involvement of toll-like receptors 2 and 4 in cellular activation by high mobility group box 1 protein." *J Biol Chem* 279(9): 7370-7377.

Park, S. and Lippard, S. J. (2011). "Redox state-dependent interaction of HMGB1 and cisplatin-modified DNA." *Biochemistry* 50(13): 2567-2574.

Pasheva, E., Sarov, M., Bidjekov, K., Ugrinova, I., Sarg, B., Lindner, H. and Pashev, I. G. (2004). "In vitro acetylation of HMGB-1 and -2 proteins by CBP: the role of the acidic tail." *Biochemistry* 43(10): 2935-2940.

Petsch, D. and Anspach, F. B. (2000). "Endotoxin removal from protein solutions." *J Biotechnol* 76(2-3): 97-119.

Pichler, W. J., Beeler, A., Keller, M., Lerch, M., Posadas, S., Schmid, D., Spanou, Z., Zawodniak, A. and Gerber, B. (2006). "Pharmacological interaction of drugs with immune receptors: the p-i concept." *Allergol Int* 55(1): 17-25.

Pirmohamed, M., James, S., Meakin, S., Green, C., Scott, A. K., Walley, T. J., Farrar, K., Park, B. K. and Breckenridge, A. M. (2004). "Adverse drug reactions as cause of admission to hospital: prospective analysis of 18 820 patients." *BMJ* 329(7456): 15-19.

PyMoL.The PyMOL Molecular Graphics System.Version 1.5.0.4.Schrödinger, LLC.

Qin, Y. H., Dai, S. M., Tang, G. S., Zhang, J., Ren, D., Wang, Z. W. and Shen, Q. (2009). "HMGB1 enhances the proinflammatory activity of lipopolysaccharide by promoting the phosphorylation of MAPK p38 through receptor for advanced glycation end products." *J Immunol* 183(10): 6244-6250.

Quintana, F. J. and Cohen, I. R. (2005). "Heat shock proteins as endogenous adjuvants in sterile and septic inflammation." *J Immunol* 175(5): 2777-2782.

Ramstein, J., Locker, D., Bianchi, M. E. and Leng, M. (1999). "Domain-domain interactions in high mobility group 1 protein (HMG1)." *Eur J Biochem* 260(3): 692-700.

Reeves, R. (2010). "Nuclear functions of the HMG proteins." *Biochim Biophys Acta* 1799(1-2): 3-14.

Rouhiainen, A., Tumova, S., Valmu, L., Kalkkinen, N. and Rauvala, H. (2007). "Pivotal advance: analysis of proinflammatory activity of highly purified eukaryotic recombinant HMGB1 (amphoterin)." *J Leukoc Biol* 81(1): 49-58.

Rovere-Querini, P., Capobianco, A., Scaffidi, P., Valentinis, B., Catalanotti, F., Giazzon, M., Dumitriu, I. E., Muller, S., Iannacone, M., Traversari, C., Bianchi, M. E. and Manfredi, A. A. (2004). "HMGB1 is an endogenous immune adjuvant released by necrotic cells." *Embo Reports* 5(8): 825-830.

Rowell, John P., Simpson, Kathryn L., Stott, K., Watson, M. and Thomas, Jean O. (2012). "HMGB1-Facilitated p53 DNA Binding Occurs via HMG-Box/p53

Transactivation Domain Interaction, Regulated by the Acidic Tail." *Structure (London, England : 1993)* 20(12): 2014-2024.

Salmivirta, M., Rauvala, H., Elenius, K. and Jalkanen, M. (1992). "Neurite growth-promoting protein (amphoterin, p30) binds syndecan." *Exp Cell Res* 200(2): 444-451.

Satoh, H., Martin, B. M., Schulick, A. H., Christ, D. D., Kenna, J. G. and Pohl, L. R. (1989). "Human anti-endoplasmic reticulum antibodies in sera of patients with halothane-induced hepatitis are directed against a trifluoroacetylated carboxylesterase." *Proc Natl Acad Sci U S A* 86(1): 322-326.

Satoh, T., Nakamura, S., Taga, T., Matsuda, T., Hirano, T., Kishimoto, T. and Kaziro, Y. (1988). "Induction of neuronal differentiation in PC12 cells by B-cell stimulatory factor 2/interleukin 6." *Mol Cell Biol* 8(8): 3546-3549.

Saunders, M., Wishnia, A. and Kirkwood, J. G. (1957). "THE NUCLEAR MAGNETIC RESONANCE SPECTRUM OF RIBONUCLEASE1." *Journal of the American Chemical Society* 79(12): 3289-3290.

Scaffidi, P., Misteli, T. and Bianchi, M. E. (2002). "Release of chromatin protein HMGB1 by necrotic cells triggers inflammation." *Nature* 418(6894): 191-195.

Schiraldi, M., Raucci, A., Munoz, L. M., Livoti, E., Celona, B., Venereau, E., Apuzzo, T., De Marchis, F., Pedotti, M., Bachi, A., Thelen, M., Varani, L., Mellado, M., Proudfoot, A., Bianchi, M. E. and Uguccioni, M. (2012). "HMGB1 promotes recruitment of inflammatory cells to damaged tissues by forming a complex with CXCL12 and signaling via CXCR4." *J Exp Med* 209(3): 551-563.

Semino, C., Angelini, G., Poggi, A. and Rubartelli, A. (2005). "NK/iDC interaction results in IL-18 secretion by DCs at the synaptic cleft followed by NK cell activation and release of the DC maturation factor HMGB1." *Blood* 106(2): 609-616.

Sgro, C., Clinard, F., Ouazir, K., Chanay, H., Allard, C., Guilleminet, C., Lenoir, C., Lemoine, A. and Hillon, P. (2002). "Incidence of drug-induced hepatic injuries: a French population-based study." *Hepatology* 36(2): 451-455.

Sha, Y., Zmijewski, J., Xu, Z. and Abraham, E. (2008). "HMGB1 develops enhanced proinflammatory activity by binding to cytokines." *J Immunol* 180(4): 2531-2537.

Shakhov, A. N., Collart, M. A., Vassalli, P., Nedospasov, S. A. and Jongeneel, C. V. (1990). "Kappa B-type enhancers are involved in lipopolysaccharide-mediated transcriptional activation of the tumor necrosis factor alpha gene in primary macrophages." *J Exp Med* 171(1): 35-47.

Shaw, P. J., Hopfensperger, M. J., Ganey, P. E. and Roth, R. A. (2007). "Lipopolysaccharide and trovafloxacin coexposure in mice causes idiosyncrasy-like liver injury dependent on tumor necrosis factor-alpha." *Toxicol Sci* 100(1): 259-266.

Sheflin, L. G., Fucile, N. W. and Spaulding, S. W. (1993). "The specific interactions of HMG 1 and 2 with negatively supercoiled DNA are modulated by their acidic C-terminal domains and involve cysteine residues in their HMG 1/2 boxes." *Biochemistry* 32(13): 3238-3248.

Siebenlist, U., Franzoso, G. and Brown, K. (1994). "Structure, regulation and function of NF-kappa B." *Annu Rev Cell Biol* 10: 405-455.

Simpson, R. J., Hammacher, A., Smith, D. K., Matthews, J. M. and Ward, L. D. (1997). "Interleukin-6: structure-function relationships." *Protein Sci* 6(5): 929-955.

Sims, G. P., Rowe, D. C., Rietdijk, S. T., Herbst, R. and Coyle, A. J. (2010). "HMGB1 and RAGE in inflammation and cancer." *Annu Rev Immunol* 28: 367-388.

Sims, J. E., Acres, R. B., Grubin, C. E., McMahan, C. J., Wignall, J. M., March, C. J. and Dower, S. K. (1989). "Cloning the interleukin 1 receptor from human T cells." *Proceedings of the National Academy of Sciences* 86(22): 8946-8950.

Stott, K., Tang, G. S. F., Lee, K.-B. and Thomas, J. O. (2006). "Structure of a Complex of Tandem HMG Boxes and DNA." *Journal of Molecular Biology* 360(1): 90-104.

Stott, K., Watson, M., Howe, F. S., Grossmann, J. G. and Thomas, J. O. (2010). "Tail-Mediated Collapse of HMGB1 Is Dynamic and Occurs via Differential Binding of the Acidic Tail to the A and B Domains." *Journal of Molecular Biology* 403(5): 706-722.

Stros, M., Stokrova, J. and Thomas, J. O. (1994). "DNA looping by the HMG-box domains of HMG1 and modulation of DNA binding by the acidic C-terminal domain." *Nucleic Acids Res* 22(6): 1044-1051.

Štros, M., Štokrová, J. and Thomas, J. O. (1994). "DNA looping by the HMG-box domains of HMG1 and modulation of DNA binding by the acidic C-terminal domain." *Nucleic Acids Research* 22(6): 1044-1051.

Takeda, M. and Kainosho, M. (2011). Protein NMR Spectroscopy : Practical Techniques and Applications. L. Y. Lian and G. Roberts. Hoboken NJ, USA, Wiley.

Tang, D., Kang, R., Livesey, K. M., Cheh, C. W., Farkas, A., Loughran, P., Hoppe, G., Bianchi, M. E., Tracey, K. J., Zeh, H. J., 3rd and Lotze, M. T. (2010). "Endogenous HMGB1 regulates autophagy." *J Cell Biol* 190(5): 881-892.

Thornberry, N. A., Bull, H. G., Calaycay, J. R., Chapman, K. T., Howard, A. D., Kostura, M. J., Miller, D. K., Molineaux, S. M., Weidner, J. R., Aunins, J. and et al. (1992). "A novel heterodimeric cysteine protease is required for interleukin-1 beta processing in monocytes." *Nature* 356(6372): 768-774.

Tian, J., Avalos, A. M., Mao, S. Y., Chen, B., Senthil, K., Wu, H., Parroche, P., Drabic, S., Golenbock, D., Sirois, C., Hua, J., An, L. L., Audoly, L., La Rosa, G., Bierhaus, A., Naworth, P., Marshak-Rothstein, A., Crow, M. K.,

Fitzgerald, K. A., Latz, E., Kiener, P. A. and Coyle, A. J. (2007). "Toll-like receptor 9-dependent activation by DNA-containing immune complexes is mediated by HMGB1 and RAGE." *Nat Immunol* 8(5): 487-496.

Travers, A. A. and Thomas, J. O. (2004). Chromosomal HMG-box proteins Chromatin Structure and Dynamics: State-of-the-Art. J. Zlatanova and S. H. Leuba. The Netherlands, Elsevier**:** 103-133

Tsung, A., Klune, J. R., Zhang, X., Jeyabalan, G., Cao, Z., Peng, X., Stolz, D. B., Geller, D. A., Rosengart, M. R. and Billiar, T. R. (2007). "HMGB1 release induced by liver ischemia involves Toll-like receptor 4 dependent reactive oxygen species production and calcium-mediated signaling." *J Exp Med* 204(12): 2913-2923.

Ulrich, E. L., Akutsu, H., Doreleijers, J. F., Harano, Y., Ioannidis, Y. E., Lin, J., Livny, M., Mading, S., Maziuk, D., Miller, Z., Nakatani, E., Schulte, C. F., Tolmie, D. E., Kent Wenger, R., Yao, H. and Markley, J. L. (2008). "BioMagResBank." *Nucleic Acids Research* 36(suppl 1): D402-D408.

Urbonaviciute, V., Furnrohr, B. G., Meister, S., Munoz, L., Heyder, P., De Marchis, F., Bianchi, M. E., Kirschning, C., Wagner, H., Manfredi, A. A., Kalden, J. R., Schett, G., Rovere-Querini, P., Herrmann, M. and Voll, R. E. (2008). "Induction of inflammatory and immune responses by HMGB1-nucleosome complexes: implications for the pathogenesis of SLE." *J Exp Med* 205(13): 3007-3018.

Van Snick, J. (1990). "Interleukin-6: an overview." *Annu Rev Immunol* 8: 253-278.

Venereau, E., Casalgrandi, M., Schiraldi, M., Antoine, D. J., Cattaneo, A., De Marchis, F., Liu, J., Antonelli, A., Preti, A., Raeli, L., Shams, S. S., Yang, H., Varani, L., Andersson, U., Tracey, K. J., Bachi, A., Uguccioni, M. and Bianchi, M. E. (2012). "Mutually exclusive redox forms of HMGB1 promote cell recruitment or proinflammatory cytokine release." *J Exp Med* 209(9): 1519-1528.

Verma, S. and Kaplowitz, N. (2009). "Diagnosis, management and prevention of drug-induced liver injury." *Gut* 58(11): 1555-1564.

Wähämaa, H., Schierbeck, H., Hreggvidsdottir, H. S., Palmblad, K., Aveberger, A. C., Andersson, U. and Harris, H. E. (2011). "High mobility group box protein 1 in complex with lipopolysaccharide or IL-1 promotes an increased inflammatory phenotype in synovial fibroblasts." *Arthritis research & therapy* 13(4).

Wakelin, S. J., Sabroe, I., Gregory, C. D., Poxton, I. R., Forsythe, J. L., Garden, O. J. and Howie, S. E. (2006). ""Dirty little secrets"--endotoxin contamination of recombinant proteins." *Immunol Lett* 106(1): 1-7.

Wang, C., Deng, L., Hong, M., Akkaraju, G. R., Inoue, J. and Chen, Z. J. (2001). "TAK1 is a ubiquitin-dependent kinase of MKK and IKK." *Nature* 412(6844): 346-351.

Wang, H., Bloom, O., Zhang, M., Vishnubhakat, J. M., Ombrellino, M., Che, J., Frazier, A., Yang, H., Ivanova, S., Borovikova, L., Manogue, K. R., Faist, E., Abraham, E., Andersson, J., Andersson, U., Molina, P. E., Abumrad, N. N., Sama, A. and Tracey, K. J. (1999). "HMG-1 as a late mediator of endotoxin lethality in mice." *Science* 285(5425): 248-251.

Wang, H., Vishnubhakat, J. M., Bloom, O., Zhang, M., Ombrellino, M., Sama, A. and Tracey, K. J. (1999). "Proinflammatory cytokines (tumor necrosis factor and interleukin 1) stimulate release of high mobility group protein-1 by pituicytes." *Surgery* 126(2): 389-392.

Waring, J. F., Liguori, M. J., Luyendyk, J. P., Maddox, J. F., Ganey, P. E., Stachlewitz, R. F., North, C., Blomme, E. A. and Roth, R. A. (2006). "Microarray analysis of lipopolysaccharide potentiation of trovafloxacin-induced liver injury in rats suggests a role for proinflammatory chemokines and neutrophils." *J Pharmacol Exp Ther* 316(3): 1080-1087.

Watson, M., Stott, K., Fischl, H., Cato, L. and Thomas, J. O. (2013). "Characterization of the interaction between HMGB1 and H3--a possible means of positioning HMGB1 in chromatin." *Nucleic Acids Res*.

Watson, M., Stott, K. and Thomas, J. O. (2007). "Mapping Intramolecular Interactions between Domains in HMGB1 using a Tail-truncation Approach." *Journal of Molecular Biology* 374(5): 1286-1297.

Weir, H. M., Kraulis, P. J., Hill, C. S., Raine, A. R., Laue, E. D. and Thomas, J. O. (1993). "Structure of the HMG box motif in the B-domain of HMG1." *EMBO J* 12(4): 1311-1319.

Yang, H., Antoine, D. J., Andersson, U. and Tracey, K. J. (2013). "The many faces of HMGB1: molecular structure-functional activity in inflammation, apoptosis, and chemotaxis." *J Leukoc Biol* 93(6): 865-873.

Yang, H., Hreggvidsdottir, H. S., Palmblad, K., Wang, H., Ochani, M., Li, J., Lu, B., Chavan, S., Rosas-Ballina, M., Al-Abed, Y., Akira, S., Bierhaus, A., Erlandsson-Harris, H., Andersson, U. and Tracey, K. J. (2010). "A critical cysteine is required for HMGB1 binding to Toll-like receptor 4 and activation of macrophage cytokine release." *Proc Natl Acad Sci U S A*.

Yang, H., Lundback, P., Ottosson, L., Erlandsson-Harris, H., Venereau, E., Bianchi, M. E., Al-Abed, Y., Andersson, U., Tracey, K. J. and Antoine, D. J. (2011). "Redox modification of cysteine residues regulates the cytokine activity of HMGB1." *Mol Med*.

Yang, H., Ochani, M., Li, J., Qiang, X., Tanovic, M., Harris, H. E., Susarla, S. M., Ulloa, L., Wang, H., DiRaimo, R., Czura, C. J., Wang, H., Roth, J., Warren, H. S., Fink, M. P., Fenton, M. J., Andersson, U. and Tracey, K. J. (2004). "Reversing established sepsis with antagonists of endogenous high-mobility group box 1." *Proceedings of the National Academy of Sciences* 101(1): 296-301.

You, Q., Cheng, L., Reilly, T. P., Wegmann, D. and Ju, C. (2006). "Role of neutrophils in a mouse model of halothane-induced liver injury." *Hepatology* 44(6): 1421-1431.

Youn, J. H., Kwak, M. S., Wu, J., Kim, E. S., Ji, Y., Min, H. J., Yoo, J. H., Choi, J. E., Cho, H. S. and Shin, J. S. (2011). "Identification of lipopolysaccharide-binding peptide regions within HMGB1 and their effects on subclinical endotoxemia in a mouse model." *Eur J Immunol* 41(9): 2753-2762.

Youn, J. H., Oh, Y. J., Kim, E. S., Choi, J. E. and Shin, J. S. (2008). "High mobility group box 1 protein binding to lipopolysaccharide facilitates transfer of lipopolysaccharide to CD14 and enhances lipopolysaccharide-mediated TNF-alpha production in human monocytes." *J Immunol* 180(7): 5067-5074.

Youn, J. H. and Shin, J. S. (2006). "Nucleocytoplasmic shuttling of HMGB1 is regulated by phosphorylation that redirects it toward secretion." *J Immunol* 177(11): 7889-7897.

Yu, M., Wang, H., Ding, A., Golenbock, D. T., Latz, E., Czura, C. J., Fenton, M. J., Tracey, K. J. and Yang, H. (2006). "HMGB1 signals through toll-like receptor (TLR) 4 and TLR2." *Shock* 26(2): 174-179.

Yuan, H., Jin, X., Sun, J., Li, F., Feng, Q., Zhang, C., Cao, Y. and Wang, Y. (2009). "Protective effect of HMGB1 a box on organ injury of acute pancreatitis in mice." *Pancreas* 38(2): 143-148.

Zanni, M. P., von Greyerz, S., Schnyder, B., Brander, K. A., Frutig, K., Hari, Y., Valitutti, S. and Pichler, W. J. (1998). "HLA-restricted, processing- and metabolism-independent pathway of drug recognition by human alpha beta T lymphocytes." *J Clin Invest* 102(8): 1591-1598.

Zheng, H., Fletcher, D., Kozak, W., Jiang, M., Hofmann, K. J., Conn, C. A., Soszynski, D., Grabiec, C., Trumbauer, M. E., Shaw, A. and et al. (1995). "Resistance to fever induction and impaired acute-phase response in interleukin-1 beta-deficient mice." *Immunity* 3(1): 9-19.

Zimmerman, H. (1999). Hepatotoxicity: the adverse effects of drugs and other chemicals on the liver. Philadelphia: , Lippincott, Williams & Wilkins.

Zou, W., Devi, S. S., Sparkenbaugh, E., Younis, H. S., Roth, R. A. and Ganey, P. E. (2009). "Hepatotoxic interaction of sulindac with lipopolysaccharide: role of the hemostatic system." *Toxicol Sci* 108(1): 184-193.